Proceedings Series

Sources and Measurements of Radon and Radon Progeny Applied to Climate and Air Quality Studies

Proceedings of a technical meeting held in Vienna, organized by the International Atomic Energy Agency and co-sponsored by the World Meteorological Organization

IAEA WMO

IAEA
International Atomic Energy Agency

SOURCES AND MEASUREMENTS OF RADON AND RADON PROGENY APPLIED TO CLIMATE AND AIR QUALITY STUDIES

Proceedings of a technical meeting held in Vienna,
organized by the International Atomic Energy Agency
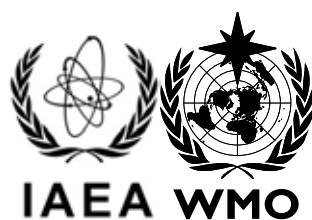and co-sponsored by the World Meteorological Organization

IAEA WMO

The following States are Members of the International Atomic Energy Agency:

AFGHANISTAN	GHANA	NIGERIA
ALBANIA	GREECE	NORWAY
ALGERIA	GUATEMALA	OMAN
ANGOLA	HAITI	PAKISTAN
ARGENTINA	HOLY SEE	PALAU
ARMENIA	HONDURAS	PANAMA
AUSTRALIA	HUNGARY	PARAGUAY
AUSTRIA	ICELAND	PERU
AZERBAIJAN	INDIA	PHILIPPINES
BAHRAIN	INDONESIA	POLAND
BANGLADESH	IRAN, ISLAMIC REPUBLIC OF	PORTUGAL
BELARUS	IRAQ	QATAR
BELGIUM	IRELAND	REPUBLIC OF MOLDOVA
BELIZE	ISRAEL	ROMANIA
BENIN	ITALY	RUSSIAN FEDERATION
BOLIVIA	JAMAICA	SAUDI ARABIA
BOSNIA AND HERZEGOVINA	JAPAN	SENEGAL
BOTSWANA	JORDAN	SERBIA
BRAZIL	KAZAKHSTAN	SEYCHELLES
BULGARIA	KENYA	SIERRA LEONE
BURKINA FASO	KOREA, REPUBLIC OF	SINGAPORE
BURUNDI	KUWAIT	SLOVAKIA
CAMBODIA	KYRGYZSTAN	SLOVENIA
CAMEROON	LAO PEOPLE'S DEMOCRATIC	SOUTH AFRICA
CANADA	REPUBLIC	SPAIN
CENTRAL AFRICAN	LATVIA	SRI LANKA
REPUBLIC	LEBANON	SUDAN
CHAD	LESOTHO	SWEDEN
CHILE	LIBERIA	SWITZERLAND
CHINA	LIBYA	SYRIAN ARAB REPUBLIC
COLOMBIA	LIECHTENSTEIN	TAJIKISTAN
CONGO	LITHUANIA	THAILAND
COSTA RICA	LUXEMBOURG	THE FORMER YUGOSLAV
CÔTE D'IVOIRE	MADAGASCAR	REPUBLIC OF MACEDONIA
CROATIA	MALAWI	TUNISIA
CUBA	MALAYSIA	TURKEY
CYPRUS	MALI	UGANDA
CZECH REPUBLIC	MALTA	UKRAINE
DEMOCRATIC REPUBLIC	MARSHALL ISLANDS	UNITED ARAB EMIRATES
OF THE CONGO	MAURITANIA	UNITED KINGDOM OF
DENMARK	MAURITIUS	GREAT BRITAIN AND
DOMINICA	MEXICO	NORTHERN IRELAND
DOMINICAN REPUBLIC	MONACO	UNITED REPUBLIC
ECUADOR	MONGOLIA	OF TANZANIA
EGYPT	MONTENEGRO	UNITED STATES OF AMERICA
EL SALVADOR	MOROCCO	URUGUAY
ERITREA	MOZAMBIQUE	UZBEKISTAN
ESTONIA	MYANMAR	VENEZUELA
ETHIOPIA	NAMIBIA	VIETNAM
FINLAND	NEPAL	YEMEN
FRANCE	NETHERLANDS	ZAMBIA
GABON	NEW ZEALAND	ZIMBABWE
GEORGIA	NICARAGUA	
GERMANY	NIGER	

The Agency's Statute was approved on 23 October 1956 by the Conference on the Statute of the IAEA held at United Nations Headquarters, New York; it entered into force on 29 July 1957. The Headquarters of the Agency are situated in Vienna. Its principal objective is "to accelerate and enlarge the contribution of atomic energy to peace, health and prosperity throughout the world".

SOURCES AND MEASUREMENTS OF RADON AND RADON PROGENY APPLIED TO CLIMATE AND AIR QUALITY STUDIES

For further information on this publication, please contact:

Terrestrial Environment Laboratory
IAEA Laboratories,
2444 Seibersdorf,
Austria
email: official.mail@iaea.org

FOREWORD

The naturally occurring radionuclide radon (^{222}Rn), together with its radioactive progeny (in particular ^{210}Pb), have been widely used to study a variety of atmospheric processes and to test and validate comprehensive global chemical transport models. In recent years, a particularly important application has been found in estimating regional scale greenhouse gas emissions. Several time series datasets have been collected of ^{222}Rn and ^{210}Pb concentrations in the planetary boundary layer (PBL) for a variety of purposes related to climate and air quality. An example of such a data collection is the use of radon monitors as a part of the World Meteorological Organization's Global Atmosphere Watch (GAW) network.

Unfortunately, the effective use of radionuclide observations is presently limited by the accuracy of source functions used by models, and by a globally uncoordinated approach to measurements, data archiving and data quality assurance, especially in relation to radon exhalation.

In June 2009 a Technical Meeting on Sources and Measurements of Radon and Radon Progeny Applied to Climate and Air Quality Studies was held in Vienna, Austria. The meeting was organized by the International Atomic Energy Agency (IAEA) and co-sponsored by the World Meteorological Organization (WMO). The meeting brought together scientists and engineers who are involved in one or more of the following: measurements and modeling of radon exhalation flux densities from the Earth's surface, measurement of atmospheric radon and radon progeny concentrations, and/or development and use of atmospheric transport models.

A major focus of the meeting was on moving towards agreed approaches to estimating radon exhalation flux densities, and to improving quality assurance of measurements both of radon exhalation flux densities and of concentrations of radon and radon progeny in the atmosphere. This is in the frame of the IAEA programme "Protection of the Marine and Terrestrial Environments" in which the transfer and behaviour of radionuclides and non-radioactive pollutants in the marine as well as terrestrial environment are investigated to develop and improve transfer models used for impact assessments with environmental issues. This publication brings together summaries of the three individual sessions of the meeting, as well as individual papers by participants.

The IAEA and WMO are grateful to the experts for their contributions to the meeting and to this report, and in particular to the session chairpersons (S. Schery, W. Zahorowski and S. Taguchi) and rapporteurs (F. Conen, R. Neubert and S. Galmarini). The support of L. Jalkanen of the World Meteorological Organization, and of C.K. Kim and A. Gondin da Fonseca of the Terrestrial Environment Laboratory, are gratefully acknowledged.

The IAEA officer responsible for this publication was P. Martin of the IAEA Terrestrial Environment Laboratory, Seibersdorf.

CONTENTS

Individual Papers

SESSION SUMMARIES

SESSION 1
RADON EXHALATION: MEASUREMENTS AND MODELLING

1. OVERVIEW OF THE CURRENT STATUS OF RADON EXHALATION MEASUREMENTS AND MODELLING

There have been a number of developments in the study of exhalation of radon from the earth's surface since the 2003 WMO/IAEA/CNRS meeting at Gif sur Yvette and the resulting report WMO/GAW [1]. Comprehensive, ground-validated radon flux density maps for China [2] and Europe [3] have been published. Production of these maps involved new algorithms relating radon flux density to closely associated variables such as soil radium or surface gamma dose rate. Schery and Huang [4] published the first global maps estimating the spatial distribution of monthly-averaged radon flux density from the oceans. On the metrology front, a paper by Mayya [5] provided a more complete analysis of the effects of back diffusion in accumulators designed to measure radon flux density. Mayya's two-dimensional analysis identified important corrections for back diffusion, not evident from earlier 1-D analyses, which should be considered in the design of accumulators and execution of their measurement protocols.

A new model-based flux density map for the land surface of the entire globe has been generated [6, 7]. That now makes at least three options: Schery and Wasiolek [8]; Conen and Robertson [9] and Goto et al. [6] available to atmospheric radon gas modellers requiring a global source term which goes beyond the earlier approximations of a constant radon flux density for most of the earth's surface. The new predictions by Goto et al. [6] still, however, assume a constant surface soil radium concentration for much of the world and that is a major limitation (as it is for the earlier maps by Schery and Wasiolek [8]).

There has been some new testing of the existing global flux density predictions that goes beyond that available at the time of the 2003 WMO/IAEA/CNRS meeting. On balance, new studies support the broad trend suggested by Conen and Robertson [9] that flux density decreases with increasing latitude in the northern hemisphere for latitudes above about 30° N [6, 10, 11]. In the current report, a paper by Yamazawa et al. [7] discusses new tests of global radon flux density predictions based on ship-board atmospheric radon gas measurements at certain northern latitudes. For the regions tested, the paper concluded that no single map was clearly superior.

There remains much work to be done to obtain higher quality predictions of radon flux density at both the regional and global scale, but especially at the global scale. There are still large regions of the earth's land surface (such as Africa and South America) for which suitable supporting data are not available. When regional predictions of flux density are combined to generate flux-density maps for a larger area, it is often found that the individual normalizations are not consistent. Large differences in average radon flux estimated for different regions (e.g. smaller in Europe than in China by almost a factor of three) may be real but could also be a result of differences between instruments and procedures used by the groups providing these estimates. Cross-comparison of instruments and field procedures may be one step necessary to resolve the issue. An ideal solution to obtaining an integrated flux

density map for the globe might be to use remote sensing data from satellites. Unfortunately, gamma rays from soil uranium and radium are too attenuated for direct use at satellite altitudes. There is a possibility that an intermediate atomic or molecular species or excitation produced from surface gamma rays might be detectable through remote sensing, but so far no one has been able to identify a specific chemical and optical scheme that appears practical.

The accuracy and reliability of flux density measurements is as an important problem limiting the usefulness of both regional and global maps. For certain regional screening studies where the goal is just to identify proportionally higher areas of radon flux density, some of the convenient but approximate techniques may suffice. However, for most studies related to development, testing, and application of atmospheric transport models for global pollution and climate change, more rigorous flux density measurements are required. For this class of measurements, increased attention should be given to quality-control protocols, such as intercomparison exercises and standards-traceable procedures, to improve the accuracy of estimates of radon flux density. In some cases on the regional scale, it may be possible to use a combination of accurate atmospheric radon measurements, back trajectory analysis and simple boundary layer box models to obtain a better normalization of regional surface flux through an inverse calculation for the average flux density in that region. In any case, the desired goal is the production and availability of new radon flux density maps with a spatial and temporal resolution that exceeds, for example, that available for many of the greenhouse gases. Should radon flux density predictions of higher quality become a reality, they could re-invigorate the field of atmospheric radon measurement and modelling which has been languishing a bit in recent years for lack of a capability to make sufficiently accurate tests of atmospheric transport models.

2. RADON FLUX DENSITY MAPS BASED ON MEASUREMENT OF GAMMA DOSE RATES

Measurements by Schery and colleagues 20 years ago around the entire continent of Australia provided evidence for a significant correlation between radon flux density and gamma dose rate [12]. Gamma dose rate is continuously measured by radiological emergency monitoring networks in Europe (including Russian Federation and Turkey), Canada, Japan and the Republic of Korea. Other countries are currently planning to install such a network (e.g. Iran). Substantial land areas have been scanned in aero-radiometric surveys carried out by geological agencies (i.e. USA, Russian Federation, Australia, parts of Canada) also providing gamma intensity and dose rate data. In Europe, an empirical function relating the magnitude of radon flux density to that of terrestrial gamma dose rate has been derived by Szegvary et al. [13] through parallel measurements of both parameters across a range of conditions. Together with information from emergency monitoring networks, it has provided a radon flux density map for Europe including estimates of seasonal variation [3, 14]. Verification of this map in Spain has shown some discrepancies with direct measurements of radon flux density because gamma dose detectors in the national monitoring network are not always installed in a location where dose rates represent the natural terrestrial background and the monitors are not calibrated in the natural gamma energy range giving a significant overestimation when this natural radiation is measured. Better estimates are made with the more detailed MARNA map [15]. In general, the European flux density map is in agreement with earlier, independent, assumptions of radon flux density decreasing with increasing latitude. Preliminary maps of radon flux density based on aero-radiometric surveys have been produced for the USA and for Russian Federation [16]. Validation of these estimates with direct flux density measurements is still outstanding.

The gamma dose rate approach to radon flux density mapping is not as fundamental as approaches based on direct radon flux density measurements or models involving surface soil radium. The dependence of radon flux density on certain other variables such as soil temperature, soil moisture, air temperature, wind speed and direction, snow cover, and atmospheric pressure change has to be dealt with by additions to the basic algorithm additions – additions that have not yet been fully formulated. However, the great power and promise of the gamma dose rate approach is the fact that a number of gamma dose rate measurements already exist for other purposes and that new measurements are relatively convenient to obtain compared with direct flux density measurements or measurements of soil radium. Thus the gamma dose rate approach is an attractive option for expanding the global coverage of radon flux density estimates.

3. FLUX DENSITY MAPS USING SOIL RADIUM CONCENTRATIONS

The WMO/GAW report [1] discussed the model developed by Schery and Wasiolek [8] for the prediction of global flux density from the earth's surface based on surface soil radium. This model simplified and reformulated the 1-D result from fundamental transport theory to give radon flux density in terms of soil radium concentration and estimates of soil moisture and soil temperature from global datasets. Zhuo et al. [2] and Yamazawa et al. [7] have used a similar approach to develop a new model for radon flux density in terms of soil radium concentration and other soil properties and meteorological variables. Their model relies on a greater number of variables, which are now more readily available from meteorological and soil datasets. Examples of these variables are bulk density, porosity, and texture of soil, measured precipitation, surface temperature, potential evapo-transpiration, and land cover classification. Using new results for soil radium in China, Zhuo et al. [2] published a map which gave an estimated average annual flux density from China of 29.7 ± 9.4 mBq m^{-2} s^{-1} (1.41 ± 0.45 atoms cm^{-2} s^{-1}). Model predictions were in good agreement with continuous measurements of radon flux density at 20 sites in China, Japan, and Korea [2, 17].

Goto et al. [6] report global predictions with a variation of the same model. However, lacking detailed data for soil radium concentration in the world they assumed a constant concentration in soil of 30 Bq kg^{-1} outside of China. The resulting global map confirmed a drop in flux density with increasing latitude similar to the predictions of Conen and Robertson [9]. The average annual flux density from the earth was estimated between 17.5 and 18 mBq m^{-2} s^{-1} (0.83 and 0.86 atoms cm^{-2} s^{-1}).

Yamazawa et al. [7] reported tests for the arctic region of three specific maps for the flux density for the globe or selected northern hemisphere countries [6, 8, 16] based upon atmospheric modelling and measurements of atmospheric radon gas from a range of ship locations in the Arctic Ocean and Bering Sea. As pointed out earlier, that paper concluded that none of the flux density predictions was clearly superior and that all had significant shortcomings for certain (but different) parts of the ship's route.

It is clear that there has been significant progress in the radium-parameter approach to prediction of radon flux density from the land's surface compared with the situation in 2003 WMO/GAW report [1]. However, it is also clear that although we now have much better regional maps for China and Europe, we are still some distance away from having equally detailed and validated maps for the whole globe. From discussion at the meeting, several suggestions were brought forth to improve the situation. One conclusion dealt with the need to get better reconciliation (consistent normalization and calibration) between maps from

different regional studies to produce consistent maps covering a larger land area. The suggestion was to do one or more of the following: (1) have groups making measurements in one region travel to a second region and make measurements with the same equipment and protocols as in the first region, (2) have only the instruments themselves temporarily exchanged between regions and used by the local groups for comparison with their own instruments, (3) have groups meet at one central location for an intercomparison exercise, each group using its own instruments, or (4) have one reference instrument based at a designated location that could be sent out to the various groups upon request as a reference or standard.

A second conclusion for improving global predictions of radon flux density deals with a more difficult problem: the lack of suitable soil radium concentration data in certain large parts of the world such as Africa and South America. Recommendations made in the WMO/GAW report [1] that as a priority new data be obtained for such regions have largely not been responded to. Such an approach is expensive, and in retrospect it seems clear that few groups have the funding or mandate from their controlling authority to carry out such large scale projects outside their own jurisdiction. As an alternative, an option of making use of presently existing geological maps and databases for the world was suggested at the present meeting. It was felt that people with expertise in uranium surface geology could make approximate estimates of radium concentration in surface soils on a country by country or smaller scale that provide significant improvement in global radon flux density maps using the surface radium approach. Even a relative classification of "below average", "about average", or "above average" would offer a major improvement over the present situation. Global reconciliation and normalization by this approach could be achieved by carrying out the process on some of the regions where the actual radium concentration has already been carefully measured.

4. RADON FLUX DENSITY MEASUREMENTS AND QUALITY CONTROL

Radon flux density is measured with a variety of devices and approaches. Grossi [18] compared four different accumulator systems in Spain, finding they generally gave similar, but not the same, results. Reference was also made during the discussion to an intercomparison exercise in 1995 where representatives from 24 institutions met with their equipment and measured radon flux density on a patch of land. The ratio between the standard deviation in the scatter in the measurements and their mean was 34% in that exercise [19]. A more recent intercomparison exercise [20] had an even poorer result for the same metric: 43%. Four major sources for such differences were discussed at the meeting:

(1) Differences in internal background and calibration of the radon or radon progeny detectors (e.g. ionisation chambers, electret devices, electrostatic deposition chambers, activated charcoal counted by gamma spectrometry, inability to reject a response from thoron (^{220}Rn) gas, incomplete mixing of radon gas inside the air space of the accumulator with a consequent effect on the radon gas concentration sampled);

(2) Accumulator effects on soil gas transport (back diffusion, induced changes in radon flux density due to advective flow caused by small persistent pressure differences between inside and outside an accumulator, temperature change, shielding from influences of sun, rain, and wind);

4

(3) Sampling bias (measurements limited to locations without stones or larger vegetation, sampling during normal working hours only, sampling only during fair weather situations, etc.);

(4) Spatial variability of radon flux density within even a small area (48 charcoal canisters exposed in a circle of 10 m diameter can provide a mean flux density for this area only with an uncertainty of ±30% [21].

Quality control should address in particular points 1)–3) because of their systematic nature. Descriptions of material and methods that accompany published radon flux density data were found to often lack the detail necessary to allow a judgment of quality and eventual bias. Potential ways to improve accuracy and minimize uncertainty were discussed. Calibration of radon detectors at a certified laboratory was seen as a necessity. Also, testing radon detectors and associated accumulation chambers, say in a radium-spiked sand box with a known radon emission, was considered. However, differences between accumulators and detectors will certainly change with environmental conditions and a sand box presents just one type of them. Back diffusion, for example, is more of a problem on dry and sandy soil than on wet clay. Furthermore, with finite-size sand boxes there are lateral boundary conditions which will vary with, and affect the results with, different size accumulators. There is a wealth of information on chamber effects on soil gas flux density in the scientific community studying CO_2 and N_2O emission that could provide helpful guidance on optimum accumulator measurements.

Recommendations regarding chamber design include maximizing the surface area of a chamber, keeping the ratio of surface area to internal height large, minimizing the chamber's closure time, and inserting a chamber base as deep as possible into ground. A comprehensive inter-comparison of instruments and methods taking all sources of uncertainty into account is best carried out by parallel measurements with different systems under a range of environmental conditions, such as occur during joint field campaigns. This provides for an integrated assessment of instrumental discrepancies as well as potential bias associated with the interaction between the instrument and the natural environment.

5. RECOMMENDATIONS FOR FUTURE WORK

There is no central archive of radon flux densities, which is making it difficult for the modelling community to make use of them. Thus, as a first step, all flux density estimates for larger regions that have been produced in the past should be made available at one place. Different flux density maps for one region are usually based on inputs of various quality and detail. It could be argued that large scale flux density estimates may be more reliable the closer they are to the area where they have been developed and validated by field measurements. This may be the case for estimates made, for example, in and for East Asia, Australia, the USA and Europe. Flux density measurement equipment and procedures are different in these regions with the potential to over- or under-estimate in one region compared to the other. To minimise eventual bias, reported differences between regional flux density estimates should be assessed by parallel measurements with two sets of instruments under a range of environmental conditions. One of them should be the instrument and procedure used in the region before. If systematic differences are discovered, they should be reported to the above archive. Ultimately, reconciled regional estimates could be merged and result in one best estimate of global radon flux density combining the work from different groups in different regions.

Ideally, a dedicated reference instrument, easy to transport and operate in a wide range of environments, is provided and held in a central location from where it is sent upon request to any group attempting to compare it with their equipment. Funding for maintenance (e.g. regular calibration at a certified laboratory) and transport may come from an international organisation. Further support would be needed in the process of making regional estimates comparable and merging them into one best global estimate by bringing together scientists, who have produced, or produce, their individual regional or global maps. For the atmospheric modelling community it would be useful to have one best estimate of radon flux density based on all available information rather than to have a number of different radon flux density maps, each with its own strengths and weaknesses.

Still, there are and will be large areas on the globe where we have little information to support our current estimates of the average radon flux density distribution. This is especially the case in the tropics, which contribute about 2/3 of the total radon emitted in the southern hemisphere. The most promising approach here would be to expand on the previous work by Schery and Wasiolek [8] and Goto et al. [6] by including more information on radium extracted from geological data. Predictions of radon flux density based on these parameters should be verified and, where disagreement is identified, adjustments should be made in the model of radon exhalation and transport from soil. Soil moisture from hydrological models or the soon-to-be-launched SMOS (Soil Moisture and Ocean Salinity) satellite could substantially improve the previous estimates in terms of accuracy and also add an estimate of temporal variations in radon flux density in regions where no continuous gamma dose rate monitoring is available.

Where emergency monitoring networks provide continuous information on gamma dose rates, these should be used for a description of spatial and temporal variations in radon flux density. Although the spatial relation between terrestrial gamma dose rate and radon flux density is known with some confidence, more work should be done on the variation of both parameters with time, such as the periods during and following rain, as well as during snow cover or rapidly changing atmospheric pressure.

6. CONCLUSIONS

The following conclusions and recommendations resulted from the meeting:

- Submit all national, regional or global radon flux density estimates to a central archive maintained by an international organization should be encouraged with an aim of eventual reconciliation and improvement of estimates of global fluxes densities.

- Render comparable reported regional flux density estimates through parallel measurements under a range of environmental conditions with two sets of instruments, one of which should be a global reference instrument.

- Improve resolving spatial and temporal variations and the accuracy of radon flux density estimates at different scales. For regions where little flux density information is currently available or likely to be obtained in the immediate future (such as Africa and South America) consider the use of models of flux density combined with expert estimates of surface radium or uranium deduced from existing data on surface geology. The aim is flux density maps providing for quantitative evaluation of global transport models and accurate estimates of trace gas fluxes by mass balance with radon.

- Encourage an international organization to publish recommended standards for flux density measurements and reporting of flux density data. The same organization should consider making available a reference flux density measurement instrument or source standard that could be used as a reference for comparison.

REFERENCES

[1] WORLD METEOROLOGICAL ORGANIZATION/ GLOBAL ATMOSPHERIC WATCH, 1st International Expert Meeting on Sources and Measurements of Natural Radionuclides Applied to Climate and Air Quality Studies, Report 155, WMO TD **1201** (2004).

[2] ZHUO, W., GUO, Q., CHEN, B., CHENG, G., Estimating the amount and distribution of radon flux density from the soil surface in China. Journal of Envir. Radioactivity **99** (2008) 1143–1148.

[3] SZEGVARY, T., CONEN, F., CIAIS, P., European ^{222}Rn inventory for applied atmospheric studies, Atmospheric Environment **43** (2009) 1536–1539.

[4] SCHERY, S.D., HUANG, S., An estimate of the global distribution of radon emissions from the ocean, Geophysical Research Letters **31** (2004) Article Number: L19104.

[5] MAYYA, Y.S., Theory of radon exhalation into accumulators at the soil-atmosphere interface, Radiation Protection Dosimetry **111** 3 (2004) 305–318.

[6] GOTO, M., MORIIZUMI, J., YAMAZAWA, H., IIDA, T., ZHUO, W., Estimation of global radon exhalation rate distribution, The Natural Radiation Environment – 8th International Symposium (PASCHOA, A.S., ed.), American Institute of Physics, Melville, NY (2008) 169–172.

[7] YAMAZAWA, H., OHYA, N., HIRAO, S., MORIIZUMI, J., IIDA, T., TASAKA, S., INOUE, M., Evaluation of radon source maps for Siberia using atmospheric radon concentration over Arctic Ocean and Bering Sea, Technical Meeting on sources and measurements of radon and radon progeny applied to climate and air quality studies, IAEA, Vienna (2009).

[8] SCHERY, S.D., WASIOLEK, M., "Modeling radon flux from the earth's surface", Radon and Thoron in the Human Environment (KATASE, A., SHIMO, M., Eds.), World Scientific, Singapore (1998) 207–217.

[9] CONEN, F., ROBERTSON, L.B., Latitudinal distribution of ^{222}Rn flux from continents, Tellus **54B** (2002) 127–133.

[10] GUPTA, M.L., DOUGLASS, A.R., KAWA, R., PAWSON, S., Use of radon for evaluation of atmospheric transport models: sensitivity to emissions, Tellus Series B - Chemical and Physical Meteorology **56** 5 (2004) 404–412.

[11] ROBERTSON, L.B., STEVENSON, D.S., CONEN, F., Test of a northwards-decreasing ^{222}Rn source term by comparison of modelled and observed atmospheric ^{222}Rn concentrations, Tellus Series B-Chemical and Physical Meteorology **57** 2 (2005) 116–123.

[12] SCHERY, S.D., WHITTLESTONE, S., HART, K.P., HILL, S.E., The flux of radon and thoron from Australian soils, Journal of Geophysical Research **94** (1989) 8567–8576.

[13] SZEGVARY, T., LEUENBERGER, M.C., CONEN, F., Predicting terrestrial ^{222}Rn flux using gamma dose rate as a proxy, Atmospheric Chemistry and Physics **7** (2007a) 2789–2795.

[14] SZEGVARY, T., et al., Mapping terrestrial γ-dose rate in Europe based on routine monitoring data, Radiation Measurements **42** 9 (2007b) 1561–1572.

[15] QUINDOS PONCELA, L.S., et al., Natural gamma radiation map (MARNA) and indoor radon levels in Spain, Environment International **29** (2004) 1091–1096.

[16] SZEGVARY, T., European ^{222}Rn flux map for atmospheric tracer applications, PhD thesis, University of Basel, Switzerland (2007).

[17] ZHUO, W., FURUKAKWA, M., GUO, Q., KIM, Y.S., Soil radon flux and outdoor radon concentrations in East Asia, Elsevier International Congress Series **1276** (2004) 285–286.

[18] GROSSI, C., Quality study of electret radon flux monitors by "in situ" intercomparison campaign in Spain, Technical Meeting on sources and measurements of radon and radon progeny applied to climate and air quality studies, IAEA, Vienna (2009).

[19] HUTTER, A.R., KNUTSON, E.O., An international intercomparison of soil gas radon and radon exhalation measurements, Health Physics **74** 1 (1998) 108–114.

[20] NEZNAL, M., NEZNAL, M., International intercomparison measurement of soil-gas radon concentration, of radon exhalation rate from building materials and of radon exhalation rate from ground, Czech Republic (2002), http://www.radon-voz.cz/pdf/radon_inv_10-2004-pdf.

[21] QUINDOS PONCELLA, L.S, Technical Meeting on sources and measurements of radon and radon progeny applied to climate and air quality studies, IAEA, Vienna (2009).

SESSION 2
MEASUREMENTS OF RADON AND RADON PROGENY
IN THE ATMOSPHERE

1. INTRODUCTION

Currently there are four major applications of ^{222}Rn in climate, air quality and pollution studies. These are: (i) tracing synoptic scale air mass transport, (ii) tracing diurnal mixing in the lower atmosphere, (iii) calibrating seasonal regional emissions of climatically sensitive tracers including CO_2, CH_4, N_2O, and (iv) validating and, to a lesser extent, parameterising, transport and mixing schemes in climate/weather models.

The focus of Session 2 of the technical meeting was intended to be on the first three applications mentioned above. Session 3 was dedicated to the last of the four applications. The actual scope of Session 2 turned out to be broader and reflected the diverse research interests of the meeting's participants.

In the last six years since the 2003 WMO/IAEA meeting [1], there has been a significant increase in applying radon atmospheric observations in atmospheric, air pollution, and climate studies. The increased activity in the field was marked by the deployment of new radon detectors. For instance, two radon dual loop detectors have been commissioned at WMO GAW stations at Mt Waliguan, China (2006) and Jungfraujoch, Switzerland (2007). Also, a number of new radon detectors have become operational within EU- and US-based greenhouse gas programs [2, 3] with a typical experimental setup involving co-located measurements of radon, greenhouse gases sampled from inlets mounted on (tall) towers.

Other important developments focused on vertical mixing characterised by ground-based radon gradient measurements within the boundary layer [4, 5] and airborne radon vertical profiles in the lower atmosphere [6]. The aim has been to develop better understanding of the mixing in general and its parameterisation in particular. The developments reflect the significance of boundary layer parameterisations in the climate and weather models.

There has been some progress in radon instrumentation. A new 270 L two filter radon detector has been built. The instrument utilises the principle of electrostatic collection in the one flow loop configuration. The development was driven by Recommendation 6 of the 2003 meeting which stated that "when considering installation of new ^{222}Rn detectors at WMO/GAW stations, preference should be given to a two-filter system, calibrated routinely using a ^{222}Rn calibration source traceable to a primary standard" [1]. This is a promising new development, initiated by and being implemented at the Deutscher Wetterdienst, Germany [6]. The established designs based on electrostatic collection and two-filter method with dual flow loop and gross alpha counting [8–10], have been improved, with emphasis on increased sensitivity on one hand, and on use of computer-based communications technologies on the other. The latter aims for better data recovery rates, remote operation, and establishment of real time output streams from field instruments.

2. PRESENTATIONS

The three major themes of Session 2 are summarized below.

2.1. Radon and radon progeny in radiation protection and pollution studies

Radiation protection

The subject was covered by three presentations. Burian and Otahal [11] discussed radon progeny levels in the boundary layer in the Czech Republic as well as in other European countries and in some locations in the US. The targeted areas included mines and waste dump surroundings, sediment fields characterised by high radon flux densities, and other areas with large numbers of low level radioactive material heaps. An intercomparison of radon progeny instruments was proposed, based on the authors' instrument. Fathabadi [12] presented a summary of selected research and monitoring activities carried out by the Environmental Radiological Protection Division of the National Radiation Protection Department of the Iran Nuclear Regulatory Authority. Particular subjects included gamma dose rates in the country, technologically enhanced naturally occurring radioactivity, radioactivity levels in soils, radon progeny levels in selected industrial and environmental settings, radon exhalation from building materials, and areas of high level natural radioactivity. Vaupotic [13] reviewed Slovenian activities related to radon levels in air (mainly in Slovenia but also in some other European and Asian locations). A wide range of radon levels in soil gas and outdoor air having been observed, radon exhalation rates were found to differ substantially on different grounds, with the highest values in the vicinity of tectonic faults. The highest radon concentrations in outdoor air have been found on carbonates, with significant diurnal variations.

Pollution studies

Zahorowski et al. [14] discussed the application of a novel metric space based on spatial variables and radon for clustering of air back trajectories corresponding to atmospheric pollution events. The performance of the new metric was shown to be better than those previously used and based on spatial variables in two or three dimensions only. The method was discussed using a multi-year dataset of collocated measurements of fine particles and ^{222}Rn in Hong Kong. Perrino et al. reported on the application of radon progeny measured in air as a tool for interpretation of atmospheric pollution events [15]. One of the outcomes was the development of "atmospheric stability indices" to quantify meteorological predisposition on any given day for pollution event(s). The indices seem to correlate well with some pollutants. It has been claimed that by studying the difference between the atmospheric stability index and the atmospheric concentration of pollutants one can identify episodes when the emission was higher than or lower than normal.

2.2. Instrumentation and measurement

Instrumentation

Steinkopff et al. [7] presented initial results obtained with a new radon detector which utilizes electrostatic collection. The instrument has a large delay volume (270 L) compared with similar instruments with electrostatic collection [8, 9] . The ^{214}Po/^{218}Po isotopic ratio has been used for quality assurance. A prototype detector has been deployed at a WMO-GAW station at Zugspitze-Schneefernerhaus (Germany). The problem of varying moisture content in the

sampled air was addressed by including an efficient drying procedure utilising Peltier elements. Time resolution of the detector is two hours.

Measurements

Schmidt et al. [16] gave an overview of a recent intercomparison of radon and radon progeny detectors as well as an outline of the French effort in radon-related research. Neubert et al. [17] discussed the findings of a two year intercomparison of co-located radon and radon progeny instruments at the Lutjewad station in the Netherlands. Both reported generally good agreement between the radon and progeny data. Aerosol wet deposition and air mass history were confirmed to be major sources of discrepancies. Similar conclusions were reached after an intercomparison at the Schauinsland station in Germany [14, 18]. It seems that using radon progeny concentration in aerosols as a quantitative substitute for radon can lead to discrepancies in most conceivable situations, caused by varying disequilibrium between radon and its progeny. These discrepancies are significant, can be expected at all time scales, including sub-synoptic time scales, and can be expected to strongly depend on local site characteristics. While changes induced by changing radon concentrations might be modelled, at least to a certain degree, the scavenging can only be simulated by a coupled, fully equipped aerosol model, which is not yet available.

2.3. Application of radon to atmospheric and climate studies

Regional emissions of terrestrial greenhouse gases

Schmidt et al. [16, 19] gave a presentation on the topical radon application related to constraining the terrestrial emissions of greenhouse gases, with the specific example under discussion concerning molecular hydrogen.

Experimental setup and parameters for model validation

Sainz et al. [20] presented a review of some experimental input parameters for model validation. They covered radon flux density rates in general and the results of the Spanish MARNA Project in particular. Related maps of potential radon in Spain were also discussed. Detailed results on soil gas concentration, integrated indoor measurements and radon flux density were given for the Spanish region of Galicia. Vargas [21] reported on a new project aimed at using radon concentrations, measured at a coastal location in Spain at 10 m and 100 m, for validation of dispersion models. The radon source term and the use of the European and MARNA radon flux density maps were discussed in some detail. An established model will be used in forward and backward models for validation.

Radon as a tracer of horizontal and vertical air movements

Zahorowski et al. [14] presented recent results on radon gradient measurements in the surface layer (Lucas Heights, Australia) and in the boundary layer (Cabauw, the Netherlands) as well as a general issue of the representativeness of local meteorological variables for air mass origin analysis.

3. PRESENTATIONS – DISCUSSION

The participants raised a number of questions specific to the presentations. Some issues, judged to be important for the near future, were raised and discussed. These were then expressed as a set of recommendations. Below is a summary of the discussions and the recommendations.

Vertical radon profiles

Benefits offered by experimentally derived vertical radon profiles in the lower atmosphere were discussed. Some suggested that potential temperature might be a better passive tracer for turbulent mixing. However, while the radon source in a given area and within a range of environmental parameters is practically constant, the same cannot be said about potential temperature. Clouds also influence the heat balance. It was agreed that the information provided by vertical radon profile measurements should be used for model validation.

Reference instrument for quality control

A reference instrument would be desirable for maintaining a common calibration scale. The participants were in favour of dedicating an instrument to that task. Such an instrument could then be transported to stations to run in parallel with different types of radon detectors. It was not clear who could organize such a comprehensive long-term intercomparison study.

Data accessibility

The accessibility of atmospheric radon concentration data seems to be lacking. Until now only a few datasets are in the public domain (or available to a large group of scientists). A central data facility would improve the visibility of the radon community. The experimentalists present at the meeting agreed in principle to submit their data. They also pointed out the fact that much public funding is conditional to releasing data after a predefined period (usually 2 years). Radon is (in principle) included in the WMO World Data Centre for Greenhouse Gases (WDCGG) in Japan [22]. The group agreed that the location is suitable for archiving and distributing the radon data. The modellers were in favour of one central facility for this purpose.

Note: A few months after the meeting in November 2009, a revised guide on data submission and dissemination was published by the WMO [23]. The guide provides definitive answers to, and comments about most discussion points documented in the proposed actions listed in Section 4.1 below.

4. CONCLUSIONS

4.1. Submission of data

The participants agreed that a number of actions are to be initiated to address the conspicuous absence of a significant number of existing radon datasets at the WDCGG site. These actions are as follows:

(1)   Participants should start submitting radon concentration datasets to the WDCGG.

(2)   In addition to the above, participants should work towards establishing a list of links to be held at, and maintained by, the WDCCG site with the data residing at sites

maintained by regional/national organisations and/or projects as well as kept by individual researchers.

(3)   Participants should develop a minimum set of requirements for the submitted data.

4.2. Intercomparison of instruments for radon and radon progeny measurements

The proposed intercomparison to be implemented on two time scales:

(1)   One or more field inter-comparisons where detectors can be inter-compared.

(2)   A multi-year program of intercomparison between a designated transportable instrument on one hand and as many as practical stationary detectors at selected sites on the other.

REFERENCES

[1]   WORLD METEOROLOGICAL ORGANIZATION/ GLOBAL ATMOSPHERIC WATCH, 1st International Expert Meeting on Sources and Measurements of Natural Radionuclides Applied to Climate and Air Quality Studies, Report Number 155, WMO TD Number 1201 (2004),   http://www.wmo.ch/web/arep/reports/gaw155.pdf.

[2]   VERHEGGEN, B., VERMEULEN, A.T., ZAHOROWSKI, W., Tall Tower Observations and Transport Modelling of Radon, Carbon Dioxide and Methane. European Geosciences Union, General Assembly 2008, Vienna, Austria, 13-18 April 2008.

[3]   HIRSCH, A.I., et al., Combining Eddy Covariance Fluxes, High-Precision Trace Gas Measurements, Chemical Transport Modeling, and Inverse Modeling to Estimate Regional CO2 Fluxes in the Southern Great Plains, USA, Eos Trans. AGU **89** (53), Fall Meet. Suppl., Abstract B54A-04 (2008).

[4]   VERMEULEN, A., VERHEGGEN, B., ZAHOROWSKI, W., ^{222}Rn vertical gradient measurements and its use for transport model calibration Transcom 2008, Utrecht, the Netherlands, 2–5 June 2008.

[5]   ZAHOROWSKI, W., et al., Diurnal boundary layer mixing patterns characterised by ^{222}Rn gradient observations at Cabauw, 18th AMS Conference on Boundary Layers and Turbulence, Stockholm Sweden, 9–13 June 2008, Extended abstract 9B.2 (2008) 5. http://ams.confex.com/ams/pdfpapers/139978.pdf

[6]   WILLIAMS, A.G., et al., Mixing and venting in clear and cloudy boundary layers using airborne radon measurements, 18th AMS Conference on Boundary Layers and Turbulence, Stockholm Sweden, 9–13 June 2008. Extended abstract 9B.4 (2008) 5. http://ams.confex.com/ams/pdfpapers/139974.pdf

[7]   STEINKOPFF, T., FRANK, G., SALVAMOSER, J., Low Level Measurements of ^{222}Rn in the Atmosphere in the Frame of the GAW-Measuring Programme at the Environmental Research Platform Schneefernerhaus / Zugspitze, Technical Meeting on sources and measurements of radon and radon progeny applied to climate and air quality studies, IAEA, Vienna (2009).

[8]   IIDA, T., IKEBE, Y., TOJO, K., An electrostatic radon monitor for measurements of environmental radon. Res. Lett. Atmos. Electr. **11** (1991) 55–59.

[9]   IIDA, T., IKEBE, Y., SUZUKI, K., UENO, K., WANG, Z., JIN, Y., Continuous measurements of outdoor radon concentrations at various locations in East Asia, Environ. International **22** 1 (1996) 139–147.

[10] WHITTLESTONE S., ZAHOROWSKI, W., Baseline [222]Rn detectors for shipboard use: Development and deployment in the First Aerosol Characterisation experiment (ACE 1). J. Geophys. Res. **103** 16 (1998) 743–751.

[11] BURIAN, I., OTAHAL, P., EER in the low layer of the atmosphere, paper presented in Technical Meeting on sources and measurements of radon and radon progeny applied to climate and air quality studies, IAEA, Vienna (2009).

[12] FATHABADI, N., Natural radionuclide research in Iran, paper presented in Technical Meeting on sources and measurements of radon and radon progeny applied to climate and air quality studies, IAEA, Vienna (2009).

[13] VAUPOTIČ, J., Review of Slovenen research on radon in air, paper presented in Technical Meeting on sources and measurements of radon and radon progeny applied to climate and air quality studies, IAEA, Vienna (2009).

[14] ZAHOROWSKI, W. et al., Baseline and non-baseline [222]Rn observations for climate and air quality studies; a review, Technical Meeting on sources and measurements of radon and radon progeny applied to climate and air quality studies, IAEA, Vienna (2009).

[15] PERRINO, C., Natural Radioactivity From Radon Progenyas a tool for the interpretation of atmospheric pollution events, Technical Meeting on sources and measurements of radon and radon progeny applied to climate and air quality studies, IAEA, Vienna (2009).

[16] SCHMIDT, M., et al., Atmospheric Radon measurements in the French greenhouse gas monitoring network (RAMCES), Technical Meeting on sources and measurements of radon and radon progeny applied to climate and air quality studies, IAEA, Vienna (2009).

[17] NEUBERT, R., LEVIN, I., KETTNER, E., ZAHOROWSKI, W., A long-term ICP experiment of two frequently-used atmospheric [222]Radon monitors, Technical Meeting on sources and measurements of radon and radon progeny applied to climate and air quality studies, IAEA, Vienna (2009).

[18] XIA, Y., et al., Variation of disequilibrium between [222]Rn and its short-lived progeny at a mountain station. Submitted to Journal of Environmental Radioactivity (2009).

[19] YVER, C., SCHMIDT, M., BOUSQUET, P., ZAHOROWSKI, W., RAMONET, M., Estimation of the molecular hydrogen soil uptake and traffic emissions at a suburban site near Paris through hydrogen, carbon monoxide and [222]Rn semi-continuous measurements. Accepted to JGR.

[20] SAINZ, C., et al., Measurements of radon and daughters in the atmosphere in the discontinuity land-sea. Experiences in radon exhalation rates as source of radon in the free atmosphere, Technical Meeting on sources and measurements of radon and radon progeny applied to climate and air quality studies, IAEA, Vienna (2009).

[21] VARGAS, A., Continuous Radon Measurement Campaign Applied to Model Validation at the 100 Meters Tower of "El Arenosillo" Station on the Huelva Coast (Spain), Technical Meeting on sources and measurements of radon and radon progeny applied to climate and air quality studies, IAEA, Vienna (2009).

[22] WORLD METEOROLOGICAL ORGANIZATION/ GLOBAL ATMOSPHERIC WATCH, 14th WMO/IAEA Meeting of Experts on Carbon Dioxide, Other Greenhouse Gases and Related Tracers Measurement Techniques, Report Number 186, http://www.wmo.int/pages/prog/arep/gaw/documents/GAW_186_TD_No_1487_web.pdf

SESSION 3
DEVELOPMENT AND USE OF ATMOSPHERIC MODELS

1. OVERVIEW OF THE CURRENT STATUS OF DEVELOPMENT AND USE OF ATMOSPHERIC TRANSPORT MODELS

There are three major applications of ^{222}Rn (hereafter radon) for the validation of climate and weather models: (i) vertical transport and mixing under conditions of deep moist convection, (ii) vertical mixing under conditions of dry convection at the lower part of the atmosphere and (iii) modeling of long range transport using global meteorological datasets. Although the scope of Session 3 of the technical meeting was dedicated to the validation of climate and weather models, most of the presentations in the session focused mainly on processes in the lower atmosphere.

Radon and its progeny have been extensively used in climate models as discussed at the 2003 WMO/IAEA/CNRS meeting at Gif sur Yvette [1]. Mass transport schemes under conditions of deep convection [2–5], vertical diffusion coefficients for the lower atmosphere [6] and model sensitivities to meteorological datasets [7] are some examples of validation studies using radon in global climate or chemical transport models (CTMs). Taken as a whole, no scheme for deep convective transport or choice of meteorological dataset yet stands out when model predictions are compared with observations. Although some differences are found in the vertical profiles in the tropics, more comparisons to free tropospheric observations of radon or another tracer transported by convective motions will be needed to identify superior convection schemes and/or the most appropriate meteorological datasets. In addition, more vertical profile observations in the tropics (recommendation No.22 in [1]) are needed but no new ones have been reported since 1991 [8]. Even in the extra-tropics, new vertical profiles of radon in the upper troposphere have not been reported since 1994 [9]. Though some radon flux density maps were tested in a global model, due to biases in large scale convective transport, no clear conclusion was obtained about which flux density map was superior [10]. On the other hand, using studies of radon in the lower atmosphere, it was possible to determine a vertical diffusion coefficient that provided better agreement with surface radon observations [6].

Although radon was used in past WMO intercomparison projects [11, 12] no new model intercomparison studies have been published using radon despite the recommendations #20 of the WMO [1]. For aerosol studies, an intercomparison project called AEROCOM was organized [13]; http://nansen.ipsl.jusseu.fr). Species to be simulated became too many for the participants, so radon was dropped from the list. For ozone studies, inter-continental transport of air pollutants and their precursors was compared in 21 CTMs in HTAP [14]; http://www.htap.org/). The aim of the HTAP program was to share knowledge of baseline ozone concentrations. Radon was listed as a species to be studied in the initial planning but was later dropped from the protocol. For carbon dioxide, an intercomparison of CTMs was conducted in the program TransCom ([15, 16]; http://purdue.edu/transcom). Radon concentrations were studied using a common flux density map but the results have not been published. Participants at the present meeting speculated that the relative inactivity of new model intercomparison exercises since the 2003 meeting could be traced in part to insufficient improvement in radon flux density maps and measurements of atmospheric radon to provide much new information.

Modellers making presentations in Session 3 discussed ways to include in their models atmospheric processes in the lower atmosphere, such as dispersal of air pollutants, diffusion,

and horizontal and vertical air movements. Using such models they were still getting significant discrepancies between predictions and measurements of radon gas and were having trouble understanding the cause of these discrepancies. Two possible causes have already been mentioned: uncertainties in flux density estimates (Session 1) and inadequate measurements of atmospheric radon (Session 2). In addition, there could be problems with the design of the models themselves, although it may be difficult to diagnose these without first having improved flux density maps and atmospheric measurements. Most modellers concentrated their attention on two key input variables in their models: (a) radon flux density and (b) boundary layer height (BLH). Another important issue for model formulation was spatial scale. Presentations generally fell into one of three spatial scales: (1) local, i.e. vertical profiles for a single point or area less than 5 km, (2) regional, i.e. wider than 5 km but not global, or (3) global.

2. LOCAL SCALE

Vertical profiles or three-dimensional structure of concentrations within a range of 5 km are studied in local models. In this meeting, an urban air quality evaluation system using stability index monitor [17, 18] and a complex numerical model of Large Eddy Simulations [19, 20] are presented.

Urban air quality was studied with a conceptual model of boundary layer in mind. Radon and pollutants exhausted in the lower atmosphere are mixed with ambient air. This mixing takes place in the atmosphere under an inversion layer, sometimes called planetary boundary layer. Atmospheric stability index (ASI) is introduced for operational monitoring of mixing efficiency due to a combined effect of the mixing below an inversion layer and entrainment of air above an inversion layer. Correlations between radon and pollutants, such as benzene, PM10 and PM2.5 at Verona, Milano and Alessandria are shown to demonstrate that concentration of radon and pollutants are varying synchronously. The ASI is monitored with commercially available equipment. The ASI allows the uncoupling of the two main factors determining primary pollution events, the dilution properties of the lower atmosphere and the emission. The ASI also distinguishes pollution due to inversion and the effect of traffic control and Sahara dust events. Performance compared to traditional Pasquill criteria was demonstrated.

Radon and its progeny in the condition of Wangara experiment are studied in an LES. The LES are conducted in grid resolution of 62.5 m × 62.5 m × 25 m in 5000 m × 5000 m × 2000 m domain with 1 second time step. The LES successfully simulated kinetic energy observed in Wangara experiment, which enabled us to study the interactions between the development of convective boundary layer and residual boundary layer developed in the previous day. The LES considered ^{222}Rn as a single source with four progenies, ^{218}Po, ^{214}Pb, ^{214}Bi, and ^{210}Pb. Due to mixing, the fractional rate of these progeny are departed from a secular equilibrium. Significant disequilibrium in neutral conditions was shown by the LES. This study is expected to assist interpretation of point observations as well as vertical profile observation of radon and process understanding of the combination of mixing and transformation (decay) of the species due to correspondence of mixing and decay time scales.

3. REGIONAL SCALE

Radon has been used to interpret emission of greenhouse gas [21], PM2.5 [22] and fetch region [23] sometimes in support of Lagrangian particle model, which trace the motion of an imaginary air mass in the three-dimensional atmosphere. Back trajectory analysis is included in this group of studies. In the meeting, in situ radon concentrations are presented with the aid

of Eulerian regional model, which estimates concentration distributions at three-dimensional domain. The Lagrangian particle dispersion model MM5v3.7-FLEXPARTv6.2 has been used in a receptor-oriented approach with different spatially heteregoneous radon exhalation flux densities to study the radon concentrations at Cabauw [24–26] and at the Spanish early warning network using the MARNA map emissions [24–26], particulary at the sites of Autilla del Pino, Murcia are discussed [24–26]. Concentrations at Beijing, Nagoya, Hateruma and Hachijo are discussed with MM5/HIRAT model [27]. Those of Cabauw are also discussed with WRF/COMMET model [28].

Radon-tracer method to estimate CO_2 flux over United States is discussed using two different weighting schemes with a synthetic Lagrangian particle model. Advantage of sensitivity-weighted averages over evenly-averaged flux is demonstrated. Aerosols measured at Hong Kong, China, are discussed with radon concentrations.

Source category and geographic region of the emission area are estimated combining radon concentrations, Ion Beam Analysis and Potential Source Contribution Function Technique. Fetch region at Sado Island is studied with back trajectory analysis. Radon flux over Honshu, Japan, is estimated as 10.6–47.9 mBq m^{-2} s^{-1} using the observed radon concentrations with fetch analysis.

Discrepancies between in situ concentrations measurement at target event are discussed from the differences in boundary layer scheme in the regional model and emission distributions given to the model. At Cabauw tower observations, discrepancy between the observations and model simulations with WRF/COMMET are discussed with the boundary layer used in the model. One boundary layer height estimates was diagnosed from European Centre for Medium Range Weather Forecast model data. And the other is the in situ observation with ceilometer. When the model failed to simulate the observations, the diagnosed boundary layer thickness are significantly different from those of ceilometer. Two boundary schemes (MRS-PBL and GS-OBL) are combined with three emission distributions; Schery and Wasiolek, Conen and Yamazawa radon flux density in MM5/HIRAT. No PBL scheme or emission distribution is superior to the others.

4. GLOBAL SCALE

Minor constituents with life time longer than a week is to be studied using global atmospheric chemistry transport model (hereafter CTM), because any air mass occupying a region is replaced by an air mass outside the region within a week. The halflife of ^{222}Rn is 3.8 days and it is not necessarily studied in a global model while there are great advantages using radon in CTMs as has been shown in the literature as well as a presentation in this meeting.

To explain the advantages, a brief description of the background of global atmospheric transport model is given here. CTM is a computer program to estimate concentrations of gas and aerosol (minor constituents) in the air at discrete time and spatial coordinates. Discrete means that concentrations are represented only at points with finite distances in space and at finite intervals in time. Domain of the computation is global horizontally and up to several kilometers in the vertical, at least 15 km which is the altitude of the tropopause in the tropics. The models have been developed for a wide range of time and spatial scales depending on the objectives of the model. Some examples of issues studied with CTM are atmospheric diffusions, atmospheric transport, source-receptor relationship, fetch, catchment area, foot print analysis, and an inverse method to estimate flux. There are some criteria to be satisfied in CTM for studying the above mentioned issues. They are positive definite concentrations, total mass conservations, no numerical diffusions to preserve shape, computational efficiency, linearity etc. It is a technical challenge to fulfill all these criteria simultaneously. These

complexities are created from the fact that the models are trying to represent continuous distributions of minor constituents at discrete points in time and space. Any models of Euralian or Lagrangian approaches cannot avoid this difficulty because the wind fields are available only at discrete time and space. All models are a consequence of trade offs among the competing requirements for an ideal perfect model. Overall performance of a model may be evaluated with some simple experiments using a constituent with a known source and observed atmospheric distributions. Radon is considered to be one of the best suitable substances for qualitative as well as quantitative evaluation of models. If the source distribution is unknown then a circulatory argument which is wrong CTM or flux is going into an endless loop. This is the same with the discussion in limited area models.

Wind fields and convective transport are studied in a CTM. Effect of convective mass flux archived in ECMWF Reanalysis is evaluated in an off-line CTM using radon [2, 6]. Although some differences are found in the vertical profiles in the tropics, more comparisons to free troposphere observations of radon or another tracer of convective transport will be needed to unambiguously identify either of the convective data sets as optimal for use in chemistry transport models. Three global emission estimates are evaluated in Goddard Space Flight Center (GSFC) off-line three-dimensional parameterized chemistry and transport model (PCTM) [10]. The PCTM analysis indicates that additional measurements of surface radon, particularly during April-October and north of 50°N over the Pacific as well as Atlantic regions, would make it possible to determine if the proposed latitude gradient in radon emissions is superior to a uniform flux scenario. Three different sets of input meteorological information: (1) output from the Goddard Space Flight Center Global Modeling and Assimilation Office GEOS-STRAT assimilation; (2) output from the Goddard Institute for Space Studies GISS II0 general circulation model; and (3) output from the National Center for Atmospheric Research MACCM3 general circulation model are evaluated in a CTM [6] using radon and lead. Taken as a whole, no simulation stands out as superior to the others in the comparison with the observations compiled into the US Environmental Measurements Laboratory RANDAB database. Transport of ^{222}Rn and methyl iodide by deep convection is analyzed in the Geophysical Fluid Dynamics Laboratory (GFDL) Atmospheric Model 2 (AM2) using two parameterizations for deep convection [4]. The shapes of the observed profiles suggest that the larger deep convective mass fluxes and associated transport in the parameterization lacking a mesoscale component are less realistic. Radon transport experiments were carried out using an atmospheric GCM with a finite-difference dynamical core, the van Leer type FFSL advection algorithm, and two state-of-the-art cumulus convection parameterization schemes [5]. Differences from 6 km to the model top are even larger, although it is not clear which simulation is better due to the lack of observations at such high altitudes.

Radon is not used in recent model to model comparison after WMO intercomparison projects [11, 12]. GEMS, for example, is a scientific research project aiming to improve the way to use satellite data [29]; http://www.ecmwf.int . The project has four components, non-reactive gas like carbon dioxide, reactive gas like ozone, aerosols and prediction of air quality using regional models. Although some models used in GEMS, IFS at ECMWF and Mozart at NCAR as the examples, were evaluated using radon in the past, radon is not listed in the current evaluations. For ozone, inter-continental transport of air pollution and their precursor are compared in 21 CTMs in HTAP (UN [14]; http://www.htap.org/). The aim of the program is to share common knowledge of baseline ozone concentrations in the models. Radon was listed as a species to be studied in the planning discussions but was dropped in the recent protocol. For aerosol, intercomparison project are organized as AEROCOM [13]; http://nansen.ipsl.jusseu.fr . Because species to be simulated are too many for participants, radon was dropped in the list. For carbon dioxide, intercomparison of CTM has been conducted as TransCom (Law et al. [15]; http://purdue.edu/transcom). Radon concentrations are collected using a common source distribution. Qualitative and quantitative evaluations are

underway. A part of the results and inverse estimate of temporal variations in the emissions are reported in this meeting.

5. SURVEILLANCE

A cautious note for homogeneous emissions of radon used carelessly in model evaluations was addressed in this session of the meeting for a case of Iran. Concentration distributions over Iran were surveyed using a technique described in the study of working environment [30]. Radon concentrations at Ramsar area are significantly high and are considered to be due to high exhalation flux density there.

6. CONCLUSIONS

As a summary of the modelling section, we have recognized the following. Distributions of radon and its progeny in the convective boundary layer are well reproduced in large eddy simulations are waited for comparison with the observations. Sensitivity study of the model by targeting events may find that one flux density map is better in one situation and another map better in another situation. Global model used radon extensively in the evaluation of its components, wind and convective transport. All evaluations are premature due to lack of data on vertical profile in the tropics especially in the upper part of the troposphere while large sensitivities in the models are detected there for different components. The measurement community is becoming aware that assessing an exposure of natural radiations to resident requires mixing and transport of atmosphere. Some models estimated emission distributions using inverse calculations. Based on the above mentioned recognitions, we may recommend the following studies in the future.

6.1. Radon concentration measurements for validation of climate/weather models

- More data should be collected in the tropics on radon in air and the accompanying BLH including vertical profiles up to the tropopause.

- For the purpose of qualitative validation of boundary layer processes: (i) the location of radon concentration observations should ideally be inland far from the coast (>100 km) and over a relatively flat topography, (ii) flux density estimates are most desirable on a daily basis, taking into account factors such as soil moisture (possibly using a surrogate parameter, such as rainfall or gamma dose rate) and the effect of flooded paddy fields.

6.2. Atmospheric radon measurements for validation of the radon exhalation flux density from the soil

For the purpose of qualitative estimate of regional-scale radon flux density, radon in air observations should be recorded hourly or better, and the BLH should be measured concurrently, for example by means of a ceilometer.

6.3. Validation of climate and weather models

- Meteorological organizations should have the capability to model atmospheric concentrations of radon.

- Modellers of global transport should recognize the importance of radon measurements for qualitative validation of their models.

6.4. Data access

The use of radon by modellers could be facilitated by (i) easier access to data for the flux density source term, and (ii) easier access to radon in air concentration datasets as discussed in Session 2.

As a consequence of whole session, we have recognized the following related to the modelling activities. Atmospheric transport models from regional to global scales need improved source information. Until then it will be not possible to distinguish between model generated uncertainty and input information intrinsic uncertainty. Excellent progress has been demonstrated in the last years in pursuing this goal.

For model validation it was also felt that effort should be put in quality checking air concentration data, and to harmonize and inter-calibrate the existing monitoring techniques. Furthermore a central organization of existing data will favour the visibility of the information which most likely will be used by a yet wider community of modellers world wide. Models could contribute to the improvement of emission inventories since they can be used in inverse modality. In fact the recent developments in inverse modeling and the good results obtained for GH gases, point to the possibility of a good contribution to the emission inventory set up.

REFERENCES

[1] WORLD METEOROLOGICAL ORGANIZATION/ GLOBAL ATMOSPHERIC WATCH, 1st International Expert Meeting on Sources and Measurements of Natural Radionuclides Applied to Climate and Air Quality Studies, Report, Number 155, WMO TD **1201** (2004).

[2] OLIVIÈ, D.J.L., VAN VELTHOVEN, P.F.J., BELJAARS, A.C.M., KELDER, H.M., Comparison between archived and off-line diagnosed convective mass fluxes in the chemistry transport model TM3, J. Geophys., Res. **109** (2004), Art. No. D11303.

[3] JOSSE, B., SIMON, P., PEUCH, V.-H., Radon global simulations with the multiscale chemistry and transport model MOCAGE, Tellus **56B** (2004) 339–356.

[4] DONNER, L.J., et al., Transport of ^{222}Rn and methyl iodide by deep convection in the GFDL, Global Atmospheric Model AM2, J. Geophys. Res. **112** (2007) DOI:10.1029/2006JD007548.

[5] ZHANG, K., WAN, H., ZHANG, M., WANG, B., Evaluation of the atmospheric transport in a GCM using radon measurements; sensitivity to cumulus convection parameterization, Atmospheric Chemistry and Physics **8** (2008) 2311–2832.

[6] OLIVIÈ, D.J.L., VAN VELTHOVEN P.F.J., BELJAARS C.M., Evaluation of archived and off-line diagnosed vertical diffusion coefficients from ERA-40 with ^{222}Rn simulations, Atmospheric Chemistry and Physics **4** (2004) 2313–2336.

[7] CONSIDINE, D.B., BERGMANN, D.J., LIN, H., Sensitivity of global modeling initiative chemistry and transport model simulations of ^{222}Rn and lead-210 to input meteorological data, Atmospheric Chemistry and Physics **5** (2005) 3389–3406.

[8] RAMONET, M., LE ROULLEY, J.C., BOUSQUET, P., and MONFRAY, P., ^{222}Rn measurements during the TROPOZ II campaign and comparison with a global atmospheric transport model, Journal of Atmospheric Chemistry **23** (1996) 107–136.

[9]   KRITZ, M.A., ROSNER, S.W., STOCKWELL D.Z., Validation of an off-line three-dimensional chemical transport model using observed radon profiles I, J. Geophys. Res. **103** (1998) 8425–843.

[10] GUPTA, M.L., DOUGLASS, A.R., KAWA, R., PAWSON, S., Use of radon for evaluation of atmospheric transport models: sensitivity to emissions, Tellus Series B-Chemical and Physical Meteorology **56** 5(2004) 404–412.

[11] JACOB, D.J., et al., Evaluation and intercomparison of global atmospheric transport models using ^{222}Rn and other short-lived tracers, J. Geophys. Res. **102** (1997) 5953–5970.

[12] RASCH, P.J., et al., A comparison of scavenging and deposition processes in global models: results from the WCRP Cambridge workshop of 1995, Tellus **52B** (2000) 1025–1056.

[13] SCHULZ, M., CHIN, M., KINNE, S., The Aerosol model comparison project, AeroCom, Phase II: Clearing up Diversity, IGAC Newsletter **41** (2009) 2–9.

[14] UNITED NATIONS, Hemispheric Transport of Air Pollution 2007, Air Pollution Studies No. 16. United Nations Publ., Sales No. E.08.II.E.5 (2008).

[15] LAW, R.M., et al., TransCom model simulations of hourly atmospheric CO2: experimental overview and diurnal cycle results for 2002, Global Biogeochemical Cycles **22** (2008) GB3009, DOI: 10.1029/2007GB003050.

[16] PATRA, P., et al., TransCom model simulations of hourly atmospheric CO2: Analysis of synoptic-scale variations for the period 2002–2003, Global Biogeochemical Cycles **22** (2008) GB4013, DOI:10.1029/2007GB003081.

[17] PERRINO, C., PIETRODANGELO, A., FEBO, A., An atmospheric stability index based on radon progeny measurements for the evaluation of primary urban pollution, Atmospheric Environment **35** (2001) 5235–5244.

[18] PERRINO, C., PIETRODANGELO, A., FEBO, A., An atmospheric stability index based on radon progeny measurements for the evaluation of primary urban pollution, Atmospheric Chemistry Physics **7** (2007) 5003-5019.

[19] VINUESA, J.-F., GALMARINI, S., Characterization of the ^{222}Rn family turbulent transport in the convective atmospheric boundary layer, Atmospheric Chemistry and Physics **7** (2007) 697–712.

[20] VINUESA, J.-F., BASU, S., GALMARINI, S., The diurnal evolution of ^{222}Rn and its progeny in the atmospheric boundary layer during the Wangara experiment, Atmospheric Chemistry and Physics **7** (2007) 5003–5019.

[21] HIRSCH, A.L., On using ^{222}Rn and CO2 to calculate regional-scale CO2 fluxes, Atmospheric Chemistry and Physics **7** (2007) 3737–3747.

[22] CRAWFORD, J. et al., Receptor modelling using Positive Matrix Factorisation, back trajectories and ^{222}Rn, Atmospheric Environment **41** (2007) 6823-6837.

[23] CHAMBERS, S., ZAHOROWSKI, W., MATSUMOTO, K., UEMATSU, M., Seasonal variability of radon-derived fetch regions for Sado Island, Japan, based on 3 years of observations: 2002–2004, Atmospheric Environment **43** (2009) 271-279.

[24] ARNOLD, D., VARGAS, A., VERMEULEN, T., VERHEGGEN B., SEIBERT, P., Analysis of radon origin by backward atmospheric transport modelling, Accepted manuscript 10.1016/j.atmosenv.2009.11.003.

[25] ARNOLD, D., Study of the atmospheric radon concentration dynamics at the Spanish radiological surveillance stations and its applications to air mass movements. Unpublished doctoral dissertation, Technical University of Catalonia, Barcelona, Spain (2009).

[26] ARNOLD, D., VARGAS, A., ORTEGA, X., Analysis of outdoor radon progeny concentrations measured at the Spanish radioactive aerosol automatic monitoring network, Applied Radiation and Isotopes **67** (2009) 833–838.

[27] NISHIZAWA, M., et al., Development of Three-dimensional Numerical model for ^{222}Rn and its decay products coupled with a mesoscale meteorological model I. Model description and validation, J. Nuclear Science and Technology **44** (2007) 1458–1466.

[28] VERMEULEN, A.T., PIETERSE, G., HENSEN, A., VAN DEN BULK, W.C.M., ERISMAN, J. W., COMET: a Lagrangian transport model for greenhouse gas emission estimation– forward model technique and performance for methane, Atmospheric Chemistry Physics Discussion **6** (2006) 8727-8779.

[29] HOLLINGSWORTH, A., et al., THE GEMS CONSORTIUM, Toward a monitoring and forecasting system for atmospheric composition, The GEMS Project, Bull. American. Meteor. Soc., (2008) 1147–1164.

[30] FATHABADI, N., GHIASSI-NEJAD, M., HADDADI, B., MORADI, M., Miners exposure to radon and its decay products in some Iranian non-uranium underground mines, Radiation Protection Dosimetry **118** (2006) 111–116.

INDIVIDUAL PAPERS

^{222}RN SOURCE TERMS DERIVED FROM TERRESTRIAL GAMMA DOSE RATES

F. CONEN
Institute of Environmental Geosciences,
University of Basel,
Switzerland

Abstract

The ^{222}Rn source terms for Europe, Russian Federation and the USA were derived from existing information on terrestrial gamma dose rates and an empirical function relating it to ^{222}Rn flux density. The procedure, its application and scope for future work are described.

Motivated by the report of a similar, preceding meeting [1], we attempted during the past several years to improve the description of the ^{222}Rn source term for some major land areas. Our two main constraints were: (a) the source term should be described on a scale relevant to atmospheric research; (b) the description should be achievable with means available to us. Constraint (a) acknowledges that a spatial resolution for atmospheric applications may be coarse (e.g. $1^o \times 1^o$). This limits its usefulness to that one purpose. Application to other areas of research, such as indoor radon risk assessment, would require a much higher resolution. At the same time, constraint (a) is a relief to constraint (b). Available means for this kind of research are limited. Two successive PhD students were chiefly working towards understanding and describing ^{222}Rn flux from soils (Lynette Robertson, University of Edinburgh; Thomas Szegvary, University of Basel) and a third PhD student (Yu Xia, University of Basel) is still dealing with aspects of it. Under mentioned constraints, our approach was to identify a parameter that is somehow related to ^{222}Rn flux and for which data on large scales is already available. Inspiration came from a study published in 1989 [2], where S. Schery and colleagues had travelled around the Australian continent, measuring ^{222}Rn flux density and other environmental parameters at about 80 locations. They found that around 60% of the variation in ^{222}Rn flux density could be explained by the variation in gamma dose rate. Latter parameter is continuously measured by emergency monitoring stations in Europe (including Russian Federation and Turkey), Canada, Japan and Republic of Korea. Other countries are currently planning to install such a network (i.e. Iran). In addition, large land areas have been scanned in aero-radiometric surveys carried out by geological agencies (e.g. USA, Russian Federation, Australia, parts of Canada and South Africa). A correlation between ^{222}Rn flux density and gamma dose rate exists because both originate from radionuclides occurring naturally in all soils. The flux of gamma rays from soil, the terrestrial dose rate component, depends on soil concentrations of ^{40}K, ^{238}U and ^{232}Th. Only ^{226}Ra, a daughter product of ^{238}U, is relevant for the source strength of ^{222}Rn. However, the relative contribution of gamma rays from ^{238}U and its daughters to the total terrestrial dose rate is pretty stable (27% to 30%) across a wide range of rock types and ages [3, 4]. At large, geological structures determine the spatial pattern of radionuclide concentrations in rocks, sediments and soils and, consequently, of gamma dose rates and ^{222}Rn flux densities. Still, there are differences for various reasons. Terrestrial gamma rays originate mainly from the upper 0.1 to 0.2 m of the soil, whereas ^{222}Rn has a scale length about an order of magnitude larger. Also, ^{222}Rn flux is modulated by grain size, affecting the emanation factor and soil gas diffusivity. An increase in soil moisture reduces diffusivity, and thus ^{222}Rn flux density. Similarly, soil moisture increases shielding and a reduction in gamma rays reaching the surface. Although the direction of change is the same, the relative magnitudes are not always the same because of the different scale lengths and fundamentally different processes

involved. Despite these limitations, it has been possible to derive an empirical function describing the magnitude of ^{222}Rn flux density as a function of terrestrial gamma dose rate ($r^2 = 0.55$) [4]. The function is based on parallel measurements of both parameters at a total of about 70 locations in Switzerland, Scotland, Germany, Finland and Hungary (^{222}Rn flux density [atom cm^{-2} s^{-1}] = 11.8 · terrestrial gamma dose rate [μS h^{-1}] – 0.15). The ^{222}Rn flux density can be converted to Bq m^{-2} s^{-1}.

A major, although not un-solvable, problem in applying this function has been to extract the terrestrial component from reported total dose rates for each station of the emergency monitoring network. In fact, the European network consists of different national networks with different sensors, site characteristics, data handling and processing procedures, etc. Total dose rate is the sum of a terrestrial, a cosmic and, sometimes, an artificial component, plus the internal self-effect of the gamma dose sensor. Fortunately, at the same time as we were doing this work, there were on-going efforts to harmonise data from the different national networks within Europe that enabled us to achieve the task with available means and generous support from colleagues at the Bundesamt für Strahlenschutz, Freiburg, Germany, and the Institute of Environment and Sustainability at the Joint Research Centre of the European Commission in Ispra, Italy [5]. Furthermore, the terrestrial dose rate had to be normalised to our reference measurement height of 1 m above ground level, which we had adhered to during establishment of the empirical function. Combining our empirical function with terrestrial gamma dose rates normalised to 1 m above ground yielded a detailed ^{222}Rn source map for Europe [6]. On a $0.5^{o} \times 0.5^{o}$ grid scale, mean annual values of ^{222}Rn flux density were estimated between 0.03 and 1.76 atom cm^{-2} s^{-1}, with half of the values between 0.40 and 0.70 atom cm^{-2} s^{-1}. A mean (0.55 atom cm^{-2} s^{-1}) close to the median (0.51 atom cm^{-2} s^{-1}) indicates a close to normal distribution. Despite the patchy distribution of weak and strong source areas, the estimated map shows a decreasing trend with increasing latitude, similar to a previous, completely independent projection [7]. Large flux density values were mainly found on the Iberian Peninsula, small values along coasts and in northern and eastern parts of Europe. Predicted mean flux density for Ireland, a place where we have not made a single ^{222}Rn measurement so far, is only 4% below an estimate based on 95 direct measurements made by another working group [8]. In contrast, verification of our estimates for Spain has shown that our approach over-estimates ^{222}Rn flux by a factor of two at three of the four visited stations. This is mainly for two reasons. First, detectors in the national monitoring network are sometimes installed at a location where measured dose rates may not represent the natural terrestrial background, such as close to the wall of a building. Although this may not compromise the initial purpose of the sensor to register an increase in dose rate caused by radioactive contamination, it is no longer a useful reference for deriving an estimate of the local ^{222}Rn flux density. Dose rates a few metres above ground are much larger when measured close to a wall (brick or concrete), than when measured by a free standing sensor over open ground. Second, actual measurement height above ground level has been found to be sometimes substantially lower than reported height. Again, this is not compromising its original purpose. Yet, when normalising measurement height to 1 m above ground, we over-compensated for loss of signal with increasing height, thereby further exacerbating the problem of over-estimating ^{222}Rn flux. Inter-comparisons at several stations in Spain have shown that the emergency monitoring network (REA) tends to report larger values than those obtained by other sensors (A. Vargas, personal communication). A better representation of natural terrestrial gamma dose rates at 1 m above ground has been made during the MARNA project [9] (L.S. Quindos Poncela, personal communication). In future, we plan to replace our initial estimates of ^{222}Rn flux for Spain with new estimates based on dose rates from the MARNA project. A large advantage of using emergency monitoring data is that it contains a temporal component, allowing estimation of seasonal variations in ^{222}Rn flux density.

Seasonal variations are larger in the northern and continental parts of Europe with a more pronounced seasonality in soil moisture. Seasonal amplitudes are smaller in the South and in regions with marine influence [6]. Hence, the loss of information through using a static estimate of dose rate in Spain will be limited.

Where gamma dose rates are derived from aero-radiometric surveys, static estimates of ^{222}Rn flux are, in principle, possible. Preliminary maps have been produced for the USA and for Russian Federation [10] (data available at: http://radon.unibas.ch). Here, a problem has been met with the application of above mentioned empirical function. It manifested itself in a step change at the border between the initial Russian and the European ^{222}Rn flux map. Most likely this has to do with the reference height of dose rates in the Russian map not being the height assumed by our function. In absence of other evidence, the estimated ^{222}Rn fluxes were divided by a chosen factor to minimise differences along the common border. For obvious reasons, the same procedure was not possible for adjusting estimates for the USA. Here, further assumptions had to be made. These assumptions were (a) no negative ^{222}Rn fluxes, (b) a mean flux of 0.87 atom cm^{-2} s^{-1} as derived from atmospheric inventories of ^{222}Rn and ^{210}Pb deposition flux [11] and (c) a similar coefficient of variation in fluxes as in Europe. Unlike the estimates for Europe, those for Russian Federation and the USA are less well supported by direct evidence. However, a likely advantage of spatial information from aero-radiometric surveys on large territories is that the data has probably been obtained with the same instruments and methods. If so, relative differences between regions are accurate and areas with larger or smaller ^{222}Rn flux densities can be identified with good confidence.

There is scope for further work. In Europe, harmonisation of radiation monitoring networks is still on-going. It may in future provide more detailed information on site characteristics, so that stations where measurements are not representative of the natural background can be excluded from estimating ^{222}Rn flux density. Also, information on the terrestrial component of gamma dose rates may become directly available to the scientific community through a web interface. Ease of access to this data is a prerequisite for it being used in environmental studies outside their initial purpose of emergency monitoring. While we think the spatial variation in ^{222}Rn flux density is well described by above mentioned empirical relation with gamma dose rate, we are not so sure about its applicability to temporal variations. To clarify the issue, more longterm parallel measurements of both parameters at a range of sites are currently being conducted. A difficult issue, where we have not found a solution so far, is the measurement of ^{222}Rn flux through deep snow. Another issue is flux estimates for regions where we have no information so far. There, it might be possible to find in archives aero-radiometric surveys carried out by geological agencies or companies. These could be used to add spatial structure to a global average of ^{222}Rn flux derived from atmospheric ^{222}Rn and ^{210}Pb inventories.

REFERENCES

[1] WORLD METEOROLOGICAL ORGANISATION, 1st International expert meeting on sources and measurements of natural radionuclides applied to climate and air quality studies, WMO TD No. 1201 (2004).

[2] SCHERY, S.D., WHITTLESTONE, S., HART, K.P., HILL, S.E., The flux of radon and thoron from Australian soils, Journal of Geophysical Research **94** (1989) 8567–8576.

[3] FRANKE, J., Flächenhafte Analyse der Zusammenhänge zwischen geologischem Untergrund und terrestrischer Radioaktivität mit Hilfe von GIS und Geostatistik. MSc Thesis, University of Hannover (2002).

[4] SZEGVARY, T., LEUENBERGER, M., CONEN, F., Predicting terrestrial ^{222}Rn flux using gamma dose rate as a proxy, Atmospheric Chemistry and Physics **7** (2007) 2789–2795.

[5] SZEGVARY, T., et al., Mapping terrestrial -dose rate in Europe based on routine monitoring data, Radiation Measurements **42** (2007) 1561–1572.

[6] SZEGVARY, T., CONEN, F., CIAIS, P., European ^{222}Rn inventory for applied atmospheric studies, Atmospheric Environment **43** (2009) 1536–1539.

[7] CONEN, F., ROBERTSON, L., Latitudinal distribution of ^{222}Rn flux from continents, Tellus **54B** (2002) 127–133.

[8] JENNINGS, S.G., CIAIS, P., BIRAUD, S., RAMONET, M., Environmental RTDI Programme 2000-2006, Irish Greenhouse Gas Emissions, Final Report, Technical Report, Environmental Protection Agency, Ireland.

[9] QUINDOS PONCELA, L.S., et al., Natural gamma radiation map (MARNA) and indoor radon levels in Spain, Environment International **29** (2004) 1091-1096.

[10] SZEGVARY, T., European ^{222}Rn flux map for atmospheric tracer applications, PhD thesis, University of Basel, Switzerland (2007).

[11] PILIPOSIAN, G.T., APPLEBY, P.G., A simple model of the origin and transport of ^{222}Rn and ^{210}Pb in the atmosphere, Continuum Mechanics and Thermodynamics **15** (2003) 503–518.

MEASUREMENTS OF RADON EXHALATION FLUX AND ATMOSPHERIC RADON IN URANIUM MINING AND PROCESSING SITES

G. GNONI, M. PALACIOS
Autoridad Regulatoria Nuclear,
Buenos Aires,
Argentina

Abstract

The Nuclear Regulatory Authority (ARN) performs an environmental monitoring of areas around the different nuclear facilities. This environmental monitoring involves a periodical sampling and analysis in the areas surrounding the operating and decommissioned facilities for the mining and milling of uranium ores. This monitoring implies the sampling and measurements of natural uranium and ^{226}Ra levels in surface waters, sediments and ground waters in each surrounding area. Moreover, radon exhalation flux measurements from uranium mill tailings and radon concentration in air are performed. Radon exhalation rate measurement is performed by activated charcoal adsorption followed by gamma spectrometry. In the case of radon gas measurements in air, they are carried out by several methods, mainly by nuclear track detectors (Makrofol and CR-39).In this work, the results related with radon exhalation flux measurements and radon concentration in air are presented and discussed. In addition, a full description of the methods used is presented.

Introduction

The Nuclear Regulatory Authority (ARN) performs environmental monitoring around the different nuclear facilities. This environmental monitoring involves a periodical sampling and analysis in the areas surrounding the operating and decommissioned facilities for the mining and milling of uranium ores and conversion facilities. The Uranium industry began its development in Argentina in 1950. Since then, several installations have operated in uranium underground mining until the late 70s, when open pit exploitation mining became the main production process. Milling plants were installed in the mining areas or nearby. The monitoring of these areas implies the sampling and measurements of natural uranium and ^{226}Ra levels in surface waters, sediments and ground waters in the influence area once a year. Moreover, radon exhalation flux and radon concentration in air measurements from uranium mill tailings are performed, as the ore tailings represent important release sources of radon gas into the atmosphere. Radon release is one of the main concerns regarding the environment in the vicinity of uranium mining and milling areas.

The routine monitoring is conducted at the following operating uranium facilities:

Facility A: it is a decommissioned uranium ore milling plant, nowadays is an operating uranium dioxide conversion plant.

Facility B: this facility is a mining and milling plant that nowadays is interrupted, but it is not decommissioned.

The environmental monitoring is also performed in the following decommissioned uranium facilities:

Facility C: milling plant.

Facilities D, E, F, G and H: mining and milling plants.

The objective of this work is to present and discuss the results arising from the radon exhalation flux and radon concentration in air measurements in the areas surrounding uranium facilities. A full description of the methods used is also presented.

Materials and methods

Radon exhalation flux

Radon exhalation flux measurements are performed using a technique described by Countess [1]. In this technique cans containing activated charcoal are placed on the ground for a known period of time, and the activity of radon adsorbed by the charcoal is subsequently measured by gamma spectrometry. This method is largely independent of the effects of atmospheric pressure, temperature and humidity during the exposure [2]. Each can (10 cm diameter, 1 dm^3 of capacity) contains a standard quantity of activated charcoal (70–75 g), held in its bottom by a filter followed by a metallic mesh. Before any radon exposure begins, the device is heated with its opening end up, for at least 3 hours at about 120°C. As soon as the heating is finished, cans are sealed with plastic caps. Once in the monitoring site the cap is removed, and the can is screwed into the ground to a depth of a few millimeters. The total number of cans needed to evaluate the area is located all over the tailing zone following a grid layout. The sampling period is generally below 36 hours, in order to achieve complete radon adsorption. Once the exposure period is finished, the cans are picked up and immediately resealed with their plastic caps. Then they are left for a period of three hours to allow the radon daughters to reach equilibrium with its parent radon gas. Counting is carried out inside a lead-brick shield to reduce the background from external radiation. A 3" × 3" NaI(Tl) crystal detector probe is placed directly onto the base of the upturned can. The ^{214}Bi peak (609 keV) is then quantified once the equilibrium between radon and its progeny is reached. This peak is chosen because of its clear separation from other emission lines and the generally low background at energies to either side of it. Before the measurements are carried out, a background counting and efficiency factor are performed. The blank counting is measured with the empty detector, under exactly the same conditions as the exposed cans are measured. The efficiency factor is determined with a can prepared exactly as the exposed cans, but it is sealed and contains a known quantity of a standard radium source.

The radon exhalation flux measurement is calculated by the following equation (Eq. (1)):

$$E = \frac{C \cdot \lambda^2}{K \cdot A \cdot \varepsilon \cdot \left(1 - e^{-\lambda t_1}\right) \cdot \left[e^{-\lambda (t_2 - t_1)} - e^{-\lambda (t_3 - t_1)}\right]} \tag{1}$$

E = radon exhalation flux (Bq m^{-2} s^{-1})

C = net counts integrated under the peak of 609 keV from ^{214}Bi

λ = decay constant of ^{222}Rn (2097×10^{-6} s^{-1})

A = can area (m^2)

ε = efficiency factor (counts / disintegrations)

K = conversion factor (1 disintegration s^{-1} Bq^{-1})

t_1 = exposure time (s)

t_2 = time from the beginning of the sampling period till the beginning of the measurement (s)

t_3 = time from the beginning of the sampling period till the end of the measurement (s)

Radon gas concentration in air

Regarding radon gas measurements in air they are carried out by nuclear track detectors, Makrofol or CR-39. Both measuring devices are shown in Figure 1. These detectors can be exposed between two and three months. [3–7]. During a monitoring campaign, the measurement devices are located around the tailing area at a height of 1.5 m.

FIG. 1. Nuclear track detectors: CR-39 (left) and makrofol (right).

CR-39 is an acrylic material and determines only the average radon concentration during the exposure period of time. On the other hand, Makrofol type E is a polycarbonate material, that measures both radon concentration and the equilibrium factor (F) between radon and its daughters, since the "Big Cup device" uses two Makrofol sheets in the same device, as it is shown in Figure 2.
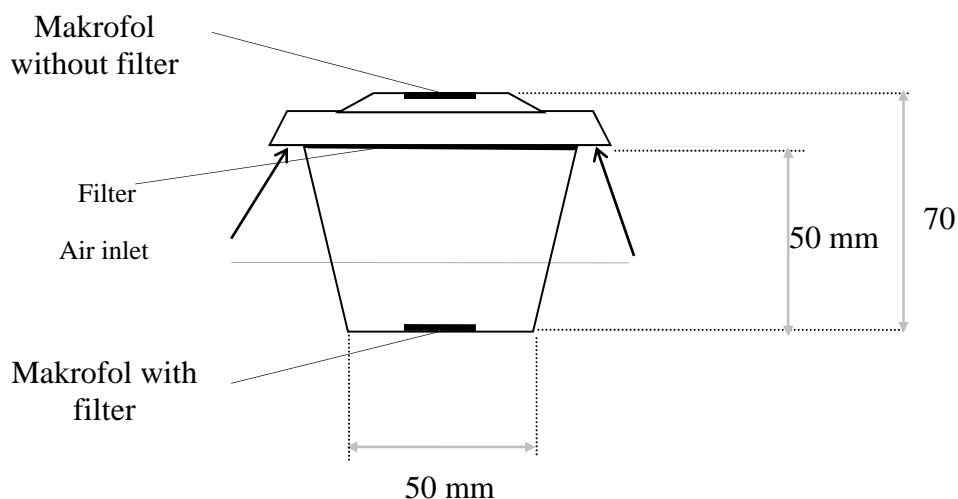
FIG. 2. Makrofol monitor used for determining radon gas concentration and equilibrium factor F.

This method was developed by the ARN radon laboratory in 2000 [8], in order to determine the equilibrium factor value, which otherwise is assumed as 0.4 as recommended by international organizations [9]. Once the exposure period finished, the Makrofol sheets are

revealed with an electroetching process, while CR-39 is revealed by chemical etching and evaluated in a microscope.

Time integrated methods give a more representative value of the radon average concentration. In addition, these detectors are resistant and inexpensive, both conditions necessary for campaigns where a large number of outdoors places have to be evaluated.

The devices are calibrated in a 1 m^3 acrylic reference chamber where controlled conditions of humidity, temperature and radon concentrations can be maintained. The lowest detection limit for CR-39 varied from 2 to 5 Bq m^{-3}, while for makrofol was between 5 and 15 Bq m^{-3}.

Results

The results related with the measurements of radon exhalation flux and radon concentration in air in the facilities for the mining and milling of uranium ores and conversion facilities are presented in this section.

Facility A

In Figure 3, average radon exhalation flux values measured at facility A, in each monitoring campaign are shown. From 1997 to 2009, a total of 19 campaigns have been performed. From 2006, the radon exhalation flux measurements frequency was settled annually. A total of about 40 cans are located in the interest area in every campaign. The values found varied from background levels to 85.7 Bq m^2 s^{-1}, the highest value measured.
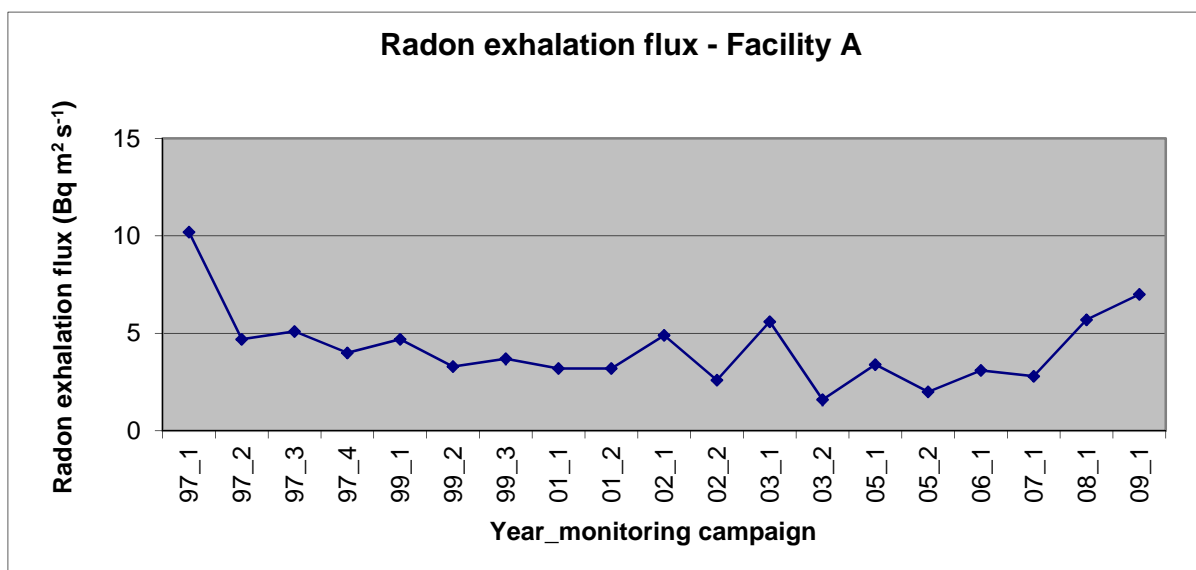
FIG. 3. Radon exhalation flux values measured at facility A in different monitoring campaigns.

The average values of radon concentration in air measured in each campaign in Facility A are shown in Figure 4. Every three months, radon concentration in air is measured in the tailing area, with a total of 15 measuring devices. It is important to remark that this facility is located right in the middle of city. This is the reason of the more frequent control performed both in radon exhalation flux and radon concentration in air. From 1998 to 2008, a total of 26 monitoring campaigns have been performed. Solid state nuclear track detectors (CR-39 or makrofol) were employed to measure radon concentration in air. In the case of makrofol

detectors, the equilibrium factor (F) between radon and its daughters was also determined. This type of detector was used in 8 campaigns. The concentration radon values determined in all the campaigns varied from 6.3 to 234.4 Bq m^{-3}. The average equilibrium factor determined was 0.56, ranging from 0.30 to 0.70.
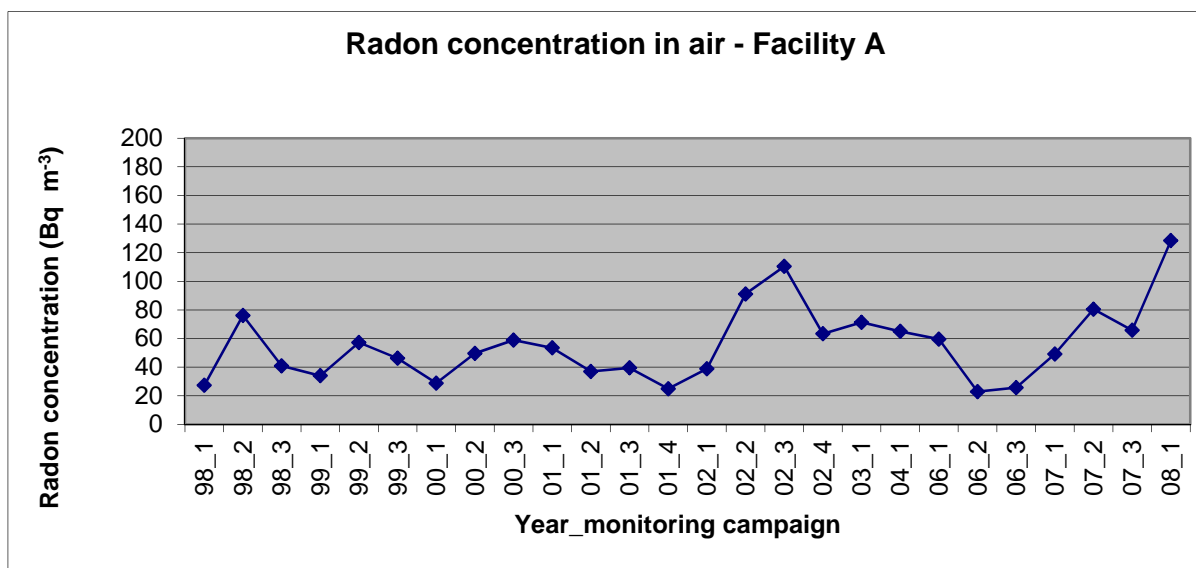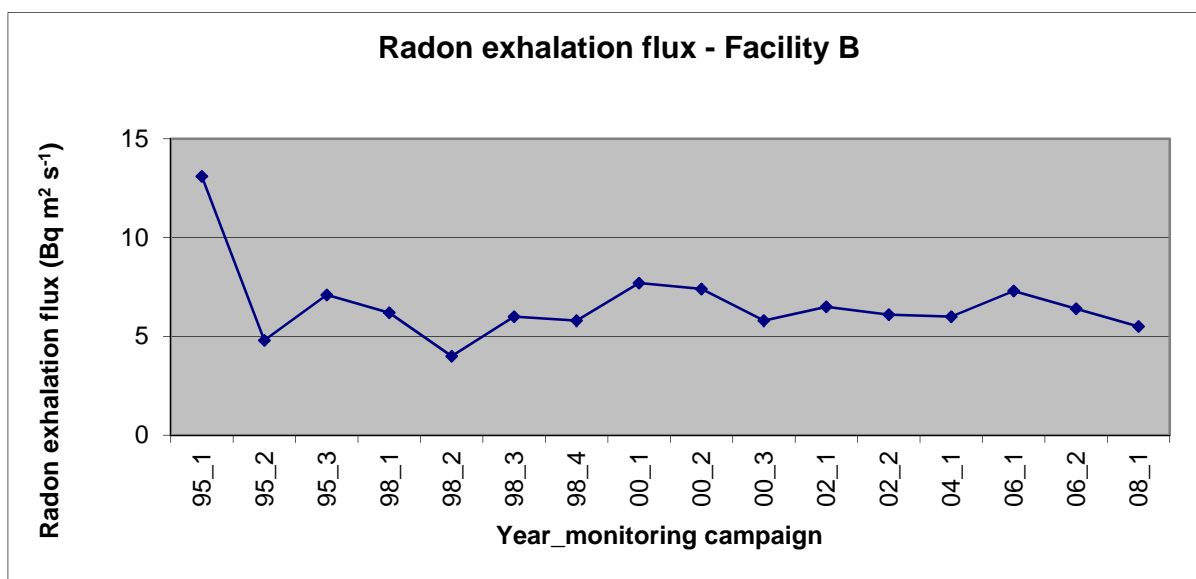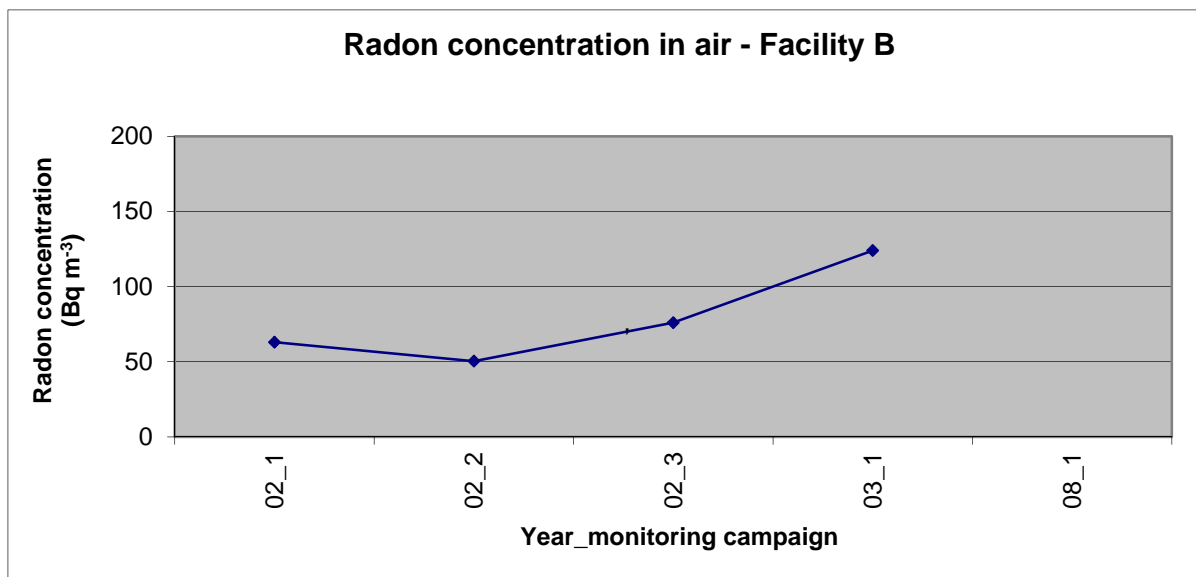

FIG. 4. Radon concentration in air at facility A in different monitoring campaigns.

Facility B

In Figure 5, the average radon exhalation flux values measured at facility B in different monitoring campaigns are shown. From 1995 to 2008, a total of 16 campaigns have been performed. Monitoring campaigns are carried out every two years. A total of about 38 cans are located in the interest area in every campaign. The values varied from background levels to 71.1 Bq m^2 s^{-1}, the highest value measured.

FIG. 5. Radon exhalation flux values measured at facility B in different monitoring campaigns.

The average values of radon concentration in air measured in each campaign in Facility B are shown in Figure 6. Radon concentration measurements in air in the tailing area were performed during 2002 and 2003, and since 2008 it was decided that this assessment will be performed once a year. It is important to evaluate radon concentration in air as this facility is located near the city, and it could be reopened in the future. A total of 25 measuring devices are employed in every campaign. Solid state nuclear track detectors were employed to measured radon concentration in air, with CR-39 or makrofol. The concentration radon values determined in all the campaigns varied from 23.0 to 386.0 Bq m^{-3}.

FIG. 6. Radon concentration in air at facility B in different monitoring campaigns.

Facility C

The average radon exhalation flux measured at facility C in different monitoring campaigns are shown in Figure 7. From 1998 to 2009, a total of 32 campaigns have been performed. From 2005, the radon exhalation flux measurements frequency was settled annually. It is important to evaluate exhalation flux as this facility is located next to the city. Though radon concentration in air is not measured in this facility, a number of dwellings in the city next to the plant are evaluated twice a year. A total of about 44 cans were located in the interest area in every campaign. The values found varied from background levels to 42.7 Bq m^2 s^{-1}, the highest value measured.
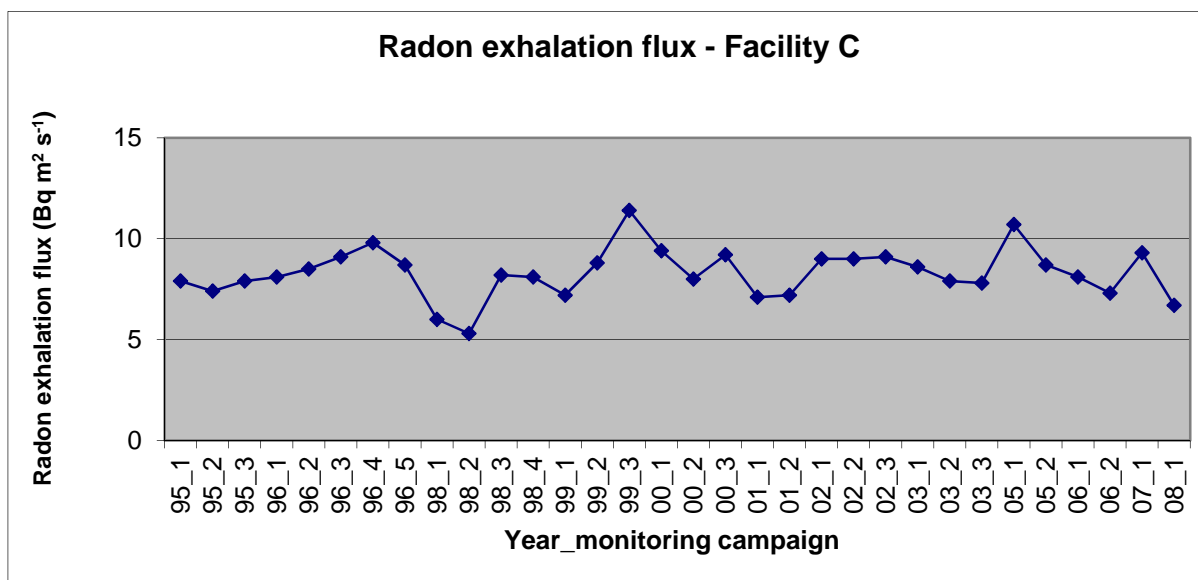
FIG. 7. Radon exhalation flux values measured at facility C in different monitoring campaigns.

Facility D to H

In Figures 8 to 12, radon exhalation flux values measured at facilities D to H in different monitoring campaigns are shown. As all these facilities are decommissioned facilities, since 2002 the monitoring campaigns frequency has been established every five years.
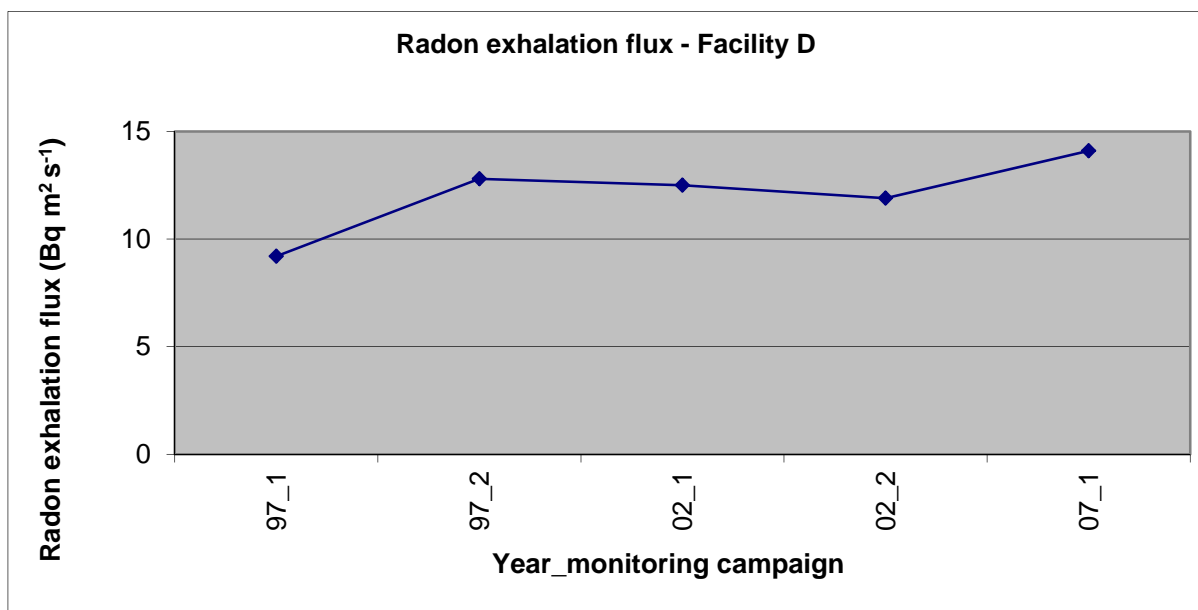

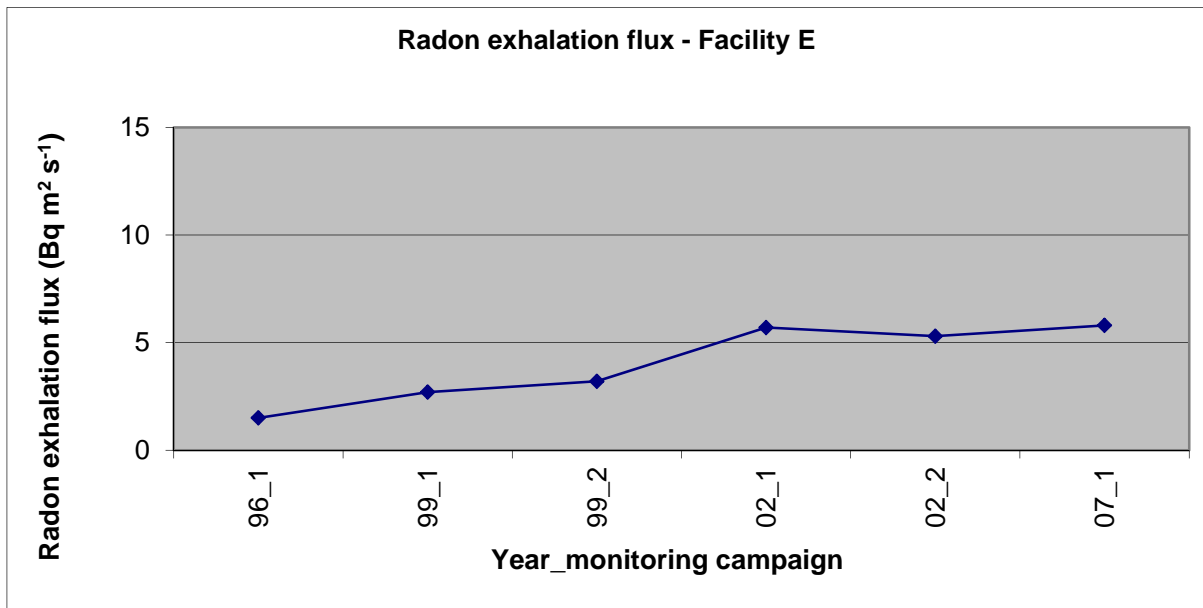FIG. 8. Radon exhalation flux values measured at facility D in different monitoring campaigns.

FIG. 9. Radon exhalation flux values measured at facility E in different monitoring campaigns.

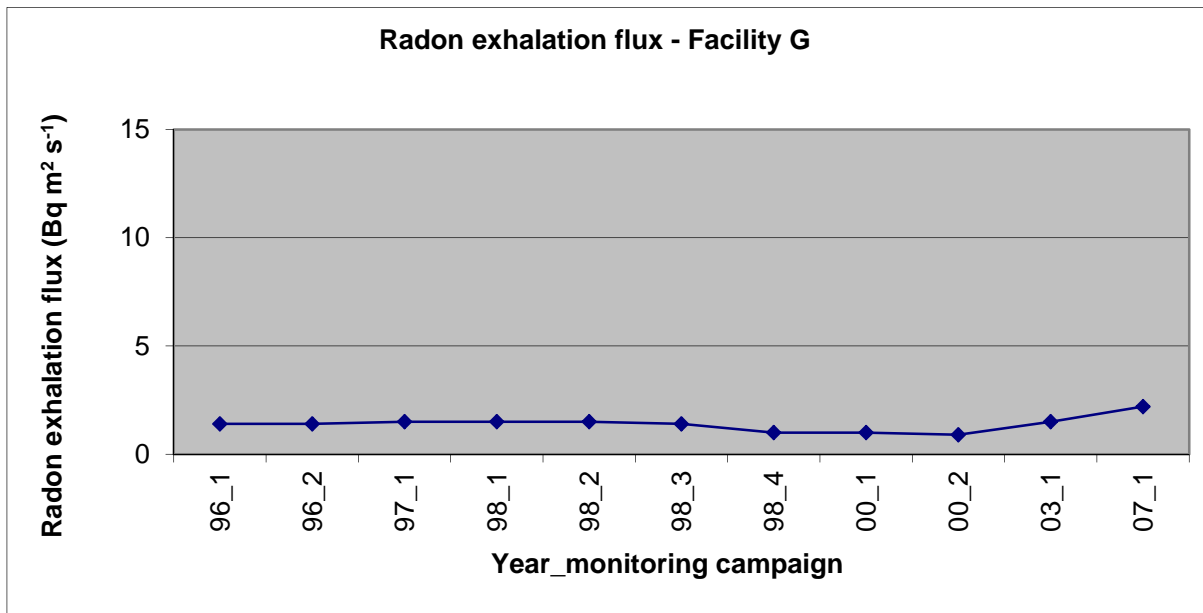*FIG. 10. Radon exhalation flux values measured at facility F in different monitoring campaigns.*

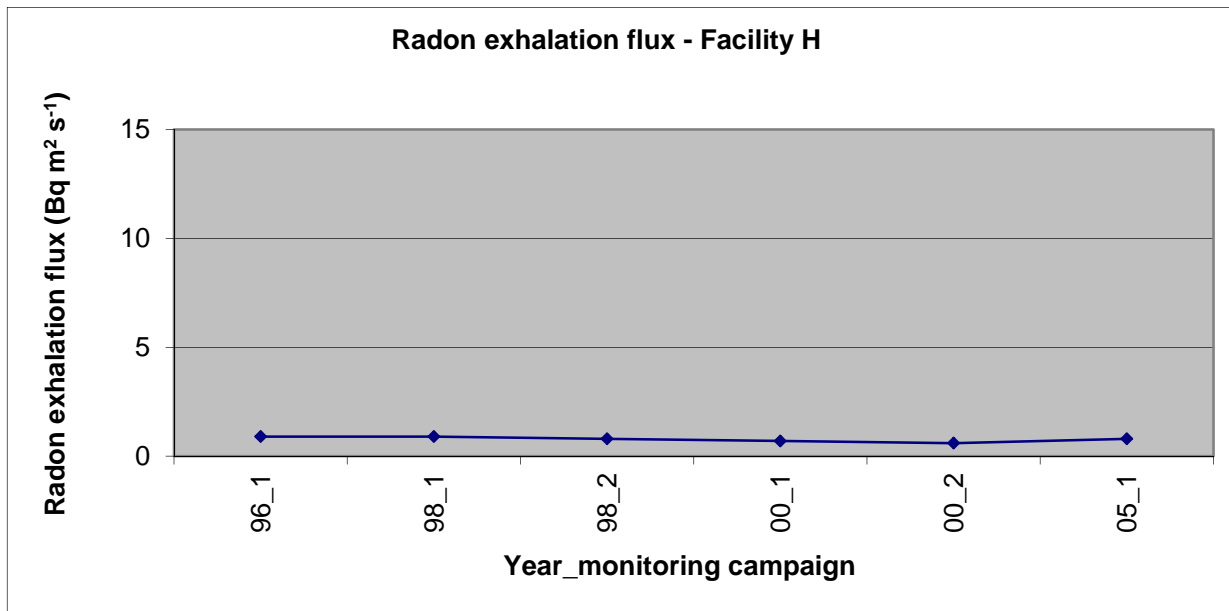*FIG. 11. Radon exhalation flux values measured at facility G in different monitoring campaigns.*

FIG. 12. Radon exhalation flux values measured at facility H in different monitoring Campaigns.

Conclusions

The results of the radon environmental monitoring around the different nuclear facilities, show that the measured values of radon exhalation flux and radon concentration in air do not present an increasing trend.

As there are no international recommendations or guidance values regarding radon exhalation flux, the results obtained from the different monitoring campaigns in each facility are analyzed considering their evolution over time. The absence of abrupt changes in the values may suggest that the actions taken to provide stabilization and isolation of the tailings are adequate so far.

There are no recommendations or guidance values regarding radon concentration outdoors either, but in this case we can compare with the criteria adopted by ICRP [9] for dwellings. The ICRP chooses an action level for annual effective dose in the 3–10 mSv range. The corresponding rounded value of radon concentration is about 200–600 Bq m^{-3}, with an annual occupancy of 7000 hours and an equilibrium factor of 0.4. It can be seen that all the average values obtained in the different campaigns for facility A and B are below the lower limit of this range. Nevertheless, it is important to remark that for indoors an occupancy factor of 0.8 (7000 hours) is applied, while the outdoor factor occupancy should be of 0.2.

It is also important to point out that there is a project for remedial actions in uranium mining and milling sites in Argentina. In this project, methods for the disposal and clean-up of residual materials associated with the facility will be selected and performed. This will provide for long-term stabilization and isolation to protect public health and the environment. This plan will take into account the results of site characterization studies, and environmental, impact and engineering assessments. The first step of this project is being carried out in Facility C, and the following steps are thought to be done in facilities A, F and H. As soon as the implementation of the plan begins, the monitoring programme will verify the effectiveness of the remedial actions applied.

Statistical analysis and modelling of the different scenarios will be implemented as future actions.

Acknowledgements

REFERENCES

[1] COUNTESS, R.J., Measurements of ^{222}Rn Flux with Charcoal Canisters. Health Phys. **31** (1976) 455.
[2] CHESNEY MASON, G., ELLIOT, G., TIANG HONG GAN, A Study of Radon Emanation from Waste Rock at Northern Territory Uranium Mines. Australian Radiation Laboratory, ARL/TR044, May 1982.
[3] URBAN, M., BINNS D.A.C., ESTRADA, J.J., Radon Measurements in Mines and Dwellings, KfK, 3866 CNEN 1101, (1985).
[4] URBAN, M., Nuclear Tracks **12** (1986) 685.
[5] AL-NAJJAR, S., OLIVEIRA A., PRIESCH E., Radiation Protection Dosimetry **27** (1989) 5.
[6] DÖRSCHEL, B., PRIESCH, E., Radiation Protection Dosimetry **54** (1994) 41.
[7] KHAN A., QURESHI, I., TUFAIL, M., Passive Dosimetry of Radon and its Daughters Using Solid State Nuclear Track Detectors (SSNTDs), Radiation Protection Dosimetry **46** (3) (1993) 149–170.
[8] LÓPEZ F.O., CANOBA, A.C., Passive method for the determination of the equilibrium factor between ^{222}Rn gas and its short period progeny, Journal of Radioanalytical and Nuclear Chemistry **258** 2 (2003) 269–274.
[9] ICPR 65 Protection Against ^{222}Rn at Home and at Work **23** 2 (1993).

QUALITY STUDY OF ELECTRET RADON FLUX MONITORS BY AN "IN SITU" INTERCOMPARISON CAMPAIGN IN SPAIN

C. GROSSI, A. VARGAS, D. ARNOLD
Institute of Energy Technologies (INTE),
Technical University of Catalonia Barcelona,
Spain

Abstract

Radon is nowadays used as a tracer for atmospheric transport model validation because of its physical and chemical characteristics. ^{222}Rn source term characterization becomes necessary for more accurate validations into the current non-stopping progression of atmospheric dispersion model development. Direct measurements of radon exhalation flux density are carried out in order to obtain a reliable map with required spatial and temporal resolutions. To measure radon exhalation flux density, the INTE (UPC) institute uses an integrated electret ionization chamber (EIC) system, also known as electret radon flux monitors. Different configurations of this device have been developed by the manufacturer and used in a comparison campaign held in the summer of 2008. In the comparison campaign, of radon exhalation flux density, measurement was carried out at four locations of the eastern Spain. The electret radon flux monitors response in different soils and with different environmental conditions was analyzed. The different electret radon flux monitor chambers show coherent results in comparison to the other integrated and continuous radon flux systems which also participated in the campaign.

Introduction

^{222}Rn is one of the radioactive daughters of ^{238}U, which is always present in soil and rocks with different concentrations. Being a noble gas, ^{222}Rn can migrate through soil pores and be finally released into the atmosphere without interacting with other chemical species during its pathway. It is liberated from the soil with variable rates, depending on soil characteristics and on external environmental parameters.

Radon gas is nowadays used as a tracer for atmospheric transport model validations because, as it is an inert gas, its concentration in air is uninfluenced neither by wet or dry depositions nor by any other chemical processes. Radioactive decay is the only removal process. Another advantage of using radon as a tracer is that it is natural occurring and it is continuously exhaled into the atmosphere. Thus, its application avoids the use of artificial releases for model validation purposes.

Besides its usefulness in atmospheric sciences, radon exhalation rate estimates also provide basic information to characterize radon-prone areas for radioprotection aims.

Thus, it is clear that the ^{222}Rn source term characterization from the land surface becomes necessary for more accurate validations into the current non-stopping progression of atmospheric dispersion model development.

Many studies have been done and are still continuing to improve ^{222}Rn source estimation according to spatial and temporal variations [1]. The scientific community is now working on developing a radon source term map which would supply input data for atmospheric transport modelling at global and local scales. Simultaneously, research for improving both integrated and continuous methods, to directly measure radon flux, is being pursued.

In this study the quality of different integrated Electret Ion Chamber (EIC) monitor geometries has been analysed. The EIC are integrated devices which are able to measure

radon exhalation from the sampled soil directly "in situ". These are commercial E-Perm instruments by the Rad. Elec. Inc. Company.

In order to compare EIC performance with other direct radon exhalation flux density measurement methods, a joint comparison campaign has been carried out in Spain [2] by the Institute of Energy Technology (INTE) of the Technical University of Catalonia (UPC), Basel University and Huelva University (UHU).

Direct methods for radon flux estimations

Development of atmospheric dispersion models has progressed to a point where improved knowledge of the ^{222}Rn source term becomes necessary for more accurate validation [1]. In spite of sufficient understanding of the theoretical processes controlling the release of ^{222}Rn from soil to the atmosphere [3], quantification of radon exhalation flux density and its distribution over the earth is still lacking because of a lack of direct and extensive ^{222}Rn exhalation flux density measurements in many regions.

Direct measurements of ^{222}Rn exhalation flux density are made using the accumulation method which allows radon gas to accumulate and to be measured in a chamber placed over the soil. Likewise, radon exhalation flux density can be directly measured both by integrated and continuous instruments which are based on the well-known accumulation method by Morawska [4]. This method is based on the accumulation of the ^{222}Rn emitted from the sampled soil surface in a known volume monitor during a time period (T). Temporal variation of the ^{222}Rn concentration in the chamber is expressed as follows (Eq. (1)):

$$\frac{dC(t)}{dt} = \frac{E_{Rn}}{V_u} - \lambda^0 C(t),$$ (1)

where C(t=0) = 0 is the initial Rn concentration (Bq m^{-3}); E$_{Rn}$ is the exhalation velocity, defined as the ^{222}Rn gas leaving the soil per time unit (Bq h^{-1}); V$_u$ is the available chamber volume (m^3) and the constant $\lambda^0 = \lambda + \lambda^*$ (h^{-1}) is given by the sum between the ^{222}Rn decay (λ) and the ventilation constant (λ^*). λ^* quantifies the possible changes between the air inside the monitor with external air due to volume leaks. Another physical factor which should be taken into account in ^{222}Rn accumulation is the so-called back-diffusion, which accounts for the possibility of ^{222}Rn being adsorbed back from the soil surface. This last factor is not significant for short-time measurements as applied in our analysis [10]. The solution of Eq. (1) is Eq. (2):

$$C(t) = \frac{E_{Rn}}{\lambda^0 V_u} (1 - e^{-\lambda^0 t})$$

(2)

The value $E_{Rn}\lambda^{0^{-1}}V_u^{-1}$ (Bq m^{-3}) is the saturation concentration value exhaled in the air-tight chamber after almost 20 days. In the case of short-time measurements and negligible leakages in the chamber, $\lambda^0 t \ll 1$ can be assumed.

Continuous monitor for radon exhalation flux density measurements are based on the simplification of Eq. (2) by developing the exponential, leading to Eq. (3):

$$C(t) = \frac{E_{Rn}}{V_u} t = \frac{F \cdot A}{V_u} t .$$

(3)

This gives a linear relation between the ^{222}Rn concentration in the chamber and time. F (Bq m^{-2} s^{-1}), is the ^{222}Rn exhalation flux density, A, the surface area covered by the accumulation chamber and V the available volume for the gas diffusion inside the monitor.

With integrated monitors for radon exhalation flux density measurement, F is calculated using the average ^{222}Rn concentration (Eq. (3)) inside the chamber over a given time T calculated by Eq. (4):

$$C(Rn)Av = \frac{1}{T}\int_0^T C(t)dt = \frac{E_{Rn}}{\lambda^0 V_u}\left[1 - \left(\frac{1 - e^{-\lambda^0 T}}{\lambda^0 T}\right)\right] = \frac{FxA}{\lambda^0 V_u}\left[1 - \left(\frac{1 - e^{-\lambda^0 T}}{\lambda^0 T}\right)\right]$$

(4)

The integrated electret ion chamber

^{222}Rn concentration in the chamber can be estimated after a given time period by integrated and passive EIC monitors. These are commercial monitors which allow measurement of the radon concentration inside a closed chamber. The monitor works as an integrating ionization chamber. The radon gas exhaled from the soil enters directly into the chamber through a Tyvek window. Inside the chamber, radon decays and the resulting ionized air discharges the positive electret voltage (700 V), which is located on the top of the monitor. The voltage drop during a measurement time (T) is proportional, by a calibration factor [7], to the radon concentration inside the chamber.

During the radon exhalation flux density measurement, completely sealed EIC monitors are used to obtain the background contribution. The sealing of the device prevents air infiltration inside the chamber, and the discharging of the electret on the top is then just due to the

environmental gamma radiation, which is considered to be the background contribution to the measurements. The background contribution is subtracted to calculate net flux result.

The sensitivity and the dynamic range of the radon exhalation flux density monitors depend on the thickness of the electret and on the chamber volume. Several combinations of electret and chambers are available. A single device scheme is illustrated in Figure 1, with a short-term ST, electret and a hemispherical chamber of 960 ml volume, H, in the so-called HST configuration.

This EIC monitors are quite inexpensive and different monitors simultaneously can be used during a measurement campaign at each site in order to get more accurate measurements. Furthermore, the voltage drop is easily measured by a portable voltage reader. The commercial availability of the stable electrets of different thicknesses, suitable chambers and a low-cost electret voltage reader has made it practical to have a viable EIC system.

Electret ion chambers (EIC) have been used for the measurement of gamma radiation since 1978 [7]. This method has not been widely used, however, because of the possible errors introduced by environmental factors such as temperature and humidity on the electret stability. These problems have been solved [8].
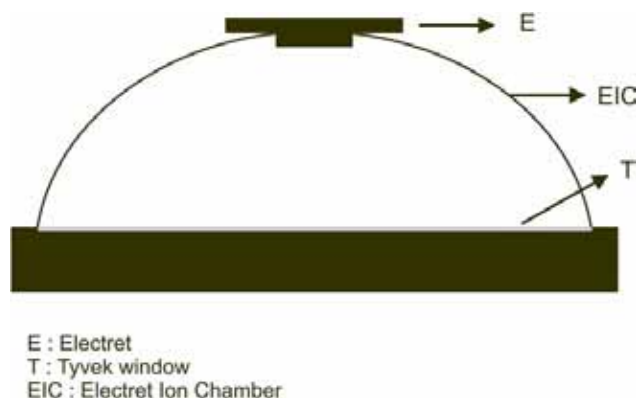

E : Electret
T : Tyvek window
EIC : Electret Ion Chamber

FIG. 1. Scheme of an Electret Ion Chamber on the soil surface.

EIC monitors are available with two different geometries. The scheme illustrated in Figure 1 needs to be placed directly on the top of the soil surface. In this case a paper towel has to be located under the monitor to prevent the Tyvek filter being contaminated by the soil. Another prototype monitor has been equipped with an aluminium collar, as is shown in Figure 2, which should, in principle, facilitate the installation of the monitor within the soil and avoid filter contamination by some stops.

The radon concentration after a time T is measured by the electret ion monitors using equation (4), where the exponential concentration increase is compensated by the radon decay and possible chamber leaks. This last factor has a non-negligible contribution to the device reliability. The ventilation constant for the EIC monitors has been certified to be equal to zero by the manufacturer [7].

FIG. 2. Radon Flux monitors with aluminium collars for in-soil installation [7].

Intercomparison campaign for EIC monitor quality study

Electret ion chamber consistency was observed under different environmental conditions and for different soil types. Additionally, the EIC monitor results have been compared with other direct methods within an intercomparison campaign. This measurement campaign has been carried out at four Spanish sites: Teruel, Los Pedrones, Quintanar de la Orden and Madrid in summer 2008 [2].

Continuous measurement devices such as the AlphaGUARD (Genitron Instruments GmbH, Frankfurt, Germany) and the Sun Nuclear model 1027 have been used for radon exhalation flux density measurements by Basel and the Huelva University, respectively. In these monitoring devices, the ^{222}Rn activity concentration is accumulated inside a closed volume, placed on the sampled soil surface, and it is then continuously measured by alpha spectrometry.

The AlphaGUARD monitor is placed near the accumulation volume chamber. The sampling air is pumped inside the monitor and concentration values are provided for each 10-min interval. A small 1-litre plastic bottle is used to prevent aerosols and ^{220}Rn from entering the AlphaGUARD [9] and [13].

The Sun Nuclear monitor is located directly inside the accumulation volume and the radon flux is measured by ^{218}Po (6 MeV) alpha spectrometry [12].

Integrated activated charcoal detectors have also been used for radon exhalation flux density measurements in the campaign study. These monitors are based on ^{222}Rn adsorption on activated charcoal [6]. The charcoal is placed on the soil surface to accumulate ^{222}Rn over a time period T. ^{222}Rn is then determined through γ spectrometry [6] of its progeny, ^{214}Pb (295 keV and 352 keV) and ^{214}Bi (609 keV) which are in secular equilibrium with radon.

Finally, the two different EIC monitor geometries described in the previous section were used in the present work. Particularly, three monitors in the HST configuration and with aluminium collars, two monitors in the HST configuration and without aluminium collars and three background monitors were used at each campaign site.

During the campaign, the atmospheric temperature and relative humidity conditions ranged from 20ºC to 35ºC and from 35% to 60%, respectively.

Results for the EIC detectors in the intercomparison campaign in eastern Spain

Figure 3 shows the radon exhalation flux density result, measured at each site by the five different EIC monitors. Results at each of the sites are in agreement and they fall into one-sigma. Radon exhalation flux density measurements done by EIC monitors with aluminium collars (C1, C2 and C3) seem to be slightly less stable than others made by monitors without collars (1, 2), maybe due to some volume definition error at the soil installation.

The weighted average value of EIC monitor results compared with radon exhalation flux density results from other integrated and continuous direct methods is presented in Figure 4. EIC monitors (vertical and green bar) show good agreement with the charcoal integrated system (pointed and red bar) and with the continuous monitors Sun Nuclear (pointed and blue bar) and AlphaGUARD (diagonal and white bar). A coefficient of variation between 10% and 23% was calculated between the two monitors. This value is in accordance with the 34% found in previous studies [10].

FIG. 3. Radon exhalation flux density results at Teruel (blue), Quintanar de la Orden (red), Los Pedrones (green) and Madrid (black) by EIC monitors with aluminium collars (C1, C2 and C3) and without collars (1, 2).
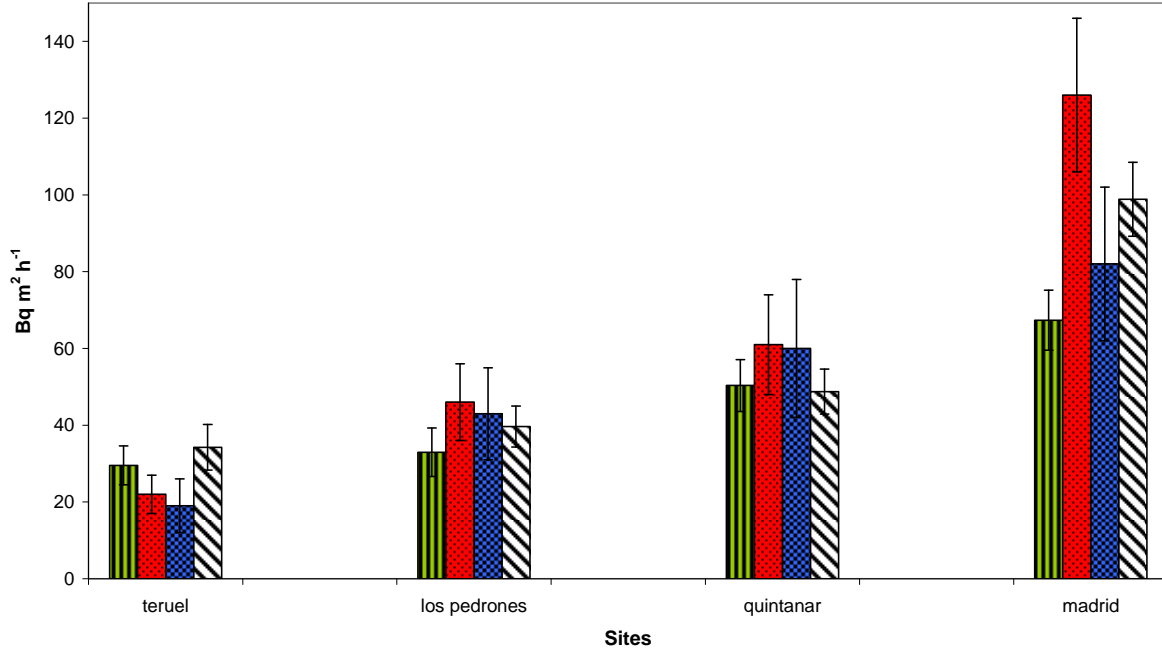
FIG. 4. ^{222}Rn exhalation flux density results at each campaign site measured by EIC (vertical and green bar), charcoal (pointed and red bar), Sun Nuclear (square and blue bar) and Alpha GUARD (diagonal and white bar) monitors.

Preliminary EIC monitor calibration

The EIC monitors, in the HST configuration, seem to have the most appropriate technical and economical features for their utilization during radon exhalation flux density site characterization. Furthermore, the EIC chambers without aluminium collars are easier to install on soil and their utilization does not lead to volume definition errors (Figure 3).

Although these monitors have shown quite good results, they are still prototype devices and more accurate calibration is needed in order to define the ventilation factor contribution during a measurement. A first monitor calibration has been performed at the Huelva University laboratory through the bed exhalation method using a well-characterized terrain with a known ^{226}Ra content of 50 Bq Kg^{-1}. The reference terrain exhalation has been calculated by the potential exhalation method [13].

After three different measurements performed by the two EIC monitors in the HST configuration and without collars, a $\lambda^0 = \lambda + \lambda^*$ of 0.20 h^{-1} has been found.

In Figure 5 the results of EIC monitor in the HST configuration, without aluminium collars are reported taking a ventilation factor of 0.20 h^{-1}.
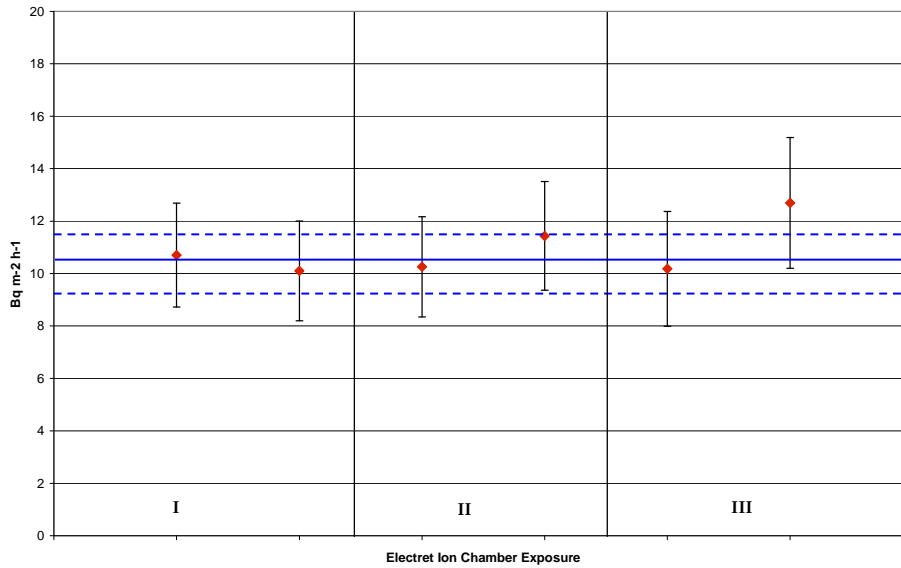
FIG. 5. Radon exhalation flux density results by EIC monitors, with a ventilation lambda of 0.2 h^{-1}, during a preliminary calibration study. Three different measurements have been performed and compared with the reference exhalation terrain.

Figure 6 presents the exhalation campaign results for the EIC monitors with and without ventilation correction at each site, only for the monitors without aluminium collars. These results are compared with radon flux values measured by AlphaGUARD monitors, which has been taken as a reference monitor. Radon exhalation flux density values by EIC monitors taking into account the ventilation factor of 0.20 h^{-1}, are also in agreement with the values measured with the AlphaGUARD. Therefore, research into this field should continue.

FIG. 6. The radon exhalation flux density results by EIC monitors with ventilation lambda equal to zero (vertical green bar) are compared with values taking into account the ventilation lambda (0.20 h^{-1}) (sky blue bar). Radon flux values by the AlphaGUARD method are also reported as a reference (diagonal white bar).

46

Conclusion

The intercomparison campaign and study shows that the EIC work properly and are in agreement with other direct methods, both integrated and continuous, for ^{222}Rn exhalation flux density measurements. In order to evaluate the quality of the EIC system, the results of an intercomparison campaign carried out at four eastern Spanish sites has been used.

Under standard environmental conditions the electret system works properly. However, the electret system could be strongly influenced by humidity condensation in the EIC chamber, which leads to electret passive discharge. Therefore, measurements with this device should not be advised when water condensation is likely. The intercomparison campaign was carried out during solar hours to avoid dew.

Mainly, it can be concluded that EIC monitors are appropriate in field campaigns due to their performance, mobility and price. The EIC monitors without aluminium collars are more practical to install because they do not have associated definition volume mistakes.

It has also been found that a crucial point for future performance analysis is the definition of a reference exhalation source in order to calibrate and carry out radon exhalation flux density detectors. Further work is planned with Huelva University to get a better quality control procedure.

REFERENCES

[1] WMO - 1st International expert meeting on sources and measurements of natural radionuclides applied to climate and air quality studies. Technical report No 155, World Meteorological Organization Global Atmosphere Watch, (2004).

[2] GROSSI, C., VARGAS, A., CAMACHO, A., et al., Inter-comparison of different direct and indirect methods to determine ^{222}Rn flux from soil, submitted to Appl. Radiat. (July 2009).

[3] PORSTENDORFER, J., Properties and behaviour of radon and thoron and their decay products in air, J. Aerosol Sci. **25** (1994) 219–263.

[4] MORAWSKA, L., PHILLIPS, C.R., Determination of the radon surface emanation rate from laboratory emanation data. Sci. of The Total Environ. **106** (1980) 253–262.

[5] LEHMANN, B.E., IHLY, B., SALZMANN, S. et al., An automatic static chamber for continuous ^{222}Rn and ^{222}Rn flux measurements from soil. Radiat. Meas. **38** (2003) 43–50.

[6] DUEÑAS, C., LIGER, E., CANETE, S., et al., Exhalation of ^{222}Rn from phosphogypsum piles located at Southwest of Spain, J. Environ. Radioact. **95** (2007) 63–74.

[7]   KOTRAPPA, P., DEMPSEY, J.C., STIEFF, L.R., Recent advances in electret ion chamber technology for radiation measurements. Radiat. Prot. Dosim. **47** (4) (1993) 461–464.

[8]   KOTRAPPA, P., STIEFF, L.R., Application of NIST ^{222}Rn emanation standards for calibrating ^{222}Rn monitors, Radiat. Prot. Dosim. **55** (1994) 211–218.

[9]   SZEGVARY, T., CONEN, F., STOHLKER, U., et al., Mapping terrestrial gamma dose rate in Europe based on routine monitoring data, Radiat. Meas. **42** (2007) 1561–1572.

[10] DE MARTINO, S., SABBARESE, C., A Method for Emanation Coefficient Measurement of ^{222}Rn and ^{220}Rn from Soils, Phys. Chem. Earth **22** (1–2) (1997) 19–23.

[11] HUTTER, A.R., KNUTSON, E.O., An international inter-comparison of soil gas radon and radon exhalation measurements, Health Physics **74** 1 (1998) 108–114.

[12] KAPLAN, I., Nuclear physics II, Addison-Wesley, Japan (1963).

[13] KELLER, G., FOLKERTS, K.H., MUTH, H., Method for the determination of ^{222}Rn radon and ^{220}Rn Thoron, exhalation rates using alpha spectrometry, Radiat. Prot. Dosim. **3** 2 (1982) 83–89.

[14] LOPEZ-COTO, I., MAS, J.L., BOLIVAR, J.P., GARCIA-TENORIO R., A short-time method to measure the radon potential of porous materials, Applied Radiation and Isotopes **67** (2009) 133–138.

DIFFUSION MEASUREMENT OF ^{222}RN THROUGH SANDY SOIL USING A NEW DEVELOPED ALPHA DETECTOR BASED ON PHOTODIODES

J. NIR, I. BRANDYS, Y. SHITRIT, A. CRAITER, R. ATIAS, E. MARCUS,
B. SARUSY, U. WENGROWICZ, Y. KADMON, Y. COHEN, Z. BERANT, A. DODY
Nuclear research Center Negev,
Beer Sheva,
Israel

Abstract

A new α detector based on photodiodes was developed in order to measure radon diffusion rate. The detector is highly efficient and low cost compared to other known detectors. Diffusion rates were measured as a function of soil porosity, grain size, soil depth and soil water content. Results showed that grain size and water content influence the diffusion rate of radon through sandy soil.

Introduction

The ^{222}Rn has a half-life of 3.8 days. It is released during the decay of ^{226}Ra, which can be found in varying amounts in rocks and in different kinds of soils. The emission products of ^{222}Rn are alpha particles (5.4897 MeV with 0.9992 probability and 4.986 MeV with 0.000785 probability) and gamma rays mainly from the decay of ^{214}Bi and ^{214}Pb daughters.

^{222}Rn has both negative and positive aspects. The negative aspect is that its transport through soil and exhalation to air may lead to lung cancer. The positive aspect is that it can be used as a natural tracer to study underground gas concentration and water transport.

There are few Radon measurement methods such as activated charcoal adsorption [1], charcoal liquid scintillation [1, 3], filtered and unfiltered alpha track detection [2, 4], electrets ion-chamber and continuous Radon monitoring.

Objectives

Measuring the effect of porosity, grain size and water content on Radon diffusion through sandy soil.

Development and construction of a continuous low cost and highly efficient ^{222}Rn measurement system based on photodiodes (for measuring α particles).

The experimental system
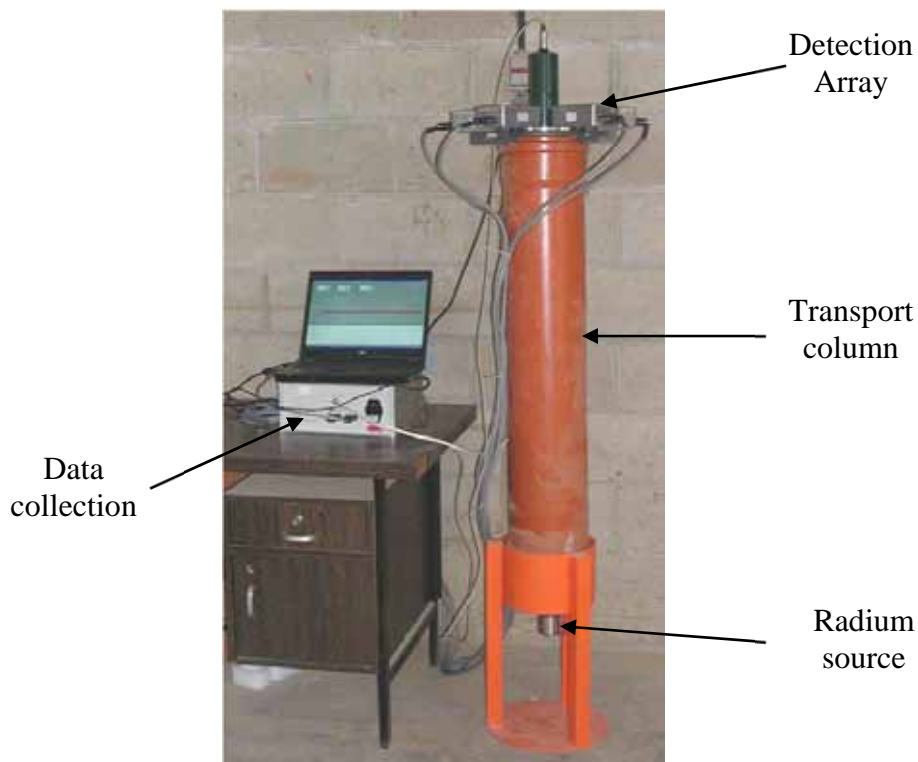
The experimental system (Figure 1) components are:

(1)   Three 8" inner diameter sealed P.V.C columns at different heights: 0.5 m, 1 m and 1.5 m.

(2)   Different grain sizes of sandy soil (with different water content), whose grain sizes are: less than 200 μm, 250–600 μm and 600–1000 μm.

(3) ^{226}Ra with 20 000 Bq activity for the creation of ^{222}Rn.

(4) A new prototype of alpha detector, which is based on 100 Silonex SLSD-71N5 commercially available solderable planar photodiodes [5], 1 cm^2 each.

  - The theoretical efficiency of the solar cells is nearly 100% response to alpha particles that hit the cells surface.

  - Every 5 solar cells are connected in parallel and installed on a separate Printed Circuit Board (PCB) – "strip".

(5) 20 solar cells PCB strips are attached to the detection head (Figure 2).

(6) A dedicated charge amplifier. This module consists of four amplification channels. Each channel includes a charge amplifier [6], a second amplification stage and a level discriminator with a TTL output. The module also utilize an OR gate that combines the output pulses of the four channels to a single TTL output.

(7) RP-11 high sensitivity NaI(Tl) scintillation gamma detector [7].

The experimental procedure

The P.V.C column is filled with sand of specific grain size and water content. The detection head is mounted on top of the column. The charge amplifiers and the gamma detector are connected to a data collection unit and a computer. The Radium source, which is located in a dedicated chamber in the bottom of the system, generates the Radon gas. Once the Radon is released it diffuses through the soil. When it reaches the detection head are the α and γ rays are measured and the data is sent to the computer.
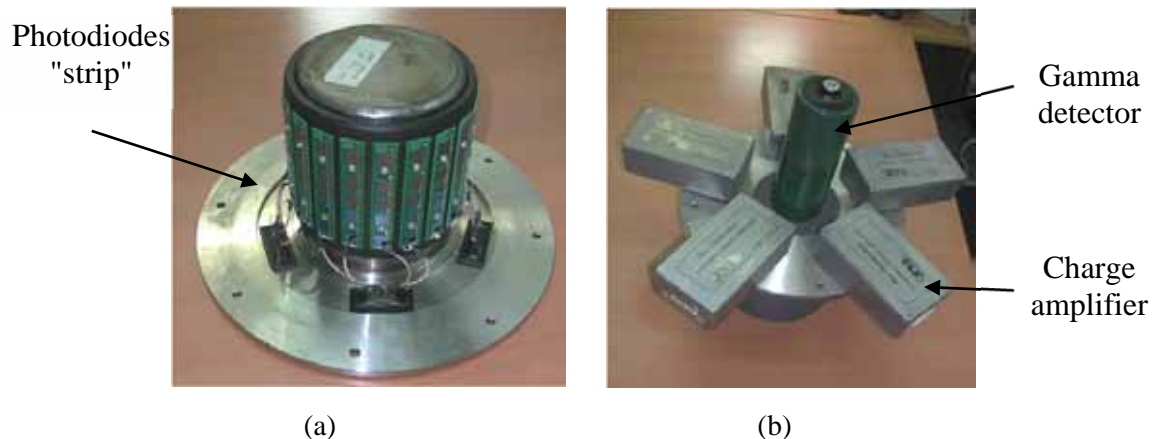

FIG. 1. The experimental system.

FIG. 2. (a) The photodiodes array (b) Gamma detector and charge amplifier for the detector.

Preliminary Results

First experimental results are presented in Figures 3 and 4. Figure 3 describes the effects of the grain size on the Radon diffusion rate. Figure 4 describes the effect of water content in soil on the Radon diffusion rate. Both figures show the α detector measurements (the γ measurements show similar behaviour).
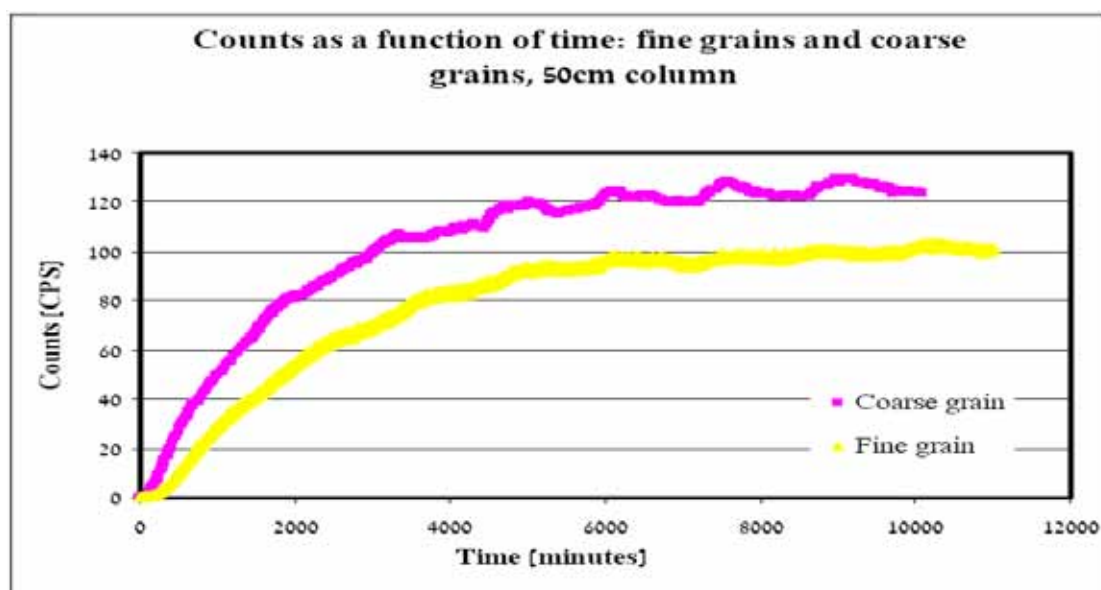

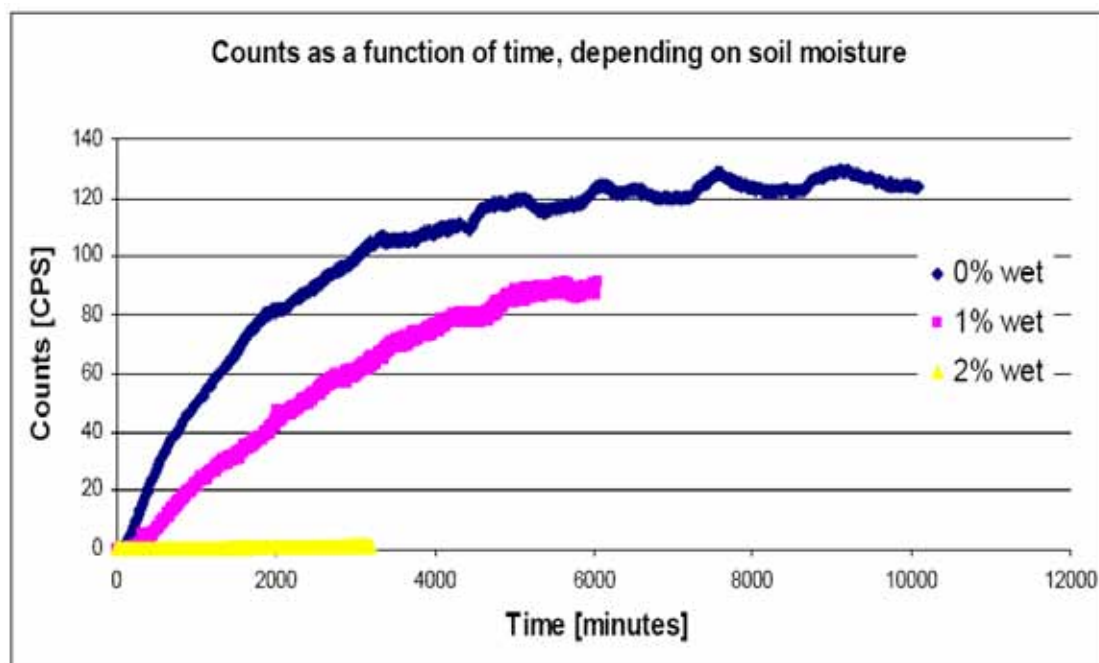FIG. 3. Effects of grain size on diffusion rate.

FIG. 4. Effect of water content on diffusion rate.

Summary

An experimental system for continuous detection of Radon transport through sandy soil was developed.

The system has a large alpha detection are and includes a gamma detector.

The study of Radon diffusion through sandy soil of different grain sizes is in progress.

REFERENCES

[1] CANOBA, A.C., LÓPEZ, F.O., OLIVEIRA, A.A., Radon determination by activated charcoal adsorption and liquid scintillation measurement, Journal of Radioanalytical and Nuclear Chemistry, **240** (1) (1999).

[2] GÖKMEN, A., GÖKMEN, I.G., YUNG-TSE H., Radon Pollution Control, Handbook of Environmental Engineering, (2005) vol. 2.

[3] COHEN B.L., COHEN E.S., Theory and Practice of Radon Monitoring With Charcoal Adsorption, Health Physics **45** (2) (1983).

[4] NIKOLAEV, V.A., ILIĆ, R., Etched track radiometers in radon measurements: a review, Radiation Measurements **30** (1999).

[5] www1.silonex.com

[6] KESTER, W., WURCER S., KITCHIN, C., High Impedance Sensors, Analog Devices Inc., Op Amp Applications, (2002) 4.39–4.67.

[7] www.rotemi.co.il/RP11/

HARMONIZATION OF AMBIENT DOSE RATE MONITORING PROVIDES FOR LARGE SCALE ESTIMATES OF RADON FLUX DENSITY AND SOIL MOISTURE CHANGES

U. STÖHLKER, M. BLEHER
Bundesamt fuer Strahlenschutz,
Germany

F. CONEN, D. BÄNNINGER
University of Basel,
Switzerland

Abstract

About 3600 stations in Europe monitor ambient dose rate for radiation protection purpose. In the absence of a nuclear emergency, natural background radiation is recorded. Variations in background radiation are largely driven by spatial differences in the concentration of natural radionuclides in soil and by temporal changes in soil moisture, which shields a varying proportion of the terrestrial component in ambient dose rate. Hence, ambient dose rate data contain information about variations in space and time of other important environmental parameters. This information can be extracted when data from the diverse European networks is harmonized.

Introduction

Monitoring of ambient dose rate in Europe has the purpose to inform about scale and intensity of radioactive contamination in case of a nuclear emergency. The data from about 3600 stations provided within the European Data Exchange Platform (EURDEP) are collected continuously within Europe. In the absence of an emergency situation, natural background radiation is monitored. This is the "normal" situation for most of the time. Small variations in background radiation contain information which can be very useful in a complementary context.

Comprehensive, ground-validated radon flux-density maps for Europe have been developed by Szegvary et al. [1]. Production of these maps involved new algorithms relating radon flux density to closely associated variables such as terrestrial gamma dose rate. Mapping gamma dose rate to radon flux-density is an alternative option for expanding the global coverage or radon flux density estimates.

The interaction between soil moisture and air temperature is significantly affected by climate change [2]. In the past years very hot and dry periods during summer months were observed in Europe. It has been reported, that these periods were preceded by a depletion of soil moisture resulting in reduced latent cooling and amplified summer temperature extremes [3]. Real-time soil moisture data would lead to the optimization of weather forecasting. Since wide area soil moisture sensor networks do not exist, we investigated the possible use of terrestrial gamma dose rate data to derive changes in soil moisture.

In this report we focus on the operational procedures for both the generation of radon flux maps on the European scale and large scale soil moisture maps with high spatial resolution. For the generation of maps, WEB services are under development, which are built on top of the so called harmonization database. The aim is to derive radon flux and soil moisture maps from ambient dose rate measurements exchanged in the EURDEP system using interpolation techniques developed within the framework of the INTAMAP project [4].

Harmonization of gamma dose rate data

It is well known that due to the diversity of European monitoring networks data from different countries show significant differences and the readings of different detector types should be corrected in order to harmonize the data on the European scale. In 2004 the European Commission initiated the so-called AIRDOS project "Evaluation of existing standards of measurement of ambient dose rate; and of sampling, sample preparation and measurement for estimating radioactivity levels in air". This project covered detailed assessment and evaluation of systems for continuous measurement of ambient gamma dose rate in the EU [5]. From this project a specific extension of the EURDEP system has been developed. The information used to characterize ambient dose rate measurement stations with respect to data harmonization needs to be provided by the individual national network operators within EURDEP. Although some of this information like geographical coordinates (in latitude and longitude), height above sea and height above ground surface are easy to obtain, this information need nevertheless continuous update. Therefore an experts group has been established recently, with the aim to define the characteristics of a data interface to the EURDEP system, which will allow all EURDEP end-users to access and to update the AIRDOS information within the EURDEP system whenever station or probe parameters have changed. Based on this specification a browser based application will be developed which will allow end-users to input data remotely. The EURDEP system will be extended accordingly and the implementation of this final extension is foreseen end of 2009. It has to be pointed out, that the continuous and immediate update of all information to the harmonization procedure is very important for the quality of the harmonization process. If the harmonization information is outdated, the harmonization procedures applied to actual ambient dose rate measurements will generate erroneous results.

Ambient dose rate and terrestrial gamma dose rate have a significant difference. Typically ambient dose rate is obtained directly from the readings of the probe. The probe detects events originating as a superset of photons from the soil and radiation of the cosmic component, which consists of muons, charged particles, gamma photons and neutrons. The terrestrial contribution is called terrestrial gamma dose rate, because from the soil only gamma photons are emitted. Therefore further important parameters for the harmonization of dose rate data are self effect of the probe, the response of the detector to secondary cosmic component and the energy dependency which is described by the sensitivity of the probe with respect to ^{137}Cs, ^{226}Ra, ^{60}Co and ^{57}Co. These parameters are less easy to obtain. For this purpose the European Radiation Dosimetry Group (EURADOS) executed inter-comparison exercises of ambient dose rate detectors used in environmental radiation surveillance systems in the years 1999, 2002, 2005 and 2008. In these inter-comparison exercises the self effect of detectors is determined at the underground laboratory UDO operated by the Physikalisch Technische Bundesanstalt (PTB) located in Braunschweig, Germany, in the Asse salt mine close to Braunschweig. Additional free field irradiation experiments are performed to determine the sensitivity of the detector and a swimming platform on a lake is used to determine the response of the detector with respect to the secondary cosmic component. In addition BfS operates the long term inter-comparison exercise (INTERCAL) at Schauinsland mountain [12], where nearly all types of probes are installed which are used in European early warning networks. The detectors are operated continuously over several years and long term stability as well as individual characteristics of the detector response with respect to the variability of the natural background radiation are investigated. Part of INTERCAL has been the experimental investigation of the detector response to the secondary cosmic component as a function of height above sea and land. In addition, the investigation of the detector sensitivity

as a function of the incident photon energy is part of the EURADOS and INTERCAL intercalibration exercises. The output of these investigations has been described in detail [12].

Using terrestrial gamma dose rate as proxy for soil radon flux

222Rn is commonly used as a natural tracer for validating climate models. To improve such models, a better source term for 222Rn than currently used is necessary. The current practice is to assume a spatially and temporally uniform flux density of 1 atom cm^{-2} s^{-1} from all ice-free land surfaces, with a lower 222Rn flux density above $60°$N (The 222Rn flux density can be converted to Bq m^{-2} s^{-1}). Szegvary et al. [1] established a method for mapping this source term by using terrestrial gamma dose rate as proxy. Simultaneous measurements of 222Rn flux and terrestrial gamma dose rate were carried out in Switzerland, Germany, Finland and Hungary in order to cover a wide range of terrestrial gamma dose rate. Spatial variations in terrestrial gamma dose rate resulted from different radionuclide concentrations in soil forming minerals. A relatively stable fraction (25–30%) of the total terrestrial gamma dose rate originates from the 238U decay series, of which 222Rn is a member (Figure 1).
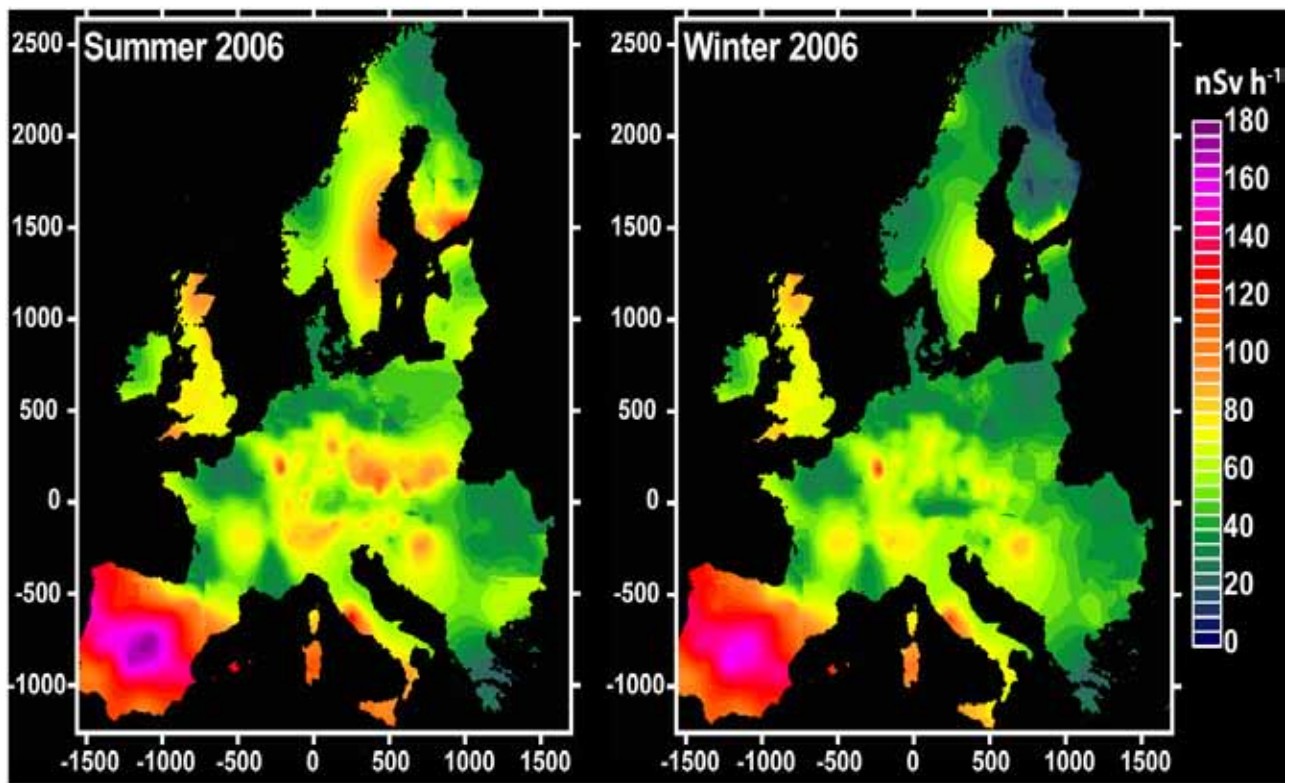

FIG. 1. Mean terrestrial gamma dose rate for summer (left) and winter (right) for 2006 in Europe [3].

Accordingly, spatial variation in terrestrial gamma dose rate was found to describe almost 60% of the spatial variation in 222Rn flux. Furthermore, temporal variation in terrestrial gamma dose rate and 222Rn were found to be correlated. Increasing soil moisture reduces gas diffusivity and the rate of 222Rn flux but it also decreases terrestrial gamma dose rate through increased shielding of photons. Prediction of 222Rn flux through terrestrial gamma dose rate for individual measurement points is imprecise but un-biased. Verification of larger scale

prediction showed that estimates of mean ^{222}Rn fluxes were not significantly different from the measured terrestrial gamma dose rate mean values.

As a result, a first map of the terrestrial gamma dose rate in Europe was derived from EURDEP. Based on spatial interpolation by kriging between monitoring stations, these European maps of terrestrial gamma dose rate have then been transformed in ^{222}Rn flux maps using the empirical relation between terrestrial gamma dose rate and ^{222}Rn flux described in Szegvary et al. [6]. These maps provide mean ^{222}Rn fluxes on a 0.5^{o} x 0.5^{o} grid for summer and winter 2006.

As described below this method has been extended and an operational system is under development. It includes the generation of flux maps with the same spatial but higher temporal resolution. Use of automated mapping procedures developed in the INTAMAP project is implemented reducing required efforts considerably. Generated spatially and temporally resolved ^{222}Rn flux would constitute a useful contribution to the ongoing effort to establish an observing system for greenhouse gas emissions in Europe.

Deriving changes in soil moisture from variations in gamma dose rate

The focus of this investigation is to derive real-time changes in soil moisture (SM) from terrestrial gamma dose rate networks. This would allow derivation of large scale soil moisture dynamics for possible use in the optimization of weather forecasting. Since large area SM sensor networks do not exist, terrestrial gamma dose rate is to be investigated to be used as a proxy for soil moisture. Because of the large spatial coverage and high temporal resolution, this technique may also be useful for calibrating spaceborne soil moisture sensors, such as the Soil Moisture and Ocean Salinity (SMOS) system [7].

It has to be pointed out, that from our point of view it is expected, that using terrestrial gamma dose rate as a proxy for SM might produce even better experimental results compared to the application of SM sensors. This is due to the fact, that terrestrial gamma dose rate detectors are integrating radiation originating from soil over an area within a 10m radius. SM sensors instead, provide data which are representative only for a very thin layer around the probe. For this reason typically a set of up to 5 SM sensors is used in parallel to improve the overall reliability of this technique. This assumption needs to proven in the future based on careful assessment of data obtained by both techniques at the Calibration/Validation sites of the SMOS project.

In most situations, free-field terrestrial component of ambient dose rate is dominated by the natural occurring radionuclides ^{40}K, ^{238}U and ^{232}Th as well as the progeny of the latter two distributed in the ground to a depth of some few centimeters. The probability of a photon to reach from a specific depth within soil profile the detector above the surface, depends on the mass of mineral particles and the water content above the layer of its origin. Assuming constant activity concentration, this component is reduced by increasing soil moisture measured by the water content of the soil. While the mass of solids can be considered to be constant, precipitation and evapo-transpiration continuously change the water content and its distribution with depth, causing variations in terrestrial gamma dose rate with time (Figure 2). Additionally, wash-out of natural air activity leads to deposition on the ground. During a precipitation event this may lead to a short-lived increase of observed dose rate. Due to the short half-lives of the dominant radionuclides ^{214}Bi and ^{214}Pb, these events have a typical duration of some few hours. Thus, proper investigations of soil moisture effects on dose rate have to eliminate these rain events.
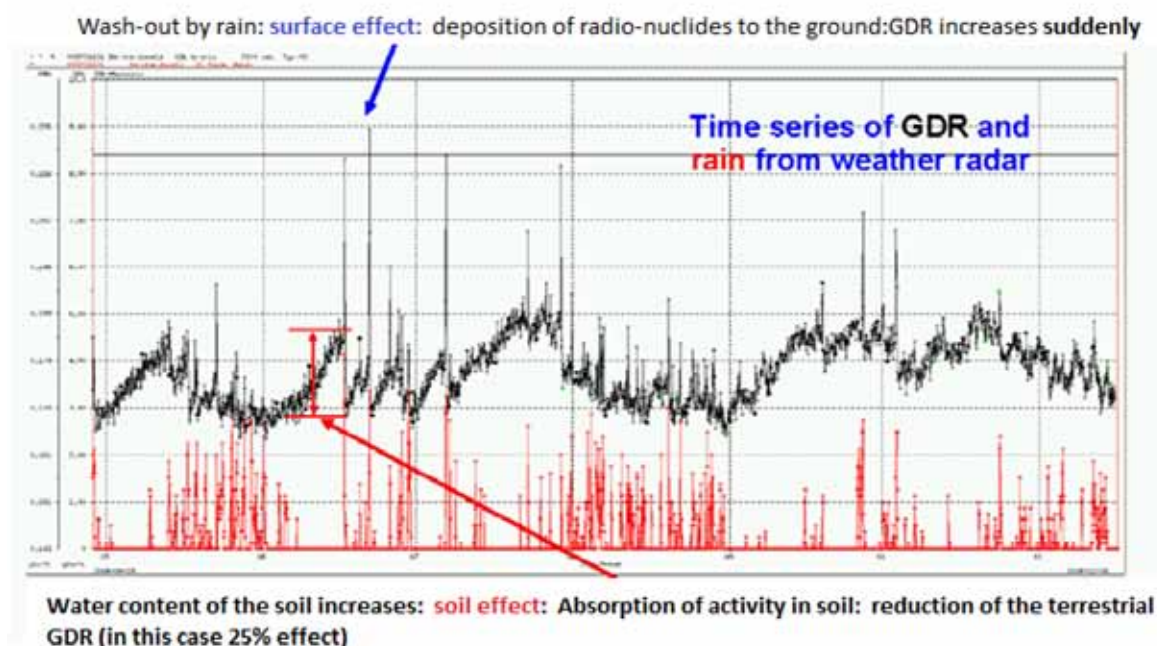
FIG. 2. The variability of the terrestrial gamma dose rate (in black) explained by surface and soil effects. The rainfall pattern provided by weather radar systems is shown in red.

In May 2008 BfS and University of Basel presented a concept to use radioactivity measurements for SM retrievals at the "Soil Moisture and Ocean Salinity (SMOS) Science Advisory Group Meeting" at ESA-ESTEC in Noordwijk, Netherlands [8] which is responsible for the scientific program of the SMOS satellite, expected to be launched in autumn 2009. The ESA advisory group proposed a cooperation with University of Munich which is operating the SMOS Upper Danube Catchment validation area.

Soil moisture experiments

As follow-up of this meeting a cooperation between the Universities of Basel, Munich and the BfS was initiated and a program was agreed on for the investigation of the correlation between soil moisture data and ambient dose rate. The program was divided in two parts.

To investigate the correlation between SM and terrestrial gamma dose rate, BfS installed early October 2008, 7 additional ambient dose rate detectors at SMOS Calibration/ Validation sites, where SM sensors are operated as part of the SMOS Calibration/Validation experiment. This would allow to directly compare data obtained by SM sensors and ambient dose rate detectors installed at the same measurement site. Soils at all sites have developed on glacial sediments, and are generally characterized by a silty texture (Table 1).

At the SMOS Calibration/Validation sites typically 8 soil moisture sensors are installed at different depths: 5 sensors at 5 cm, 1 sensor at 10 cm, 20 cm and 40 cm depth, each. The SM sensors provide data averaged over one hour. In our preliminary study we compared 2h mean values of SM and terrestrial gamma dose rate data obtained between April and Mai 2009. At all 7 stations we calculated the correlation between one of the SM sensors installed at 5 cm depth and the terrestrial gamma dose rate. Since only data related to the soil effect have to be taken into account, increased values of gamma dose rate caused by precipitation were

eliminated. For 2 and 24 hour averages almost normally distributed data sets for dose rate were obtained. For the used gamma dose rate probe the statistical uncertainty of 2h mean values is in the order of 1%. Soil moisture data show statistical uncertainties below 1 %. However, data from different sensors at the same site and the same depth may differ significantly. Furthermore, soil moisture data show significant deviations from normal distribution. To get a first estimation of the correlation between both observation methods, the Spearman's rank correlation coefficient (SRCC) was calculated. For 24 h mean data, Table 1 shows correlation coefficients between -0.59 and -0.84.

TABLE 1. SPEARMAN'S RANK CORRELATION COEFFICIENT FOR OBSERVED DATA OF SOIL MOISTURE (SENSORS AT DEPTH OF 5 CM) AND DOSE RATE. THE ANALYSIS WAS PERFORMED FOR 2 H MEAN DATA AND 24 H MEAN DATA AT SEVEN STATION IN BAVARIA IN APRIL TO MAI 2009. SOIL MOISTURE AND TEXTURE DATA WERE PROVIDED BY F. SCHLENZ, UNIVERSITY OF MUNICH (LMU).

	2h mean gamma dose rate	Spearman's rank correlation coefficient	
Station	Soil type [13]	2 h mean	24 h mean
Neusling	sandy silt [Us]	-0.66	-0.78
Steinbeissen	sandy silt [Us]	-0.56	-0.74
Frieding	sandy silt [Us]	-0.50	-0.59
Lochheim	sandy-loamy silt [Uls]	-0.57	-0.68
Rothenfeld	medium-silty sand [Su3]	-0.66	-0.77
Engersdorf	sandy silt [Us]	-0.62	-0.76
Karolinenfeld	sandy silt [Us]	-0.76	-0.84

TABLE 2. SPEARMAN'S RANK CORRELATION COEFFICIENT FOR OBSERVED DATA OF SOIL MOISTURE (FOUR SENSORS AT DIFFERENT DEPTHS) AND DOSE RATE. DATA ARE OBTAINED FROM APRIL TO MAI 2009 AT NEUSLING (LOWER BAVARIA).

sensor	depth	Spearman's rank correlation coefficient	
		2 h mean	24h mean
SM005	5 cm	-0.63	-0.75
SM105	5 cm	-0.66	-0.78
SM105	10 cm	-0.56	-0.68
SM010	20 cm	-0.18	-0.19

In addition we calculated the correlation between all SM sensors and the terrestrial gamma dose rate for station Neusling. It can be seen from Table 2, that the correlation between terrestrial gamma dose rate and SM is the best for SM sensors close to the soil surface. This

behavior is in agreement with our knowledge about the contribution of different soil layers to the resulting terrestrial gamma dose rate. As an example in Figure 3 the correlation at station Steinbeissen is shown.
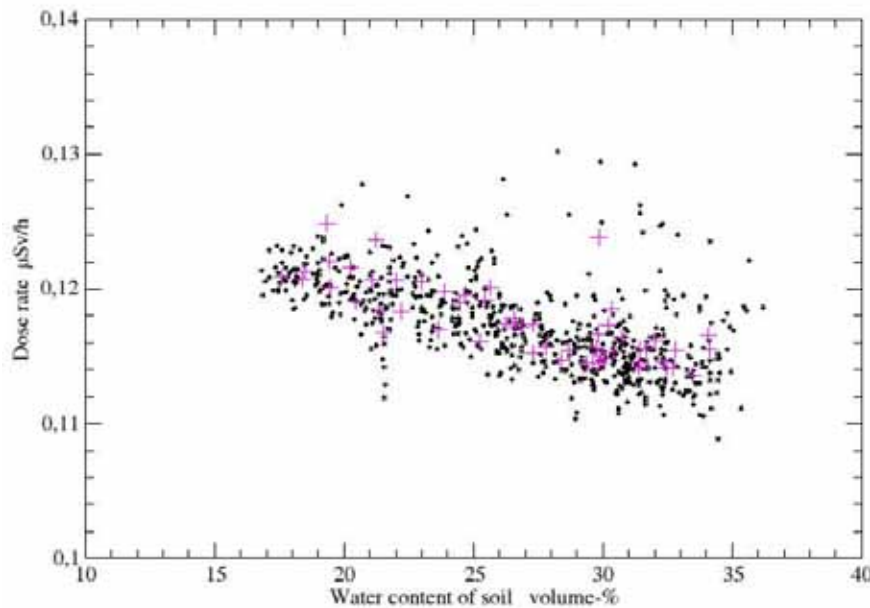

FIG. 3. Correlation of observed data for soil moisture (Sensor SM105 of Table 2) and dose rate. Data are obtained from April to Mai 2009 at Neusling (Lower Bavaria). Stars show 2h mean data and crosses indicate 24 h mean data.

The investigations reported in this paper give preliminary results. Further investigations should overcome the following problems: They should consider soil type characteristics for the different monitoring stations. Furthermore, the influence of air pressure on secondary cosmic component of dose rate should be taken into account as well as the impact of natural air activity concentration on terrestrial dose rate.

Correlation between soil moisture and terrestrial gamma dose rate - large scale

A second investigation focused on the comparison of SM data provided by the PROMET SM model with terrestrial gamma dose rate data obtained experimentally at the 1800 stations of the German ambient dose rate network. PROMET (PRocess-Oriented Model for Evapo Transpiration) is a physically based land surface model. The model describes the actual evapotranspiration and water balance at different scales. The model is described in detail in [9] and [10]. Basically, the model consists of a kernel model which is based on five sub-modules (radiation balance, soil model, vegetation model, aerodynamic model, snow model) to simulate the actual water and energy fluxes and a spatial data modeller, which provides and organizes the spatial input data on the field-, micro- and macroscale. PROMET was used to calculate the soil moisture on an hourly basis. The preliminary results of this investigation taking into account dose rate and model data between 2001 and 2009 showed no correlation between the PROMET model calculations of SM with terrestrial gamma dose rate. Since comparison of the experimental point observations of SM and terrestrial gamma dose rate are in rather satisfactory agreement, we assume that the output of the current version of the PROMET soil moisture model provides information averaged over larger areas. SM data calculated by PROMET are difficult to be used for the comparison with point observations of

SM data derived from ambient dose rate obtained at the measurement sites of the early warning network. Actually the PROMET model is in the process of optimization. After availability of a new version of PROMET the comparison of modeled SM and measured terrestrial gamma dose rate data will be repeated.

Ground calibration of the SMOS Satellite using dose rate data

As has been described, the results of the intercomparison of point measurements based on soil moisture sensors and gamma dose rate probes are encouraging to some extend. BfS together with Universities of Munich and Basel are engaged in the SMOS Upper Danube Catchment validation area. It is intended to continue this work and to develop techniques for the large scale estimation of ground based soil moisture data for the calibration of the remote sensing SMOS satellite.

The generation of daily maps of terrestrial dose rate on the European scale

BfS mapped the harmonization information provided by EURDEP/AIRDOS in the database structure shown in Table 1. The database includes the data section, where ambient dose rate data together with the statistical uncertainty are stored. Parameters found in the "station" and "probe" tables are used to characterize ambient dose rate measurement stations in general with respect to the aspect of data harmonization.

In a first step the ambient dose rate data from EURDEP needs to be preprocessed with respect to the measurement time period. Internationally there exists no common standard concerning measurement periods of ambient dose rate networks. To EURDEP for example, data with about 40 different measurement periods from 3 min to 24 h are reported. The first task is thus to harmonize all data with different measurement periods to a common period of one hour - which is the recently agreed standard within EURDEP. In a second step the harmonization database allows to process all data with respect to their physical properties as well as taking into account station and site characteristics.

The sensitivity of a detector for the cosmic radiation varies with different altitude. Each detector type has an individual type specific response and the over- or underestimation of different detector types ranges from 5% to 160%. The response of a detector to the secondary cosmic component is an empirical factor which was in case of the probes used in the German network determined experimentally [11]. From this response of a detector to secondary cosmic component (SCR) the factor "response to SCR" is derived. To get the cosmic response, the known dose rate due to the cosmic radiation is calculated from the height above sea, stored in the "station" table using the formula described in [11]. The cosmic contribution to the ambient dose rate is than multiplied with the factor "response to SCR" stored in the "probe" table. The self effect of a probe (also called the internal background or zero-effect of the probe) varies from 2–50 nSv/h for different ambient dose rate probes and needs to be determined experimentally.

The terrestrial dose rate is obtained from the measured ambient dose rate after subtraction of self effect and the calculated cosmic response. Finally one has to apply a correction related to the height of the probe above ground, which typically – and recommended – is one meter above ground, but even installations of more than 10 m are reported within EURDEP. The terrestrial gamma dose rate as a function of the height of the probe above ground has been

obtained experimentally at the Schauinsland look-out tower in cooperation with University of Basel [3].

In case of natural background radiation one has to apply an additional factor describing the sensitivity of the probe relative to ^{226}Ra (which is called "response@Ra226"). To compensate for the energy dependency of a probe in an emergency situation, one has to apply the correction factors "response@Cs137", "response@Co50" or "response@C57" depending on the contamination situation.

Where applicable, an artificial component from ^{137}Cs has to be subtracted.

TABLE 3.   STRUCTURE OF THE HARMONIZATION DATA BASE.

Table	Table	Table
Parameters of station	Parameters of probe	Measurement results
station ID	probe ID	ambient dose rate / μSv/h
Coordinate (latitude, longitude)	self effect / μSv/h	terrestrial dose rate / μSv/h
height above sea / meter	height above land / meter	statistical uncertainty / μSv/h
site status	response to SCR	cosmic response / μSv/h
site type	response @ Cs137	time-stamp
^{137}Cs contamination / μSv/h	response @ Ra226	status
	response @ Co60	
	response @ Co57	

Data for self effect, response of the detector to SCR, to Cs-137, Ra-226, Co-60 and Co-57 determined in EURADOS and INTERAL exercises need to be provided by the network operators since, and as already mentioned, the AIRDOS extension of the EURDEP database needs to be updated continuously.

Data visualization tool

For the visualization of ambient dose rate data together with interpolation results on a global, European or regional scale, BfS developed a WEB client application in the framework of the INTAMAP project. The advantages of WEB client applications are platform independency, the standardized interaction with other Web Services, the easy access via browser. In addition BfS developed a desktop GIS application running on UNIX/Linux systems in an X11 environment. This application is used for the validation of data in the contents of the routine validation procedure with the need to plot and select data in maps and time series and to change the status of individual elements in the database.

Both applications allow to handle ambient dose rate data together with those attributes which are selected from the harmonization data base like self-effect, height above ground height above sea level etc.

The layout of the presentation was chosen in accordance with the requirements defined in the German Integrated Measurement and Information System (IMIS). The measurement results are presented as point data in the same color scheme used for the interpolated information. Shapefiles are loaded to define country boarders and clipping is used to restrict interpolations methods to areas over land.

Meanwhile the above described automatic procedures to calculate terrestrial gamma dose rate from raw data as output of the harmonization application can be used on an operational basis to generate interpolated maps of the terrestrial gamma dose rate on an local and European level. The purpose of this application is to provide harmonized gamma dose rate data for scientific applications. Further work is needed to make the application accessible to external users. It is intended to provide a first operational system end of 2009.

Conclusion

Available data from routine monitoring of gamma dose rates in Europe contain information on spatial and temporal variations of radon flux density and on soil moisture. They are driven in similar ways by geological and meteorological factors as is the terrestrial component of the dose rate. Results from a number of projects aiming at an inter-comparison and harmonization of dose rate sensors and network characteristics within Europe now provide for the extraction of the terrestrial component from reported total ambient dose rates, which include to varying degrees also cosmic components and instrumental self effects. Empirical relations with radon flux density and soil moisture have been worked out. In the near future, a WEB client application will enable the scientific community to tap into and use the information on radon flux density and soil moisture contained in data from routine monitoring of gamma dose rates in Europe.

REFERENCES

[1] SZEGVARY, T., et al., Mapping terrestrial γ-dose rate in Europe based on routine monitoring data, Radiat. meas. **42** (2007) 1561–1572.
[2] SENEVIRATNE, S.I., LUTHI, D., LITSCHI, M., SCHAR, C., Land-atmosphere coupling and climate change in Europe. Nature **443** (2006) 205–209.
[3] FISCHER, E.M., SENEVIRATNE, S.I., LUTHI, D., SCHAR, C., Contribution of land-atmosphere coupling to recent European summer heat waves. Geophysical Research Letters 34, article number L06707 (2007).
[4] PEBESMA, E.J., et al., INTAMAP: an interoperable automated interpolation web service; Proceedings of StatGIS09: GeoInformatics for Environmental Surveillance, Milos, Greece, 17–19 June 2009.
[5] BOSSEW, P., et al., AIRDOS: Evaluation of existing standards of measurement of ambient dose rate; and of sampling, sample preparation and measurement for estimating radioactivity levels in air. JRC ref. N 21894-2004-04 A1CO ISP BE, European Joint Research Commission (2007).
[6] SZEGVARY, T., LEUENBERGER, M.C., CONEN, F., Predicting terrestrial ^{222}Rn flux using gamma dose rate as a proxy. Atmos. Chem. Phys. **7** (2007) 2789-2795.

[7]   BARRÉ, H.M.J.P., DUESMANN, B., KERR, Y.H., SMOS: The mission and the system. IEEE Transcations on Geoscience and Remote Sensing **46** (2008) 587–593.

[8]   STOEHLKER U., CONEN, F., Radioactivity use for SM measurement, The Soil Moisture and Ocean Salinity (SMOS) Science Advisory Group, Minutes of the Twenty-Third Meeting, 21–22 May 2008, ESA-ESTEC, Noordwijk, Netherlands.

[9]   MAUSER, W., SCHDLICH, S., Modelling the spatial distribution of evapotranspiration using remote sensing data and promet; Journal of Hydrology **213** (1998) 250-267.

[10] MAUSER, W., BACH, H., Promet a physical hydrological model to study the impact of climate change on the water flows of medium sized mountain watersheds, Journal of Hydrology, submitted paper (2008).

[11] WISSMANN, F., RUPP, A., STÖHLKER, U., Characterization of dose rate instruments for environmental radiation monitoring, Z. Kerntech. **4** (2007) 193-198.

[12] STÖHLKER U., BLEHER M., SZEGVARY TH., CONEN F., Inter-calibration of gamma dose rate detectors on the European scale, ECORAD 2008, Bergen June 2008, Radioprotection **44** 5 (2009) 777–783.

EVALUATION OF RADON FLUX MAPS FOR SIBERIAN AND EAST ASIAN REGIONS BY USING ATMOSPHERIC RADON CONCENTRATION OBSERVED OVER OCEANS

H. YAMAZAWA, S. HIRAO, J. MORIIZUMI, T. IIDA,
Nagoya University,
Nagoya,

S. TASAKA
Gifu University,
Gifu,

Japan

Abstract

Regional to global radon flux maps presently available for Siberian and East Asian regions were compared to each other and tested by using them as input source terms of long-range atmospheric radon transport simulations and comparing the result with atmospheric radon concentrations observed over down-wind oceans, such as the Arctic Ocean and Bering Sea. The comparison of maps showed that the absolute values of differences in radon exhalation flux density between maps are as large as 10 to 20 mBq m^{-2} s^{-1}. The observed atmospheric radon concentrations were better explained by small fluxes density of 5 to 15 mBq m^{-2} s^{-1} predicted by Yamazawa's map [1, 2] and Conen's map [3, 4] in the arctic rim of the Siberian region. Whereas, in the far-eastern region of the continent especially in the mid-latitudinal areas, relatively large radon exhalation flux more than 30 mBq m^{-2} s^{-1} estimated by Schery's map [5] is more likely than the smaller values estimated by the other maps.

Introduction

Atmospheric radon has been used as a tracer of contaminants originating from land masses because of its similarity in the geometry of sources and its physicochemical properties. There are multiple global and regional radon flux maps available. However, the radon flux values are substantially different from each other. This uncertainty in the radon flux distribution and its seasonal variations have been the main limitations in applying radon as a tracer in atmospheric transport studies. Reduction of the uncertainties in the radon flux maps will enhance the usefulness of radon as an atmospheric tracer.

Some of the maps are based on a theoretical formulation of physical processes of radon exhalation from the ground surface and uses relatively similar but still different formulae describing dependency of radon flux on radium and water contents of soil and other parameters [1–5]. Differences in these parameters used to calculate radon flux are also main causes of inconsistent flux values between maps in addition to inherent differences in the theoretical formulations. Other maps use the environmental gamma dose rate as a proxy of radon flux [4]. This idea seems promising if dose rate measurement networks with a proper density and extent are available and the relation between the radon flux and the dose rate is reasonably determined by considering locality of dose rate measurements.

Direct measurements of radon fluxes are the most reliable means of testing the maps [9]. However, especially for maps with a large spatial extent, this method is no longer effective and feasible since a flux measurement suffers from very small-scale locality both in space and time. In this study, the radon flux maps are tested by using them as input source terms of long-range atmospheric transport simulation [6, 7] and by comparing the calculated surface

concentration with observations carried out on a research vessel in the downwind of northern and eastern parts of Eurasian Continent (Russian Federation, China, etc.). Although this strategy of radon map testing suffers from uncertainty in the long-range simulations, [8] the atmospheric radon concentration observation recently carried out in the arctic region is expected to narrow down the uncertainty in the radon flux in the area of interests.

Radon flux maps

The flux maps tested are Schery's (hereafter, referred to as S-map) [5], Conen's (C-map) [3] and Yamazawa's (Y-map) ones [2].

Y-map is based on the Goto's formulation [1] using the JRA-25 reanalysis meteorological data (JMA and CRIEPI) for soil moisture, but UNSCEAR data are newly used for the area other than China. Terrain ruggedness is not considered in this map. The flux values may increase by a factor of 1.0 to 1.2 if the terrain ruggedness is taken into consideration. Global distribution of radon exhalation flux density of Y-map is shown in Figure1. The original map is given as a grid data with the latitudinal and longitudinal resolutions of 1° for each month from 1979 to 2007. The global average of the flux (land area weighted average) for this period is 20.8 mBq $m^{-2} s^{-1}$. The spatial distribution of radon flux in this map is mostly determined by soil moisture in addition to country-to-country difference caused by difference in radium content. Therefore, the exhalation flux density has seasonal variations with maximums in the late summer to autumn in the northern hemisphere when the soil moisture is low. The amplitude of seasonal variation in the radon flux is estimated to be about 5 mBq $m^{-2} s^{-1}$. It is evident that the radon flux is small in the northern area of the Eurasian and American continents due to high soil moisture content as compared with arid areas at mid latitudes.

Global distribution in terms of zonal mean flux is compared in Figure2 (a). Although the latitudinal variations are similarly depicted by S-map and Y-map, the absolute values of radon exhalation flux density are substantially different by about 10 mBq $m^{-2} s^{-1}$ in the tropical to subtropical zone and by about 20 mBq $m^{-2} s^{-1}$ or more in the northern mid to high latitudinal zone. The difference is evident in the area of interest as shown in Figure2 (b) for Siberia. S-map has high radon flux density of a little more than 30 mBq $m^{-2} s^{-1}$, whereas C-map and Y-map are 10 to 20 mBq $m^{-2} s^{-1}$. Y-map shows clear latitudinal dependency, which is caused by higher soil water content in the higher latitudinal areas.
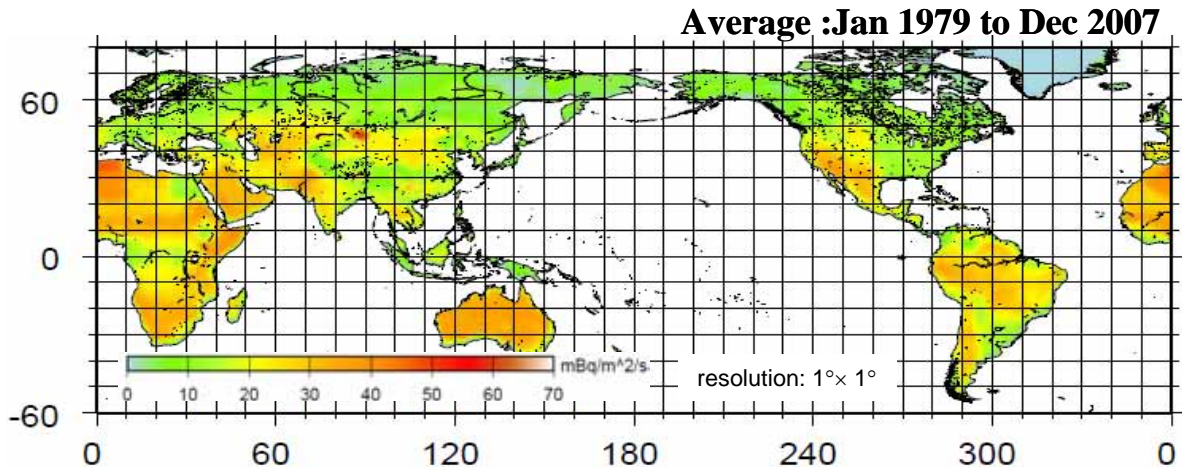
FIG.1. Global distribution of radon exhalation flux density of Y-map averaged over 29 year period from 1979.
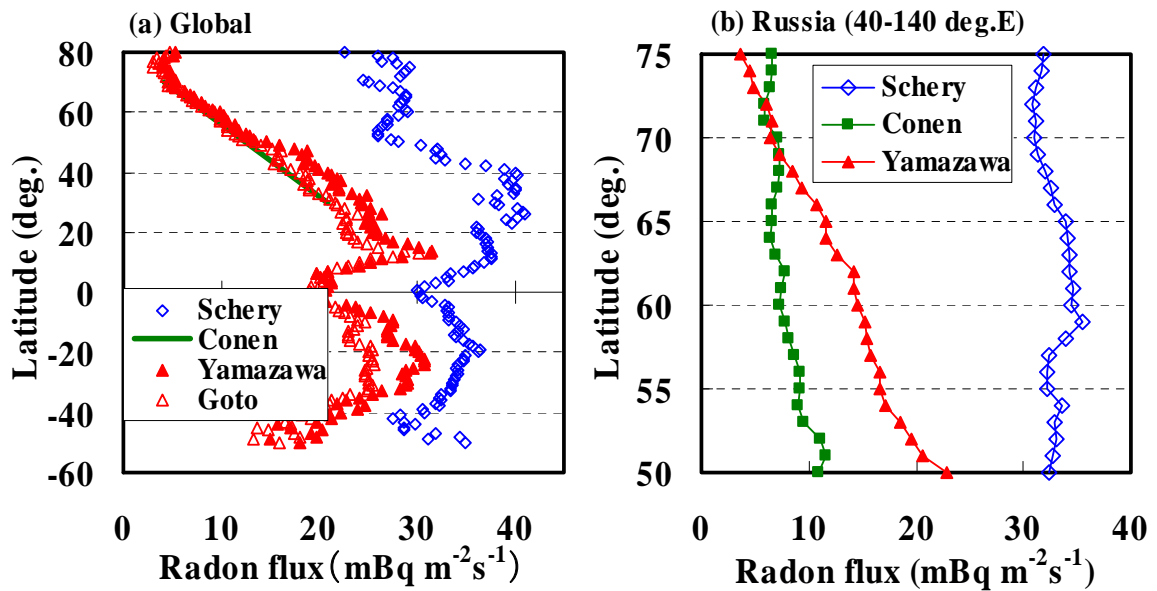

FIG. 2. Zonal mean of radon exhalation flux density for (a) the globe and (b) Russian Federation.

Atmospheric radon concentration observation in the Arctic region

The atmospheric radon concentration data used as reference in the test of radon flux maps were the result of the observation cruises, MR 08-04 and -05, on the research vessel Mirai during the period from mid August to mid November, 2008. The round cruise started from Japan, through northwestern Pacific Ocean and the Bering Sea, to the Arctic Ocean. The vessel was in the Arctic Ocean during whole September in trying to go further northward. Hourly-averaged radon concentration in air at a 12.5 m height was continuously measured with an electrostatic-type radon monitor, which has a 70 L air container equipped with a PIN photodiode for alpha spectrometry. The minimum detection limit of the monitor for hourly concentration is less than 0.1 Bq m^{-3} and the statistical error in the concentration value is about 8% at 1 Bq m^{-3}.

The observed concentration showed clear spatial differences superimposed by seasonal variations. Over the Arctic Ocean in September, the average concentration was 0.5 Bq m^{-3} with a range from concentrations lower than the detection limit to as high as 6.0 Bq m^{-3}. Rises of concentration were observed when the vessel encountered continental air masses. Over the Bering Sea in mid-October, rapid and large variations in concentration were observed, of which mean, minimum and maximum concentrations were 2.0, 0.2 and 6.2 Bq m^{-3}, respectively. The concentration over the northwestern Pacific Ocean in late October and early November showed very large variation caused by long-range transport of radon by synoptic systems. The range of variation was 0.5 to 9.5 Bq m^{-3} with a mean value of 2.9 Bq m^{-3}.

Atmospheric radon transport simulation

Model

Since the model used in the present application is the same with ones described in other literatures [6, 7] only a brief description will be made here. The model is a combination of the meteorological model, MM5, and an Eulerian transport model, HIRAT, for radon and its decay products. These models are off-line connected through a data set of three-dimensional wind, turbulence and precipitation. This model was favourably validated by using surface radon concentrations observed at several stations in the East Asian region [6, 11]. The model domain was set to be a 9072 km square with the horizontal resolution of 72 km to cover the Arctic Ocean, the Bering Sea and the northern part of the Pacific Ocean, and potential radon source areas of Eurasian and North American Continents. The global meteorological analysis data from JMA and the sea surface temperature data from NCEP were used as input data to MM5.

Results

An example of simulation results is shown in Figure 3, in which surface concentrations over the Arctic Ocean calculated by the model for the locations along the cruise trajectory are compared with the observation. Values shown in this figure are 5-hour running averages. The calculation results are for the lowest model layer which is 50 m deep. The calculation results obtained from the three radon flux maps showed temporal variations similar to each other in shape but clearly different in absolute value of concentration. The overall similarity of the calculated concentration variation with the observed concentration implies the validity of the long-range transport simulation. Simulation showed that the increases in the concentration were caused by passages of the vessel through radon-bearing air masses originated from continents. We can deduce merits and demerits of each radon flux map from the degree of agreement and/or disagreement in the absolute value with the observation as discussed in the following section.
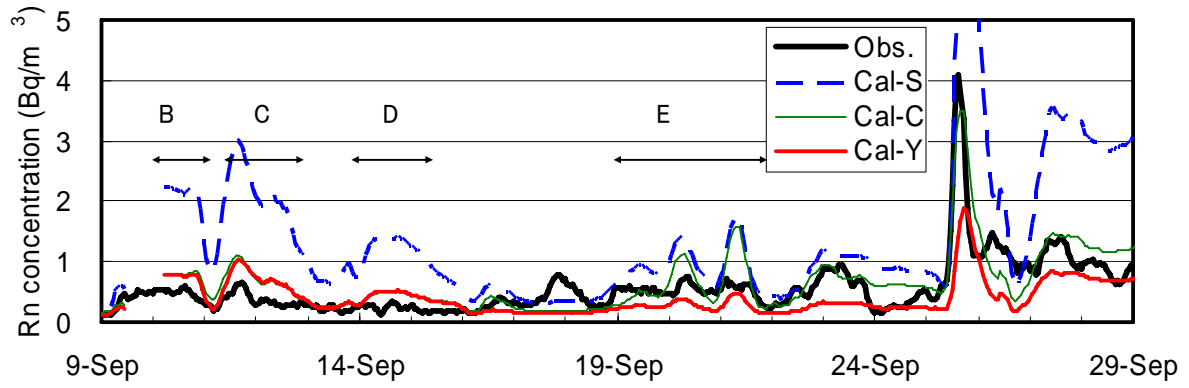
FIG.3. Calculated and observed radon concentration in surface air over the Arctic Ocean.

Discussions

Map performance for source areas

The source areas of air masses which caused observed surface radon concentration variations are shown in Figure 4. Each label in the figure corresponds to a radon concentration peak as shown in Figure 3. Since this analysis of source areas was carried out by repeatedly viewing an animation of surface concentration distribution, the spatial distribution of the source area is qualitative. The atmospheric transport simulations were carried out with the three radon flux maps. Table 1 summarizes ratio of simulated to measured surface radon concentrations for air masses originated from different continental source areas.

For the arctic rim of the Eurasian Continent, that is areas B to D and G to I, it is evident that S-map is considerably larger than unity, implying that the radon exhalation flux density is overestimated. Similar but less serious overestimations by a factor of 1.6 to 2.0 were found for the areas B to D in C-map and Y-map. Radon flux at eastern part of this arctic rim (G and I) of C-map resulted in simulated atmospheric concentration very close to observed one whereas that of Y-map gave underestimation by a factor of about 2. For the Alaskan areas, A, E and F, S-map is evidently better than Y-map although it still resulted in overestimation of surface radon concentration by a factor of 1.2 to 1.8. The under estimation by a factor of 2 to 3 was found for this area in Y-map.

The Okhotsk-Sea and Japan-Sea basin areas, J to M, S-map gave the best simulation results of the surface concentration of radon among the three maps. However, the fluxes at the northern and southern parts of this region are respectively overestimated and underestimated by S-map. It is interesting to notice that, although both C-map and Y-map resulted in underestimation, the underestimation is more serious at the southern part, implying latitudinal gradient of surface radon flux as was found in the case of S-map.

FIG.4. Source areas of radon that have contributed to concentration measured during the cruise observation over the Arctic Ocean and the Bearing Sea.

TABLE 1. RATIO OF CALCULATED TO OBSERVED RADON CONCENTRATIONS FOR THE AIR MASSES ORIGINATED FROM DIFFERENT AREAS.

Area	S-map	C-map	Y-map
A	1.15	-	0.35
B	4.52	1.68	1.61
C	5.35	1.85	1.79
D	5.45	1.97	1.98
E	1.78	-	0.54
F	1.40	-	0.41
G	2.21	1.04	0.51
H	3.85	1.36	0.97
I	2.11	0.85	0.50
J	0.49	0.30	0.22
K	1.56	0.60	0.57
L	0.85	0.46	0.34
M	1.60	0.66	0.49

Flux estimation

From the ratios of measured to observed radon concentration in surface air summarized in Table 1, surface radon exhalation flux density F can be estimated as Eq. (1):

70

$$F = F_{cal} \frac{C_{obs}}{C_{cal}} \qquad (1)$$

where F_{cal} is the flux density of the source area used in the atmospheric transport simulation, C_{cal} and C_{obs} the calculated and observed radon concentrations, respectively. The result of the flux estimation is shown in Figure 6. Since radon measured during a certain period is not only from the areas shown in Figure 5 but a mixture of radon originating from various areas, and the source areas shown in the figure are still a result of preliminary and simple analysis, the source estimation with the above equation resulted in somewhat different values of flux density if the different flux maps were used. The values in Figure5 are averages of results from three flux maps. For example, 4.2 and 72.1 mBq m^{-2} s^{-1} for Areas A and G are averages of values from 2.6 to 6.3 mBq m^{-2} s^{-1} and 69.5 to 77.3 mBq m^{-2} s^{-1}, respectively. For this reason, although the values are shown with the minimum digits of 0.1 mBq m^{-2} s^{-1}, a difference less than about a few mBq m^{-2} s^{-1} might be insignificant.
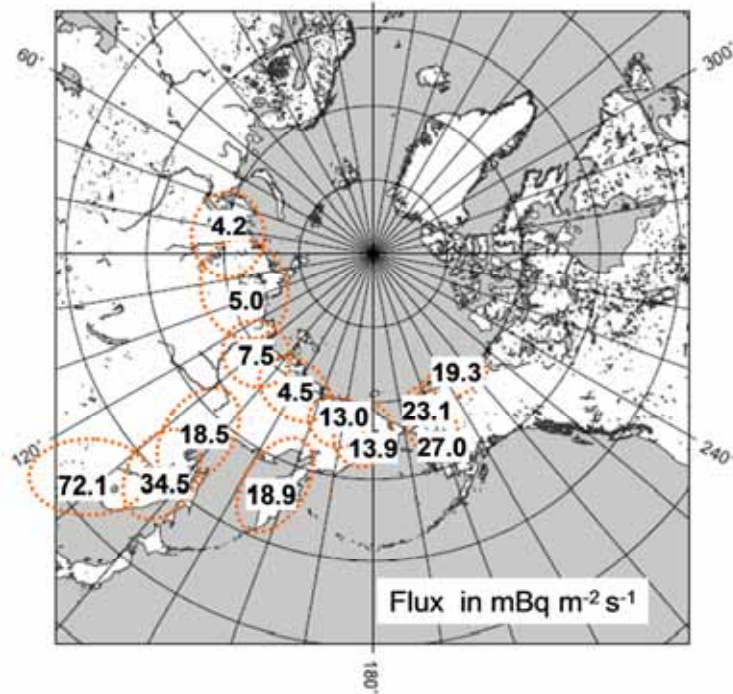
FIG.5. Radon flux estimated in the present study.

The estimated flux density shows clear west-to-east and north-to-south increases. Along the Arctic rim, the radon flux density is around 5 mBq m^{-2} s^{-1} in the longitudinal range from 70° to 120°, 10 to 15 mBqm^{-2}s^{-1} at the east end of the continent and 20–30 mBq m^{-2} s^{-1} in Alaska. This feature is predicted in Y-map although the absolute values are underestimated. In the far eastern region, the radon flux density was estimated to be 20–35 mBq m^{-2} s^{-1} in the latitudinal range from 50°–60°N and more than 35 mBq m^{-2} s^{-1} in the latitudes lower than 50°N. This latitudinal distribution is also qualitatively predicted by Y-map except for the underestimation of absolute values.

Conclusion

Radon flux maps currently available for the Sybrian and East-Asian regions were compared and tested in atmospheric transport simulations with reference data of atmospheric radon concentration observed over the Arctic Ocean and the Bering Sea. The comparison showed that the radon exhalation flux density predicted by the maps are inconsistent in the sense that one map shows clear latitudinal distribution but the others do not, and that the difference in absolute value of flux density between maps is as large as 20 mBq m^{-2} s^{-1} for this area of interest. It was found that there is no single map which is superior to the others in all aspects. Schery's map gives best estimate for the far-eastern region at latitudes lower than 50°N and Alaska while it considerably overestimate the flux density on the Arctic rim of Russian Federation. Flux densities for the Artic rim in the Conen's map were found to be best while its values at lower latitudes were found to be too small. The latitudinal and longitudinal distributions of Yamazawa's map were supported by the observed atmospheric radon concentration, however the absolute value of flux density was indicated to be substantially smaller than that expected by the observation. A preliminary estimation of radon exhalation flux density from the observed atmospheric radon concentration was carried out. The flux density in this area of interest was estimated to be 5 to 70 mBq m^{-2} s^{-1}. Since this analysis is a simple one, there are uncertainties in specifying source areas. An inverse modelling will be the next step of this study. Although the long-range atmospheric model used in this study has been validated, uncertainty inherent in it is also a source of uncertainties of the present analysis.

Acknowledgements

REFERENCES

[1] GOTO, M., et al., Estimation of Global Radon Exhalation Rate Distribution, Proc. 8th Int. Symp. Natural Radiation Environment, Buzios, Brazil, AIP Conference Proceedings 1034 (2007) 169.

[2] YAMAZAWA, H., et al, Radon exhalation flux for eastern part of Eurasian Continent estimated from soil moisture data and its test with observed atmospheric radon concentration, (in preparation).

[3] SZEGVARY, T., et al., Mapping terrestrial γ-dose rate in Europe based on routine monitoring data. Radiation Measurements **42** (2007) 1561.

[4] CONEN, F., ROBERTSON L.B., Latitudinal distribution of ^{222}Rn flux from continents, Tellus **54B** (2002) 127.

[5] SCHERY, S.D., WASIOLEK, M.A., Modeling Radon Flux from the Earth's Surface, in RADON AND THORON IN THE HUMAN ENVIRONMENT, World Scientific Publishing, Singapore (1998) 207.

[6] HIRAO, S., et al., Development and Verification of Long-Range Atmospheric ^{222}Rn Transport Model, Journal of Nuclear Science and Technology, Supplement **6** (2008) 166.

[7] HIRAO, S., et al., Development and Verification of Long-range Atmospheric Transport Model of ^{222}Rn and Lead-210 Including Scavenging Process, Proceedings of 8th International Symposium on the Natural Radiation Environment, (2007) 407.

[8] YAMAZAWA, H., et al., Modeling of atmospheric radon transport in East Asian region, Proceedings of International symposium on Environmental Modeling and Radioecology, (2006) 119.

[9] ZHUO, W., et al., Modeling Radon Flux Density from the Earth's Surface, J. Nucl. Sci. Tech., **44** (2007) 1100.

[10] UNSCEAR, Sources and effects of ionizing radiation, UNSCEAR, New York (2000).

[11] MORIIZUMI, J., et al., Continuous Observation of Atmospheric ^{222}Rn Concentrations for Analytic Basis of Atmospheric Transport in East Asia, Journal of Nuclear Science and Technology, Supplement **6** (2008) 173.

A NOTE ON THE CONTRIBUTION OF TROPICAL REGIONS TO THE EARTH'S RADON FLUX

P. MARTIN
Agency's Laboratories Seibersdorf, IAEA,
Vienna,
Austria

Abstract

According to the radon exhalation flux density model of Schery and Wasiolek [1], the region between the Tropic of Cancer and Tropic of Capricorn contributes about 38% to the total worldwide annual average radon flux. The tropical component is very different between the two hemispheres, being 28% for the northern hemisphere, but 66% for the southern hemisphere. Consequently, an understanding of the factors affecting radon exhalation in the tropics is important if we are to improve modelling of radon behaviour, and the present lack of data from such regions is very unfortunate.

Discussion

A large number of studies have been undertaken in temperate and high-latitude regions on the topic of sources and concentrations of radon and radon progeny in the air, especially indoors. Far fewer studies have been carried out in the tropics and subtropics. The reasons for this include a lower contribution to radiological dose due to the generally greater ventilation in houses in hotter climates [2, 3], and a lower technical capacity and/or requirement to carry out environmental radioactivity measurements in many tropical countries.

The purpose of this note is to point out the importance of the tropical regions to the global radon flux from the Earth's surface, especially in the southern hemisphere. Unfortunately, the usual practice of employing a linear scale on a latitude axis tends to de-emphasize the contribution of the tropics to many surface-area related processes such as radon flux. Figure 1 shows the estimated mean annual latitudinal radon exhalation flux density plotted against latitude. In this plot, the latitude axis is scaled such that the area enclosed by the curve between any two latitudes is proportional to the radon flux (Bq s^{-1}) for that area. The main factor influencing the mean flux density at each latitude is the proportion of the surface with ice-free land. Therefore the Southern Hemisphere, with large oceans and ice-covered land areas (primarily Antartica) contributes only about 26% of the Earth's total radon flux.

The region between the Tropic of Cancer and Tropic of Capricorn contributes about 38% to the total flux. The tropical component is very different between the two hemispheres, being 28% for the northern hemisphere, but 66% for the southern hemisphere.

The radon exhalation flux density for ice-free soil is affected by a number of factors. Of the temporally variable factors, soil moisture has the greatest influence [4]. The relationship is complex, but in general rainfall results in a reduction in exhalation. Most studies of seasonal variability show reductions in the wetter months, i.e. in general winter in temperate zones [5] and wet monsoon in the tropics [6]. This combined with increased ice and snow cover in winter in the high latitudes means that the tropical contribution to a hemisphere's total flux should be higher in winter than in summer. For locations with long dry seasons of very low rainfall and/or wet seasons with highly variable daily rainfall, it is likely that the wet season flux will be not only lower than the dry season flux, but also much more variable [6].

Given these considerations, an understanding of the factors affecting radon exhalation fluxes in the tropics is important if we are to improve modelling of radon behaviour, especially for the southern hemisphere, and the present lack of data from such regions is very unfortunate.
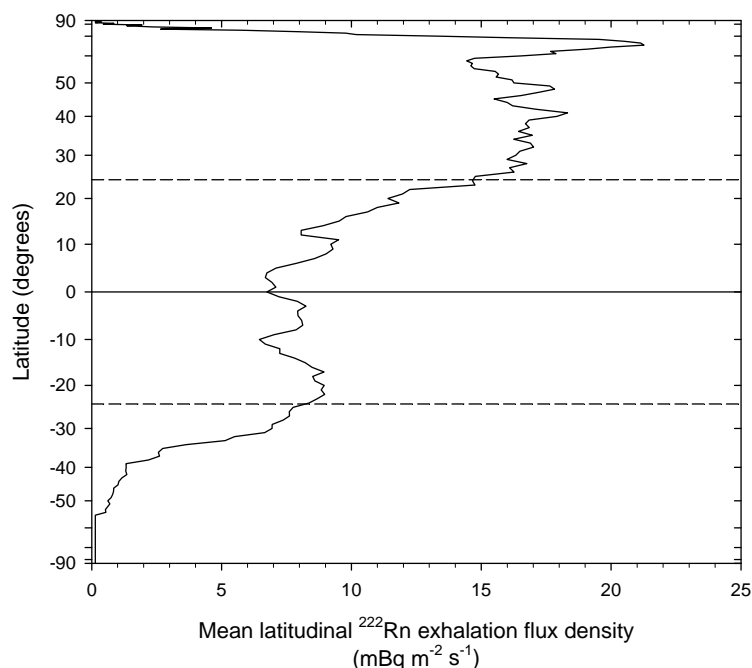

FIG.1. Estimated mean annual latitudinal radon exhalation flux density. Data were obtained from http://www.nmt.edu/~schery/mapdata.html [1] and have a latitudinal resolution of one degree.

REFERENCES

[1] SCHERY, S.D., WASIOLEK M.A., Modelling ^{222}Rn flux from the Earth's surface. In: ^{222}Rn and Thoron in the Human Environment, KATASE A & SHIMO M (Eds), World Scientific (1988) 207–217.

[2] ARAGUNJO, A.M., OHENHEN H.O., OLOWOOKERE S.P., A re-evaluation of the occupancy factors for effective dose estimate in tropical environment, Radiation Protection Dosimetry **112** (2004) 259-265.

[3] ROCHEDO E.R.R., LAURIA D., International versus national regulations: Concerns and trends, Applied Radiation and Isotopes **66** (2008) 1550–1553.

[4] JHA S., KHAN A.H., MISHRA U.C., A study of the ^{222}Rn flux from soil in the U mineralised belt at Jaduguda, Journal of Environmental Radioactivity **49** (2000) 157-169.

[5] WHITTLESTONE S., ZAHOROWSKI W., SCHERY S.D., Radon flux variability with season and location in Tasmania, Australia, Journal of Radioanalytical and Nuclear Chemistry **236** (1998) 213-217.

[6] LAWRENCE C.E., AKBER R.A., BOLLHÖFER A., MARTIN P., ^{222}Rn exhalation from open ground on and around a uranium mine in the wet–dry tropics. Journal of Environmental Radioactivity **100** (2009) 1-8.

222RN OBSERVATIONS FOR CLIMATE AND AIR QUALITY STUDIES

W. ZAHOROWSKI, S. CHAMBERS, J. CRAWFORD, A.G. WILLIAMS, D.D. COHEN,
Australian Nuclear Science and Technology Organisation,
Kirrawee,
Australia

A.T. VERMEULEN, B. VERHEGGEN
Energy Research Centre of the Netherlands,
Petten,
The Netherlands

Abstract

This paper identifies the current major applications for 222Rn in atmospheric research. Two of these applications – air mass transport and vertical mixing in the lower atmosphere – are illustrated by four separate case studies: (1) Using 222Rn to identify the geographical extent, strength and seasonal variability of land and oceanic emissions; (2) Using 222Rn in pollution studies to improve the performance of clustering algorithms used to define source regions; (3) Using near-surface hourly 222Rn gradient observations from towers as tall as 200 m to investigate diurnal dilution effects in the boundary layer with changing atmospheric stability; and (4) Using vertical 222Rn profile "snapshots" measured from light aircraft up to 4 km above ground level to contrast boundary layer entrainment rates between clear-sky, convective and stratiform cloud cases. Lastly, a recent set of 222Rn and 222Rn progeny observations is used to discuss the 222Rn/progeny equilibrium factor and illustrate some common problems associated with using 222Rn progeny as a proxy for 222Rn.

Introduction

222Rn (radon) is a naturally occurring radioactive tracer of air movement at different spatial and temporal scales. At present, the primary applications of radon in weather, climate, air pollution, and other atmospheric research include:

Tracing air mass transpor

This is a well established application of radon as a tracer of local, regional and global air mass transport on mainly synoptic time scales (2–10 days) [1, 2]. Measurement platforms include ground stations and research or commercial ships. The majority of ground stations are located at coastal or island sites; there are relatively few continental sites. Although most ground-based measurements stations are within the boundary layer, some mountain sites probe tropospheric air for at least a fraction of each day.

Tracing vertical mixing in the lower atmosphere

Historically, this was one of the first application of radon as a tracer of air movement (e.g. [3]). Radon profiles made using light aircraft provide insight into vertical mixing processes on a time scale limited by the duration of the flight. In contrast, radon gradient measurements that sample air from tower inlets provide continuous coverage of the full diurnal and seasonal cycles, but are limited in their vertical extent. Given the technical complexities and resources required, extensive vertical mixing datasets are relatively rare.

Calibrating regional fluxes of greenhouse gases

This includes terrestrial emissions of carbon dioxide, methane, nitrous oxide, molecular hydrogen and other gases. The spatial reach of this technique is regional and the temporal scale extends from seasons to years. This application has become increasingly popular since the late nineties, and the first comprehensive publication on the subject appeared in 2000 [4]. This subject is discussed in the current volume by [5].

Parameterisation and validation of transport and mixing schemes in weather and climate models

Early contributions to this field appeared in the late eighties. The research effort includes local, regional, and global circulation models of different complexity (e.g. [6]). A full day session was dedicated to this subject during the meeting as well as a number of contributions in this volume.

This paper focuses on the first two of these applications, by means of four case studies: (1) a fetch analysis conducted for a WMO GAW station; (2) the use of radon as a non-spatial metric for clustering trajectories of atmospheric pollution events; (3) vertical gradient measurements of radon in the surface layer (<50m) and lower boundary layer (<200m); and (4) vertical radon profiles in the lower troposphere using motorised gliders (<4000m above ground level). These examples are based on experimental radon time series and vertical radon gradients / profiles measured in Australia (Cape Grim, Goulburn and Lucas Heights), China (Hong Kong) and the Netherlands (Cabauw). The last section gives a short account of recent work on the ^{222}Rn / progeny equilibrium factor and its variability at a mountain site in Schauinsland (Germany), and provides an example of expected differences in the signal obtained from collocated detectors: a one filter radon progeny detector, and a two filter radon detector.

Air mass origin: analysis of main fetch areas at a WMO GAW station

Identifying the predominant air mass fetch regions of ground stations has long been a key application of long-term radon observations (e.g. [7]). The example reported here focuses on results from Cape Grim, Tasmania (40º40'56"S, 144'41"18"E), a WMO GAW station.

Angular radon concentration distributions at Cape Grim, based on hourly radon observations in the period 2001–2008, are shown in Figure 1a; also indicated are the primary wind sectors, labelled according to local convention. In each 10º wind direction sub-sector the radon concentration distribution is characterised by the 25th, 50th and 75th percentiles (contour lines). The angular radon distribution is highly anisotropic and shows a strong, clearly-defined land influence from the Australian mainland and, to a lesser extent, Tasmania. On the scale chosen for Figure 1a the influence of the oceanic radon source function appears negligible. This extreme example of consistent and distinctive land and oceanic fetch regions is unique among baseline stations around the globe. Despite the compelling evidence of Figure 1a, the oceanic influence on the Cape Grim hourly atmospheric radon signal is not negligible. Figure 1b shows the range of radon concentrations, between the 10th and 90th percentile values (i.e. 80% of observations), in each of the three designated wind sectors: Baseline, Mainland and Tasmania. The following discussion focuses on the Baseline and Mainland sectors only.

In apparent contradiction of Figure 1a, and despite more than two orders of magnitude difference between typical oceanic and terrestrial radon source functions, a significant overlap in the ranges of radon concentration between the Baseline and Mainland sectors is evident in Figure 1b. This indicates that the distinction between radon events originating from these sectors defined by wind direction alone is not clear-cut. It will be demonstrated, however, that this result is an artefact of the event selection technique employed. By further refining the event selection criteria, it is indeed possible to demonstrate a clear distinction between events representing Australian mainland and oceanic fetch regions.
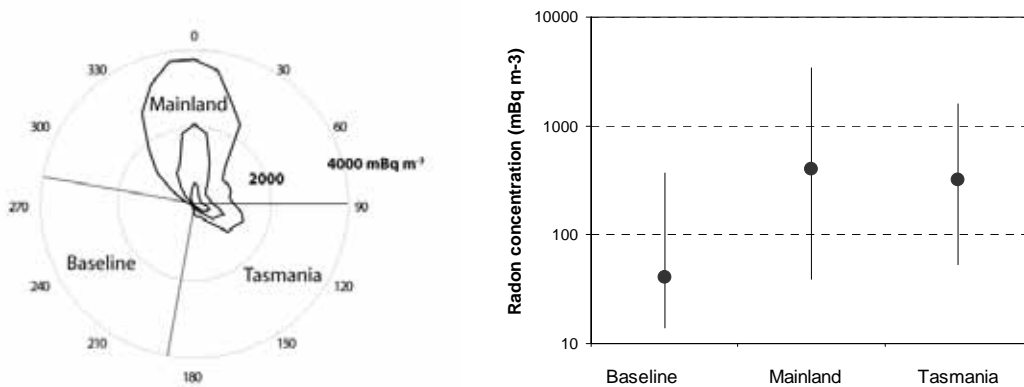
FIG. 1. (a) Angular radon concentration (mBq m^{-3}) distributions in 2001–2008 characterised by 25th, 50th, and 75th percentiles; (b) Radon concentration (mBq m^{-3}) distributions for the three wind sectors at Cape Grim.

The most suitable methods by which to categorise events arriving at Cape Grim from distinct fetch regions are: (a) spatial analysis of back trajectories, which approximate air parcel paths *en route* to the site; and (b) temporal analysis of composite radon concentration distributions in the respective wind sectors (i.e. how radon concentrations evolve on average as a function of time after a local wind direction change to a given sector).

A composite Baseline event from the 2001–2008 Cape Grim radon dataset is shown in Figure 2. Of particular interest is the evolution of radon concentration with time after change to the Baseline sector, which rapidly decreases over the first 24 hours. After approximately one day in the sector, concentrations become both low and relatively stable (note the semi-log scale). This situation persists for the next three days in the sector, indicating that the corresponding air parcels are likely to be in equilibrium with the oceanic radon source function during this period. Events persisting in the Baseline sector for more than one, but less than five days, will henceforth be referred to as "oceanic" events.
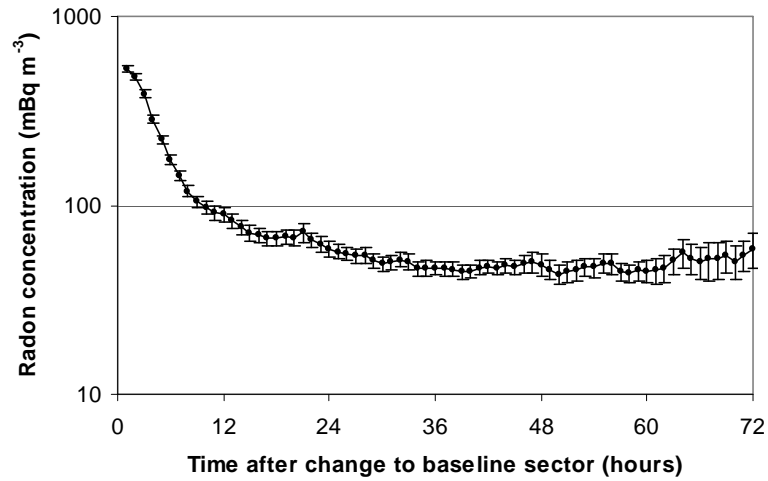
FIG. 2. Radon concentration means in consecutive 1 hour composite periods after a change to the baseline sector based on the 2001–2008 radon dataset.

A detailed examination of back trajectories corresponding to all oceanic events revealed a small number of events (on average 30 per year over the 8-year period) that were affected – to varying degrees – by Australian mainland emissions. Excluding these events provided a far superior approximation of the range of radon concentrations expected in air that is in equilibrium with the oceanic radon source function. Radon concentration distributions corresponding to: (a) all Baseline events (i.e. selected by local wind direction alone); (b) oceanic events; and (c) oceanic events with any Australian mainland influence over the past 10 days removed, are summarised in Table 1, along with a selection of other comparative statistics.

TABLE 1. SEASONAL RADON CONCENTRATION (mBq m^{-3}) DISTRIBUTIONS FOR SELECTED EVENTS IN THE BASELINE SECTOR IN 2001–2008 CHARACTERISED BY THE 10th, 25th, 50th, 75th, AND 90th PERCENTILES. OCEANIC EVENTS ARE DEFINED AS THOSE BASELINE EVENTS WHICH PERSISTED IN THE SECTOR FOR LONGER THAN 1 DAY AND LESS THAN 5 DAYS.

Season (Southern Hemisphere)	Hours	Means	Radon concentration (mBq m^{-3})		Median		
			10th percentile	25th percentile		75th percentile	90th Percentile
All baseline events							
Summer	7818	142	8	19	32	71	351
Autumn	6525	230	18	30	48	143	574
Winter	6491	154	21	31	45	92	338
Spring	7846	144	13	23	38	81	281
All	28680	165	14	25	40	93	370
All oceanic events (all)							
Summer	2258	31	8	16	25	36	53
Autumn	1830	57	14	24	37	55	114
Winter	1815	71	19	28	42	59	161
Spring	2135	47	11	19	30	52	91
All	8038	50	12	21	32	50	87
Oceanic events (air parcels with no contact with land within at least 10 days before arrival at Cape Grim)							
Summer	1947	30	9	17	25	36	52
Autumn	1315	56	13	22	35	53	87
Winter	1189	59	20	29	42	55	98
Spring	1563	47	11	19	30	52	87
All	6014	46	12	20	32	48	76

The most important quantitative aspect of the three Baseline radon concentration distributions shown in Table 1 is that their range becomes progressively narrower with the increasingly restrictive selection criteria imposed on the hourly observations. In fact, 80% of Baseline observations (i.e. with radon concentrations between the 10th and 90th percentile values), are within 356, 75, and 64 mBq m^{-3} concentration ranges, respectively, for the three Baseline sets considered. The same ranges, expressed as a ratio of their respective median radon concentrations, are: 8.8, 2.3, and 2.0. This progressive reduction in the range of radon concentrations confirms the efficacy of the chosen selection criteria in identifying purely oceanic air masses, since the narrower the range of concentrations, the more homogenous the oceanic radon source probed by the observations. By comparison, the similarly normalised concentration range for *all* Mainland observations, and only those events that exclusively traversed the Australian mainland (as detailed below), are 8.5 and 3.1, respectively.

For the Baseline and Mainland wind sectors, the normalised concentration range defined above can be considered to be an index of the homogeneity of the radon source function. Whereas the values of the index for Baseline and Mainland events defined by wind sector alone are similar (8.8 and 8.5, respectively), when the more refined selection criteria are applied the resulting index values for the (exclusively) oceanic and mainland events differ significantly (2 and 3.1, respectively). This difference most likely reflects the fact that the terrestrial radon source is less homogenous than the oceanic source.

The extent of the oceanic fetch region based on the complete 2001–2008 dataset is shown in Figure 3. Fetch regions typical of summer, winter and all observations are contrasted in the

first three panels of this figure. Figure 3d, based on all observations, represents the mean time required for air parcels to reach Cape Grim expressed in units of ^{222}Rn half life. A seasonal dependence is evident between Figures 3a and 3b. In general, winter fetch regions are shifted north towards the Australian mainland compared to the summer fetch consistent with the seasonal migration of the subtropical ridge. Consequently, winter oceanic events are more likely to be affected by Australian continental radon emissions than summer oceanic events. This effect can be better quantified by calculating and comparing the relevant radon distributions. (Table 1).
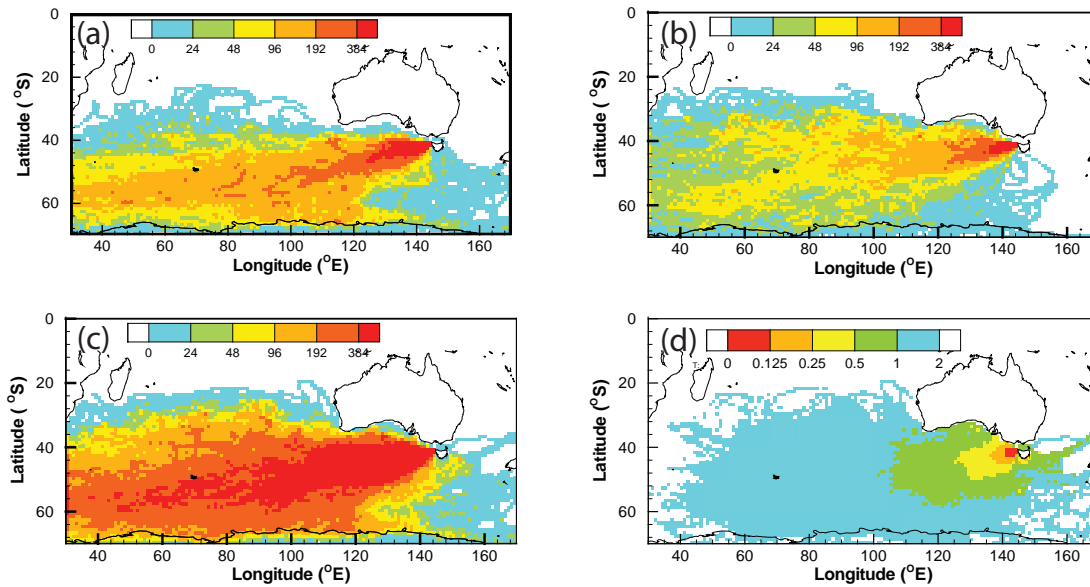
FIG. 3. 2001–2008 seasonal back trajectory [8] density functions for selected Baseline events at Cape Grim. Each density function plot indicates the number of times a 1°× 1° grid cell was traversed by a Baseline event trajectory. Composite density function plots of events persisting in the Baseline sector for more than 1 day, but less than 5 days, are shown for: (a) Southern Hemisphere summer, (b) Southern Hemisphere winter, and (c) all events. Plot (d) indicates the mean time required for corresponding air parcels to reach Cape Grim (in units of $^{222}Rn\,\tau_{1/2}$ =3.82 days).

In contrast to Baseline observations, persistency in the Mainland sector is not an effective selection criterion for isolating Mainland events that have specifically traversed the Australian mainland. The best selection method in this case is one based on back trajectory analysis [8] alone. Analysis of 10-day back trajectories for Mainland events between 2001 and 2008 indicated that only 39% of all designated Mainland events traversed the Australian mainland exclusively. Of the remaining trajectories, 27% were exclusively of oceanic origin, 11% traversed the ocean and Tasmania, while the remaining 23% were of mixed origin.

An important aspect of Cape Grim observations which traverse the Australian mainland is the extent and shape of their potential continental fetch. Figure 4 depicts the 2001–2008 back trajectory density function plots for these events. In contrast to the oceanic fetch, it is obvious that the continental fetch is strongly seasonal. In summer, only parts of Victoria are well represented, whereas in winter a larger portion of continental Australia south of 28ºS is well covered (compare Figure 4a and 4b).
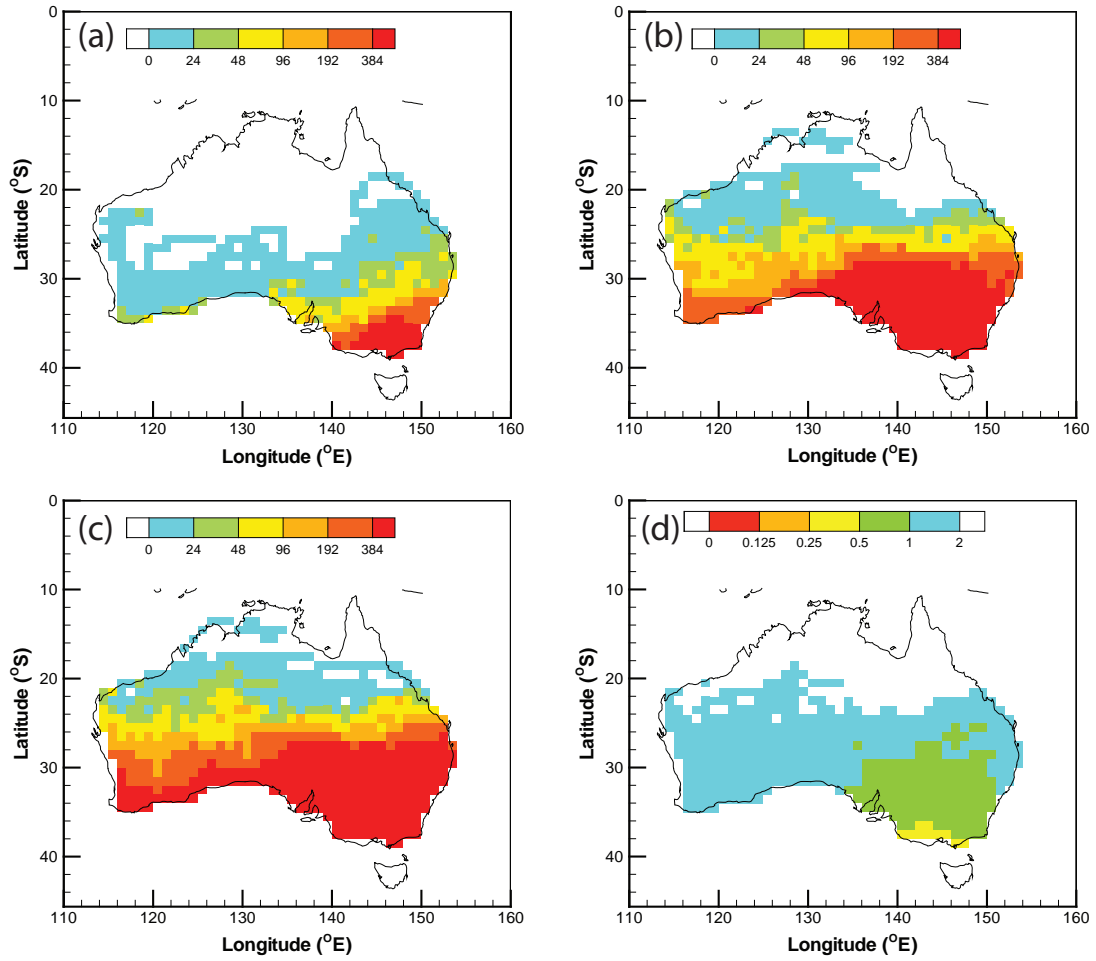
FIG. 4. 2001–2008 back trajectory density function plots for selected Mainland events at Cape Grim. Composite plots, including only trajectories of air parcels that have traversed the Australian mainland, are shown for: (a) Southern Hemisphere summer, (b) Southern Hemisphere winter, and (c) all events. Panel (d) indicates the mean time required for the corresponding air parcels to reach Cape Grim (in units of $^{222}Rn \, \tau_{1/2} = 3.82$ days). For reasons of clarity the density function has not been plotted for oceanic grid cells.

The strength of interaction of air parcels with the Australian mainland is shown using Potential Source Contribution Functions calculated for the lowest and highest quartiles of the corresponding radon concentration distributions in summer (Figure 5a and 5b) and winter (Figure 5c and 5d). See [9] for more details. For example, the PSCF value in grid cell (i, j) for the 1st quartile in summer, $PSCF_{i,j}$, is given by $m_{i,j}/n_{i,j}$ where $n_{i,j}$ represents the number of trajectory end points falling in the grid cell for the summer events, and $m_{i,j}$ is the number of these events corresponding to radon measurements falling in the lowest 25% of the summer radon measurements. From these plots, it is again clear that the widest (and strongest) interaction of air parcels with land emissions on their way to Cape Grim is in winter.
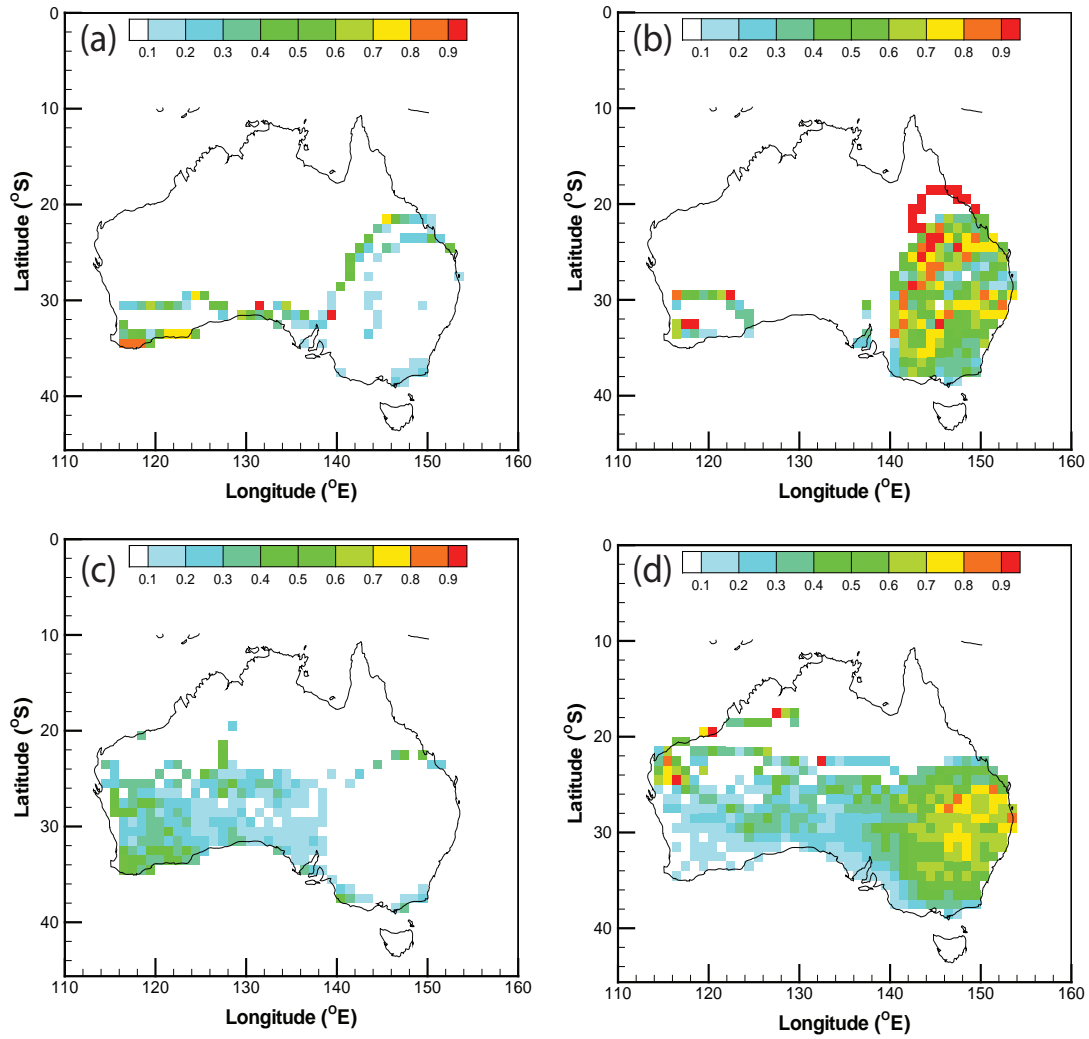
FIG. 5. *Potential Source Contribution Functions (PSCF) [9] for selected Mainland events: Southern Hemisphere summer PSCFs are shown for (a) the 1st and (b) the 4th quartiles of radon observations, and Southern Hemisphere winter PSCFs are shown for (c) the 1st and (d) the 4th quartiles of radon observations. For reasons of clarity the density function has not been plotted for oceanic grids cells.*

Air mass origin: using ^{222}Rn for clustering trajectories of atmospheric pollution events

Air pollution studies frequently use back trajectories to better understand sources of pollution and transport of entrained pollutants, as well as how these change on synoptic, seasonal, and inter-annual time scales. All these factors are important, as they are likely to affect the type and severity of pollution at a receptor site.

In this context, a commonly employed analysis technique is to group trajectories into clusters representing distinct fetch areas and air transport patterns. Clustering is performed numerically. Irrespective of the details of the clustering algorithms employed, each one assumes a specific measure of the distance between two trajectories. The measure (also called metric) is constructed in such a metric space that best quantifies how close (or distant) the two trajectories are. A clustering algorithm thus defines cluster membership by minimising the

distance between trajectories in similar clusters and maximising the separation between trajectories belonging to different clusters.

Commonly used metric spaces for cluster definition employ only spatial variables in two or three dimensions (e.g. [10]). In this section we summarise the recent work of Crawford et al. [11] who proposed to extend the definition of metric space to include hourly observations of radon concentration at a receptor site. The study used data from a 3-year sampling program (2001–2003) of $PM_{2.5}$ aerosols and hourly radon observations at Hok Tsui (Hong Kong). Each $PM_{2.5}$ sample represents a 24-hour integrated measurement, for which the total aerosol mass ($\mu g/m^3$) was determined, as well as source fingerprints using Positive Matrix Factorisation (see also [12]).

The experimental and fingerprint information was used to investigate and compare the performance of four metric spaces, defined in Figure 6. The first two of these metrics (M1 and M2; standard and normalised 2-D spatial metrics), are the most common in the literature. M3 includes height as a third spatial component, and M4 (the present metric of interest) introduces radon as the first non-spatial metric component. Clustering was performed using the Partitioning Around Medoids program [13].

$$D_{i,j} = \frac{1}{n} \sum_{k=1}^{n} d_{i,j}(k)$$

$$D_{i,j} = \frac{1}{n} \sum_{k=1}^{n} \left(\frac{d_{i,j}(k)}{R_{k,x}} \right)$$

$$D_{i,j} = \frac{1}{n} \sum_{k=1}^{n} \left(\frac{d_{i,j}(k)}{R_{k,x}} + \frac{|z_i(k) - z_j(k)|}{R_{k,z}} \right)$$
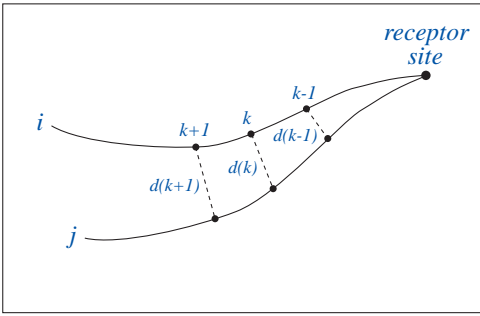
$$D_{i,j} = \frac{1}{n} \sum_{k=1}^{n} \left(\frac{d_{i,j}(k)}{R_{k,xy}} + \frac{|z_i(k) - z_j(k)|}{R_{k,z}} + \frac{|r_i - r_j|}{R_r} \right)$$

FIG. 6. *Equations defining the four metric spaces, where $d_{i,j}(k)$ is the great-circle distance (m) between the two end points of trajectory i and j at time k, $h_i(k)$ and $h_j(k)$ is the height (m) of trajectory i and j, respectively, at the kth end-point, r_i and r_j are the radon (mBq m^{-3}) measurements of trajectory i and j, respectively, and n is the number of hours considered for the back trajectory. Normalisation factors R represent the largest distance or radon concentration change amongst all pairs of trajectories in the dataset.*

The performance of each metric was assessed by investigating the variation of the aerosol mass corresponding to trajectories in each cluster. The principal assumption in the assessment was that the better the cluster identifies a uniform footprint area and transport pattern, the smaller should be the intra-cluster variation of its aerosol mass. Since each aerosol sample spans a full day, 24 hourly back trajectories are calculated, corresponding to each hour of that day. Each hourly trajectory on a collection day was allocated $1/24^{th}$ of the corresponding aerosol mass for that day. This method of allocation is based on the assumption that on diurnal time scales trajectories within a cluster point to areas of approximately uniform aerosol emissions. To strengthen the validity of this assumption, the mean and standard deviations of mass for clusters were taken into account for sampling days in which 13 or more trajectories were classified in the same cluster. The coefficient of variation, the measure used for metric performance, was then calculated as the standard deviation of mass within a cluster divided by the mean mass in the cluster.

Cluster analysis was then performed in the four metric spaces (M1 - M4) using 1, 3, 5 and 7-day back trajectories. The clustering program was run for each of the 16 cases, generating between 3 and 15 clusters for each case. Two criteria were applied to identify the optimum range of clusters. The first criterion is based on the idea of average silhouette width [13]. The second involves the use of the coefficient of variation of the aerosol mass within a cluster. Figure 7 shows the average coefficient of variation of the measured aerosol mass for each of the four metric spaces using 7-day back trajectories. The horizontal axis represents the number of clusters considered. Classifications based on lower number of clusters are characterised by higher variability of total aerosol mass. The quality of the classification is optimal for cluster numbers between 8 and 12. Finally, a visual inspection of the results for 8 to 12 clusters demonstrated that 12 clusters offered a higher degree of detail on separation of air transport patterns, hence 12 clusters were used for the analysis.
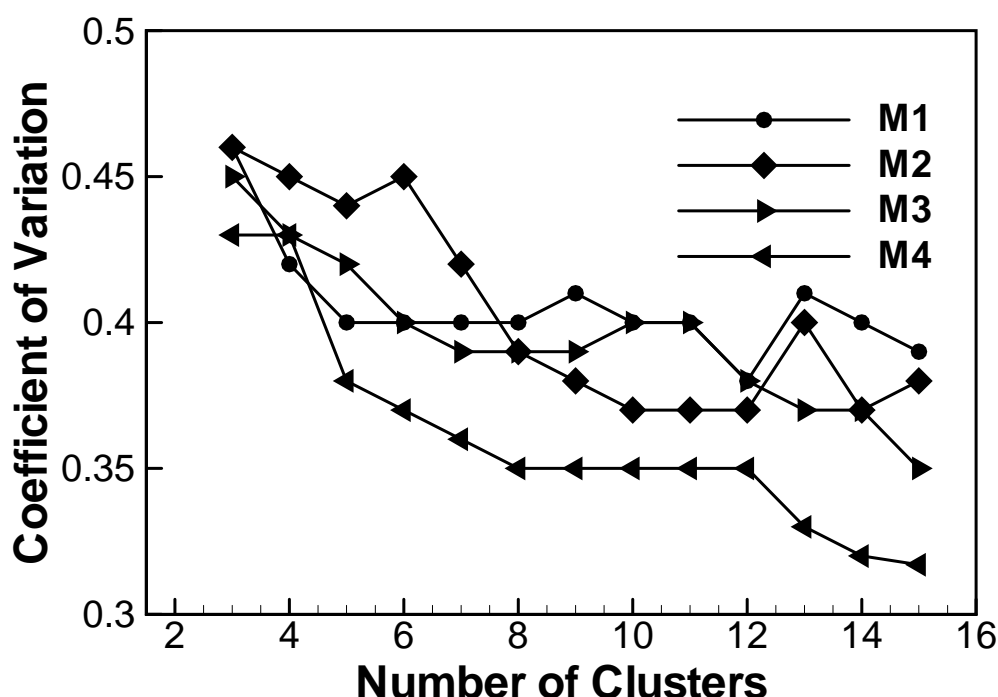
FIG. 7. Average variation of measured aerosol mass for each of the four metric spaces using 7-day back trajectories. Adapted from [11].

Figure 8 shows the average aerosol mass coefficient of variation for the 12 clusters identified using the four metric spaces for 1, 3, 5 and 7-day trajectories. It is clear that M4 results in a significant decrease in the coefficient of variation. Normalising the distance between trajectories at each end point and adding trajectory altitude, as in M2 and M3, respectively, has little impact on the variation of the measured mass within a cluster. Increasing the length of the back trajectories results in less intra-cluster variation. A similar analysis performed on the source fingerprints showed that the optimum back trajectory length depended on the type of aerosol under consideration, which was related to the atmospheric residence time.
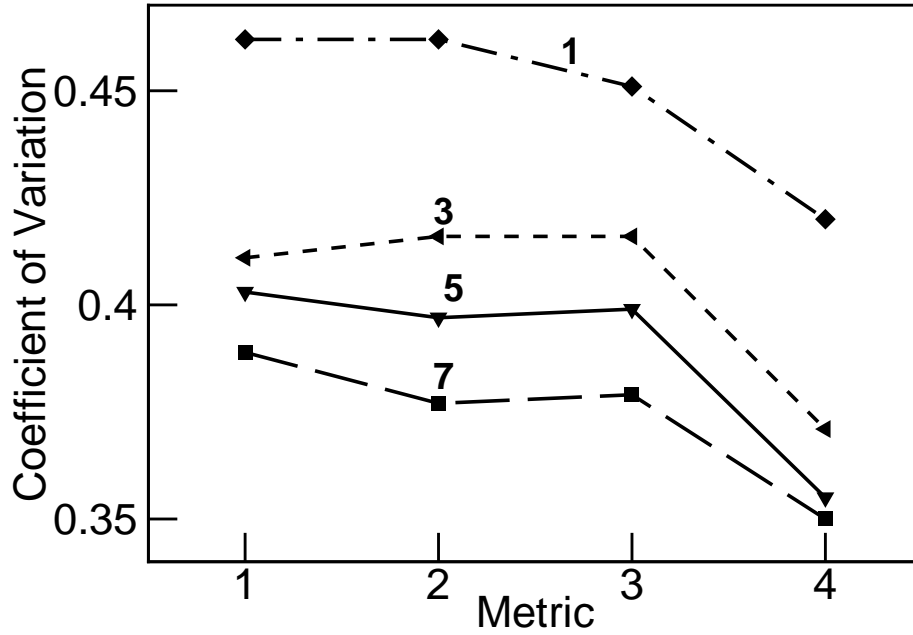
FIG. 8. Average coefficient of variation of measured aerosol mass for clusters defined using four metrics and 1, 3, 5, and 7-day back trajectories (numbered). Adapted from [11].

In summary, the overall performance of the new metric space (M4) which, for the first time, included a non-spatial variable, is better than any of those used previously. The above findings also point to the fact that, for optimum performance of clustering algorithms, the choice of metric space is crucial and that including a suitable tracer with the usual spatial variables should be considered.

Mixing in the lower atmosphere: diurnal boundary layer mixing patterns characterized by ^{222}Rn gradient observations at Lucas Heights (NSW, Australia) and Cabauw (the Netherlands)

Accurate representation of the atmospheric boundary layer, through which most energy, trace gas, and aerosol exchanges take place, continues to be problematic in contemporary weather and climate models. To evaluate, and ultimately improve, boundary layer mixing schemes it is first necessary to construct quantitative measures of vertical mixing and exchange within the lower atmosphere at a temporal resolution sufficient to resolve the diurnal cycle. One way to quantitatively characterize near-surface mixing processes on diurnal time scales is to make continuous, high temporal resolution, radon gradient measurements.

We measured radon gradients at two sites (Cabauw, the Netherlands: 51.971°N, 4.927°E; and Lucas Heights, Australia: 34.053°S, 150.981°E) using pairs of 1500 L dual flow loop, two filter radon detectors [14, 15]. The 20–200 m gradient measurements at Cabauw targeted mixing in the lower boundary layer, whereas the 2–50 m gradient measurements at Lucas Heights targeted mixing in the surface layer. At both sites the radon signal was influenced by atmospheric processes occurring on three distinct temporal scales: seasonal, synoptic and diurnal.

At the Cabauw site, there was a pronounced variability in seasonal median radon concentration at both measurement heights. The lowest concentrations were observed in winter and summer, when the dominant air mass fetch was the Atlantic Ocean, and the highest concentrations were observed in spring and autumn, when a larger proportion of the air mass fetch was over western and/or central Europe. Approximately 40% of air masses arriving at Cabauw in autumn had a predominantly continental European fetch, compared to 26% in summer. Furthermore, on occasions when the air mass fetch was oceanic in spring and autumn, it was often over the North Sea, leeward of the British Isles, where radon concentrations are likely to be perturbed from (larger than) usual oceanic baseline values ($\leq$100 mBq m^{-3}). In autumn, the median radon concentration from the mainland European fetch (i.e. wind sector 50º to 220º) was 3.3 times larger than the corresponding concentration from the Atlantic/North Sea regions. The 90th percentile European radon concentration in autumn (i.e. representing the most consistent terrestrial fetch) was 5360 mBq m^{-3}. By contrast, the 10th percentile concentration from the oceanic sector in summer (i.e. the most consistent oceanic fetch) was 255 mBq m^{-3}.

A pronounced diurnal variability was evident in the 20 m Cabauw observations, characterized by an early morning maximum and early afternoon minimum, reflecting expected changes in mixing depth. Based on seasonal composites, the amplitude of this cycle ranged from 470 mBq m^{-3} in winter to 1420 mBq m^{-3} in spring. The 200 m Cabauw data exhibited a modest mid-morning maximum, consistent with upward mixing of radon from the surface as the nocturnal inversion breaks down.

The 20 m radon signal at Cabauw is affected by both local and remote influences. The remote signal represents the effects of radon source variations in the air mass' recent (<2-week) fetch, due to its 3.8-day half-life. The local signal is a combination of local source variations and diurnal changes in the local mixing depth. Under low wind conditions, local contributions dominate and vice versa. We separated contributions based on arbitrarily chosen wind speed thresholds: low <3 m s^{-1} and high >7 m s^{-1}. Low wind conditions (typical of summer; Figure 9 a) exhibited a pronounced diurnal cycle. At such times nocturnal 20–200 m radon gradients of 2000–5000 mBq m^{-3} were commonly observed due to the suppression of turbulent mixing. Under high wind speed conditions (typical of winter; Figure 9 b), with near neutral stability and a deeper mechanically mixed surface layer, there was little gradient (<500 mBq m^{-3}) or diurnal change in radon concentration. Under these conditions, the primary source of variability in the observed radon signal was due to synoptically driven changes in the recent air mass fetch. Changes in radon concentration due to short term fetch variations in winter can be comparable in magnitude to the largest of the near-surface gradients in winter.

Unambiguously disentangling the synoptic and diurnal influences on the Cabauw radon signal is an important step towards characterising and quantifying diurnal vertical mixing at the site. Once estimates of the regional terrestrial radon source function have been made, the observed radon time series and gradient observations will be compared with a column or regional model under conditions dominated by local and remote sources to evaluate mixing and transport schemes.

A pronounced seasonal variability was also evident in the 2 and 50 m Lucas Heights radon time series for the 2-year period 2006–2007. The lowest median monthly concentrations were observed from November to February. Based on 10-day back trajectory analysis, these months were characterised by synoptic conditions that favoured east to south easterly winds and, given the site's proximity to the coast, land fetches as short as 20 km.
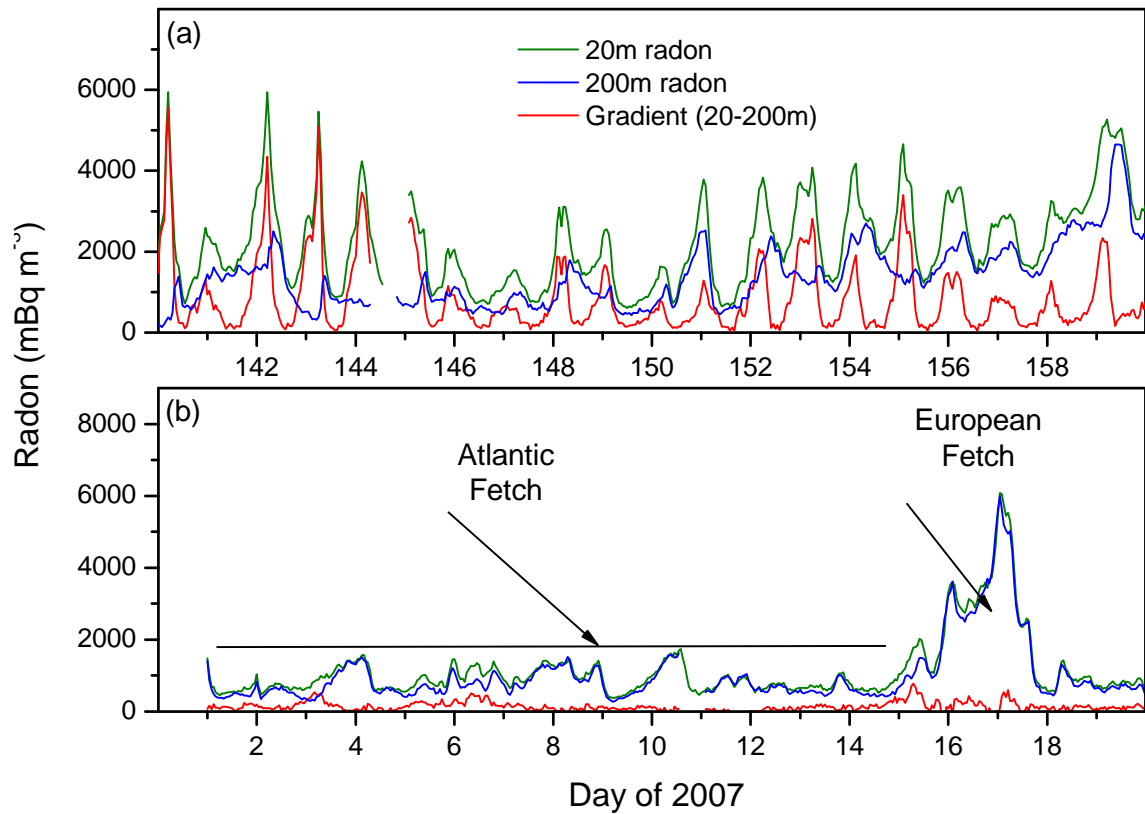
FIG. 9. Comparison of radon observations between 20 and 200 m on the Cabauw meteorological tower: (a) when diurnal influences prevail under low wind speed conditions in summer, and (b) when synoptic fetch conditions prevail under high wind speed conditions in winter. Adapted from [15].

The highest median monthly concentrations were recorded from April to August when prevailing synoptic conditions brought air masses more than 1000 km across south eastern Australia. The amplitude of the seasonal radon cycle at this site, based on median monthly concentrations, was 2350 mBq m^{-3}.

The diurnal cycle of 2 m radon concentrations at Lucas Heights was characterised by peak concentrations near sunrise and minimum concentrations late in the afternoon. The amplitude of seasonal composite diurnal cycles varied from 1200 mBq m^{-3} in summer to 2100 mBq m^{-3} in winter. The comparatively small diurnal cycle at this site is in part attributable to the oceanic influence on measurements, since the site is only 20 km from the coast. In summer, air masses representing the most extensive oceanic fetch had radon concentrations of 170 mBq m^{-3}. Radon concentrations from air masses with the longest land fetches in winter had radon concentrations of 5650 mBq m^{-3}.

The summer observations at Lucas Heights were characterised by light winds and frequently cloudless nights. These conditions favoured the development of strong nocturnal stratification, with nocturnal boundary layers often shallower than 50 m, resulting in 2–50 m radon gradients that exceeded 2000 mBq m^{-3} (Figure 10). Despite the typically longer land fetches in winter at Lucas Heights, stronger winds and more frequent cloud cover often resulted in near-neutral nocturnal stratification and less pronounced diurnal change in mixing depth. Consequently, the 2–50m gradient in winter was often less than 500 mBq m^{-3} (Figure 10).
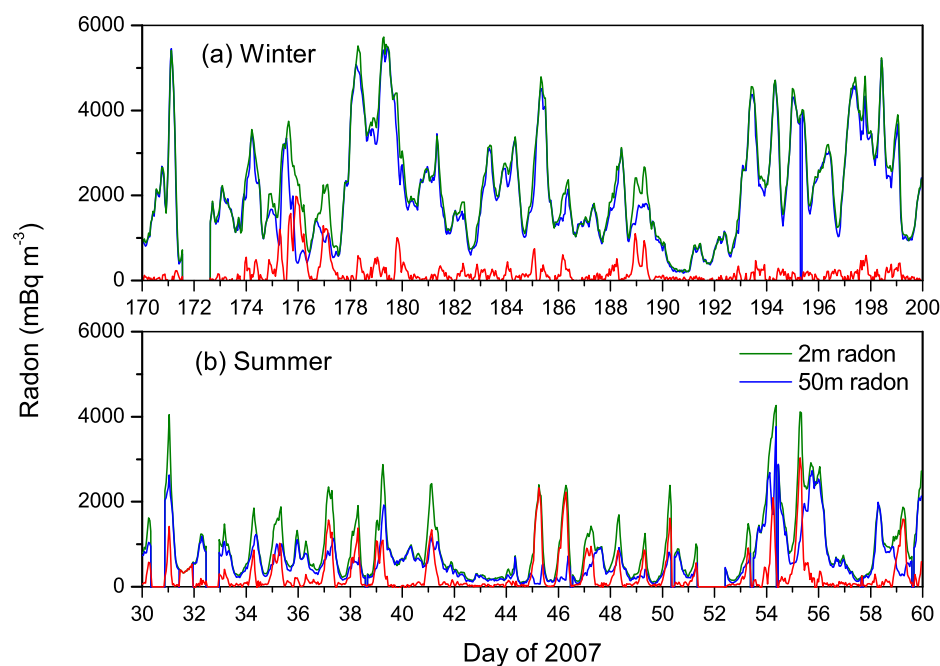
FIG. 10. Comparison of radon observations between 2 and 50 m on the Lucas Heights meteorological tower: (a) when synoptic fetch conditions prevail under high wind speed conditions in winter, and (b) when diurnal influences prevail under low wind speed conditions in summer. Colour code as in Fig. 9.

Mixing in the lower atmosphere: boundary layer mixing studies using airborne radon measurements

Parameterisation of mixing and entrainment processes in the atmospheric boundary layer under clear and cloudy conditions continues to be a topic of intensive research. The accuracy of representations of these processes in regional and global weather and climate models remains a central issue limiting their performance in predicting the distribution of thermodynamic variables and pollutants in the lower atmosphere on diurnal, seasonal and inter-annual timescales. Progress in this field is hampered by a lack of naturally ubiquitous tracer species that are conveniently measurable and have simple and accurately known source and sink functions as well as a spatial distribution that is suitable for unambiguous interpretation of vertical mixing and exchange processes within the lower atmosphere. ^{222}Rn satisfies these requirements over land. Furthermore, radon's half-life is optimum for boundary layer mixing studies, as it is long compared with typical turbulent timescales (<1 hour) but short enough to constrain its concentration in the free troposphere to be typically 2 orders of magnitude lower than its near-surface values.

ANSTO has developed a charcoal trap based sampling system for accurate absolute measurements of atmospheric radon concentrations using airborne platforms. The airborne radon sampler is small and light enough to be mounted in the under-wing pod of a motorised research glider (Figure 11), and can capture up to 10 radon samples per flight. The exposed traps are transported to our α-decay counting laboratory at Lucas heights in Sydney Australia,

where the radon is extracted and its activity determined. The lower limit of detection for this method is estimated to be equal to or better than 10 mBq m^{-3} (less than 5 atoms per litre).

FIG. 11. ANSTO 10-trap radon sampler installed in an underwing pod of the ECO-Dimona instrumented motorized glider operated by Airborne Research Australia.

We present here profiles of radon activity collected in clear and cloudy daytime boundary layers during airborne field campaigns near Goulburn in rural inland New South Wales, Australia [16]. The terrain under the flight pattern was relatively flat, dry and homogeneous, being used mainly as grazing pasture in this low-rainfall region. Flights were conducted using an instrumented motorised glider operated by Airborne Research Australia, a research group attached to Flinders University of South Australia. Other instrumentation aboard the aircraft simultaneously recorded meteorological and navigational quantities to supplement the radon sampling. A 10m mast erected at a nearby farm recorded continuous meteorological quantities and near surface (2m) radon concentrations using an ANSTO 1500 L dual flow loop, two filter detector [14].

Figure 12 shows radon profiles for 19 fully developed clear sky convective boundary layers sampled during the Goulburn campaigns. In all cases, there is a very marked drop in activity from high values within the (surface-coupled) mixed layer to near-zero values in the free troposphere above. This contrast is present under a range of conditions, from light-wind strong convection to high-wind near-neutral boundary layers, and is predominantly a consequence of radon's 3.8 day half-life. In the presence of this large jump, the "top-down" diffusion process associated with entrainment across the interface leads to a large range of radon gradients in the upper half of the mixed layer (evident in Figure 12) that are sensitive to the degree of entrainment.

Venting of air from the mixed layer is further enhanced by the presence of active boundary layer clouds. Figure 13 shows radon profiles for 21 convective boundary layers topped with coupled active (non-precipitating) cumulus clouds, sampled during the Goulburn campaigns. Significant radon concentrations are present throughout the coupled cloud layers, gradually reducing with increasing altitude as the sub-cloud and cloud layer air mixes. The lack of any discontinuity in the profiles at cloud base confirms that the sub-cloud and cloud layers are fully coupled. Given that the aircraft flew mainly in the spaces between clouds, the measured

radon concentrations indicate the extent to which air is being detrained out of the clouds in what is effectively an enhanced boundary layer venting process.
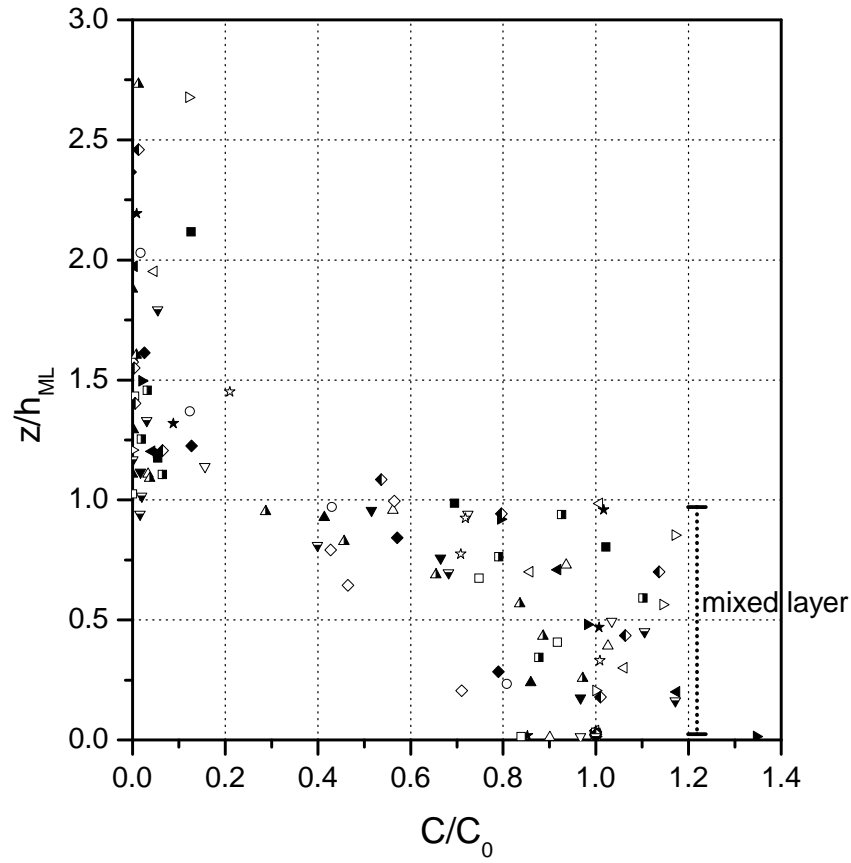
FIG. 12. Profiles of radon activity normalized with surface values, for 19 clear sky convective boundary layers in rural inland New South Wales, Australia. The altitude (z) axis is normalized with the mixed layer depth. Adapted from [16].
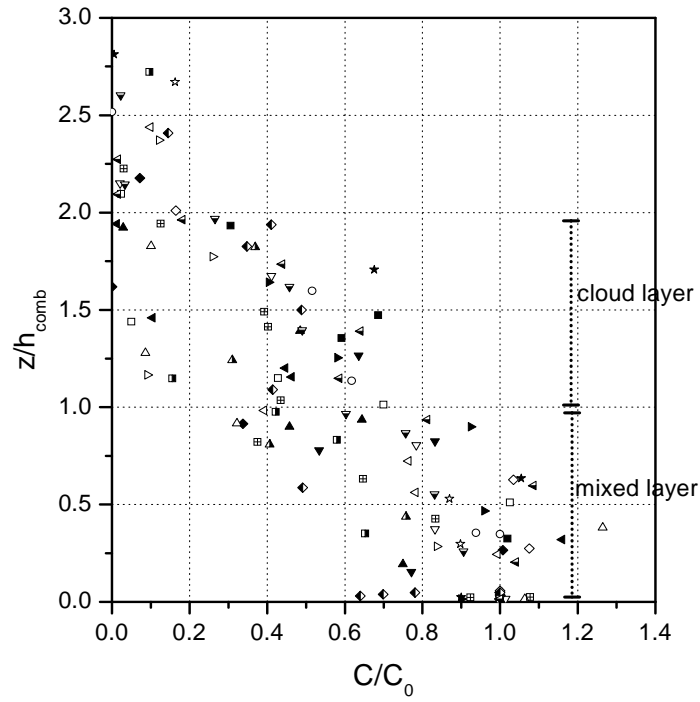
FIG. 13. Profiles of radon activity normalized with surface values, for 21 convective boundary layers topped with coupled active cloud layers in rural inland New South Wales, Australia. The altitude (z) axis is scaled such that the cloud layer falls in the range 1–2. Adapted from [16].

These examples demonstrate that radon is a powerful tracer of mixing and exchange processes in the atmospheric boundary layer. It is hoped that results from these studies will aid in the validation of large eddy simulations and chemical transport models, and ultimately lead to the development of improved parameterisations of vertical transport processes in regional and global climate models.

Disequilibrium between [222]Rn and its short-lived progeny at a ground station

Since the 2003 WMO/GAW-IAEA meeting a number of studies have investigated the relationship between [222]Rn and [222]Rn progeny signals, which is often described in terms of an equilibrium or disequilibrium factor (e.g. [5, 17]).

Large variations in the [222]Rn/progeny equilibrium factor have been observed world-wide. While values from individual studies in the literature vary from 0.2 to 1.0, values are more typically between 0.5 and 0.7 [18]. Consequently, routine calibration of one filter [222]Rn progeny detectors in the field is not only impractical, but almost impossible to implement. Only in a certified [222]Rn chamber, where [222]Rn and [222]Rn progeny concentrations as well as environmental factors like humidity and temperature can be controlled, could such a calibration be conducted successfully [19].

To illustrate this problem, we summarize here the findings of a recent field study on the [222]Rn/progeny equilibrium factor conducted near the top of the Schauinsland mountain in South-West Germany (47°54′15′′ N, 7°54′33′′ E, 1200 m asl) [20]. The objective of the study was to quantify the effects of precipitation (wet-deposition) and the vegetation canopy (roughness-induced dry deposition) on the [222]Rn/progeny equilibrium factor. The vegetation canopy in the fetch region of the Schauinsland summit site is highly heterogeneous, changing

with wind sector from pasture to forest. Hourly measurements of [222]Rn and its short-lived progeny were made using separate detectors between November 2007 and April 2008. The detector inlets were collocated at 2.5 m above ground level. [222]Rn was measured with a dual flow loop, two-filter detector [14] and the [222]Rn progeny with a one-filter detector [21].

Two factors contributed to the observed differences in concentration between [222]Rn and its progeny: (a) the [222]Rn/progeny equilibrium factor; and (b) instrumental effects. A subset of observations was selected during which progeny removal effects were assumed to be minimal or negligible. This involved excluding precipitation events and selecting only observations from wind sectors with low surface roughness (i.e. high aerodynamic resistance). The sector 120°–180° faced a steep valley that was dominated by pasture. It was assumed that [222]Rn and its progeny in air coming from that direction would be in equilibrium when reaching the station. Observations from this sector were used as a reference for observations made under more complex fetch conditions. Differences that then remained between concentrations of [222]Rn and its progeny in this reference sector under non-precipitating conditions (Figure 14) were assumed to be due to instrumental effects.
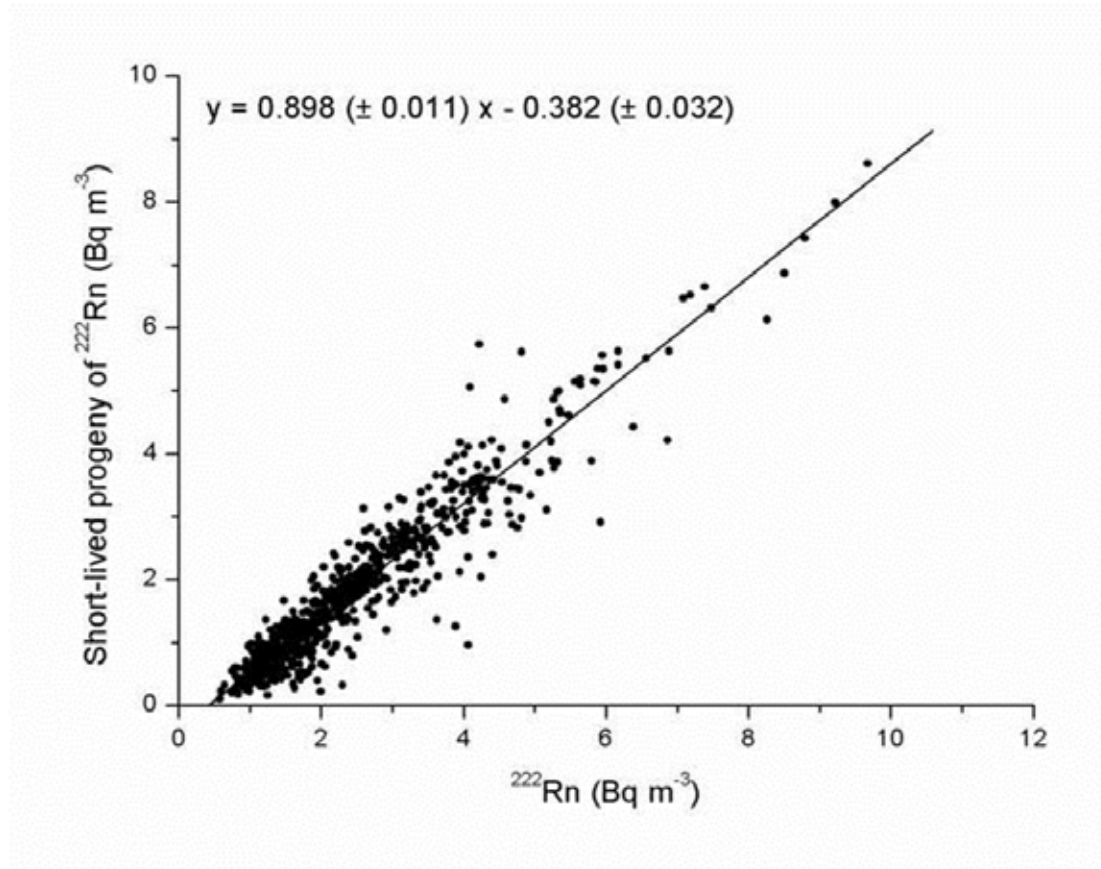
FIG.14. Correlation between [222]Rn and its short-lived progeny concentrations determined by two independent instruments for events with negligible surface wet deposition and wind from the reference sector (values in brackets are standard errors of regression parameters) Adapted from [20].

After categorizing the data by wind sector and meteorological conditions, the effects of precipitation, canopy type and combinations thereof on the [222]Rn/progeny equilibrium factor were quantified for air parcels coming from the two forested wind sectors. The [222]Rn/progeny equilibrium factor calculated for the forested regions varied throughout the observation

period. For non-precipitating conditions, equilibrium factors for the two forested sectors (240°–300° and 0°–60°), were 0.86 and 0.87, respectively, compared to the reference sector. These levels of disequilibria were attributed entirely to dry-deposition of ^{222}Rn progeny on the rough forest canopy. Under precipitating conditions, the average equilibrium factor for the forested sectors was 0.74, compared to the reference sector. This ~13% reduction in equilibrium factor was attributed to wet-deposition effects. While some evidence was found to suggest that increasing precipitation intensity was positively correlated with the ^{222}Rn/progeny equilibrium factor, no clear relationship could be determined which would enable progeny observations to be converted to ^{222}Rn concentrations under those conditions.

In conclusion, the results above indicate that significant disequilibrium between ^{222}Rn and its progeny can be expected to occur on all time scales, including sub-synoptic time scales, and that the degree of disequilibrium is strongly dependent on site characteristics as well as prevailing meteorology.

REFERENCES

[1]   CHAMBERS, S., ZAHOROWSKI, W., MATSUMOTO, K., UEMATSU, M., (2009). Seasonal variability of radon-derived fetch regions for Sado Island, Japan, based on three years of observations: 2002–2004. Atmospheric Environment **32** 271–279.

[2]   ZAHOROWSKI, W., CHAMBERS, S., HENDERSON-SELLERS, A., Ground based ^{222}Rn observations and their application to atmospheric studies, Journal of Environmental Radioactivity **76** (2004) 3–33.

[3]   WIGAND, A., WENK, F., Der Gehalt der Luft and Radium-Emanation, nach Messungen bei Flugzeugaufstiegen. Annalen der Physik, Vierte Folge, Band 86, **13** (1928) 657–686, (in German).

[4]   BIRAUD, S., et al., (2000). European greenhouse gas emissions estimated from continuous atmospheric measurements and ^{222}Rn at Mace Head, Ireland. Journal of Geophysical Research **105** D1 (2000) 1351-1366.

[5]   SCHMIDT, M., et al., Atmospheric Radon measurements in the French greenhouse gas monitoring network (RAMCES), 2009.

[6]   JACOB, D.J., et al., (1997) Evaluation and intercomparison of global atmospheric transport models using ^{222}Rn and other short lived tracers. Journal of Geophysical Research **102** (D5) 5953–5970.

[7]   ZAHOROWSKI, W., et al., ^{222}Rn in boundary layer and free tropospheric continental outflow events at three ACE-Asia sites. Tellus **57B** (2005) 124–140.

[8]   DRAXLER, R.R., ROLPH, G.D., HYbrid Single-Particle Lagrangian Integrated Trajectory, HYSPLIT v4.0 (2003). HYSPLIT (HYbrid Single-Particle Lagrangian Integrated Trajectory) Model access via NOAA ARL READY Website (http://www.arl.noaa.gov/ready/hysplit4.html).

[9] HOPKE, P.K., LI, C.L., CISZEK, W., LANDSBERGER, S., The use of bootstrapping to estimate conditional probability fields for source locations of airborne pollutants. Chemometrics and Intelligent Laboratory Systems **30** (1995) 69–79.

[10] DORLING, S., DAVIS, T., Cluster analysis: a technique for estimating the synoptic meteorology controls on air and precipitation chemistry – method and application. Atmospheric Environment **26A** (1992) 2575–2581.

[11] CRAWFORD, J., ZAHOROWSKI, W., COHEN, D.D., A new metric space incorporating [222]Rn for generation of back trajectory clusters in atmospheric pollution studies. Atmospheric Environment **42** (2009) 371–381.

[12] CRAWFORD, J., et al., Receptor modelling using positive matrix factorisation, back trajectories and [222]Rn. Atmospheric Environment **41** (2007) 6823–6837.

[13] KAUFMAN, L., ROUSSEEUW, P.J., (2005). Finding Groups in Data, an Introduction to Cluster Analysis. John Wiley and Sons, Inc. New York. ISBN 0-471-87876–6.

[14] WHITTLESTONE S., ZAHOROWSKI, W., Baseline [222]Rn detectors for shipboard use: Development and deployment in the First Aerosol Characterisation experiment (ACE 1). Journal of Geophysical Research **103** (1998) 16743–16751.

[15] ZAHOROWSKI, W., et al., (2008). Diurnal boundary layer mixing patterns characterised by [222]Rn gradient observations at Cabauw. American Meteorological Society's 18th Symposium on Boundary Layers and Turbulence, 9–13 June 2008, Stockholm, Sweden.

[16] WILLIAMS, A.G., et al., A mixing and venting in clear and cloudy boundary layers using airborne radon measurements. American Meteorological Society's 18th Symposium on Boundary Layers and Turbulence, 9–13 June 2008, Stockholm, Sweden (2008).

[17] NEUBERT, R., LEVIN, I., ERNESTO KETTNER, E., ZAHOROWSKI, W., A long-term ICP experiment of two frequently-used atmospheric [222]Radon monitors, (2009).

[18] UNSCEAR 2000, United Nations, Sources and Effects of Ionizing Radiation, Annex B (Exposures from natural radiation sources).

[19] WORLD METEOROLOGICAL ORGANIZATION/ GLOBAL ATMOSPHERIC WATCH, 1st International Expert Meeting on Sources and Measurements of Natural Radionuclides Applied to Climate and Air Quality Studies, Report Number 155, WMO TD Number 1201 (2004).

[20] XIA, Y., et al., (2009). Variation of disequilibrium between [222]Rn and its short-lived progeny caused by surface deposition. Submitted to Radiation Measurements.

[21] STOCKBURGER, H., SITTKUS, A., Unmittelbare Messung der natürlichen und künstlichen Radioaktivität der atmosphärischen Luft, Zeitschrift für Naturforschung **21a** (1966) 1128–1132 (in German).

EER IN THE LOW LAYER OF THE ATMOSPHERE

I. BURIAN, P. OTAHAL, J. MERTA
State Institute for Nuclear, Chemical and Biological Protection,
Milin,
Czech Republic

Abstract

The fundamental factor influencing radon (and its decay products) in the lower level of the atmosphere is radon exhalation flux density from the surface. The flux is not dependent only on the concentration of radium in the bedrocks, but also on the physical characteristics of the soil. Many studies were realized in the Czech Republic by our organization (State Institute for NCB Protection, v.v.i.). These measurements could help us understand the behavior of radon and its decay products (RnDP) not only in the free atmosphere, but also for the transport from soil. Many papers describe a possibility of using the dose rate for the estimation of radon exhalation flux density. In this paper we present a set of results and analyses to try to show the limited range of this approach.

Keywords: radon, equilibrium equivalent concentration of radon (EER), outdoor air, solid state nuclear track detector (SSNTD)

Introduction

Radon and its decay products (RnDP) are frequently used as tracers for dynamic processes in the atmosphere to study climatic changes and for construction of climatic models. The source of radon is radium in soil, the flux from the soil to free atmosphere [Bq m^{-2} s^{-1}] can be measured. [1] Unscear (2000) estimated the worldwide mean 0.016 Bq m^{-2} s^{-1}. Many studies attempt to estimate flux by using the results of the dose rate measurement (mostly using planes). These approaches follow the following scheme:

dose rate (gamma) ← ^{226}Ra in bedrock

$\rightarrow$ ^{222}Rn in soil $\rightarrow$ radon exhalation flux density$\rightarrow$ outdoor radon

The first step of the scheme supposes that radium content under the surface is responsible for a part of the global dose rate (in many cases measured 1 m above the surface). The remaining parts of the scheme describe the flow of other dependencies.

Dose rate and radium in soil

About half of the photon dose rate is caused by cosmic rays (this part of the dose rate is changing with altitude). The rest is caused by terrestrial radiation. Using all our results, it is possible to estimate the approximate relation between radium concentration and dose rate: Eq. (1)

$$H = 0.00038 \ a_{m,Ra} + K \qquad (1)$$

(Here, H is the dose rate or kerma rate in μGy h^{-1}, and K=0.19 μGy h^{-1}; mass activity of ^{226}Ra a$_{m,Ra}$ is in Bq kg^{-1}).

A part of our results are shown in the following figure 1 (for lower radium concentrations).

Dose rate [µGy/h]
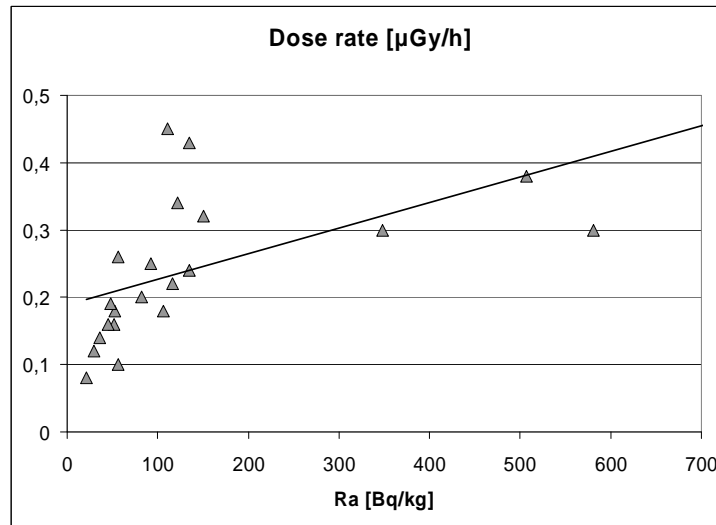
FIG. 1 Relation between content of ^{226}Ra (for lower values and terrestrial gamma dose rate)

For the region of extremely low values, the dependence changes significantly: Eq. (2)

$$H = 0.00233 \ a_{m,Ra} + 0.028 \qquad (2)$$

But the variance is similar like above. The graphic presentation of these results us in the Figure 2.
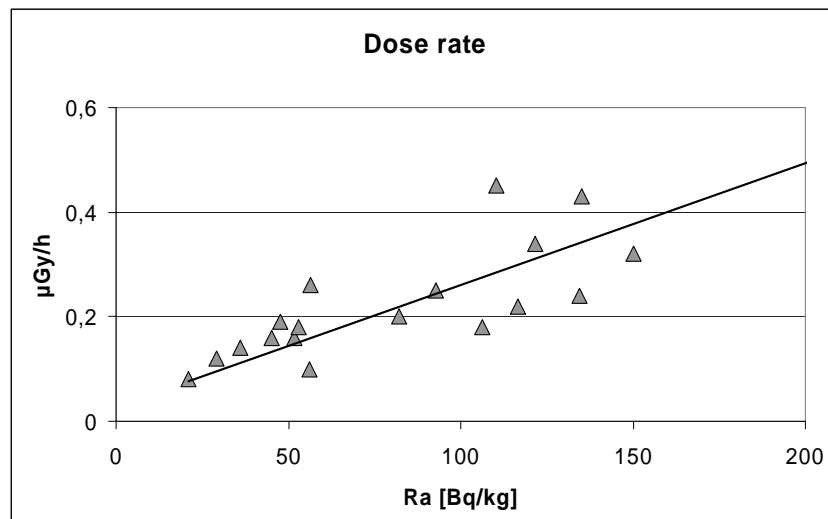
Dose rate

FIG. 2. Relation between more content of ^{226}Ra (the lowest values) and terrestrial dose rate.

Radium content and radon in soil concentration

Radium in bedrock is distributed heterogeneously linked with specific bedrock type, its geographical and stratigraphical position. Moreover, a fundamental factor influencing the radon transport is diffusion length (settled by porosity). In the layer close to the surface, the diffusion length is influenced by water content. The radon concentration, therefore, changes with time [2].

The reason for this is the solubility of radon in water: Eq. (3)

$$k = 0.106 + 0.401 \exp(-0.051T) \tag{3}$$

k – the coefficient of solubility of radon in water is dependent on water temperature T [$°C$].

The ratio of radon in soil and mass activity of mother radium is 690±500 in Bq m^{-3}/ (Bq kg^{-1}) = kg m^{-3} for all 24 results. When some outliers are excluded, the spread decreases (580 ± 280 for 21 results). The mass activity of radium 150 Bq kg^{-1} corresponds to the radon concentration (in soil) 100 kBq m^{-3}.

Figure 3 below shows the results of measurement of both quantities for lower values only.
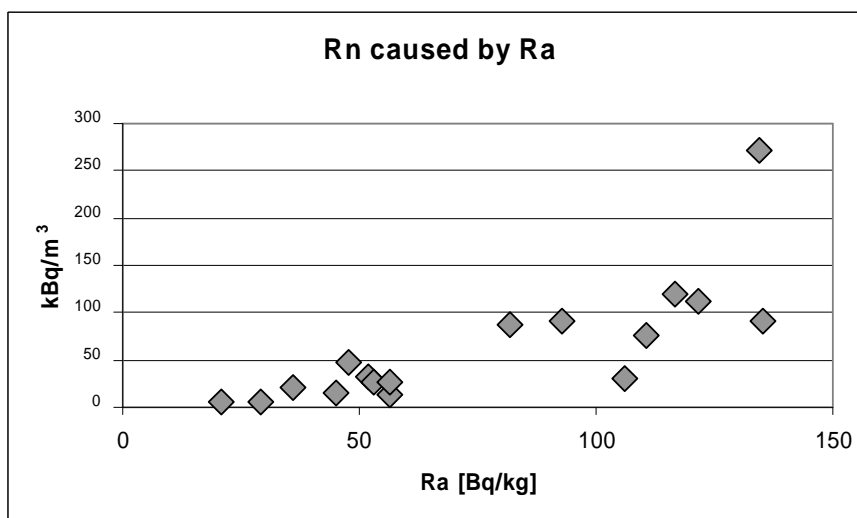
FIG. 3. Relation between concentration of radium and content of radon in soil.

Radon concentration in soil and radon flux

In many cases, we compared radon in soil concentration with radon exhalation flux density. In the Figure 4, the point corresponds to the third quartile from 15 measurements of radon in soil concentration and the average of two radon exhalation flux density measurements.
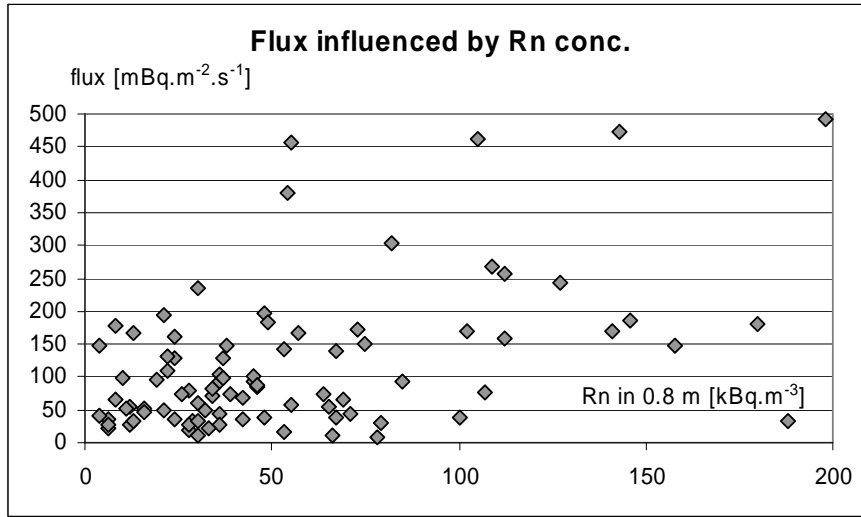
FIG. 4. The comparison of radon flux and concentration of radon in soil.

The ratio of flux / radon concentration is 3.4 ± 4.8 in (mBq m^{-2} s^{-1}/ kBq m^{-3}) = μm s^{-1} for all 93 results, after excluding two outliers 2.8 ± 2.6 in the same units.

For the most frequent region of radon concentration of 20–200 kBq m^{-3}, the ratio is 2.3 ± 2.0 (μm s^{-1}) for 77 measurements.

Unfortunately, we found the same dispersion in the case of more measurements. Every point in Figure 5 represents an average of 8 measurements of radon exhalation flux density:
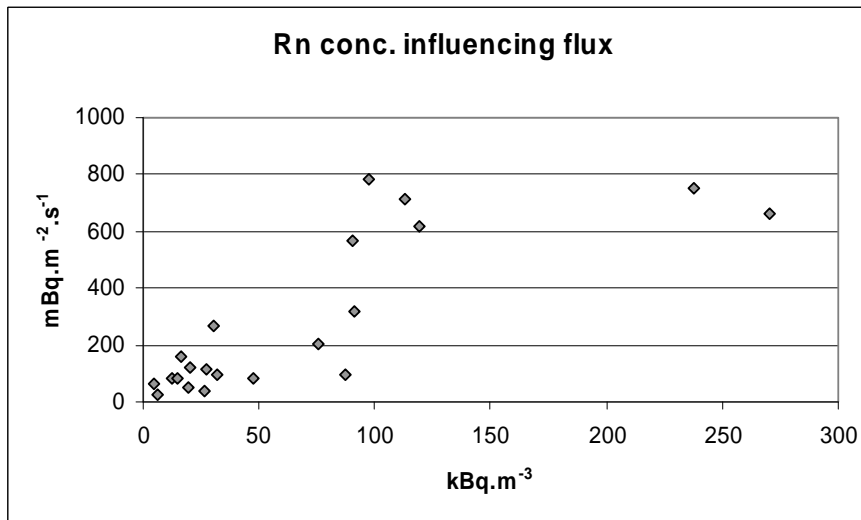
FIG. 5. The results of comparison between average radon flux (8 measurements on the same place) and concentration of radon in the soil.

The relation 5.04 ± 2.87 μm s^{-1} (excluding one outlier leads to 4.69 ± 2.35) is again connected with enormous SD.

The flux is, in our opinion, influenced by several parameters. First of all, permeability of soil depends on the soil's moisture (changing when RH is not stable). What is important for flux is the difference of barometric pressure and pressure of air in the soil.

The flux not only changes by location, but also in time. We measured the flux 15 times over the course of 30 hours and the values ranged between 48 to 120 mBq m^{-2} s^{-1}. At the same time, radon in the soil was only changing from 110 to 150 kBq m^{-3}.

Radon exhalation flux density and outdoor concentrations

Our measurements were realized in many circumstances.

One of the very differing locations was deponies of the former uranium mill. Here, the flux was, of course, very high – 74 000 mBq m^{-2} s^{-1}. The results of EER measurement were 1.0 ± 0.2 Bq m^{-3} in 2009. Similar results were gained in the past by different methods – continuous, integral.

The other point was near the neogenic sediments of the Wienas basin (calcium sands and clays) near the city of Brno. Similar to the first case, the points of sampling were also within a radius of 1 km. EER values are described by a value of 12.7 ± 2.42 Bq m^{-3}. Here radon exhalation flux density was relatively low – 71 mBq m^{-2} s^{-1}, so according to the first of point of view, there is no reason for the elevated values.

What was the reason for such absurd results? The difference in weather – in the first case, it was sunny and moderately windy, in the second case it was foggy and no wind. One can deduce that the atmosphere behavior plays a more important role than local "soil" parameters.

We registered similar anomalies many times and some of them are described below.

The influence of presence or absence of radon exhalation flux density was studied in another measurement set: Near the town Jachymov, in a valley surrounded by uranium tailings, full of radium, originally from the 1950s (flux up to 600 mBq m^{-2} s^{-1}) only insignificantly elevated values of EER were registered (the mean was 7.4 Bq m^{-3} at 7 a.m.).

The other measurement set was organized around a lake with surface area of 8 000 000 m^2. In this case, no difference was registered between results in the case of the leeward side and the windward face was seen.

Radon and EER in the lower layer of the atmosphere — results of different measurements

The concentration of radon and RnDP are change dynamically during the day. Seasonal variation is also frequently observed. It is caused by the changing state of soil (moisture, pressure) and the changing state of the atmosphere. According to [3] E.M. Scotta (2003), the lower level of the atmosphere is comprised of the roughness layer (0–1 m), the surface layer (1–200 m), and the transition layer (200–2000 m). The thickness of layers is different, influenced by the character of surface protrusions.

Figure 6 shows the high dependence of radon concentration in roughness and surface layers.

Here the measurements were realized with the help of SSNTD in diffusion chambers, so the results are valid for radon gas (many of prior number are EER values). Diffusion chambers hung on a 40-metre-high chimney in the spring of 2008.
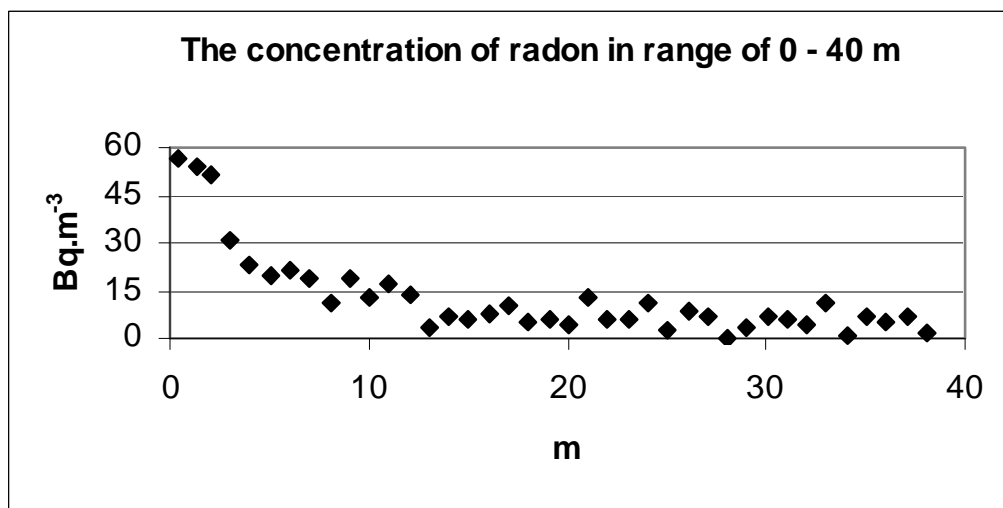

FIG. 6. *The high dependence of concentration of radon in the low level of atmosphere.*

Not only vertical tendency was studied. EER was measured in towns throughout the Czech Republic at 7:00 a.m. in the roughness layer. The average of all values was 2.7 ± 1.4 Bq m^{-3} (3 measurements). We have registered a medium increase of EER values throughout the decades, but this value is lower than the average found in 1986 (5.5 Bq m^{-3}) – it was calculated for four seasons.

Monthly measurements of EER, which were continuously monitored using TS-96, were realized in three towns of our country. Figure 7 shows relative changes - the result was divided by the global mean in this location. Since the distance is 300 km between two regional cities, one could be surprised that the fluctuations in concentrations are nearly identical when concentrations themselves vary.
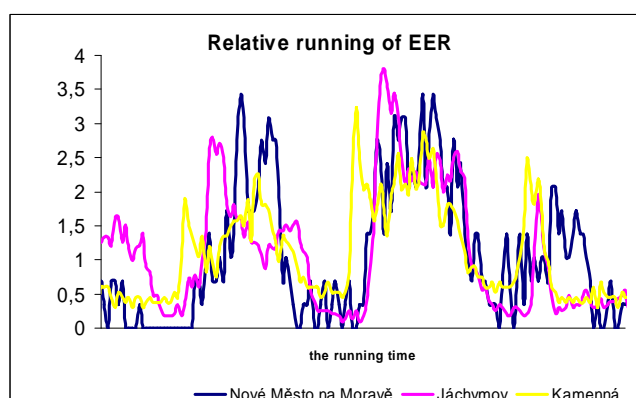
FIG. 7. *The weighted values of EER in three towns in the Czech Republic.*

Conclusion

It is nearly impossible to estimate the radon (or EER) outside in context with dose rate in a local setting. All our results show that throughout the transformation, the relationship between the dose rate and outdoor radon is very uncertain. It is of course possible, that these relations are caused by complicated geologic structures of the Czech Republic.

Maybe the correlation between the radon exhalation flux density and the rate is possible on a global scale or in the case of a simple geologic structure (selected cratogenic areas, on smaller scales of the sedimentary basin)**.**

REFERENCES

[1] UNSCEAR, Sources and Effects of Ionizing Radiation. United Nations Scientific Committee on the Effects of Atomic Radiation Report to the General Assembly with Scientific Annex B: Exposure from natural sources. United Nations, New York, NY, (2000).
[2] NEZNAL, M., NEZNAL, M., Measurement of radon exhalation rate from the ground surface: Can the parameter be used for a determination of radon potential of soils? Radon investigations in the Czech Republic IX (2002) 16–25.
[3] SCOTT, E.M., Modelling radioactivity in the environment, Radioactivity in the environment, **4** (2003), Elsevier.

LOW LEVEL MEASUREMENT OF [222]RN IN THE ATMOSPHERE IN THE FRAME OF THE GLOBAL ATMOSPHERIC WATCH PROGRAMME

G. FRANK, T. STEINKOPFF
Deutscher Wetterdienst,
Offenbach,

J. SALVAMOSER
IGU, Institut für angewandte Isotopen-, Gas- und Umweltuntersuchungen,
Wörthsee,

Germany

Abstract

[222]Rn is a useful tool evaluating air transport models and identifying atmospheric exchange conditions. In conjunction with other natural and artificial radionuclides, such as ^{210}Pb and [7]Be in aerosols, ^{3}H in hydrogen or in water, ^{14}C as [14]CO_2 and [14]CH_4, [85]Kr and ^{133}Xe, also [222]Rn data are useful in long range transport studies. The sampling locations are supposed to be without local [222]Rn sources. In the frame of the Global Atmospheric Watch Programme of the World Meteorological Organization measurements are also performed by the German Meteorological Service.at the environmental research platform Schneefernerhaus UFS SFH (2,650 m a.s.l.) below the top of Germany's highest mountain Zugspitze. A measuring device was constructed being able to measure concentrations of 30 mBq m^{-3} based on the principle of electrostatic deposition of [222]Rn daughters. The air is pumped through an aerosol filter which removes the ambient progeny of [222]Rn, thus only air and gaseous radon passes. The air then flows continuously through a measuring chamber with a rugged silicon surface barrier as detector. In a strong electric field the decay products of [222]Rn, [218]Po and [214]Po are deposited at the detectors surface and its α-decay is measured. The measuring device is operated automatically with a measuring interval of two hours. Temperature, pressure and humidity are recorded in 10 minute intervals. It was demanded from the system to achieve a minimized manual handling and an easy way of calibration. The sensitivity of the instrument is dependent on the volume of the decay chamber, the chamber and detector geometry; progeny capture efficiency, humidity, sampling interval and counter efficiency. The calibration procedure was performed using a [222]Rn calibration source traceable to a primary source. The sensitivity accuracy and the instrumental background were evaluated.

The global atmospheric watch program of the world meteorological organization

Established in 1989 by the Eleventh World Meteorological Congress (Cg-XI) as a major priority programme, the "Global Atmospheric Watch (GAW)" programme is one of "World Meteorological Organization's (WMO)" most important contributions to the study of environmental issues in the post-UNCED period (United Nations Conference on Environment and Development, 1992). The mission of GAW is to make reliable, comprehensive observations of the chemical composition and selected physical characteristics of the atmosphere on global and regional scales.

During the past three decades, the largely separate communities making observations and modelling of natural and partly artificial radio nuclides and of chemical constituents began to merge. Thus, at many of the Regional, Global and Contributing-partner stations in the GAW network of the WMO, radio nuclides are measured.

As a result of a meeting in 2004 [1] the current situation with respect to measurements of natural radio nuclides and modelling of their global cycles was documented and recommendations for improving sources, measurements and modelling were made mainly that WMO/GAW, WCRP and IAEA should emphasize to their communities the need for better

knowledge of ^{222}Rn flux from Earth's surface, more accurate atmospheric ^{222}Rn flux measurements and to encourage in Africa and South America measurements of ^{226}Ra in rocks and surface soil and estimation of ^{222}Rn exhalation, flux and transport in the atmosphere.

Measurement of ^{222}Rn in the atmosphere

A very sensitive method for ^{222}Rn measurement is the sampling of Radon with enrichment, adsorption and desorption on activated charcoal followed by scintillation counting or proportional counting. But this method is complicated to realize for continuous measurements. Other methods are measuring the activity of the decay products of ^{222}Rn.

One-filter method

This method is often operated by working level monitors and for radiation protection applications. ^{222}Rn concentration in air is approximated by the measurements of specific radioactivity of ^{222}Rn daughters attached to atmospheric aerosol particles. Air is pumped through an aerosol filter, the decay products of ^{222}Rn are filtered, and α-particles from the α-decay of ^{214}Po and ^{218}Po or γ- or ß-decay of ^{214}Bi or ^{214}Pb, attached to aerosols are counted [2]. With this method there are site- and experiment-specific assumptions necessary regarding equilibrium of ^{222}Rn concentration and the aerosol specific radioactivity [2, 3].

The measurement of natural specific activities of gaseous ^{222}Rn demands for methods with higher sensitivity and nuclide specific separation. The aim for ^{222}Rn measurements is the direct measurement of ^{222}Rn and in addition the easy calibration with ^{222}Rn sources traceable to a primary standard.

Two filter methods

In this method the air passes two filters, a first filter retains ^{222}Rn decay products, in a decay chamber ^{222}Rn decay products ^{218}Po, ^{214}Pb, ^{214}Bi and ^{214}Po are built up and sampled on a second filter where they are measured with different detectors.

The measured activity is dependent from the air velocity, the volume of the decay chamber, the adsorption rate of decay products on areas inside the chamber, aerosol retain of filter and sensitivity of the detector.

^{222}Rn detectors deployed up to now at the WMO/GAW stations are based on the counting of the two alpha emitting ^{222}Rn progeny ^{218}Po and ^{214}Po collected as aerosol on a second filter, counted with a scintillation photo multiplier tube or a surface barrier detector assembly. These instruments are of two types: one flow loop or dual flow loop and are described in more detail below.

One flow loop, two-filter detector:

The instrument [4, 5] can be configured with a 500 or 1,000 litre delay chamber and set up to 60-min or 30-min sampling and counting. Sample air is pumped through a decay chamber at flow rates ranging from 350 to 400 litres min^{-1}. For a 60 minute sample collection followed by a 60 minute alpha count, the lower limit of detection is equal to about 55 mBq m^{-3}. The response time of the detector is about 60 minutes.

Dual flow loop, two-filter detector:

The detector [6] is a major redesign of an earlier instrument [7]. It aims at measurement of very low levels of ^{222}Rn and low power consumption which might be an essential requirement at remote locations. Two air flow paths are used to separate the high flow rate required in the original two-filter design to prevent loss of ^{222}Rn progeny to the walls of the detector, and the low flow rate needed to change the air sample in the instrument. The high flow rate path is achieved by using a second blower inside the chamber and results in the progeny being transported through the second filter within about a minute of their production. The change of the air inside the detector is set to be completed on a timescale of about half an hour to ensure that the overall time resolution of the instrument is less than 45 minutes. There are three detectors of this type deployed at the GAW stations (Cape Grim, Cape Point, and "Mauna Loa Observatory (MLO)". The lower limit of detection for a 60 minutes count depends on the volume of the main detector delay chamber, and is about 20 mBq·m^{-3} and 10 mBq·m^{-3} for MLO and Cape Point, and Cape Grim, respectively.

Continuous direct measurement of ^{222}Rn

It was our aim to develop a system which enables us for the direct and continuous measurement of ^{222}Rn. The measuring system employs the electrostatic collection of the alpha emitting ^{222}Rn decay products ^{218}Po and ^{214}Po produced in the measuring chamber followed by alpha particle spectrometry using a surface barrier detector. Figure 1 shows the basic principle of the sampling and measuring procedure. In our system ^{218}Po and ^{214}Po are directly measured. This is in contrast to measuring systems which measure the decay products being attached to aerosol particles and then accumulated on filters. The electrostatic deposition is in principle a well known method. A comparable system with electrostatic deposition and α-counting is used since years in our laboratory for measuring traces of ^{226}Ra in water sample through measuring its daughter ^{222}Rn. In this case a smaller counting chamber is used. Water samples are degassed, stored for a time and the built up ^{222}Rn is detected. A detection limit of <10 mBq L^{-1} for ^{226}Ra is reached. This system and its conditions was the pattern for the low level ^{222}Rn system developed here.
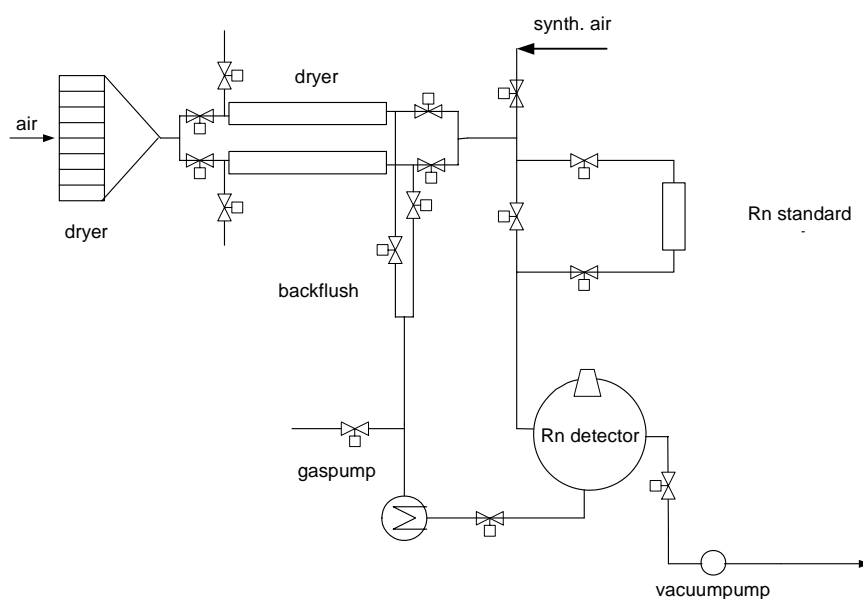
FIG. 1. Schematic diagram of the ^{222}Rn low level detection system.

The air is sampled through an aerosol-filter in order to remove aerosols and the radon daughters attached to aerosols. Moisture in the sample air is carefully removed by a more step drying system. In a first step the incoming air is kept at constant level with a heat exchanger. At the Zugspitze temperatures range from -40°C to +20°C at very different humidity are to be expected. In the further steps air is dried to a partial pressure of <1 mbar.

Finally a ^{226}Ra free drying agent was used to remove still remaining parts of water vapour. Stable conditions are important for counting. Only air with gaseous radon will be allowed to enter the sensitive volume of the detector. Here ^{222}Rn decays to ^{218}Po. The positive charged ^{218}Po is electrodeposited in a strong electric field by means of a high voltage between the chamber and a surface barrier detector. After deposition of ^{218}Po the α-decays of ^{218}Po and ^{214}Po are recorded. Peak identification is carried out with a multichannel analyzer, where a distinction between ^{218}Po and ^{214}Po is possible. Figures 2a and 2b demonstrate the ratio of ^{218}Po and ^{214}Po deposited on the surface barrier detector.
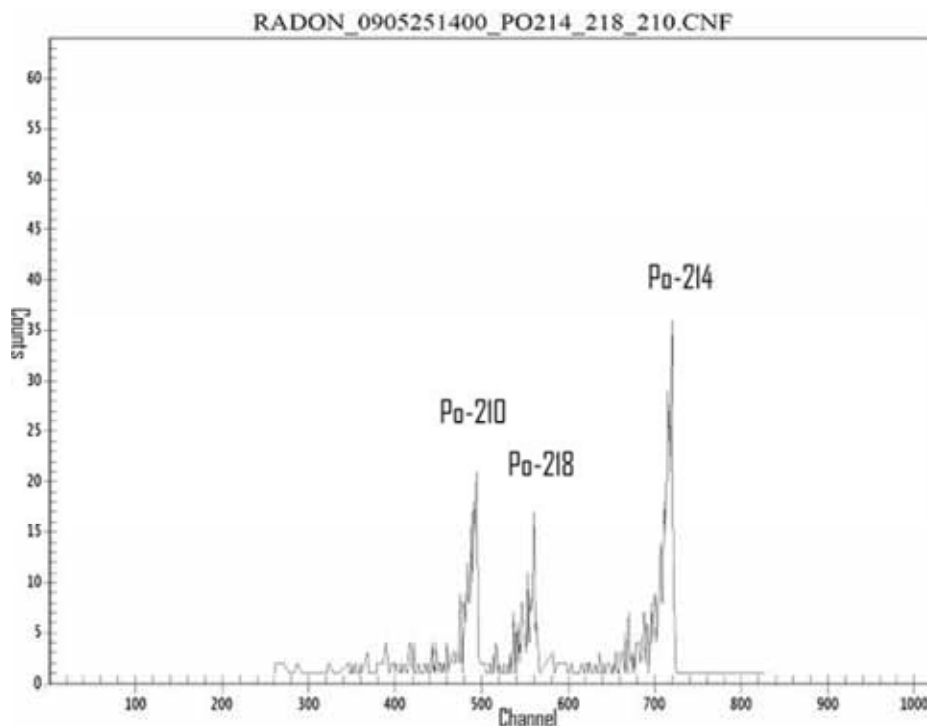
FIG. 2a. α-spectrum of ^{218}Po and ^{214}Po, recorded at UFS-SFH, May 2009.

Figure 2a shows the ^{218}Po and ^{214}Po with a ratio of ^{214}Po/^{218}Po >1.This effect is stronger for measurements at the UFS-SFH than for measurements carried out in Offenbach (Figure 2b). We think the higher count rate of ^{214}Po results from sample gas composition and a slightly changed deposition efficiency. Figure 2a also shows the accumulation of ^{210}Po after a longer time of measuring. The detector surface will have to be cleaned carefully in the course of maintenance to restrict to ^{218}Po and ^{214}Po.
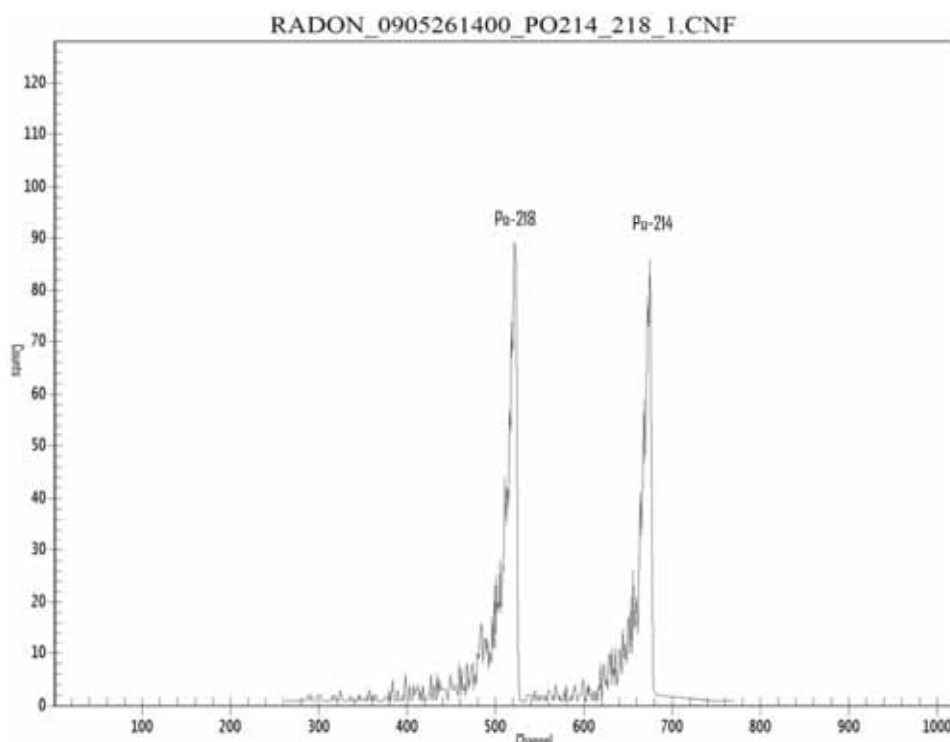
FIG. 2b. α-spectrum of ^{218}Po and ^{214}Po, recorded at DWD Offenbach, May 2008.

The complete evaluation of counting and spectrometry is done with commercially available nuclear measurement systems. The energy calibration is performed with an alpha standard source containing ^{241}Am, ^{239}Pu and ^{244}Cm. The total sampling and measuring device is calibrated with ^{222}Rn being emanated from a ^{226}Ra source. The chamber volume is 300 L.

Instead of accumulating radon daughters on a filter and measuring the different decay products, ^{222}Rn and its daughter ^{218}Po, produced in the measuring chamber, is directly measured. ^{218}Po is continuously produced and deposited. After 20 minutes radioactive equilibrium is reached (90%). It takes 10 times longer for ^{214}Po to be in radioactive equilibrium.

The sensivity of the electrostatic deposition is independent of the air flow over a wide range [8]. This will be documented through measurements with different air flows to check the time resolution and response characteristics.

The efficiency depends on the preparation of the counting gas and the applied high voltage, responsible for the electric field for collecting the ions of the electrostatic deposition. The mean residence time of the sample gas in the chamber is very short compared to the half life of ^{222}Rn; this means, that the sensivity of the system is independent from the air flow over a wide range. This is an advantage to the two filter method, where the mean residence time of the air or the gas velocity in the decay chamber affects the sensivity [9].

Figure 3 shows the plateau for a given geometry. Saturation in ion collection is already reached at a voltage of 25 kV. These measurements were carried out with a ^{222}Rn standard of 25 Bq absolute.
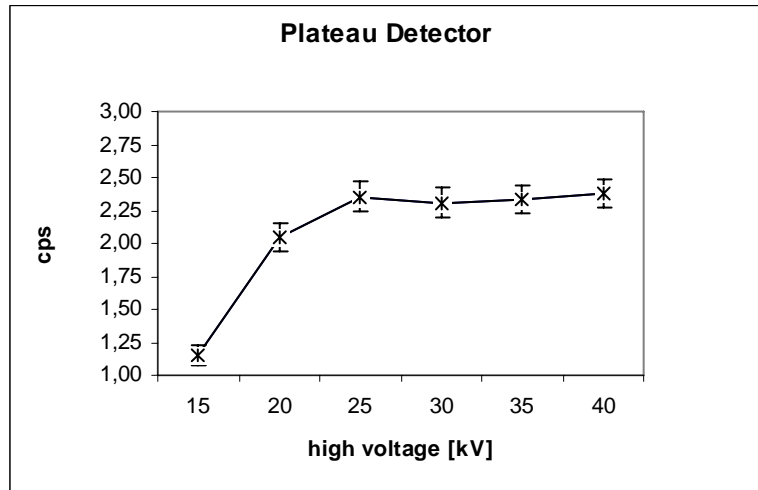
FIG. 3. High voltage of detector for electrostatic deposition.

In equilibrium count rates of ^{218}Po and ^{214}Po are nearly the same. This is the ideal case (Figure 2b); in general ^{214}Po has a higher count rate than ^{218}Po (Figure 2a). This is explained by small amounts of remaining contaminants like water vapour or electro negative, ion neutralizing gases or other trace gases [9] and also a deposition of ^{218}Po which is <100%. The variation of the deposited isotope ratio over a period of some months is shown in figures 4a, 4b and 4c. In March 2009 the sampling site and the flow path were changed. The isotope ratio shows a higher fluctuation from March to May. The mean ratio measured from December 2008 to February 2009 with a value of 1.47 ± 0.17 changed to 1.69 ± 0.33 from March 2009 to May 2009. The reason is not yet clearly explained. In addition to the ^{222}Rn measurements pressure, temperature, humidity of incoming air and humidity after drying are measured in intervals of 10 minutes. These data and all other data being available for hydrocarbons, sulphur compounds and NO_x should be compared with the isotope ratio in order to develop a correction term as reported in [10].
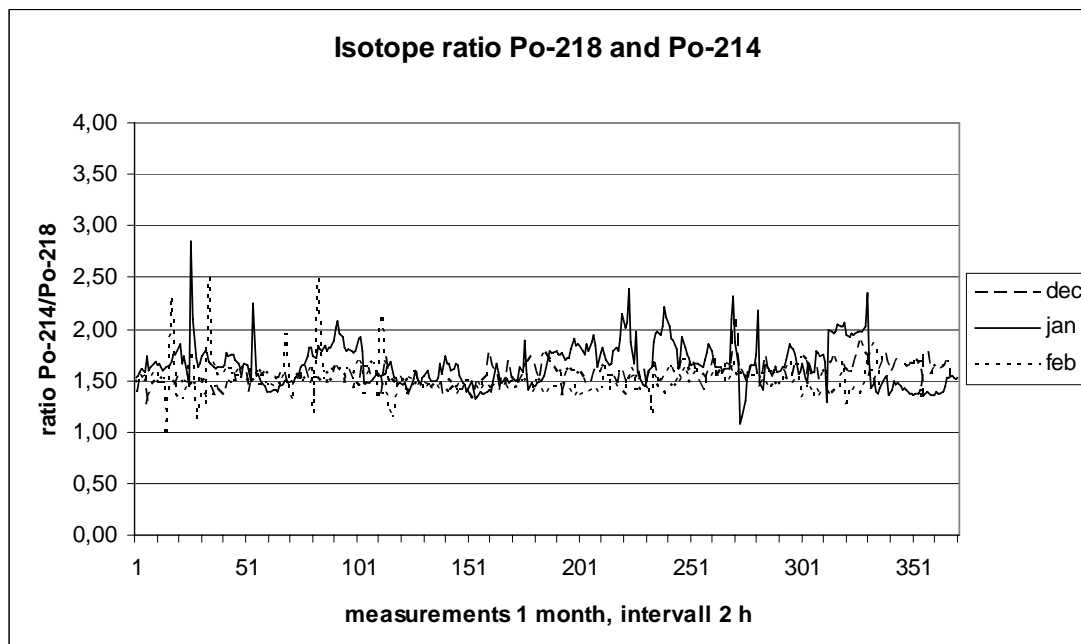
FIG. 4a. Isotope ratio of ^{214}Po / ^{218}Po from measurements over three months in a two hour interval from December 2008 to February 2009 at the UFS-SFH 2,600 m altitude.
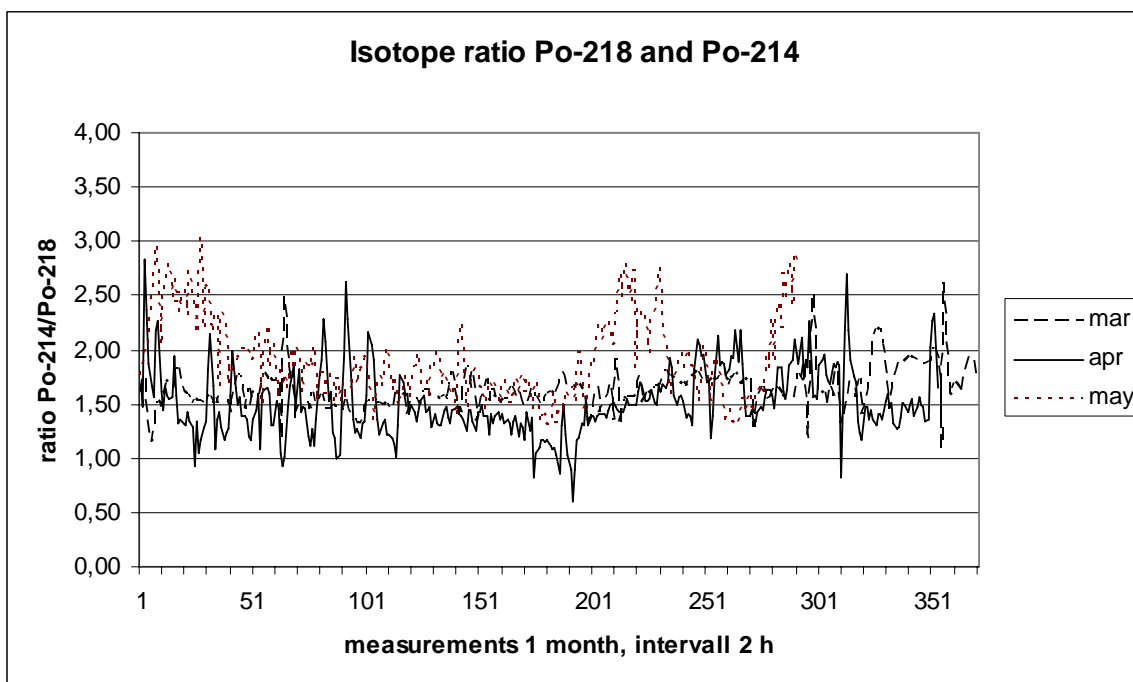
FIG. 4b. Isotope ratio of ^{214}Po / ^{218}Po from measurements over three months in a two hour interval from March 2009 to May 2009 at the UFS-SFH, 2,600 m altitude.
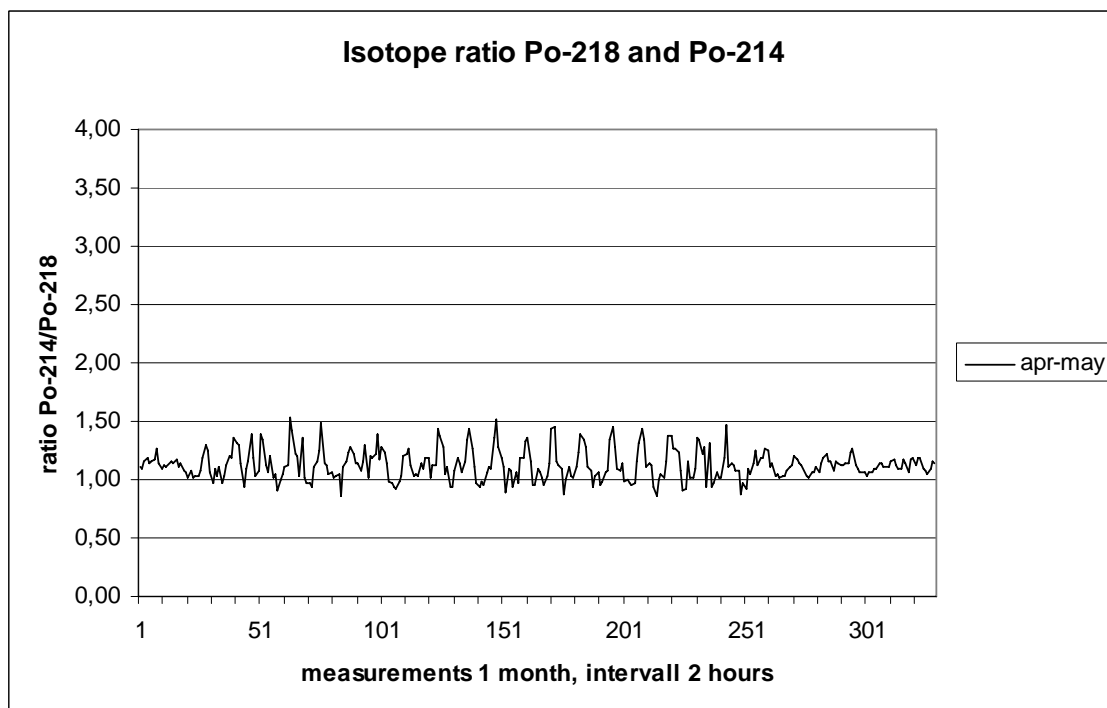
FIG. 4c. Isotope ratio of $^{214}Po/^{218}Po$ in a two hour interval from April 2008 to May 2008 at Offenbach, DWD Laboratory in 10th floor.

Figure 4c shows the ratio of ^{214}Po / ^{218}Po at the sampling site Offenbach. The ratio is nearly 1 (1.13 ± 0.13) and obviously a daily variation. Compared with figures 4a and 4b the ^{214}Po / ^{218}Po ratio has a lower fluctuation, a slightly higher deposition of ^{218}Po (ratio ^{214}Po / ^{218}Po ≈ 1) and daily variation, which is seen at the UFS-SFH only in a period of few days. Maybe the air pressure influences the process of deposition and the deposition efficiency. Comparing the sampling sites UFS-SFH and Offenbach the total efficiency did not change.

Detection limit of ^{222}Rn

In our measuring device an air sample with a ^{222}Rn concentration of 0.05 Bq m^{-3} generates about 10 counts in 2 hours. Due to the given conditions (volume and efficiency), this count rate is significantly higher than the background and easily to be distinguished from the background rate with 0.5 counts per hour (10 counts / day). A detection limit of 0.03 Bq m^{-3} with a counting error of ± 0.02 Bq m^{-3} is easily achievable.

Results

In November 2008 the system has been installed at the GAW measuring site UFS-SFH (2,600 m a.s.l) below the top of Germany's highest mountain the Zugspitze. Meanwhile the system successfully works since beginning of 2009 and different tests at the sampling site were carried out. In summer 2009 different sampling locations for the air inlet pipe were tested, because some locations are slightly influenced from local ^{222}Rn being emanated from the surrounding rocks.

A measurement series at the UFS-SFN of Deutscher Wetterdienst at the Zugspitze was performed (Figure 5) demonstrating that the system is ready to be used operationally. Figure 5 presents the results of ^{222}Rn concentration at the UFS-SFH during end of May. There seems to be still a small influence of local ^{222}Rn, which may be explained through a lot of activities with blasting, drillings and building activities for the construction of a new cable car. The building activities will be finished in the end of 2009 and normal environmental conditions should be expected then, meaning lower fluctuation in the isotope ratio.
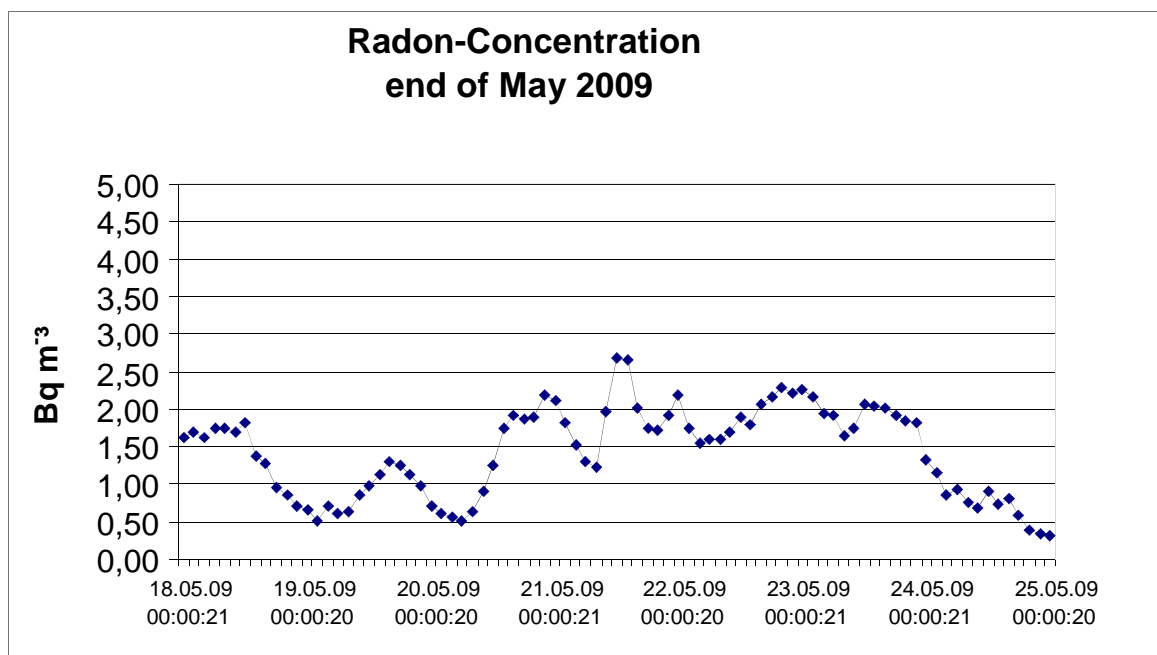
FIG. 5. Radon concentration at UFS-SFH int the end of May 2009.

A radon monitoring system being able to detect ^{222}Rn directly at low concentration levels was successfully constructed and operated at the UFS-SFH. The main target was to show that the system is working automatically based on the above mentioned sampling and measuring principles.

Future tasks

Our aim is to decrease the limit of detection to <10 mBq m^{-3}. This should be mainly done by increasing the deposition efficiency, for total efficiency is the product of counting efficiency (in our case 50% as a 2π-geometry) and the deposition efficiency. Further approach will be done in the explanation of the fluctuation of the isotope ratio ^{214}Po/^{218}Po and therefore the approach to reach stable conditions in the isotope ratio and a higher deposition rate of ^{218}Po. Count rates of ^{218}Po and ^{214}Po should then be added to reach a higher sensitivity. A further aim is the correlation of the ^{222}Rn measurements to atmospheric conditions. The measurements of tritium in water vapor, ^{14}C in CO_2 and ^{85}Kr may be embedded in future, too.

REFERENCES

[1] WORLD METEOROLOGICAL ORGANIZATION (WMO) GLOBAL ATMOSPHERIC WATCH, 1st International Expert Meeting on Sources and Measurements of Natural Radionuclides Applied to Climate and Air Quality Studies, Gif sur Yvette, France, 3-5 June 2003, No. 155, April 2004.
[2] SCHMIDT M., et al., Carbon Dioxide and Methane in continental Europe: A climatology, and ^{222}Rn-based emission estimates. Tellus **B 48** 4 (1996) 457–473.
[3] PAATERO J., et al., A Comprehensive Station for Monitoring Atmospheric Radioactivity. Radiation Protection Dosimetry **54** 1 (1994) 33–39.
[4] HUTTER, A.R., et al., ^{222}Rn at Bermuda and Mauno Loa: Local and Distant Sources. J. Radioana. And Nuclear Chem. **193** (1995) 309–318.

[5]   GUGGENHEIM, S.F., NEGRO, V.C., Automatic Filter Changer for Environmental ^{222}Rn Measurements. Winter Annual Meeting of the American Society of Mechanical Engineers, 90-WA-DE-2, Dallas Texas, 25–30 November, 1990.

[6]   WHITTLESTONE, S., ZAHOROWSKI, W., Baseline ^{222}Rn detectors for shipboard use: Development and deployment in the First Aerosol Characterisation experiment (ACE 1). J. Geophys. Res. **103** 16 (1998) 743–751.

[7]   SCHERY, S.D. et al., Two-filter monitor for atmospheric ^{222}Rn. Rev. Sci Instrum., **51** 3 (1980) 338–343.

[8]   WICKE, A., Untersuchungen zur Frage der natürlichen Radioaktivität der Luft in Wohn- und Aufenthaltsräumen Grundlagen zur Abschätzung der Strahlenexposition durch Inhalation von Radon und Thoron Zerfallsprodukten, Dissertation Gießen 1979.

[9]   KIKO, J., Detector for ^{222}Rn measurements in air at the 1 mBq/m³ level. Nucl. Instr. Methods in Physics Research, **A 460** (2001) 272–277.

[10] HOPKE, P., Use of electrostatic collection of ^{218}Po for measuring Rn, Health Physics, **57** 1 (1989) 39–42.

REVIEW OF RADON RESEARCH IN SLOVENIA

J. VAUPOTIČ
Radon Center, Department of Environmental Sciences,
Jožef Stefan Institute,
Ljubljana,
Slovenia

Abstract

Results of radon research in Slovenia in last two decades are reviewed, with emphasis on radon in soil gas and outdoor air. Track etch detectors were exposed all over the country, in boreholes at a depth of 80 cm and in outdoor air at a height of 150 cm above ground. Arithmetic mean values of radon concentration in soil gas were 40.9 kBq m^{-3} and 45.1 kBq m^{-3} for two consecutive years, and in outdoor air, 15.3 Bq m^{-3} in summer and 14.4 Bq m^{-3} in winter. In both cases, higher values were found in the south-west part of the country covered by carbonates and crossed by a number of tectonic faults.

Introduction

The first measurements of radon (^{222}Rn) in Slovenia were carried out by the Jožef Stefan Institute in the Žirovski vrh uranium mine in 1969 [1]. Once regular radon monitoring had been introduced and was performed by the mine company radiation protection service, our attention was extended to other workplaces, such as underground mines [2], show caves [3], spas [4] and a phosphate mill [5]. These measurements were limited, being based only on the use of alpha scintillation cells, and no radiation doses were calculated. The situation changed in 1991 when the national radon survey in Slovenia was initiated. Since then, radon has been dealt with from two main aspects: (1) radiation protection, comprising radon in indoor air at homes and at various workplaces, and (2) radon in geosciences, comprising radon in outdoor air, soil gas, thermal waters and seawater. Following the first aspect, radon has been surveyed in about a thousand randomly selected dwellings [6], 730 kindergartens [7], 890 schools [8], the Postojna Cave [9], 26 major hospitals, 10 waterworks, 7 wineries, 5 spas, and in a number of other public buildings, such as bus and railway stations, health care centres, university premises, police and customs offices, and others [10–11]. In more than 59 buildings the radon problem has been successfully mitigated. In addition to radon (Rn), concentrations of radon short-lived decay products (RnDP), equilibrium factors (F) between Rn and RnDP, and unattached fraction (f_{un}) of RnDP have also been monitored at some workplaces [12]. In a small number of dwellings and public buildings, also thoron (^{220}Rn) was recently monitored [13].

Radon concentration has also been measured in soil gas all over Slovenia, in outdoor air in Slovenia and at Mt. Etna, Italy [14], and in seawater at selected points in the Mediterranean Sea [15]. Radon has also been monitored continuously at selected Slovenian thermal water springs and in soil gas at several tectonic faults both in Slovenia and elsewhere, in order to understand its role as a potential earthquake precursor [16–22]. In this review, results on radon in outdoor air and soil gas are presented and discussed.

Experimental

Several complementary techniques have been used. Radon scintillation cells [22] are in use to obtain instantaneous radon concentrations. Average radon concentrations have been measured by exposing various types of track etch detectors provided from several sources in Slovenia (Jožef Stefan Institute), Germany (Karlsruhe Forschungszentrum), Norway (Radonlab, Oslo), Poland (Henryk Niewodniczański Institute of Nuclear Physics, Polish Academy of Sciences, Kraków) and Japan (National Institute of Radiological Sciences, Chiba). After exposure, detectors were sent back to the provider for etching and data evaluation. AlphaGuard radon monitors (Genitron, Germany), Barasol probes (Algade, France), RadonScout monitors (Sarad, Germany) and Radim monitors (Plch, SMM, Czech Republic) have been used to follow diurnal variations of radon (Rn) concentration only, and various EQF radon devices (Sarad, Germany), for concentrations of RnDP, F, and f_{un}. All these devices have been checked at intercomparison experiments organised regularly by the Slovene Nuclear Safety Administration [23], and were recently calibrated in the Radon Chamber of the Laboratory of Radiometric Expertise at the Henryk Niewodniczański Institute of Nuclear Physics, Polish Academy of Sciences, Kraków, Poland [24].
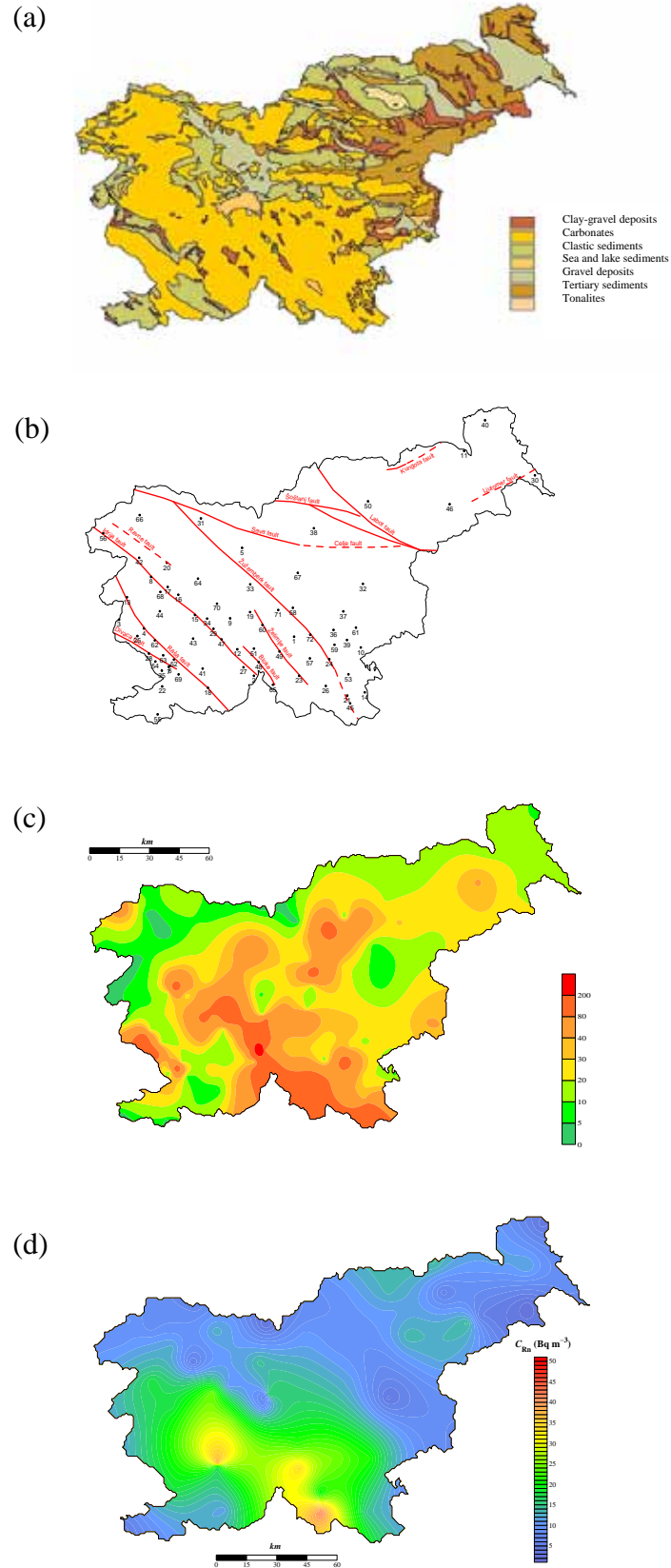
Some radon concentrations in soil gas and all radon exhalation rates were measured by the Laboratory of Radiometric Expertise from Kraków, using the AlphaGuard equipment described elsewhere [25]. The same laboratory also performed gamma spectrometric analyses of soil samples.

Results and discussion

Radon survey in soil gas

Radon activity concentrations were measured in soil gas, using alpha scintillation cells and etch track detectors, at a depth of 80 cm at 70 points in 2006 and 72 points (23 repeated from 2006) in 2007 all over the country (a surface area of about 20,273 km^2), mostly located close to meteorological stations, at which gamma dose rate is permanently monitored by exposing thermoluminescent dosimeters. The density of points was higher in the south-west part of the country which is covered by carbonates (Figure 1a) and crossed by a number of tectonic faults (Figure 1b), where higher radon levels were found previously in indoor air [6-8].

Radon concentrations ranged from 1 kBq m^{-3} to 200 kBq m^{-3}, with arithmetic means of 40.9 kBq m^{-3} and 45.1 kBq m^{-3} for 2006 and 2007 [26], which is comparable to those in some other European countries, such as Austria with 75 kBq m^{-3}, Czech Republic with 28 kBq m^{-3}, Slovakia with 22 kBq m^{-3}, Germany with 55 kBq m^{-3}, France with 58 kBq m^{-3} and Croatia with 26 kBq m^{-3} [27]. Based on this data, a map of radon levels in soil gas has been made (Figure 1c).

FIG. 1. Maps of Slovenia: (a) with petrographic units, (b) with main tectonic faults and points for radon measurements in soil gas, (c) iso-concentration contours of radon concentration in soil gas, and (d) iso-concentration contours of radon concentration in outdoor air.

At a number of places, radon exhalation rate was measured as well as radon, and soil samples were collected for gamma spectrometry. Good correlations are seen between radon concentration and [226]Ra content in soil (Figure 2a), while correlations between exhalation rate and radon concentration and radon concentration and [226]Ra content in soil are weak, with correlation coefficients of less than 0.30 (Figs. 2b and 2c).

a)

b)

c)
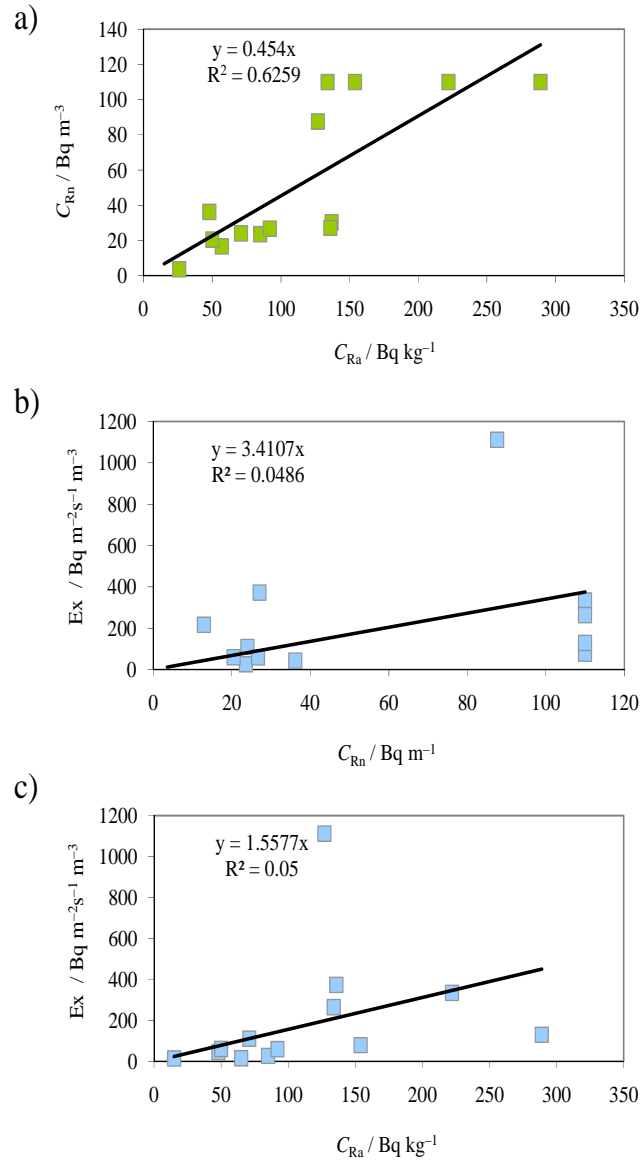
FIG. 2. Relationships of (a) radon concentration in soil gas (C_{Rn}) and [226]Ra content in soil (C_{Ra}), (b) exhalation rate (Ex) and radon concentration in soil gas (C_{Rn}), and (c) exhalation rate (Ex) and [226]Ra content in soil (C_{Ra}).

Radon survey in outdoor air

Radon concentration in outdoor air was measured by exposing track etch detectors between March and June 2005, June and September 2005 and from September 2005 to March 2006, at 60 points all over the country (Figure 3a) [28], coinciding with points for radon measurements in soil gas. Results of all three exposures fit well a lognormal distribution (Figure 3b).
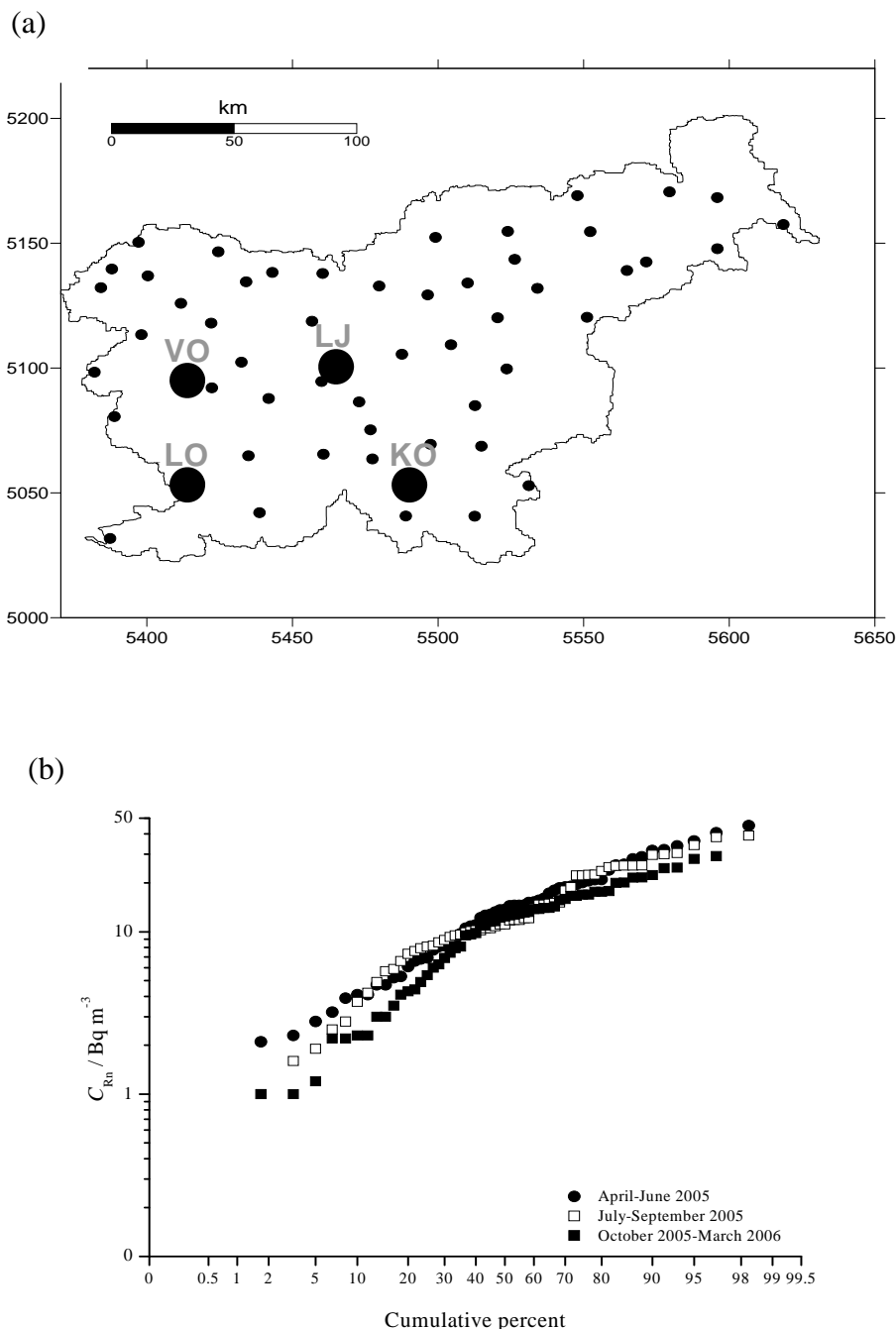
FIG. 3. *Radon measurements in outdoor air: a) 60 locations with indicated 4 locations (LJ, LO, KO, VO) where continuous monitoring was performed, b) lognormal plots of radon concentration in outdoor air (C_{Rn}), measured by exposing track etch detectors in periods: March – June 2005, June – September 2005 and September 2005 – March 2006.*

According to the *t*-test, datasets for different periods do not differ significantly from one another and the arithmetic mean for summer was 15.3 Bq m^{-3} and for winter, 14.4 Bq m^{-3}. Based on this data, a map of outdoor air radon has been made (Figure 1d). The regions of elevated values are seen in the south- west part of the country covered by carbonates (cf. Figure 1a) and crossed by faults (cf. Figure 1b). Higher values in the regions of uranium mining at Žirovski vrh, mercury mining at Idrija and coal mining at Kočevje are ascribed not only to geology, but also to temperature inversions, that occur frequently in wintertime. Elevated values were expected but not found in the granite region near Maribor at the Austrian border, where gamma dose rate is higher by a factor of 2–3 than anywhere else in the country. Obviously, emanation from the compact granite is lower. Thermal and mineral waters rich in ^{226}Ra are abundant in the most north-eastern part of the country. Elevated outdoor radon levels have not been observed here because of a surface layer of clay which, if it is not dry, is an effective barrier for radon transport from the ground [29].

A relatively good correlation between radon levels in outdoor air and in soil gas measured at the same point is seen (Figure 4).
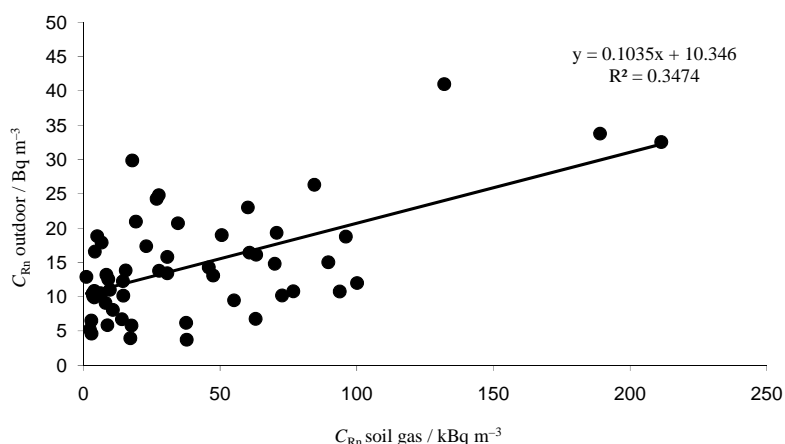
FIG. 4 Correlation between radon concentrations in outdoor air (C_{Rn} outdoor) and in soil gas (C_{Rn} soil gas).

Continuous radon monitoring in outdoor air

At four points out of the 60 indicated in Figure 3a, radon, together with air temperature and relative humidity, barometric pressure and rainfall, was monitored continuously in outdoor air and indoors in a nearby house, using two AlphaGuard instruments, for about ten days. The points were at: Ljubljana (LJ), the capital, the northern part located over river sediments and southern part over clay, 299 m a. s. l. (above sea level), continental climate with hot summer and cold winter, 1393 mm annual precipitation; Kočevje (KO), located on carbonate and clay, close to an abandoned coal mine, 467 m a.s.l., continental climate, 1523 mm annual precipitation; Lokev (LO), located over carbonate and terra rossa (clayey red soil), 449 m a.s.l., Mediterranean climate with hot summer and mild winter, 1420 mm annual precipitation; and Vojsko (VO), located over dolomite in a remote forest area, 1067 m a.s.l., Alpine climate with mild summer and cold winter, 2456 mm annual precipitation.

For consideration of space, time series of the parameters measured outdoors are not presented here. In all, a typical diurnal variation of radon concentration was seen. While amplitudes at LJ were similar during the period of measurement, they differed substantially from day to day at KO, being the lowest during rainy days when wet soil hampered radon exhalation. Correlation coefficients were calculated (Table 1) for relationships between radon concentration in outdoor air and radon concentration indoors, outdoor air temperature, barometric pressure and relative humidity. The correlation coefficients are highest at LJ and lowest at VO. They have the same sign at all points, with the exception of T_{out} at VO, where the low value hardly allowed a correlation to be calculated. Big differences in correlation coefficients are a warning that radon levels in outdoor air should be discussed site specifically and any generalisation is risky.

TABLE 1. CORRELATION COEFFICIENTS FOR RELATIONSHIPS BETWEEN RADON CONCENTRATION IN OUTDOOR AIR (C_{Rn}^{out}) AND RADON CONCENTRATION INDOORS (C_{Rn}^{in}), OUTDOOR AIR TEMPERATURE (T_{OUT}), BAROMETRIC PRESSURE (P_{OUT}) AND RELATIVE HUMIDITY (RH_{OUT}), FOR POINTS AT LJUBLJANA (LJ), VOJSKO (VO), LOKEV (LO) AND KOČEVJE (KO).

	LJ	VO	LO	KO
C_{Rn}^{in}	0.71	0.27	0.32	0.46
T_{out}	−0.72	0.13	−0.39	−0.14
P_{out}	0.42	0.20	0.22	0.49
RH_{out}	0.85	0.03	0.31	0.40

Conclusions

The following conclusions result from the nation-wide radon surveys, using etch track technique, in soil gas and outdoor air in Slovenia:

- Radon activity concentrations in soil gas ranged from 1 kBq m^{-3} to 201 kBq m^{-3}, with arithmetic means of 40.9 kBq m^{-3} and 45.1 kBq m^{-3} for 2006 and 2007 measurements,

- Radon activity concentrations in outdoor air ranged from 3.2 Bq m^{-3} to 47.2 Bq m^{-3}, with arithmetic means of 15.3 Bq m^{-3} and 14.4 kBq m^{-3} for summer and winter periods,

- The patterns of diurnal variations of radon concentration at four geologically and geographically different site differed substantially; therefore, radon levels in outdoor air should be discussed site specifically,

- Analysis of time series of radon levels in outdoor air should be based on the synoptic maps and not only on air temperature, pressure, humidity and rainfall.

Acknowledgements

REFERENCES

[1] KRISTAN, J., KOBAL, I., A modified alpha scintillation cell for the determination of radon in uranium mine atmosphere, Health Phys. **24** (1974) 103.

[2] KOBAL, I., VAUPOTIČ, J., UDOVČ, H., BURGER, J., STROPNIK, B., Radon concentrations in the air of Slovene (Yugoslavia) underground mines, Environ. Int. **16** (1990) 171.

[3] KOBAL, I., SMODIŠ, B., ŠKOFLJANEC, M., Atmospheric ^{222}Rn in tourist caves of Slovenia, Health Phys. **52** (1987) 477.

[4] KOBAL, I., FEDINA, Š., Radiation doses at the Radenci health resort, Radiat. Prot. Dosim. **20** (1987) 257.

[5] BRAJNIK, D., KRIŽMAN, M., KOBAL, I., STEGNAR, P., Sources of technologically enhanced natural radioactivity and their impact in Slovenia, Radiat. Prot. Dosim. **24** (1988) 551.

[6] KRIŽMAN, M., ILIĆ, R., SKVARČ, J., JERAN, Z., "A survey of indoor radon concentrations in dwellings in Slovenia", Radiation Protection in Neighbouring Countries in Central Europe – 1995 (Proc. Symposium Portorož, Slovenia), Jožef Stefan Institute, Ljubljana, Slovenia (1995) 66–70.

[7] VAUPOTIČ, J., et al., Systematic radon and gamma measurements in kindergartens and play schools in Slovenia, Health Phys. **66** (1994) 550.

[8] VAUPOTIČ, J., ŠIKOVEC, M., KOBAL, I., Systematic radon and gamma-ray measurements in Slovenian schools, Health Phys. **78** (2000) 559.

[9] VAUPOTIČ, J., et al., Methodology of radon monitoring and dose estimates in Postojna Cave, Slovenia, Health Phys. **80** (2001) 142.

[10] VAUPOTIČ, J., Indoor radon in Slovenia, Nucl. Technol. Radiat. Prot. **18** (2003) 36.

[11] VAUPOTIČ, J., Slovenian Approach in managing exposure to radon at workplaces, Nukleonika (in press).

[12] VAUPOTIČ, J., KOBAL, I., The importance of nanosize aerosols of radon decay products in radon dosimetry, Croat. Chem. Acta **80** (2007) 565.

[13] VAUPOTIČ, J., ČELIKOVIĆ, I., SMREKAR, N., ŽUNIĆ, Z.S., KOBAL, I., Concentrations of ^{222}Rn and ^{220}Rn in indoor air, Acta Chim. Slovenica **55** (2008) 160.

[14] VAUPOTIČ, J., ŽVAB, P., GIAMMANCO, S., Radon in outdoor air in the Mt. Etna area, Italy, Nukleonika (in press).

[15] VAUPOTIČ, J., GREGORIČ, A., KOTNIK, J., HORVAT, M., PIRRONE, N., Dissolved radon and gaseous mercury in the Mediterranean seawater, J. Environ. Radioact. **99** (2008) 1068.

[16] ZMAZEK, B., TODOROVSKI, L., DŽEROSKI, S., VAUPOTIČ, J., KOBAL, I., Application of decision trees to the analysis of soil radon data for earthquake prediction, Appl. Radiat. Isotopes **58** (2003) 697.

[17] ZMAZEK, B., et al., Radon in soil gas: how to identify anomalies caused by earthquakes, Appl. Geochem. **20** (2005) 1106.

[18] FUJIYOSHI, R., et al., Meteorological parameters contributing to variability in ^{222}Rn activity concentrations in soil gas at a site in Sapporo, Japan, Sci. Total Environ. **370** (2006) 224.

[19] ŠEBELA, S., VAUPOTIČ, J., KOŠ'TÁK, B., STEMBERK, J., Micro-displacements and radon air concentrations in Postojna Cave, Slovenia, J. Cave Karst Studies (in press).

[20] VAUPOTIČ, J., RIGGIO, A., SANTULIN, M., ZMAZEK, B., A radon anomaly in soil gas at Cazzaso, NE Italy, as a precursor of a $M_L = 5.1$ earthquake, Nukleonika (in press).

[21] VAUPOTIČ, J., et al., Radon in soil gas at the Ravne fault in NW Slovenia, European Geoscience Union General Assembly 2009 (Book Abstracts Vienna, Austria), p. 9496.

[22] VAUPOTIČ, J., ANČIK, M., ŠKOFLJANEC, M., KOBAL, I., Alpha scintillation cell for direct measurement of indoor radon, J. Environ. Sci. Health **A27** (1992) 1535.

[23] KRIŽMAN, M., Report on the intercomparison experiment on radon and progeny in air, Slovene Nuclear Safety Administration Report URSJV RP **47** (2001).

[24] VAUPOTIČ, J., et al., Calibration of radon measuring devices of the Radon Center in the IFJ-KR-600 Radon Chamber, Jožef Stefan Institute Report IJS-DP–10103 (2009).

[25] ŽUNIĆ, S.Z., et al., High natural radiation exposure in radon spa areas: a detailed field investigation in Niška Banja (Balkan region), J. Environ. Radioact. **89** (2006) 249.

[26] VAUPOTIČ, J., et al., Radon mapping in Slovenia based on its levels in soil gas, 33rd International Geological Congress, (Book of Abstracts Oslo, Norway 2008), Abstract no. S. [l.: s. n].

[27] EUROPEN COMMISSION (EC), An overview of radon surveys in Europe, EUR 21892 EN, PUBSY 1429 (2005).

[28] VAUPOTIČ, J., KOBAL, I., KRIŽMAN, M., Background outdoor radon levels in Slovenia, Nukleonika (in press).

[29] SHWEIKANI, R., HUSHARI, M., The correlation between radon in soil gas and its exhalation and concentration in air in the southern part of Syria, Radiat. Meas. **40** (2005) 699.

INFLUENCE OF HETEROGENEOUS AND DISTANT RADON SOURCES ON LOCAL AND REGIONAL RADON TRANSPORT

D. ARNOLD, A. VARGAS, C. GROSSI
Institute of Energy Technologies,
Technical University of Catalonia,
Barcelona

C. PARAGES
Spanish Nuclear Safety Council,
Madrid

Spain

P. SEIBERT
Institute of Meteorology, University of Natural Resources and Applied Life Sciences,
Vienna,
Austria

Abstract

This work presents a sample of how considering a complex spatial heterogeneous radon exhalation flux density as a source term in modelling studies, using a receptor-oriented approach, influences the modelling results in comparison with the traditionally used $1 \, atom \cdot cm^{-2} \cdot s^{-1}$ radon exhalation flux density over land and $0 \, atom \cdot cm^{-2} \cdot s^{-1}$ over water bodies. Results show that when high accuracy is needed, for instance in validation of atmospheric transport models, the use of an accurate spatial varying radon exhalation flux density gives may significantly improve the modelling results.

Introduction

Radon has been largely used as a passive atmospheric transport tracer at different scales and with several applications [1–3], including model validation. However, the influence of the radon source term definition on the accuracy of the model results has always been a topic of concern [4]. Traditionally, a simple constant radon exhalation flux density of $1 \, atom \cdot cm^{-2} \cdot s^{-1}$ over land and 0 over water bodies, or at most a latitude-dependent flux, has been used by the modelling community. Nevertheless, much more complex definitions are currently available. In Europe, a 0.5 degree European radon flux map (http://radon.unibas.ch/), based on the correlation of radon exhalation rate and terrestrial gamma dose rate, has been developed and it is free for use. Based on the same correlation function used in the aforementioned European map, but using the high-resolution (1 km) terrestrial gamma dose rate MARNA map [5] already existing in Spain, a radon exhalation flux density map for the Spanish region has been constructed. This heterogeneous radon source maps still carry, though, some limitations and approximations that may negatively influence the model results, for instance, the lack of temporal variations in the radon exhalation flux densities. One way to address this problem would be using accurate models to make an estimation of the radon source through inversion techniques, but this would require, at the same time, the use of a very accurate and well validated model, which in turn would require again a good radon source term.

Within this context two case studies have been set to make a preliminary evaluation of the influence of a heterogeneous radon source term on the estimation of the measurements at stations in Cabauw and Spain.

Methods

To make a first inspection of the differences of the modelled versus the measured radon ambient concentrations, a receptor-oriented approach was taken. For each of the sites of interest, backwards transport simulations were performed with the Lagrangian particle dispersion model FLEXPART version 6.2 [6, 7] (see also http://transport.nilu.no/flexpart) driven with operational analyses from the European Centre for Medium-Range Weather Forecasts [8] with a horizontal resolution of 0.5º and 60 vertical levels. The output of such simulations are given as gridded source-receptor sensitivities (SRS) [9, 10], which describe the sensitivity of each of the receptor concentration values to each of the possible source elements. In the absence of radioactive decay, the concentration at a specific time would be obtained by multiplying the SRS values for all grid elements with the respective radon exhalation flux density value and summing over all these contributions. Decay could have been calculated directly in FLEXPART, however, it is computationally more efficient to introduce it as a correcting factor depending on the respective transport times in this post-processing step. Once the SRSs are obtained for each of the sites under study, they can therefore be folded with different gridded radon exhalation flux densities to obtain the modelled radon ambient concentrations for each of the radon source terms defined. Differences can be then studied by comparison with measurements through simple visual inspection supported, if necessary, by some statistical metrics such the Root Mean Square Error (RMSE), the bias or the correlation. For this study three different radon exhalation flux density sources have been used (Figure 1).
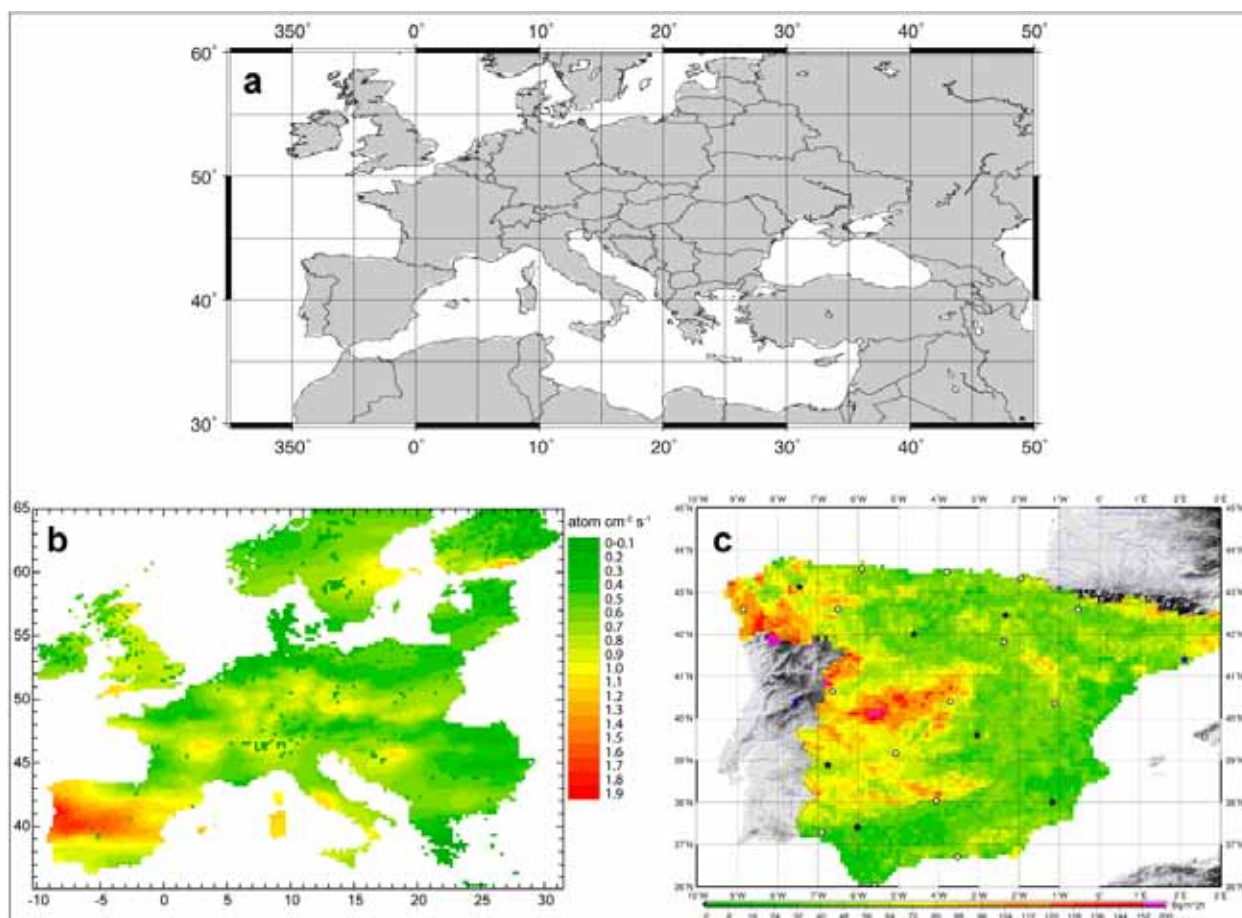
FIG. 1. Radon exhalation flux density maps used as radon source term in the atmospheric dispersion modelling, a constant 0.66 atom cm^{-2} s^{-1} over land and 0 over water bodies (a), the spatially variably European radon flux map (b) and the one obtained from the MARNA map(c).

The simplest assumption for the radon source would be a constant radon exhalation flux density over land, typically of 1 atom cm^{-2} s^{-1}, and 0 over water bodies. (The ^{222}Rn flux density can be converted to Bq m^{-2} s^{-1}). In this work, this simple source term adopts a radon exhalation flux density of 0.66 atom cm^{-2} s^{-1} (50 Bq m^{-2} h^{-1}) above land, chosen after the work of Levin et al. [11] who gave an average of 50–60 Bq m^{-2} h^{-1} for Heidelberg and the whole of western Europe. The second, more complex, source term is the European radon flux map of Szegvary et al. [12, 13], which gives a spatially variable radon exhalation flux density for Europe. It is known, though, that this map overestimates the radon exhalation flux density over Spain [14], therefore, and to be applied over this region, a third radon source term was defined. It is based on the same formula used in the European radon flux map but using the high resolution terrestrial gamma dose rate map available for Spain, the MARNA. This map is at an approximate maximum resolution of 1 km, which can be downsampled at the desired resolution. In the present work, a maximum resolution of 0.02 degrees was used.

Additionally, this study has been used as a first evaluation test of the new version of FLEXPARTv6.2 able to work with MM5 output fields (MM5V3.7-FLEXPARTV6.2; [15, 16]), that is, using more realistic wind fields able to represent local scale phenomena better.

Case studies

Cabauw

The Cabauw station (latitude 51.97ºN, longitude 4.93ºE, altitude –0.7 m a.s.l.) is located in the Netherlands at about 50 km east from the North Sea. The soil type in the southerly region is mainly river-clay. North of the tower, the soil type is peat or peat on clay. Therefore, radon exhalation flux densities in the vicinity of the station are expected to be low and quite homogeneous as shown in the European radon flux map. In this moderately maritime region there is a predominance of westerly flows which will be poor in radon. However, eastern and southern continental air masses often reach the area, hence a radon increase can be expected in such situations. The station includes a 213-m-high tower which provides vertical profiles of the meteorological data as well as trace gas data including ^{222}Rn. ^{222}Rn is continuously measured at two different heights, 20 m and 200 m above ground level, with an ANSTO radon monitoring device [17, 18] based on the two-filter technique.

The location and surroundings of the site make it also a perfect target station to make first evaluations of newly developed models. Therefore, the dispersion calculations were performed not only with FLEXPARTv6.2 version but also with the new version driven with MM5 output using a maximum horizontal resolution of 1km in the innermost domain. Moreover, in this case study, a whole period of one month (April 2007) was simulated since it allows then to evaluate the model behaviour and the influence of the definition of a heterogeneous source term under different synoptic situations and the transition periods between them.

REA stations- Autilla del Pino and Murcia

The Spanish environmental radiological surveillance is carried out by the Spanish Nuclear Safety Council. One of the existing surveillance systems consists of 25 automatic radiological stations (REA stations) equipped with a BAI 9850 monitoring device from the Berthold Company. The REA stations provide gamma dose rate, radon ambient concentration, derived from the pseudo-coincidences due to ^{214}Po / ^{214}Bi, alpha and beta air concentration and meteorological data on real time [19].

The location and topographic surrounding of the REA stations (Figure 2a) vary considerably ranging from rooftop stations in cities, to single ground-level stations on mountain ridges or coastal borders. Moreover, the complex geology of the Spanish region leads to a wide range of variation of the expected radon exhalation flux density within the country. From the meteorological point of view, the REA station locations are not less heterogeneous. Influences from the oscillation of the Azores high-pressure system together with the influence of the European continent and the warm Mediterranean Sea, produce a high climatic variability within the country with complicated wind patterns. A predominance of westerly and northerly flows is often seen in most stations. However, due to the often low pressure gradient situations occurring in the Iberian Peninsula (IP) mainly in summer, the development of mesoscale circulations such as mountain-valley systems and land-see breezes, are also predominant in some stations. This varied meteorological situation also modulate the radon ambient concentrations.

Initially the whole 25 REA stations under 11 typical synoptic situations affecting the Iberian Peninsula were studied. However, in the present work, results from only two representative stations, Autilla del Pino and Murcia, and for selected meteorological episodes are shown. Autilla del Pino is located in central Spain (Figure 2b) and has a quite homogeneous radon exhalation flux density in the surrounding of the station. Murcia is located near the coast (Figure 2c) and a strong discontinuity in the radon exhalation flux density appears due to the nearby sea.
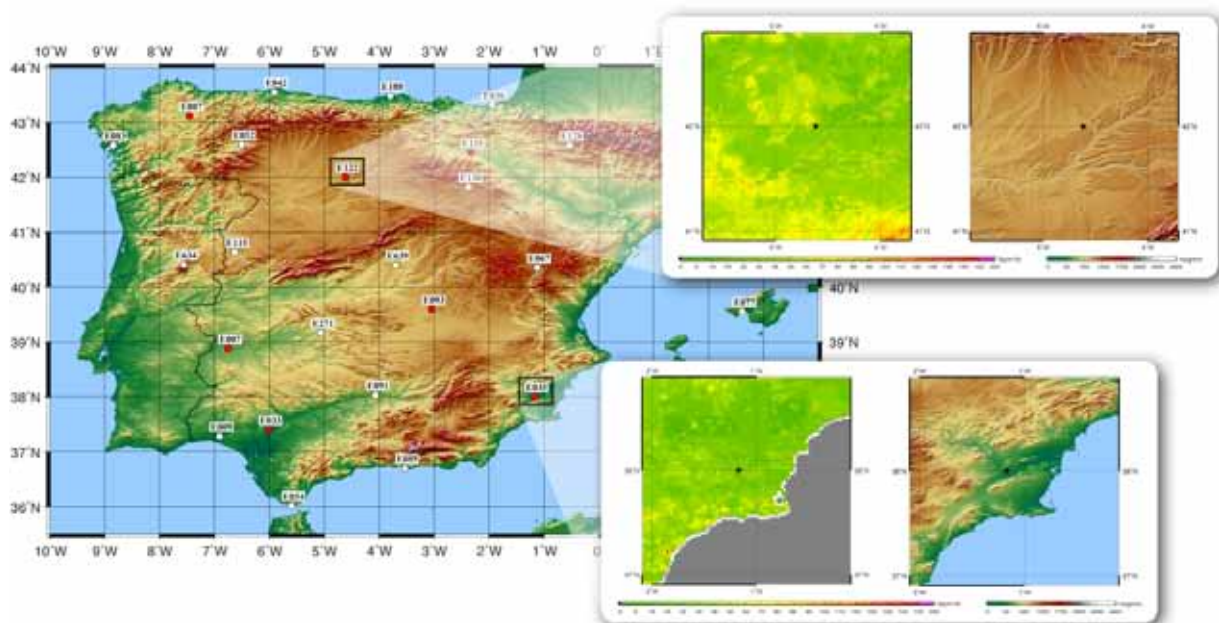
FIG. 2. Map with the locations of the REA stations on the Iberian Peninsula. Zoomed in are the two stations Autilla del Pino and Murcia, together with the radon exhalation flux density map in the vicinity of the station.

Results and discussion

Cabauw

Measured radon ambient concentration during April 2007 (Figure 3) includes different transport conditions. During the first two weeks of the month, a predominance of strong westerly flows, with air coming from the sea and hence poor in radon, gives low radon ambient concentrations with smoothed diurnal cycles. This period is followed by low wind speeds predominantly from the European continent, with the subsequent raise in the radon baseline and marked diurnal cycles. A shift to westerly and north-westerly flows is afterwards found finally ending with a period with again continental inflows with an increase of the radon baseline. Modelled time series show fair agreement with the measurements for the two versions of FLEXPART (Figure 3) and using both the constant radon source term and the European radon flux map. However, significant differences appear. The radon time series obtained using FLEXPARTv6.2 together with the 0.66 atom cm^{-2} s^{-1} show a clear overestimation of the night-time maxima while the synoptic variation is properly captured. This may be due to a combination of a too shallow nocturnal stable boundary layer given by the model and an overestimation of the radon exhalation flux density in the surrounding of the station, being 0.66 atom cm^{-2} s^{-1} too high. The combination of FLEXPARTv6.2 together with the European radon flux map as a source term does not present such overestimated night-time maxima since the flux in the close vicinity of the station is between 0.2 and 0.4 atom cm^{-2} s^{-1} according to the European radon flux map, nevertheless, the day-to-day accumulation during the periods with lower wind speeds and air coming from the European continent, it is clearly underestimated, reaching even the 50% of the measured concentrations.
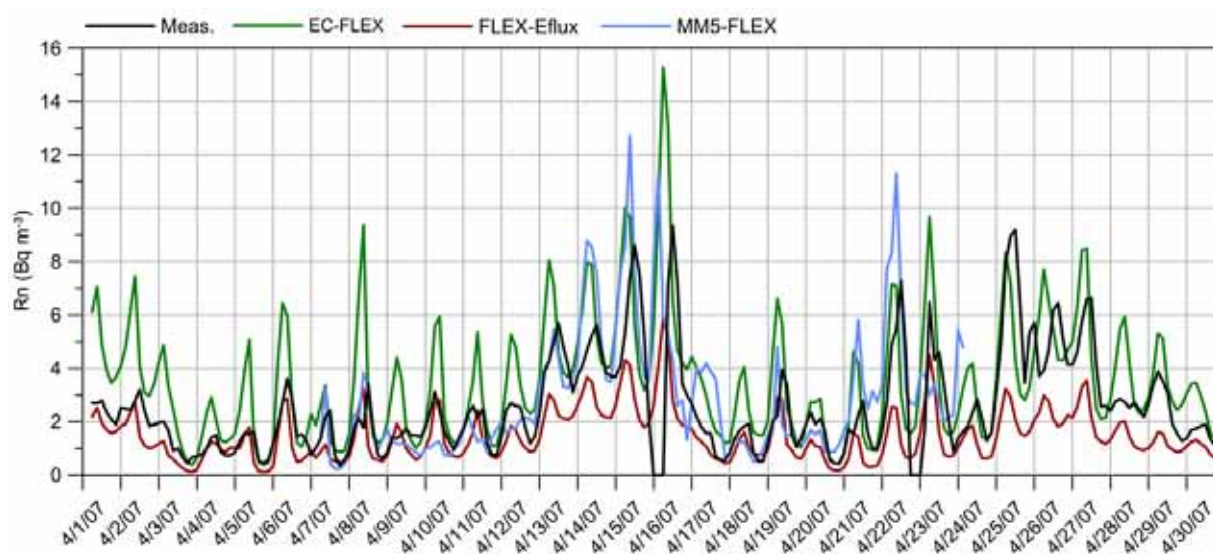
FIG. 3. *Measured (black) and simulated radon time series at 20m a.g.l at Cabauw station using FLEXPARTv6.2 model with a constant 0.66 atom cm^{-2} s^{-1} above land radon source term (green), with the European radon flux map (red) and MM5V3.7-FLEXPARTv6.2 using the constant 0.66 atom cm^{-2} s^{-1} radon exhalation flux density above land and 0 over water bodies (blue).*

As stated in the preceding section, and being one of the main applications of an accurate radon exhalation flux density map, this case study included also the first evaluations of the new version of MM5V3.7-FLEXPARTv6.2 which is able to work with MM5 high resolution meteorological fields. Since MM5 simulations are computationally very expensive, even using hpc, only the central part of the target month was simulated. The gridded output of MM5V3.5-FLEXPARTv6.2 was folded with the simpler constant radon source term and compared with its equivalent ECMWF driven FLEXPARTv6.2 modelled time series (Figure 3). Results of MM5V3.5-FLEXPARTv6.2 are generally in better agreement, specially regarding the absolute value of the night-time maxima and its high frequency characteristics.

REA Stations

All the dispersion calculations in this case study were performed with FLEXPARTv6.2 using both the simple constant 0.66 atom cm^{-2} s^{-1} over land and the radon source term derived from the MARNA map with a maximum resolution of 0.02 close to the station and 0.2 for the rest. The resulting time series were used to highlight the differences appearing in the modelled radon ambient time series when different source terms were used in regions like the Spanish one, with high variability of radon exhalation flux density. Additionally this work helped to identify the main radon sources that could affect some of the stations.

Autilla del Pino

Three different meteorological episodes within January 2003 were selected to study the behaviour of ambient radon concentration time series at Autilla del Pino. Episode 9 (Figure 4, Ep9) corresponds to a strong easterly advection with strong synoptic forcing. For this specific case, the modelled time series, with the two different radon source term, behave similarly with no significant differences between them, both showing a non-realistic dampened diurnal cycle.
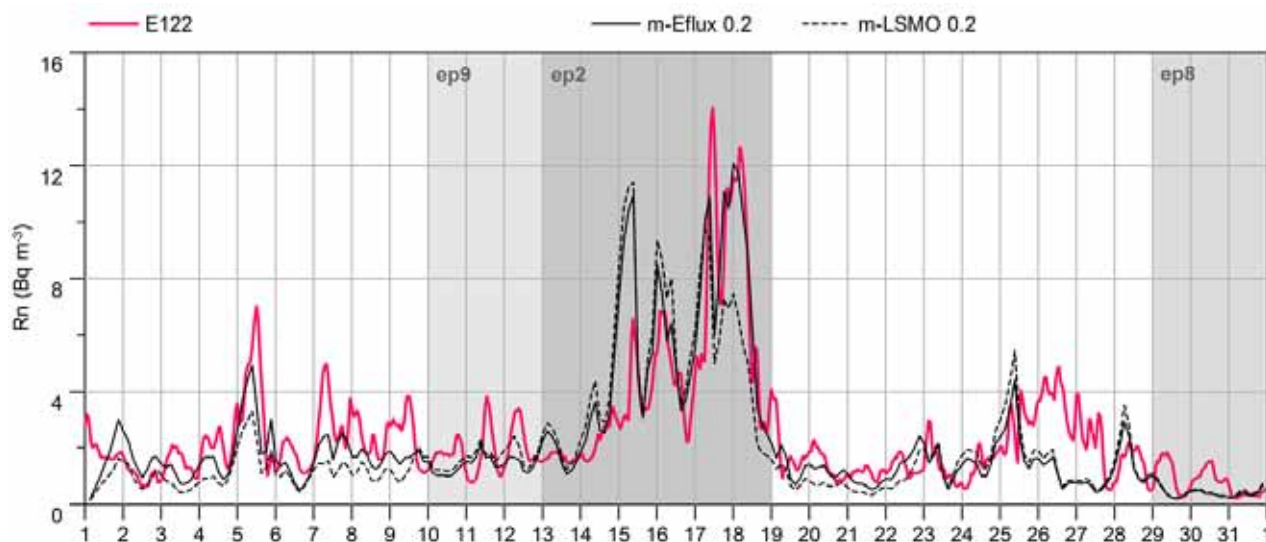
FIG. 4. *Measured (pink) and modelled radon time series (black) at Autilla del Pino station using the constant 0.66 atom cm^{-2} s^{-1} radon exhalation flux density above land and 0 over water bodies (dashed) and the one derived form the MARNA map (solid).*

Episode 2 (Figure 4, Ep2) shows a typical winter high pressure situation which may remain over the Iberian Peninsula for long periods. These weather conditions lead to a day to day accumulation reflected in the noticeable increase of the radon baseline in up to 4 Bq m^{-3}. Radon ambient concentration baseline is well represented by the model but, again, the nocturnal boundary layer is poorly represented being in some cases underestimated or overestimated in others. However, this episode presents a very interesting feature. During the last two days of this period, a significant difference appears according to the two radon source terms used. This behaviour can be explained looking at the SRSs (Figure 5), which mainly spread over the Iberian Peninsula (IP), with higher contributions from the western part of it during these measurement times. The western part of the IP has very high radon exhalation flux densities due to the mainly granitic composition of the soil below. Therefore, 0.66 atom cm^{-2} s^{-1} clearly undervalues the real fluxes leading to an important underestimation of the radon ambient concentrations. On the contrary, the resulting time series when the radon source term derived from the MARNA map is use, represent properly the measurements. It becomes here evident, the need of a better resolved radon exhalation flux density map to be used as a source term in model evaluation, with, at least, the spatial variability included.

FIG. 5. SRM with two zooms in on the right for a sample day of Episode 2 at Autilla del Pino. Day 17.01.2003 at 06:00

Episode 8 (Figure 4, Ep8) corresponds to a very strong northerly advection with air coming from the Atlantic and with strong winds that dampen the diurnal cycles and decrease the radon baseline. In this case the selection of the radon source term definition makes no difference in the final modelled time series.

Murcia

Two typical summertime meteorological episodes were selected to study the behaviour of radon ambient concentration time series at Murcia station. Episode 5 (Figure 6, Ep5) corresponds to thermal low conditions which commonly go together with a heat wave. During this synoptic situation, a low pressure gradient on the surface usually appears and the strong insolation favours the development of mesoscale phenomena. FLEXPARTv6.2 simulates strong diurnal cycles, but with both radon sources, the baseline is overestimated indicating that the region contributing to the baseline has been assigned a too high radon flux.

Episode 3 (Figure 6, Ep3) shows a pressure swamp situation which often appears during summertime in Spain, giving episodes of high levels of pollutants. It is characterised by a

very low pressure gradient which favours stagnation and recirculation processes. Measured radon ambient concentrations show clearly marked diurnal cycles which are not properly modelled by FLEXPARTv6.2 probably due to a poor representation of the height of the boundary layer during night-time. Again, the baseline is overestimated indicating that the radon source terms used are both higher than the real one.
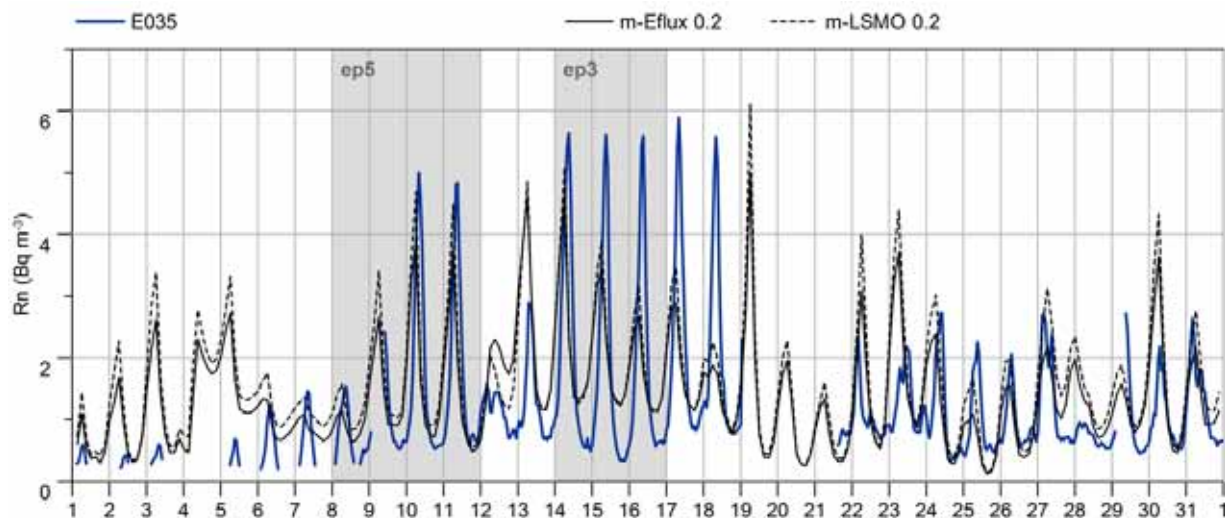

FIG. 6. Measured (blue) and modelled radon time series (black) at Murcia station using the constant 0.66 atom·cm^{-2}·s^{-1} radon exhalation flux density above land and 0 over water bodies (dashed) and the one derived from the MARNA map (solid).

Conclusions

This preliminary case studies show the significant influence of the emission inventory on the final model results. This influence is smoothed when there is strong synoptic forcing with strong winds, vigorous mixing and dampening of the diurnal cycles. However, when there is advection from continental areas and not very strong mixing, differences appear and can easily reach differences of 40%. They are especially noticeable during night-time conditions where nearby heterogeneities in the surrounding radon exhalation flux densities strongly influence the measurements and also when air that has passed over areas with high radon exhalation flux density reaches the measurement station. Therefore, depending on the accuracy desired in the results and also the scope of the study and the meteorological episode in which it takes place, a simple radon source term could then work reasonably fine. When very accurate simulations are needed (f.i. in model validation studies) in places with very heterogeneous radon exhalation flux densities and under meteorological conditions that would favour their influence on the measurements, an accurate radon source term, variable both in space and also in time, would be necessary. This detailed radon source term, though, is still missing, and additional work is needed to fulfil the needs of the atmospheric modelling community.

REFERENCES

[1]   LEE, H.N., LARSEN, R.J., Vertical diffusion in the lower atmosphere using aircraft measurements of ^{222}-Rn. J. Appl. Meteorol. **36** (1997) 1262-1270.

[2]   LUPU, A., CUCULEANU, V., Code for calculating the vertical distribution of radon isotopes and their progeny in the atmosphere, Computer Physics Communications **141** 1 (2001) 149–162.

[3]   CONEN, F., ROBERSTON, L.B., Latitudinal distribution of ^{222}Rn flux from continents, Tellus **54B** (2002) 127–133.

[4]   WMO - 1st International expert meeting on sources and measurements of natural radionuclides applied to climate and air quality studies. Technical Report No 155, World Meteorological Organization Global Atmosphere Watch (2004).

[5]   QUINDÓS, L.S., et al., Natural gamma radiation map (MARNA) and indoor radon levels in Spain, Environ. Int. **29** (2004) 1091-1096.

[6]   STOHL, A., HITTENBERGER, M., WOTAWA, G., Validation of the Lagrangian particle dispersion model FLEXPART against large scale tracer experiments. Atmos. Environ. **32** (1998) 4245–4264.

[7]   STOHL, A., FORSTER, C., FRANK, A., SEIBERT, P., WOTAWA, G., Technical Note: The Lagrangian particle dispersion model FLEXPART version 6.2. Atm. Chem. Phys. **5** (2005) 2461–2474.

[8]   ECMWF (edited by: White, P.W.): IFS Documentation, ECMWF. Reading, UK, 2002. (available online at http://www.ecmwf.int)

[9]   WOTAWA, G., et al., Atmospheric transport modelling in support of CTBT verification - Overview and basic concepts. Atmos. Environ. **37** (2003) 2529–253.

[10] SEIBERT, P., FRANK, A., Source-receptor matrix calculation with a Lagrangian particle dispersion model in backward mode. Atm. Chem. Phys. **4** (2004) 51–63.

[11] LEVIN, I., et al., Observations of atmospheric variability and soil exhalation rate of ^{222}Rn at a Russian forest site: Technical approach and deployment for boundary layer studies. Tellus **54B** (2002) 462–475.

[12] SZEGVARY, T., LEUENBERGER, M.C., CONEN, F., Predicting terrestrial ^{222}Rn flux using gamma dose rate as a proxy. Atm. Chem. Phys. **7** (2007) 2789–2795.

[13] SZEGVARY, T., et al., European ^{222}Rn inventory for applied atmospheric studies. Atm. Chem. Phys. Disc., (2008) acpd-2008-0017.

[14] GROSSI, C., et al., Inter-comparison of different direct and indirect methods to determine ^{222}Rn flux from soil. Radiat. Meas. (submitted, 2009).

[15] SEIBERT, P., SKOMOROWSKI, P., Untersuchungen der orografischen Besonderheiten der Probenahmestellen Schauinsland und Freiburg und deren

Auswirkungen auf die Genauigkeit von adjungierten atmosphaerischen Ausbreitungsrechnungen, Schriftenreihe Reaktorsicherheit und Strahlenschutz, (2007) BMU - 2008 - 713, on-line at http://www.bmu.de/41875.

[16] ARNOLD, D., Study of the atmospheric radon concentration dynamics at the Spanish radiological surveillance stations and its applications to air mass movements. Unpublished doctoral dissertation, Technical University of Catalonia, Barcelona, Spain (2009).

[17] WHITTLESTONE, S., ZAHOROWSKI, W., Baseline radon detectors for shipboard use: development and deployment in ACE-1. Journal of Geophysical Research **103** D13 (1998) 6743-16751.

[18] ZAHOROWSKI, W., CHAMBERS, S.D., HENDERSON-SELLERS, A., Ground based ^{222}Rn observations and their application to atmospheric studies. J. Environ. Radioactiv. **76** (2004) 3-33.

[19] VARGAS, A., ARNOLD, D., ORTEGA, X., PARAGES, C., Influence of natural radioactive aerosols on artificial radioactivity detection in the Spanish surveillance networks. Appl. Radiat. Isotop. **66** (2008) 1627–1631.

MEASUREMENT AND SIMULATION OF RADON TRANSPORT IN EAST ASIA AND THEIR IMPLICATION ON SOURCE DISTRIBUTION

S. HIRAO, H. YAMAZAWA, J. MORIIZUMI, T. IIDA
Nagoya University, Furo-cho, Chikusa-ku, Nagoya, Japan

Abstract

Outlines of the continuous monitoring of atmospheric radon concentration at several locations in East Asia, the development and validation of a long-range atmospheric transport model, and a trial of estimating and reducing uncertainty in radon exhalation flux density maps were presented. Atmospheric radon concentration data observed at a small solitary island in the Pacific Ocean were successfully used to improve the vertical diffusion scheme in the model although the uncertainty in the radon flux density data was the limitation. It was also pointed out that a kind of source-receptor analysis using the radon concentration observed at these islands would reduce uncertainty in the radon flux density maps.

Introduction

Atmospheric radon has a potential of being used as a tracer for atmospheric transport of meso- to synoptic scales because of its half life. Its typical application is a use in a validation of long-range atmospheric transport models as reference data. Since the source of radon is somewhat uniformly distributed over land, advantages of using radon as a tracer are more apparent in examining vertical diffusion calculations of the models than in testing horizontal transport and diffusion calculations. Main limitations of radon as an atmospheric tracer come from uncertainty in the radon exhalation flux density [1]. The commonly used exhalation flux density value of 1 atom of radon per square centimeter per second is now considered to be not sufficiently accurate and a few radon flux density maps estimated by more physically sound models from radium content and soil moisture data became available [2, 3]. However, differences in flux density values between maps are still large and the uncertainty in values of radon flux map is roughly a factor of 1.5 to 2 [1].

The authors have been operating an atmospheric radon monitoring network in the East Asian region, in which surface radon concentration have been measured at several points including small solitary islands in the Pacific Ocean.[4] They have also developed a long-range atmospheric transport model for radon and its decay products. The model was tested and improved by using observed radon data from the network [5, 6]. With the above-mentioned background, this paper briefly demonstrates how atmospheric radon data are used to test and improve an atmospheric transport model and how the inconsistency between the radon exhalation flux density maps appears in the simulations.

Radon concentration observation

The radon monitoring network has been operational since around 2000. The observation points of the present network are shown in Figure 1, in which also shown are observation points already closed. The network is designed to capture outflow of air masses from the Asian Continent. For this reason, most of the observation points are aligned along a west-east line. Among the points, Hachijo Island is the best located and maintained station, where the observation point is located at the northwestern edge of the island to have a pure fetch over sea when the prevailing wing from the northwestern sector. The local radon exhalation flux density from this island has been measured to be less than 1 mBq m^{-2} s^{-1} because the surface of the island is covered by scoria of basalt due to relatively recent volcanic activities [7].

Radon concentration at each site is measured with an electrostatic-type radon monitor with a 16.7 L vessel. Its minimum detection limit is 0.3 Bq m^{-3} for one hour average concentration. Hourly concentrations are stored.
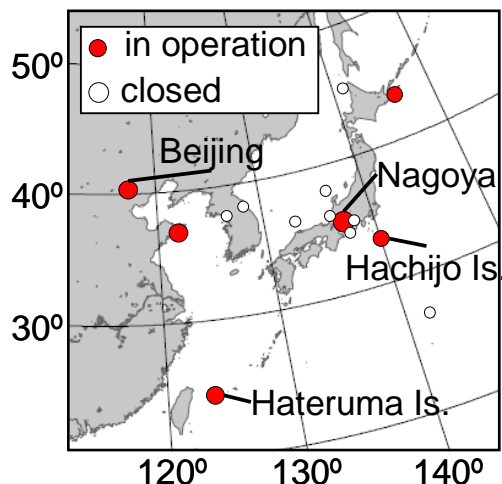

FIG. 1. Location of surface air radon concentration observation in the East Asian region.

Model

The long-range transport model consists of a meteorological model, MM5, and an Eulerian type transport model [5, 6]. These two models are off-line connected with three-hourly meteorological data feed. The original version of this model used the MRF-PBL model in MM5 to calculate the vertical eddy diffusivity. This model is a first-order turbulence model with a relatively simple modelling of turbulence quantities in terms of mean meteorological variables. As shown later in this paper, this model is replaced by the GS Model, a 1.5-order turbulence closure model, to achieve better performance for radon transport simulations. Although treatments of lateral boundary conditions, numerical schemes for advection and diffusion calculation and quality of sea surface temperature data were also tested by using radon data as reference, their results are not presented here.

The calculation domain for is 9792 km (W-E) × 7776 km (S-N) × 10 km, divided by horizontal grid of a 72 km square. Meteorological data and SST data used are the global analysis data from Japan Meteorological Agency and the monthly SST data from NCEP. Although the Schery's radon monthly flux map [2] was mainly used in the model test, Yamazawa's map (NU map) [8] based on the radon exhalation modelling by Goto [3] was also used to discuss effects of uncertainty in the radon exhalation flux density.

Results and Discussion

Performance of the original model

Simulation results are compared with the concentration observed at Hachijo Island and Nagoya in Figure 2. The concentration variations with several-day cycle observed at Hachijo Island were simulated well except that the absolute value was systematically underestimated. The good performance of the model for several-day cycle concentration variations and the general tendency of underestimation of absolute value of the concentration were commonly found for other locations in this region [5]. Similar underestimation was found at Nagoya, where diurnal variations were pronounced. The underestimation of the daily minima at Nagoya is considered to be caused by possible underestimation in radon flux and/or shortcomings in vertical transport (diffusion) calculation in the model.

The bias of the simulated concentration for each month are shown in Figure 3 (left). It is defined by Eq.(1)

$$b_n = \sum_i \left(C_i - M_i \right) \bigg/ \sum_i M_i \tag{1}$$

where C_i and M_i are the calculated and measured concentrations, respectively. Underestimation of surface concentration is evident especially in the cold season when the northwesterly monsoon form the continent prevails.

Improvement of PBL model

According to the detailed analysis of the potential temperature profiles, it was found that the simulated PBL at Hachijo Island was generally deeper than observation. This tendency of the MRF-PBL model resulted in more dilution of radon and hence lower concentration in the PBL. With the purpose of improving this point by using a more sophisticated turbulence scheme, the first-order MRF-PBL model was replaced by a 1.5-order GS-PBL model. This replacement resulted in shallower PBL depth (closer to observation), higher surface radon concentration by a few tens of percent and hence better values of bias at Hachijo Island (Figure 3: right). However, the improvement in the bias values was not evident at the other locations although there were slight improvements.
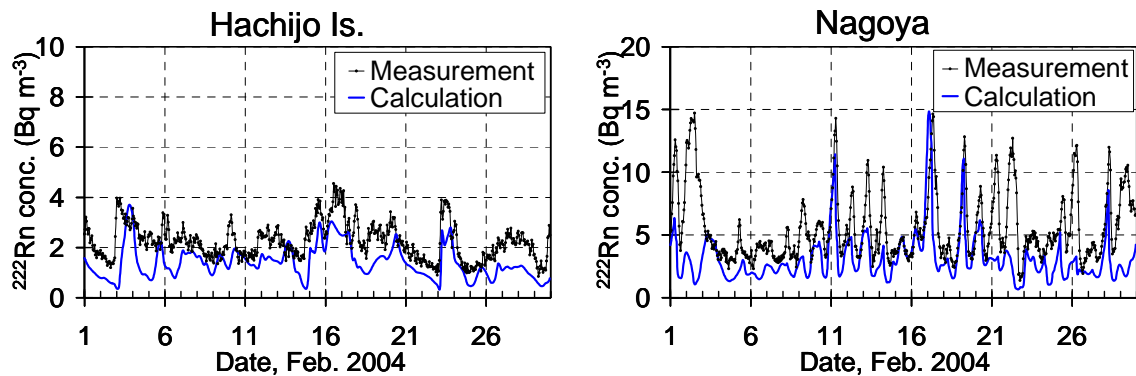
FIG.2. Comparison of simulated surface radon concentration with observation.
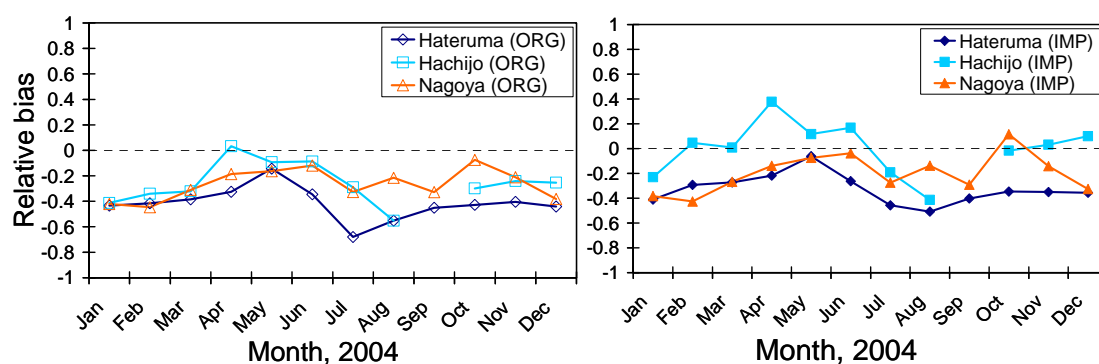
FIG. 3. Monthly averaged normalized bias of the concentration simulated by the original model with the MRF-PBL model (left) and the GS-PBL model (right) from the Schery's flux map.

Effects of uncertainty in radon flux maps

The improvements of the long-range atmospheric transport model were supported by the comparison with the observed radon concentration in addition to the comparisons of potential temperature profiles. However, this conclusion is based on the assumption that the radon exhalation flux density map is reliable. As pointed out by the presentation by Yamazawa in this meeting, there are substantial differences in values between radon flux density maps [8]. In addition, radon flux density may change in time due to change in soil moisture, and in space due to spatial distribution of radium content and other soil properties. Therefore, when simulation results of atmospheric radon concentration are compared with observations, we must be careful about the fact that both atmospheric transport model models and radon flux density maps have their own uncertainties.

It is not easy to separately discuss the effects of these two sources of uncertainties in a comparison between simulated and measured radon concentrations. A straightforward way of inferring effects of uncertainty in radon flux density maps is to use more than one radon flux density maps. An example of the comparison on simulation results from different radon flux maps (Figure 4) with observation results is shown in Figure 5 for a month in winter of a year different from that in Figure 2. The model used is the improved one. The flux density maps are the Schery's map [2] and the NU map [3, 8].

The results from the Schery's map show good agreement with the observation although slight underestimation in the first 10days and large overestimation for some peak concentrations. Whereas, the simulation with the NU map generally underestimated the concentration. This is consistent with the results found for the atmospheric radon concentrations at the Bering Sea and the Arctic Ocean [8].
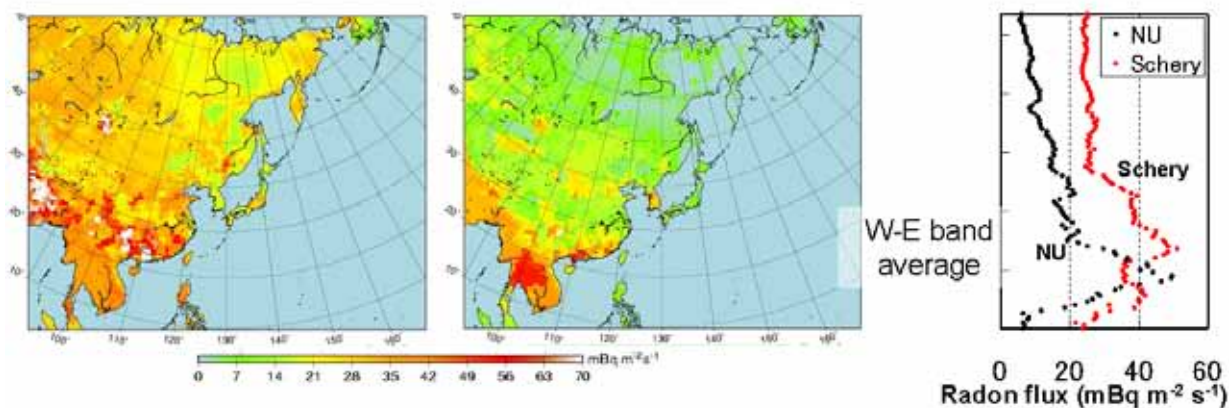
FIG. 4. *Radon flux maps used in the ATM simulation and differences in flux density values.*
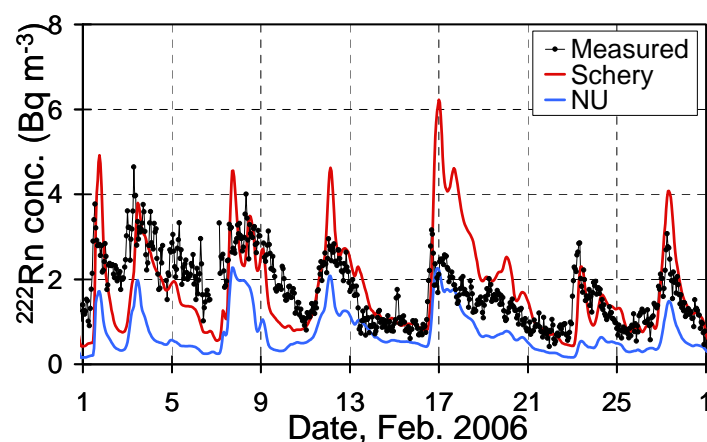
FIG. 5. *ATM simulation results from two different radon flux density maps compared with observation in February 2006 .*

A kind of source-receptor analysis was carried out for this month. The land area of the model domain was divided into 10 sub-areas. Simulations were carried repeatedly, each being with flux from only one sub-area was allowed. Since the source-receptor relation or the dilution factor, that is the concentration at the receptor contributed by a source divided by the strength of the source, can be reasonably calculated by the improved model, the discrepancy of the simulation results from the observation can be attributed to uncertainty in radon flux density at each sub-area. This analysis indicated that in the case of Schery's map, the overshoot of concentration at peaks were mainly contributed by radon from west Siberia and mid to north China, for which average radon exhalation flux density values of 29.4 and 28.2 mBq m^{-2} s^{-1} are assigned. Reduction in these values will result in better agreement with the observed radon concentration. Also pointed out for the Schery's map was that larger flux density at the Korean Peninsula would give better results. Whereas, for the NU map, the underestimation of concentration was found to be mainly caused by small flux density values for the mid to north China and east Siberia, for which the map predicts flux density to be 13.7 and 5.5 mBq m^{-2} s^{-1}, respectively. Little larger flux densities at other locations except for the Korean Peninsula also improve the comparison with the observation. This trial-and-error type procedure of testing flux density values will be replaced by a more systematic statistical method such as one with

Bayesian statistics to have more quantitative insight in the radon exhalation flux density distribution.

Summary

The outlines of the continuous atmospheric radon monitoring at the surface level in the East Asia and the development and improvement of long-range atmospheric transport model by using radon monitoring data were described. Usefulness of the atmospheric radon as a tracer highly depends on continuous measurements of radon concentration at various locations with a certified uncertainty and a reliable radon exhalation flux density map properly describing spatial and temporal variations. The radon concentration data have become more available then before although most of them are surface level data. On the other hand, radon flux distribution has not been determined accurately enough to precisely discuss ATM performance. An example way of narrowing down the uncertainty in radon flux density map was demonstrated in this paper. Reduction of the uncertainty in radon flux density maps is the key and urgent task.

References

[1] YAMAZAWA, H., et al., Modeling of atmospheric radon transport in East Asian region, Proceedings of International symposium on Environmental Modeling and Radioecology (2006) 119.

[2] SCHERY, S.D., WASIOLEK, M.A., Modeling Radon Flux from the Earth's Surface, in RADON AND THORON IN THE HUMAN ENVIRONMENT, World Scientific Publishing, Singapore (1998) 207.

[3] GOTO, M., et al., Estimation of Global Radon Exhalation Rate Distribution, Proc. 8th Int. Symp. Natural Radiation Environment, Buzios, Brazil, AIP Conference Proceedings 1034 (2007) 169.

[4] MORIIZUMI, J., et al., Continuous Observation of Atmospheric ^{222}Rn Concentrations for Analytic Basis of Atmospheric Transport in East Asia, Journal of Nuclear Science and Technology, Supplement 6 (2008) 173.

[5] HIRAO, S., et al., Development and Verification of Long-Range Atmospheric ^{222}Rn Transport Model, Journal of Nuclear Science and Technology, Supplement 6 (2008) 166.

[6] HIRAO, S., et al., Development and Verification of Long-range Atmospheric Transport Model of ^{222}Rn and Lead-210 Including Scavenging Process, Proceedings of 8th International Symposium on the Natural Radiation Environment, (2007) 407.

[7] OHKURA, T., et al., Monitoring Network of Atmospheric ^{222}Rn Concentration in East Asia and Backward Trajectory Analysis of ^{222}Rn Concentration Trend at a Small Solitary Island on Pacific Ocean, Journal of Japan Society for Atmospheric Environment **44** (1) (2009) 42 (in Japanese).

[8] YAMAZAWA, H., et al., Evaluation of radon flux maps for Siberian and East Asian regions by using atmospheric radon concentration observed over oceans, (2009).

VERTICAL DISPERSION OF RADON AND CONVENTIONAL POLLUTANTS: SOME TESTS ON EXISTING AND NEW MODELS

M. MAGNONI[*]

ARPA Piemonte, Centro Regionale Radiazioni Ionizzanti e Non Ionizzanti,
Ivrea,
Italy

Abstract

The atmospheric mixing height was recognized as the most relevant parameter affecting the accumulation of major urban pollutants as well as radon. In this work a simple model for the evaluation of the mixing height, by means of radon activity concentration measurements (Bq m^{-3}), is proposed and tested with published and new data, gathered in Milan and Alessandria (Po Plain). Moreover, the radon exhalation flux density for the area of interest (Po Plain) was estimated in the range 4.2 mBq m^{-2} s^{-1} – 8.6 mBq m^{-2} s^{-1}.

Introduction

The use of radon for the studies of the accumulation of conventional pollutants was suggested by several authors in the last two decades [1–3]. This issue is of great concern in Italy, especially in the North. It is well known that Northern Italy, and in particular the Po Valley, the largest Italian agricultural and industrial area (45 000 km^2, around 20 million inhabitants) is characterized by condition of high air stability, especially in winter. For that reason, high and sometimes very high concentration levels of the typical pollutants mainly coming from motor vehicles traffic (benzene, PM10, PM2.5, Nitrogen Oxides) are often reached.

The basic idea underlying this framework is that radon, being produced in the Earth crust by the radioactive decay of radium at a fairly constant rate, after the diffusion in the atmosphere, is only affected by the changing of meteorological conditions. For that reason, the variation of outdoor radon levels, being relatively independent on the variations of the source strength, can be considered as a good indicator for the prediction of acute pollution phenomena of man made pollutants. There are some experimental evidence that the most acute pollutions events are strongly related with atmospheric conditions of high atmospheric stability. When these conditions occur the pollutants concentrations at ground level rise quickly and are often fairly independent on their emission rates, usually related to motor vehicles traffic [4]. For that reason radon can be seen as a tool for the prediction and the calculations of acute pollution phenomena.

In these situations, when advection is absent or negligible, the accumulation and the dynamics of radon as well as all the other pollutants are strongly affected by a parameter, the 'mixing height', i.e. the depth of the Planet Boundary Layer. In this paper a model for the evaluation of the atmospheric mixing height by means of measurements of radon concentrations performed outdoor, near the ground, is described. In order to test the model, some experimental data on radon and some conventional pollutants (benzene, PM10, NO$_2$) were collected in Alessandria, a small town (around 80 000 inhabitants) located in the south border of the Po Plain, not far from the Monferrato hills. Other experimental radon data, collected and published by other researchers in Milan were also used for model validation. The results obtained using our model are also compared with those calculated by means of different software and mathematical models and also by direct experimental measurements.

---

[*] With contributions from D. Bianchi, L. Erbetta, S. Gastaldo, P. Rabbia and V. Garbero

Material and methods

The radon detection system

The radon concentration in atmosphere was measured in Alessandria by means of a quite high sensitivity radon detector, the Pylon-TEL, coupled with MR-1 Miam control device (Minimum Detectable Activity = 0.9 Bq m^{-3}, for 30' counting). The detection system is based on a large ZnS scintillation electrostatic cylindrical chamber (18.5 litres) into which the air is driven by a pump. The counting efficiency of the chamber is increased by collecting the radon progeny to the cathode, a coaxial cylinder of aluminized mylar that overlays a scintillator (ZnS), see Figure 1.
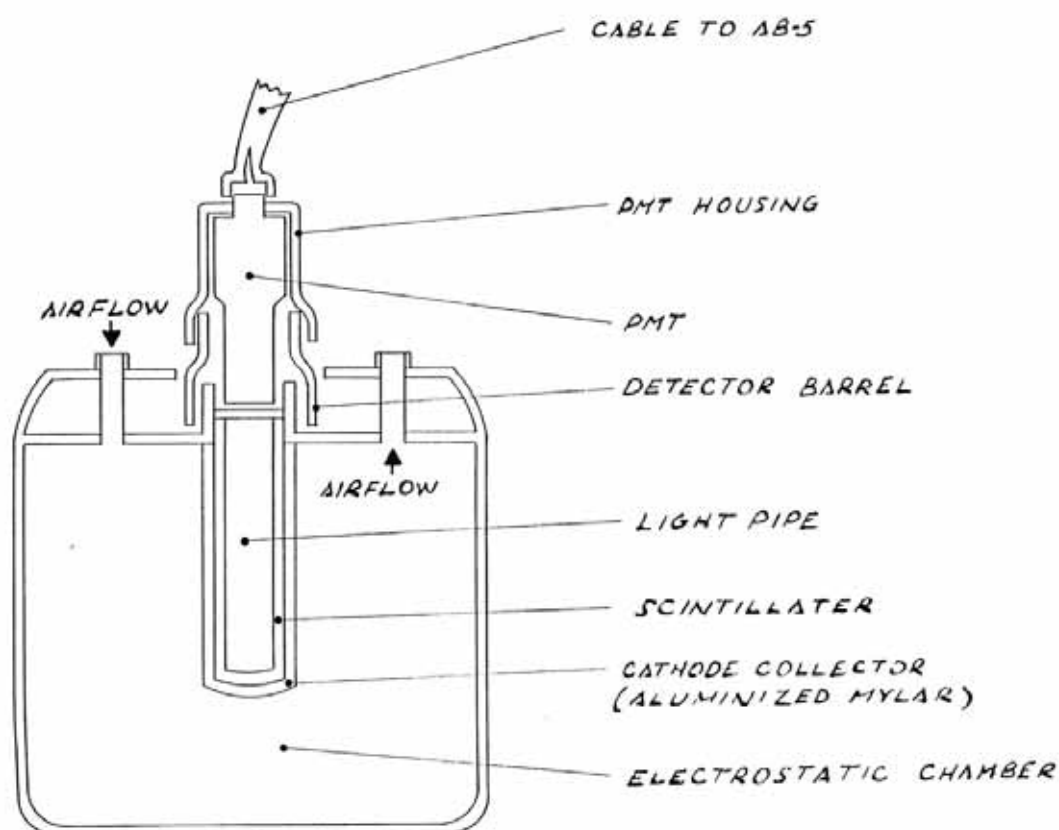
FIG. 1. Scheme of PMT-TEL detection probe.

The detection system was installed on the roof a building, approximately 4 m above the ground: it was then possible to follow the daily fluctuations of radon due to the atmospheric motions and then to compare them with the levels of the other conventional pollutants, such as benzene, PM10 and NO$_x$, mainly coming from motor vehicles, simultaneously recorded at a sampling station located in the same urban area (1 km far away).

Theoretical model

The radon exhalation flux density *J* coming from the Earth surface can be described by the well known balance equation (1):

$$divJ + \frac{\partial C}{\partial t} = 0 \qquad (1)$$

where *C* is radon concentration (Bq m^{-3}). If we assume that radon motion in the free atmosphere could be modelled in one dimension (i.e, considering only the vertical coordinate *z*) and if we neglect advection, we can write for *J* equation (2):

$$J = -D \cdot \frac{\partial C}{\partial z} \qquad (2)$$

where *D* is the coefficient of eddy diffusivity; putting equation (2) in the expression (1), we get the following second order differential equation (3):

$$D \cdot \frac{\partial^2 C}{\partial z^2} - \lambda \cdot C = 0 \qquad (3)$$

in which λ is the radon decay constant. The equation is straightforward integrated, giving equation (4):

$$C(z) = A \cdot e^{-z \cdot \sqrt{\frac{\lambda}{D}}} + B \cdot e^{z \cdot \sqrt{\frac{\lambda}{D}}} \qquad (4)$$

where *A* and *B* are constants whose value will depend on the boundary conditions describing the real physical phenomenon.

The motion of air masses in the lower atmosphere, in the Po Plain, especially during winter, is largely affected by thermal inversion that, in particular during night time, limits the vertical circulation. The stronger the thermal inversion, the higher the accumulation of conventional pollutants and radon as well. In these cases the pollutants can be roughly considered as uniformly distributed within the so called 'mixing layer', defined by a parameter, the 'mixing height', *h* the value of which strongly affects the concentration levels of radon as well as all the other pollutants.

Therefore, in order to mathematically describe the accumulation phenomena in this layer we can consider the motion of the radon and all the air particles restricted to a limited layer (*0, h*), where *h* is actually the mixing height.

For the boundary condition in *z=0*, if we want to correlate the radon concentration at the soil-air interface C_0 with an external and measurable physical parameter, i.e. with the radon exhalation flux density ϕ (Bq m^{-2} h^{-1}]) coming from the ground, we have to put a condition on the radon flux itself, *J(0)=ϕ,* that is equivalent to the following equation (5):

$$\frac{\partial C(0)}{\partial z} = -\frac{\phi}{D} \tag{5}$$

For the boundary condition in $z=h$, because the diffusion of pollutants and radon above the mixing height h is forbidden, i.e. the flux of radon is zero, the derivative of C in h should vanish. We have therefore equation (5a):

$$\frac{\partial C(h)}{\partial z} = 0 \tag{5a}$$

$$D \cdot \left(-A \cdot \sqrt{\frac{\lambda}{D}} + B \cdot \sqrt{\frac{\lambda}{D}}\right) = \phi \tag{6}$$

$$-A \cdot \sqrt{\frac{\lambda}{D}} \cdot e^{-h \cdot \sqrt{\frac{\lambda}{D}}} + B \cdot \sqrt{\frac{\lambda}{D}} \cdot e^{h \cdot \sqrt{\frac{\lambda}{D}}} = 0$$

These boundary conditions define the following algebraic system, for the unknown A and B whose solution, together with equation (4), allows the calculation of the vertical profile of the radon concentration (Eq. (7)):

$$C(z) = \frac{\phi \cdot \left\{ e^{-z \cdot \sqrt{\frac{\lambda}{D}}} + e^{-(2h-z) \cdot \sqrt{\frac{\lambda}{D}}} \right\}}{\sqrt{\lambda \cdot D} \cdot (1 - e^{-2h \cdot \sqrt{\frac{\lambda}{D}}})} \tag{7}$$

Equation (7) depends on a parameter, the mixing height h, that varies accordingly to the changing of the meteorological conditions and generally decreases during the night, especially in winter when strong inversions occur. It can be easily seen that the (7) is able to predict the increasing of the concentration levels while the mixing height h decreases, as confirmed by all the available experimental data. In fact we have, for example, at ground level ($z=0$) equation (8):

144

$$C(0) = \frac{\phi \cdot (1 + e^{-2h \cdot \sqrt{\frac{\lambda}{D}}})}{\sqrt{\lambda \cdot D} \cdot (1 - e^{-2h \cdot \sqrt{\frac{\lambda}{D}}})} > \frac{\phi}{\sqrt{\lambda \cdot D}} \tag{8}$$

where the expression at the right side of the inequality is the ground level ($z=0$) concentration for very great h ($h \rightarrow +\infty$).

Results and discussion

Experimental measurements

The experimental campaign in Alessandria started in spring 2008 and allowed to collect a considerable amount of data on radon and typical motor vehicles pollutants; hourly data of more than 200 days were gathered [5]. The comparison between radon and the conventional pollutants showed a significant correlation of radon with benzene, and to a lesser extent, also with PM10 and NO_2. In particular the correlation between radon and all urban pollutants appears quite good ($R^2 > 0.7$) considering monthly averaged data (see, for example, Figure 2).
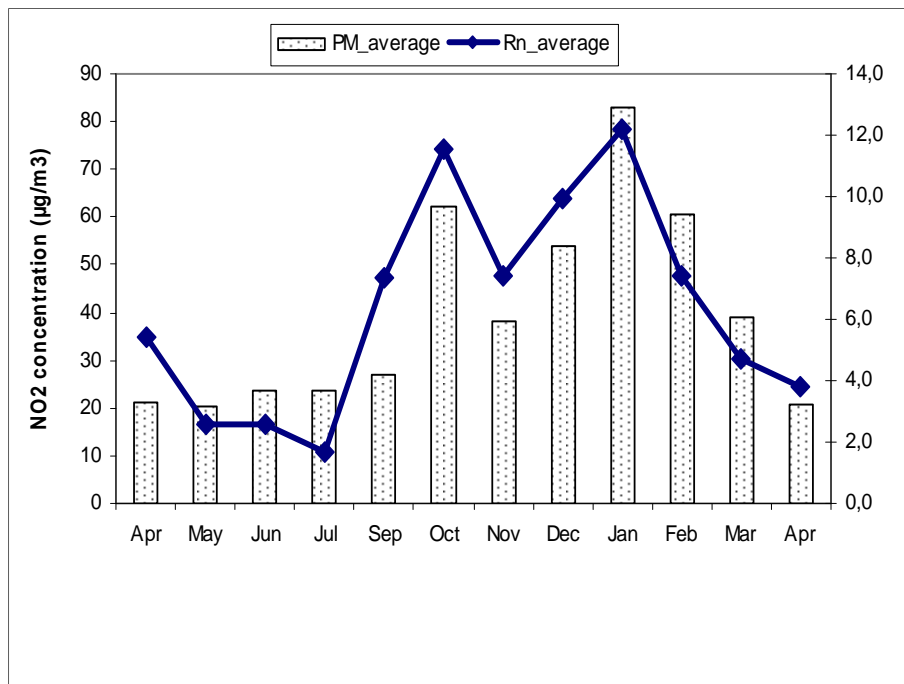
FIG. 2. Monthly averaged data of PM10 and radon in Alessandria (2008–2009).

The correlation worsens considerably considering hourly data, as the Pearson correlation matrix shows (Table 1), while it is still quite good for benzene, a volatile chemical species that exhibits a gaseous behaviour.

TABLE 1. PEARSON CORRELATION MATRIX

	RADON	PM10	BENZENE	NO$_2$
RADON	1.000			
PM10	0.393	1.000		
BENZENE	0.625	0.545	1.000	
NO$_2$	0.323	0.623	0.721	1.000

In order to study the mean trend of the radon concentration during a typical day, averaging the hourly data, we calculated for each month or season a 'typical average day'. In Figure 3 the typical daily trends for summer, winter and two months (April and September) are shown.
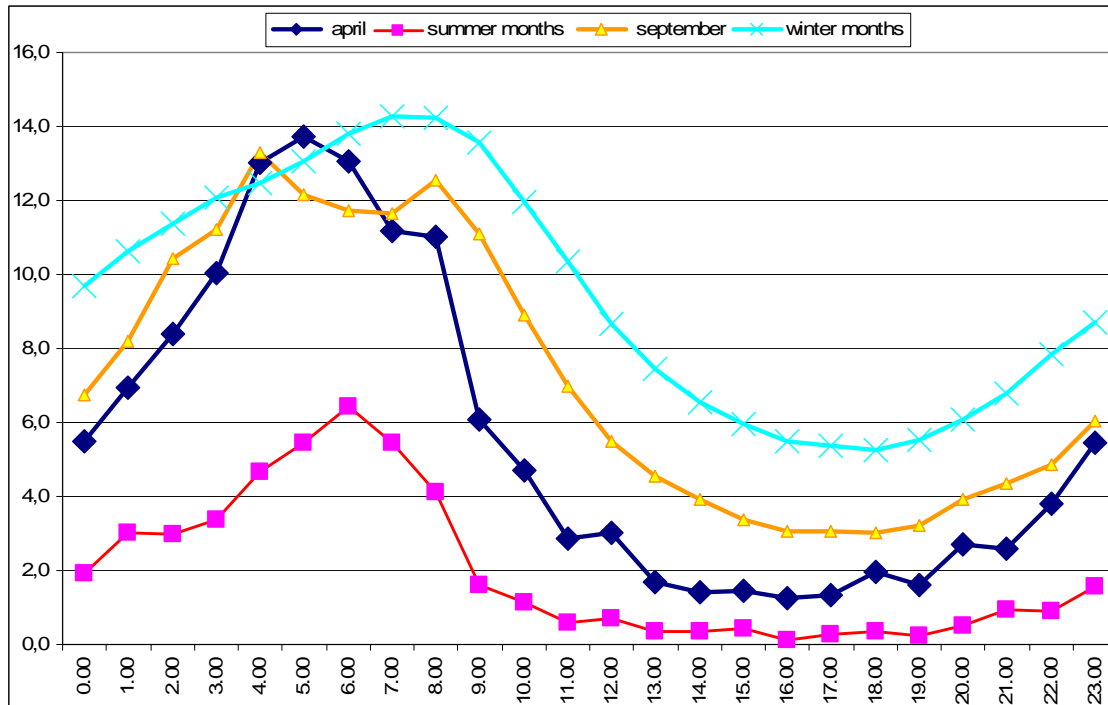
FIG. 3. *Radon typical average day in different months and seasons in Alessandria: in summer the morning maximum is substantially lower (by a factor of 2 or 3) than in winter, while the minimum approaches the Minimum Detectable Activity (<1 Bq m^{-3}).*

Model test

In order to test the model we have first to consider the input parameters:

- The radon exhalation flux density from the ground ϕ, assumed constant in the time range of the observations
- The coefficient D, a dispersion coefficient related to the atmospheric conditions while the parameter to be determined is of course the mixing height h.

146

It can be shown that (see Figure 4), for a wide range of 'acceptable' D values (say, from 3000 m^2 h^{-1} to 50 000 m^2 h^{-1}), the dependence of C(z) is relatively weak. Therefore, one can assume a constant value for D too, even if the 'true' D value is known with poor accuracy.
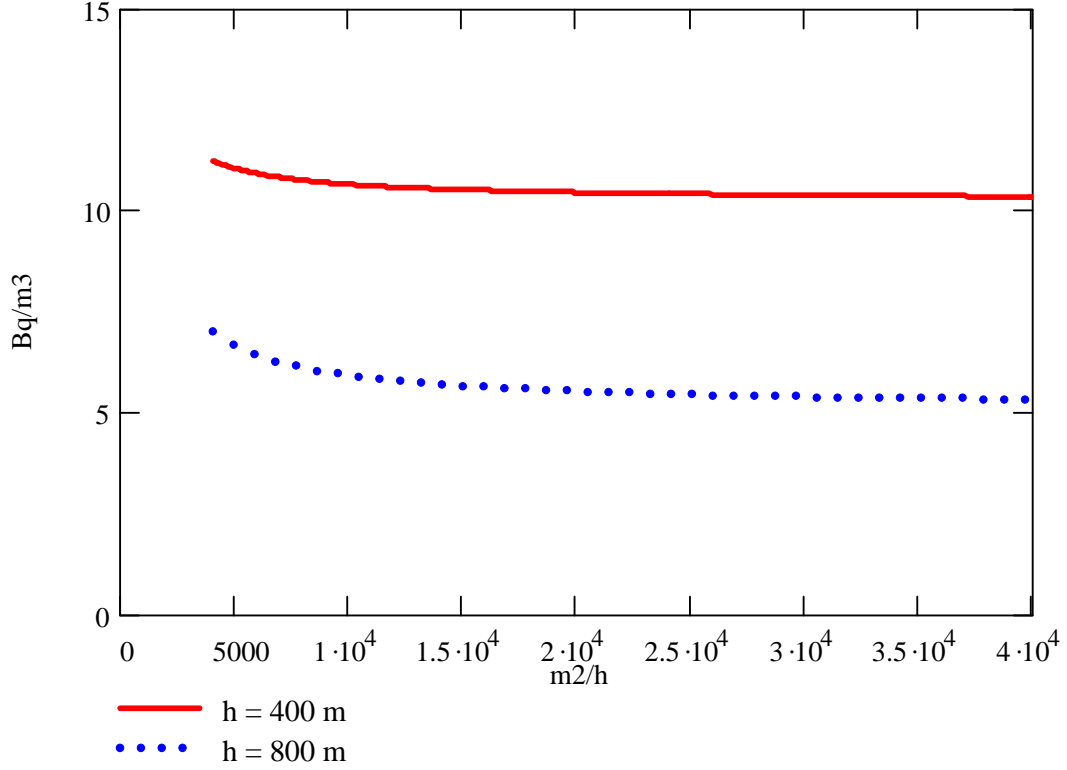
FIG. 4. Variation of the radon concentration for two different mixing heights as a function of D.

Thus, the application of the model and the calculation of the mixing height should be straightforward, provided the value ϕ of the radon exhalation flux density is known. Unfortunately, in the area of interest (Po Plain) there are no reliable direct measurements of the radon flux. The researchers of the University of Milan that a few years ago studied the problem and proposed a box model[6] for the evaluation of the mixing height used for ϕ the value of 72 Bq m^{-2} h^{-1} (20 mBq m^{-2} s^{-1} or 0.95 atom cm^{-2} s^{-1}), taken from global scale flux accepted data. However, this value seems to be quite high because it doesn't fit well with the observed radon concentration.

For that reason, for the determination of the value of ϕ as the input data for the model, we followed a "fitting approach". We left free the all the 3 parameters of the model and we made a least square regression of the experimental data with the function $C = C(\phi, D, h)$, the quantity to be minimized being equation (9):

$$\chi^2 = \sum_j (C_j - C(\phi, D, h))^2 \qquad (9)$$

where the C_j are the hourly values of a "typical average day", calculated for each month.

We performed the regressions not only on our new data (Alessandria) but also on previous published data, gathered in city of Milan, about 80 km from Alessandria [7].

The average best fit value of the radon flux ϕ in Alessandria was $\phi = 15$ Bq m^{-2} h^{-1} (4.2 mBq m^{-2} s^{-1}), while for the flux in Milan we found a greater value, $\phi = 31$ Bq m^{-2} h^{-1} (8.6 mBq m^{-2} s^{-1}), but less than ½ of the value used in the box model calculation previously used.

The fitted values for D were found are in the range 3600–8100 m^{-2} h^{-1}, with a mean value of 5250 m^{-2} h^{-1}.

Once estimated and fixed ϕ and D, we are then able to calculate the mixing height h from the C_j experimental radon concentration data: these calculations were performed for Alessandria data and also for the available (published) Milan data.

The mixing heights h calculated in this way were found in the range 150–2800 m, the average values being 486 m for Milan and 682 m for Alessandria: the h values in typical average days are shown in Figure 5.
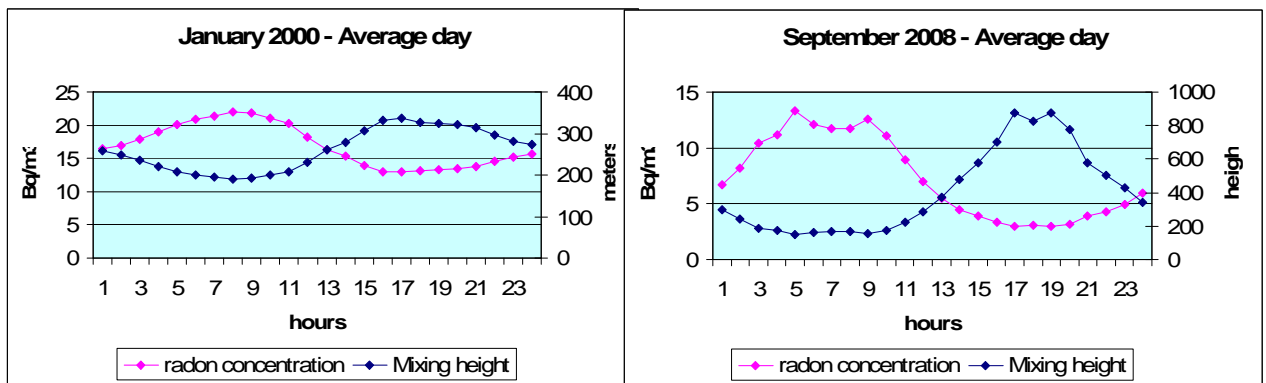
FIG. 5. Radon concentration and related mixing height for typical average days in Milan and Alessandria.

These results seem in quite good agreement with those calculated with the CALMET meteorological software model and especially with those obtained using a thermodynamic model based on the Gryning-Batcharova model, as can be seen from Figure 4, where the cumulative frequencies of the calculated mixing heights for the site of Milan are compared with our calculations (red line) [8].
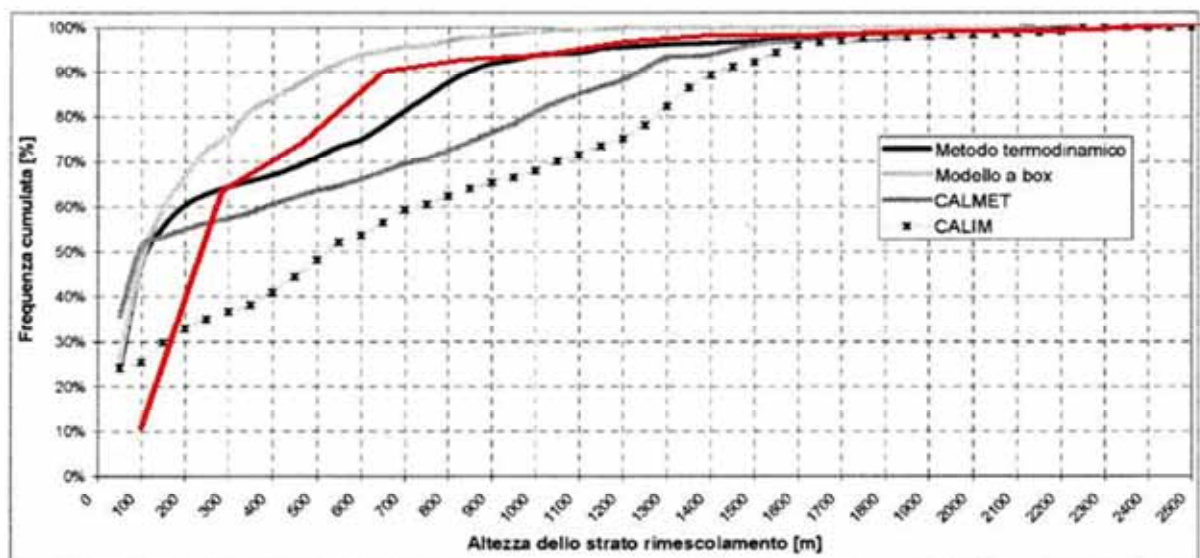
FIG. 6. Cumulative frequency for the mixing heights in Milan: our predictions (red line) are in quite good agreement with those obtained with the CALMET software model and a thermodynamic model based on the Gryning-Batcharova model, while differ substantially from the radon box model calculations (light grey line).

Conclusions

A simple model for the calculation of the mixing heights from the radon concentration measurements was developed and tested using new experimental data gathered in Alessandria and previously published data (Milan). The model gave results in good agreement with other models based on different approaches and thus appears as an useful tool for the predictions of acute conventional pollution phenomena in the Po Valley.

Moreover, the values of radon exhalation flux density, estimated fitting with our model the radon concentration data, are quite different in Alessandria (15 Bq m^{-2} h^{-1})) and Milan (31 Bq m^{-2} h^{-1})). All these values are substantially lower than those previously used in this area (72 Bq m^{-2} h^{-1}) and estimated on a global basis. An improvement of the model, taking into account also for the time variation of the mixing height, $h(t)$, is now in progress.

REFERENCES

[1]   ALLEGRINI, I., FEBO, A., PASINI, A., SCHIARINI, S., Monitoring of the nocturnal mixed layer by means of particulate radon progeny measurement, Journal of Geophysical Research **99** (1994) 18765–18777.
[2]   MARCAZZAN, G.M., TESTA, A., Radioactive aerosols as tracers of turbulent diffusion: measurements in the city of Milan, J. Aerosol Sci. **26** (1995) 847–848.
[3]   SESANA, L., BARBIERI, L., FACCHINI, U., MARCAZZAN, G.M., [222]Rn as a tracer of atmospheric motions: a study in Milan, Radiation Protection Dosimetry, **78** (1998) 65–71.
[4]   PERRINO C., PIETRODANGELO, A., FEBO, A., An atmospheric stability index based on radon progeny measurements for the evaluation of primary urban pollution, Atmospheric Environment **35** (2001) 5235–5244.

[5] GARBERO, V., DELLACASA, G., BIANCHI, D., MAGNONI, M., ERBETTA, L., Outdoor radon concentration measurements: results and correlation with atmospheric stability condition and air quality, Radiation Protection Dosimetry, (in press), (2009).

[6] MARCAZZAN, G.M., PERSICO, F., Evaluation of layer mixing depth in Milan town from temporal variation of atmpspheric radioactive aerosol, J. Aerosol Sci. **27** (1996) 21- 22.

[7] SESANA, L, CAPRIOLI, E., MARCAZZAN, G.M., Long period study of outdoor radon concentration in Milan and correlation between its temporal variations and dispersion properties of atmosphere, Journal of Environmental Radioactivity **65** (2003) 147–160.

[8] CASADEI, S., et al., Evaluation of the mixing layer depth in the urban area of Milan, (in Italian), Ingegneria Ambientale, XXXV (2006) 144–157.

NATURAL RADIOACTIVITY FROM RADON PROGENY AS A TOOL FOR THE INTERPRETATION OF ATMOSPHERIC POLLUTION EVENTS

C. PERRINO

C.N.R. Institute of Atmospheric Pollution Monterotondo Stazione (Rome), Italy

Abstract

Natural radioactivity from radon short-lived decay products can be used to obtain reliable information about the mixing properties of the lower boundary layer. Continuous monitoring of natural radioactivity is obtained by means of a dedicated automatic sampler. This technique allows the interpretation of the time variation of atmospheric pollutants concentration in terms of relative weight of atmospheric dilution vs. changes in pollutant emissions and chemical transformation. Many examples of application of this technique to the interpretation of atmospheric pollution episodes concerning primary and secondary pollutants as well as particulate matter are reported.

Introduction

The knowledge of the dilution properties of the surface atmospheric layer is an essential tool for understanding the accumulation of pollutants and, in general, the time evolution of any pollution process. It is well known, in fact, that air pollution is the result of a complex interaction between chemistry and meteorology and that the atmospheric concentration of pollutants depends on their emission, transformation and deposition rate as well as on their dilution in the planetary boundary layer. In a given area, the difference from day to day in the emission rate of primary atmospheric pollutants are not so relevant, while their concentration may vary up to one order of magnitude as a consequence of atmospheric stabilization. Even more complex is the situation for secondary pollutants, whose concentration is very much dependent on the accumulation of precursors, which takes place in stable air masses. Conversely, an increased mixing of the lower atmosphere favours the dilution of both primary and secondary pollutants determining a substantial improvement of air quality.

We can obtain useful information about the dilution potential of the planetary boundary layer, which is not directly measured by any standard meteorological procedure, by monitoring a ground emitted and chemically stable compound whose emission rate can be considered to be constant in the space and time scale of our observations. This is the case of Radon and of its short-lived decay products, as the variation in the emanation rate of Radon from the soil can be considered to be negligible in a time scale of some days and a space scale of some kilometres, a time and space scale suitable for the description of pollution phenomena. It follows that the concentration of Radon and Radon progeny in the air strictly depends on the dilution properties of the atmosphere where the measurement is carried out. By determining natural radioactivity due to the Radon progeny attached to atmospheric particles we can obtain a reliable picture of the capability of the atmosphere to favour or reduce atmospheric pollution events. Radon and Radon progeny have been successfully used as good natural tracers of the mixing properties of the lower boundary layer in the studies of Allegrini et al. [1], Febo et al. [2], Gariazzo et al. [3], Kataoka et al. [4], Perrino et al. [5], Sesana et al. [6], Vecchi et al. [7].

We describe in this paper the application of the natural radioactivity technique to the interpretation of primary and secondary atmospheric pollution phenomena recorded in Central Italy.

Experimental

Natural radioactivity was measured by means of an automatic stability monitor (PBL Mixing Monitor, FAI Instruments, Fontenuova, Italy), essentially consisting of a sampler for the collection of particulate matter on filter membranes and a Geiger-Muller counter for determining the total beta activity of the short-lived Radon progeny attached to particles. The instrument operates on two filters at the same time: sampling is performed on the first filter for a 1-h sampling duration, then this filter undergoes the beta measurement phase while a second filter undergoes the sampling phase. These instrumental features assure that the short-lived beta activity of the particles is determined continuously over an integration time of 1 h and that the beta measurement period is long enough to guarantee a good accuracy of the results; the residual radioactivity is taken into account by a software procedure. The accuracy of the determination is improved by the automatic subtraction of the background radiation (cosmic rays), the continuous monitoring of the stability of the high voltage to the Geiger detector and normalisation of this value to a reference value [8].

Results

Primary pollutants

Typical outputs of the natural radioactivity monitor are shown in Figure 1, which refers to one summer month (August, left panel) and one summer month (December, right panel) in Rome.

During the warm months, which in Italy are generally characterised by large-scale high-pressure systems, the temporal pattern of radioactivity shows a well-modulate, regular shape, with night time maximum values (nocturnal atmospheric stability) and daytime minima (convective mixing of the lower atmosphere that dissipates the inversion layer). The mixing period starts very early in the morning and lasts until the late evening. During the winter period, instead, atmospheric stability periods, lasting for several days, alternate to advection periods. During advection natural radioactivity always shows very low values (e.g. 5–6, 15, 21–22, 28 and 31 December in Figure 1); during wintertime stability, instead, the nocturnal inversion only slackens during the day hours and natural radioactivity keeps high values also during the day day (e.g. 2, 8, 19, 24 December). During the winter period, the diurnal mixing is not only weak but also of limited duration, from the late morning to the early afternoon.
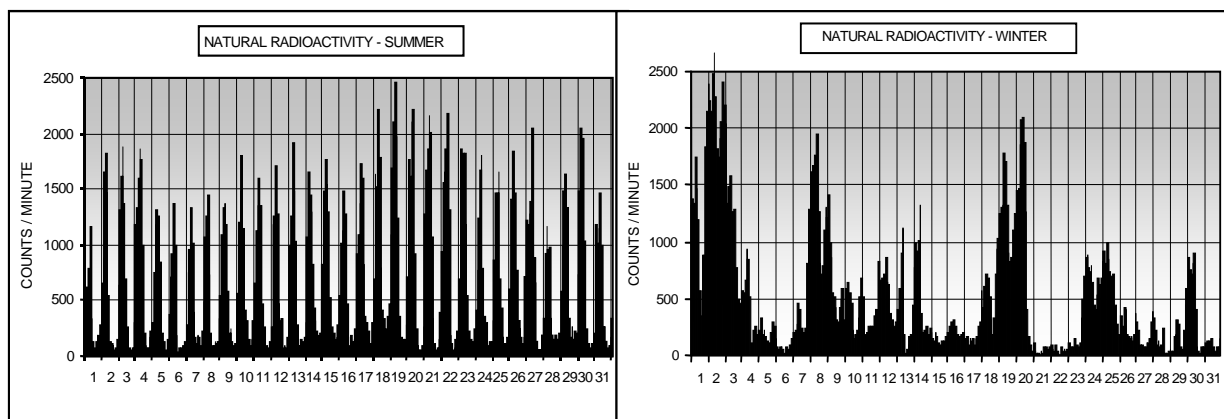
FIG. 1. Time pattern of natural radioactivity in Rome, during a summer and a winter month.

The very different duration of the atmospheric mixing phase along the year has an important consequence for atmospheric primary pollution. By monitoring traffic flows in Rome, it can been shown that during both summer and winter the numer of moving vehicles increases between 7 and 8 a.m., keeps a high value during the whole day and decreases between 8 and 10 p.m. The pattern of natural radioactivity reveals that during the summer the lower atmosphere is already well mixed when the traffic flow increases and that the night-time stability occurs when the traffic flow has already distinctly decreased. During the winter period, instead, the morning increase of the traffic flow corresponds to a still undeveloped mixed layer and the evening stability occurs when the traffic flow is still high. This causes the heavy pollution events typical of the winter.

Figure 2 reports the time pattern of natural radioactivity and of carbon monoxide during the first five days of December at the urban background station of Rome. Typically, the concentration pattern of primary non-reactive pollutants, such as CO, shows a first peak in the morning, when traffic emissions accumulate into the stable layer, a decrease during the warm hours, when traffic emissions can dilute, and a second stronger peak in the evening, when the emission flux superimposes again on atmospheric stability (e.g. December 1st). However, when atmospheric stability persists also during daytime, the decrease of primary pollutant concentration during warm hours is less distinct and a quite high primary pollution level can be detected also during the central part of the day (e.g. December 2nd). In the case of advection, instead, (e.g. from the afternoon of 4th until the end of 5th) CO concentration keeps very low values, and only small increases during the morning and the evening are observed. This close link between the time pattern of primary pollutants and natural radioactivity confirms the reliability of this parameter in describing pollution events.
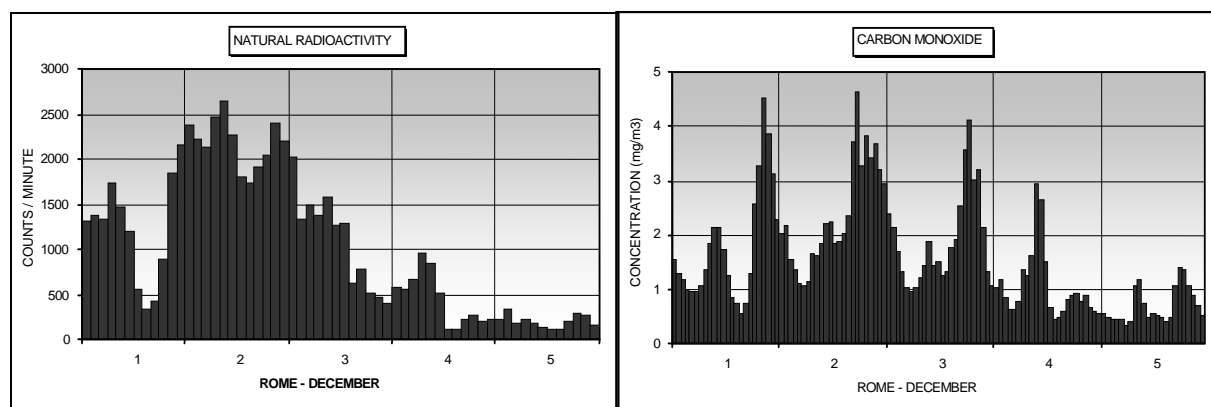
FIG. 2. Time pattern of natural radioactivity and of CO at the urban background station of Rome.

In order to make the information contained in the pattern of natural radioactivity more easily perceived and interpreted, an Atmospheric Stability Index (ASI) able to characterise each day in terms of meteorological predisposition to the occurrence of a primary pollution event has been developed. The Index is a proper combination of natural radioactivity values and of their time derivatives during the times of the day that favour the occurrence of primary pollution (early morning and evening).

The very good agreement between the ASI values and the average concentration of a primary non-reactive pollutant such as benzene, reported in Figure 3 for the year 1999–2000, shows that the mixing of the lower atmospheric layer, well described by the ASI, is of primary

relevance in determining the average concentration of non-reactive primary pollutants in the urban area of Rome. The satisfactory values of the correlation coefficient (R=0.89) indicate that the ASI is a reliable tool for the interpretation of primary pollution events. A better correlation between ASI and pollution values is, nevertheless, not expected, since the ASI takes into account only one of the two driving forces that determine pollutant concentration, that is the meteorological factor, while it does not take into account the day-to-day variations in the emission fluxes. In other words, the two data sets should coincide only if the emission fluxes were constant in time. The study of the differences between the two data sets, anyway, can be useful to identify situations when atmospheric pollution is heavier than predictable on the only basis of the meteorological situation (e.g. in case of heavy traffic episodes) or lighter (e.g. in case of traffic restriction measures or of holidays). For example, a lower correlation is expected during August, when the emission flux is distinctly lower than during the rest of the year, due to summer holidays (see Figure 3).
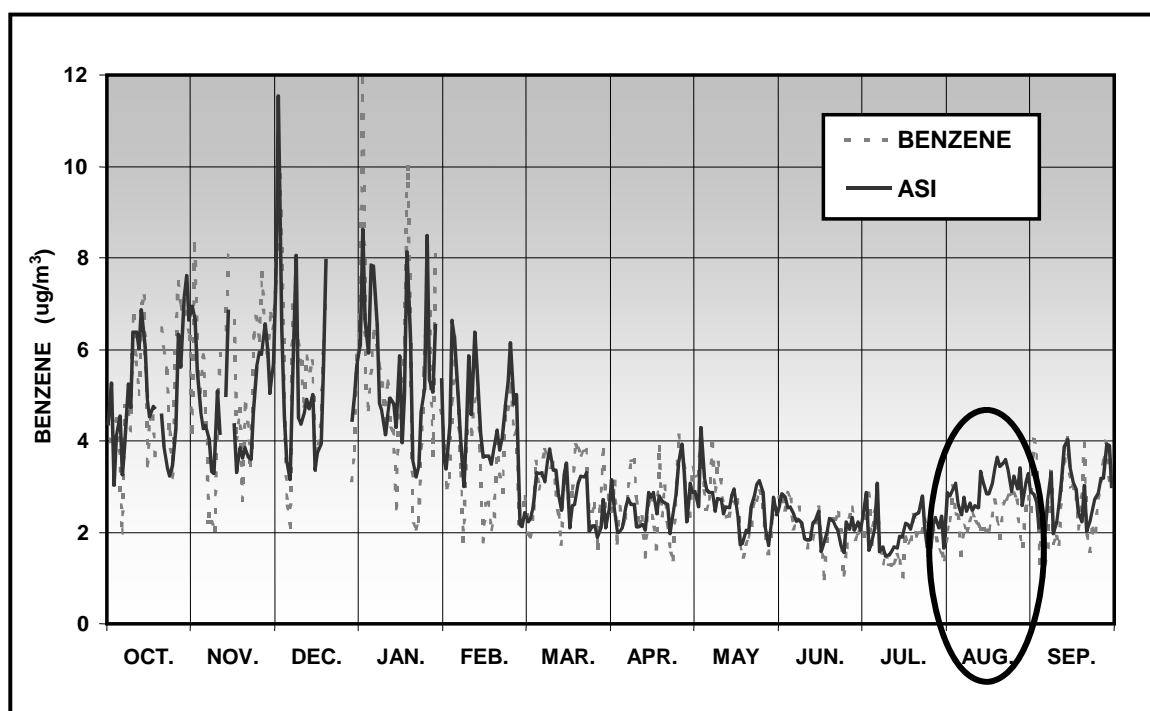
FIG. 3. Atmospheric Stability Index (ASI) and average daily concentration of benzene at the urban background station of Rome.

Ozone

Natural radioactivity also constitutes a robust key for the interpretation of ozone time pattern. The example reported in Figure 4, which refers to the area of Gallese, a village in Central Italy about 50 km from Rome, shows that in most cases ozone exhibits its typical behaviour, with increasing during daylight hours and very low values during the night (Figure 4, upper panel). The main exceptions can be observed on November 3–5, 7–8 and 19–23, when ozone keeps high values also during the night (25–30 ppb, which is the ozone background value at that latitude and time of the year). The time pattern of natural radioactivity (lower panel) shows that prolonged advection occurred during these periods, making it possible the prevalence of ozone vertical transport from the upper atmospheric layer over the chemical loss at the ground. During the rest of the period, the mechanical mixing (convection) only occurs during the central part of the day, while during the night the lower atmospheric layer is

154

uncoupled from the residual upper layer and the removal reactions (NO titration) cause the decrease of ozone concentration to about zero (see, for example, the nights 2–3, 8–9, 9–10).

It is interesting to note that when stability conditions occurred also during the daytime, such as in the case of November 24–27 and 30, ozone concentration always kept very low values, below 10 ppb. This can be explained by considering that in these conditions the lower atmospheric layer are decoupled from the residual layer not only during the night but also during the middle of the day. As a consequence, the ozone amount available in the lower layer is quickly consumed by the titration reaction and cannot be replaced, as a further ozone transport from the upper layers is prevented.
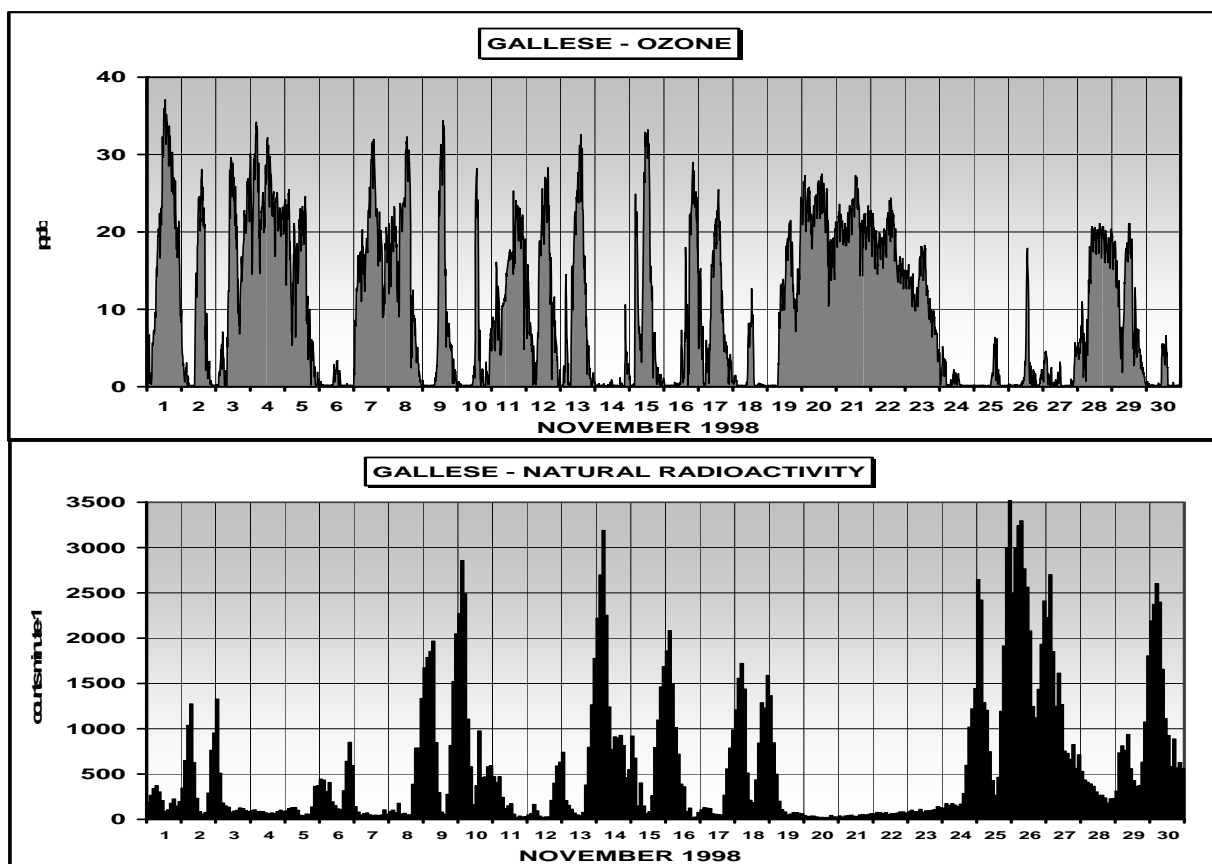
FIG. 4. Time pattern of ozone and of natural radioactivity during the field campaign carried out in the rural area of Gallese.

Particulate matter

The link between the dilution properties of the lower atmosphere and the accumulation of suspended particles is highlighted by comparing the graphs in Figure 5, where an interesting episode occurred in Rome on December 2003 is reported. The time pattern of the atmospheric concentration of particles smaller than 10 micrometers in diameter (PM_{10}), recorded at the background station of Rome (upper graph) shows that during the first part of the period (December 16–21) the concentration of particulate matter was quite high, while in the second period (22–31) the values were generally lower, with the clear exception of the 27th, when a sudden increase of PM_{10} (from about 30 to about 60 $\mu g\ m^{-3}$) was observed. The graph of the

traffic flow during the same period (middle graph of Figure 5) did not show any important variation neither during the whole period, nor specifically on the 27th. The study of natural radioactivity (lower graph) indicates that during the first six days of the period conditions of increasing stabilisation of the atmosphere occurred in the area of Rome. In particular, a strong nocturnal stability can be observed during the nights of 17th, 18th, 19th and 20th, with a very weak convective mixing during the daytime hours of the 19th (high values of natural radioactivity not only during the night but also during the middle hours of the day). These conditions, which favour the accumulation of all pollutants, caused the build up of PM_{10} concentration. Starting from the first hours of the afternoon of 21st, an advection episode caused a sudden change of the air masses and allowed a rapid dilution of the accumulated pollutants. The pattern of PM_{10} concentration shows a sudden decrease and keeps values lower than 20 µg m^{-3} for the following four days. At about 6 p.m. of the 26th, the atmospheric circulation showed a new variation, with a sudden and strong stabilisation of the lower atmosphere that persisted during the night and also during the day-hours of the 27th. This situation caused the observed sudden increase in the concentration of PM_{10}, which decreased again on December 28th, when a new increase of the dilution potential of the atmosphere occurred (low values of natural radioactivity).
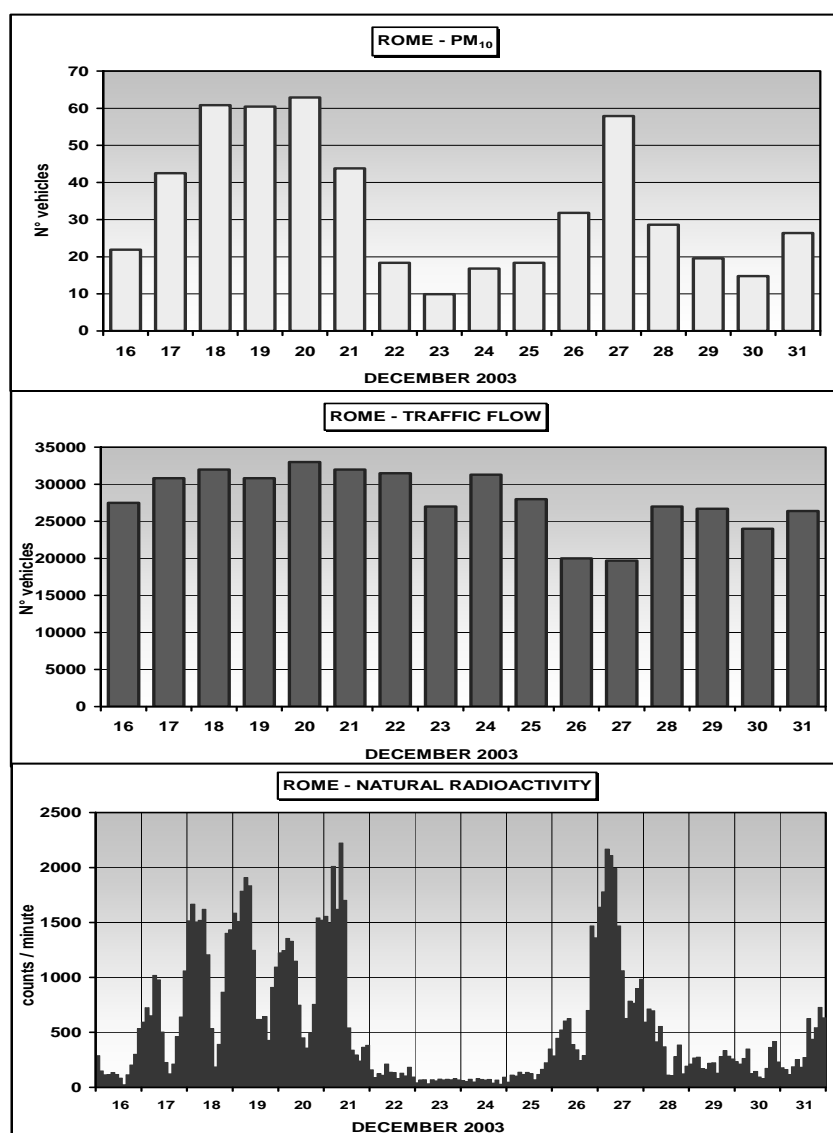
FIG. 5. Time pattern of PM_{10} concentration (upper graph), of traffic flow (middle graph) and of natural radioactivity (lower graph) in the urban area of Rome.

This example demonstrates the ability of natural radioactivity to identify also particulate pollution events that are due to a decrease in the dilution properties of the lower atmosphere. This ability has led to the development of an Atmospheric Stability Index for particulate matter (ASIpm), calculated with an algorithm specific to particulate matter pollution. Again, the comparison between the values of the ASIpm and the concentration of atmospheric particles (PM_{10}), reported for the winter months of 2004 in Figure 6, shows that the index exhibits satisfactory performance in reproducing the time pattern of PM concentration on the only basis of natural radioactivity values (R=0.88), and confirms that the mixing of the atmosphere is a driving force also in the build up of a pollutant of heterogeneous composition and origin such as particulate matter.
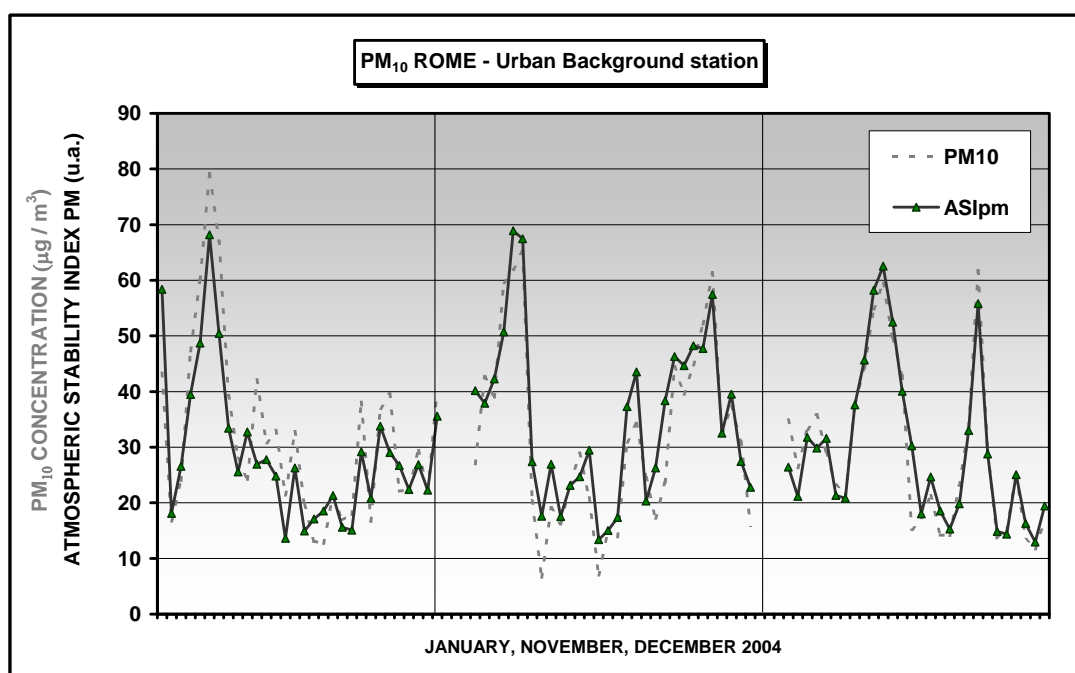
FIG. 6. Comparison between the values of the ASIpm and the concentration of atmospheric particles (PM_{10}) at the urban background station of Rome during the winter months of 2004.

As in the case of primary pollutants, deviations of the measured PM concentration from the ASIpm value indicate the occurrence of a change in the emission/formation/transport of particles in the area of study. The example reported in Figure 7 shows the case of December 2004, when a strong episode of dust transport from north-African desert area to Central and South Italy was recorded. The occurrence of the dust transport is confirmed by the simulation of the Dust Regional Atmospheric Model (DREAM), which predicts the atmospheric life cycle of the eroded desert dust (http://www.bsc.es/projects/earthscience/DREAM/). In this case, the value of the ISApm indicates the concentration of PM_{10} that would have been measured on December 2–4 in the absence of the transport episode (around 30 µg m^{-3}). Chemical analysis of the collected particles shows that the difference between the PM_{10} value

indicated by the ASIpm and the measured value (from 70 µg m^{-3} on December 2nd to 25 µg m^{-3} on December 4th) are almost totally to be ascribed to crustal components (64 µg m^{-3} on December 2nd) [9].

The possibility of a very fast identification of particulate pollution episodes due to natural events (desert dust, sea-salt transport, volcanic eruptions etc.), to be further confirmed by chemical analysis of the particles, can be particularly useful to local Authorities, who in these cases can avoid the application of traffic restriction measures that are generally undertaken during periods when PM level exceeds a fixed value.

Similarly, local Authorities can benefit from the application of the natural radioactivity method to identify the results of the application of traffic restriction measures. Only a decrease of the pollutant concentration well below the ASI value indicates, in fact, a real contribution of the restriction measure to air quality improvement. A decrease of both pollutant concentration and ASI value would reveal, instead, a simple improvement of the dilution ability of the atmosphere.
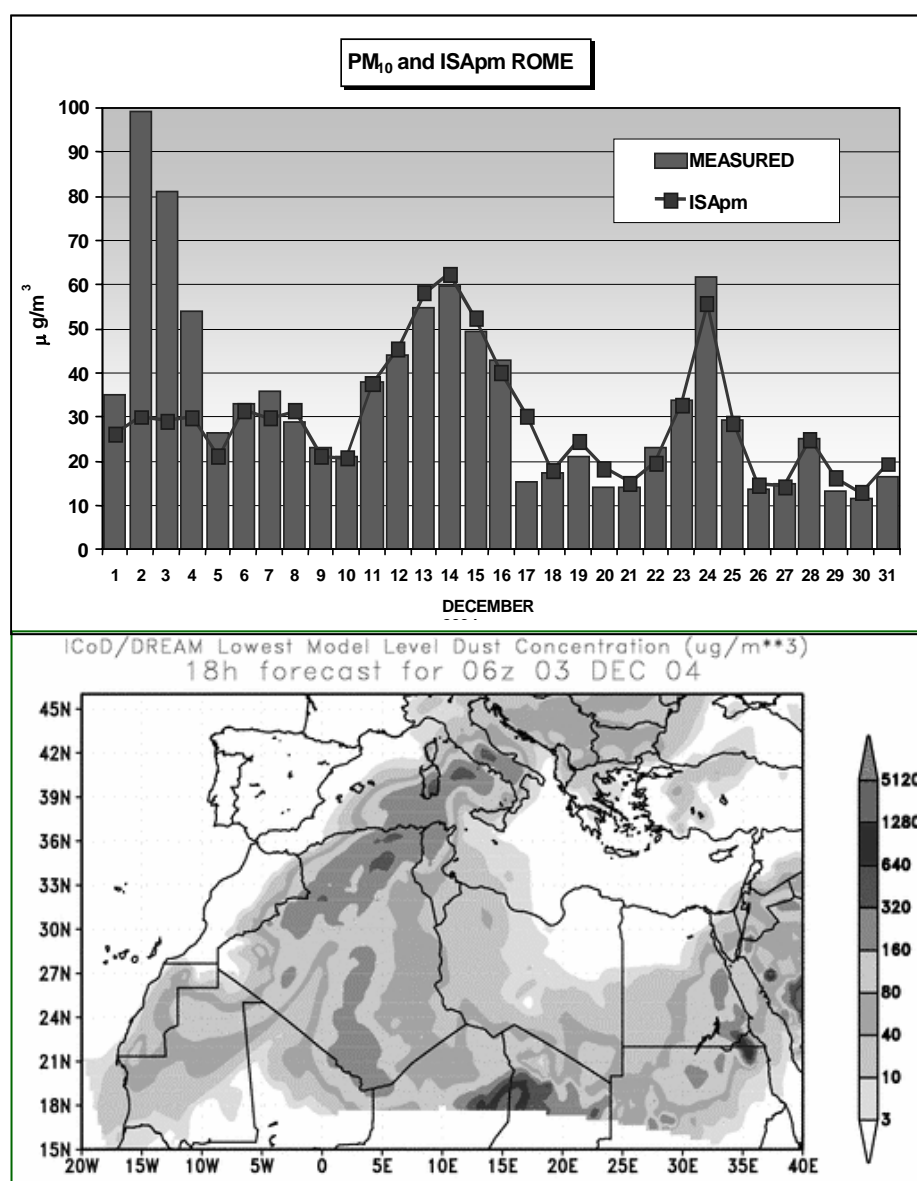
FIG. 7. PM$_{10}$ concentration measured and predicted by the ISA during a desert dust transport event (upper panel); simulation of the event by the Dust Regional Atmospheric Model (DREAM) (www.bsc.es/projects/earthscience/DREAM/).

Conclusions

The dilution properties of the lower boundary layer and their influence on the dispersion and accumulation of atmospheric pollutants can be evaluated on the basis of the measurement of the natural radioactivity due to Radon progeny.

This method allows a clear distinction of the relative weight of the emission flux variations and of the atmospheric dilution in determining the modulation of the air concentration of both primary and secondary pollutants.

REFERENCES

[1]   ALLEGRINI, I., et al., Monitoring of the nocturnal mixed layer by means of particulate radon progeny measurement, J. Geophys. Res. **99** (1994) 18.765.

[2]   FEBO, A., et al., A method for the interpretation of ground level ozone measurements in air quality networks, EMEP/CCC Report 10/97 (Proceedings of the EMEP-WMO Workshop on Strategies for Monitoring of Regional Air Pollution in relation to the need within EMEP, GAW and other international bodies), J. Schaug and K, Uhse Eds. (1997) 165–171.

[3]   GARIAZZO, C., et al., Analysis of Radon, surface turbulence and SODAR data to evaluate meteorological effects on air pollutants, Proceedings of 12th International Symposium on Acoustic Remote Sensing, Cambridge (2004).

[4]   KATAOKA, T., et al., A study of the atmospheric boundary layer using radon and air pollutants as tracer, Boundary-Layer Metereol. **101** (2001) 131.

[5]   PERRINO, C., et al., An atmospheric stability index based on radon progeny measurements for the evaluation of primary urban pollution, Atmos. Environ. **35** (2001) 5235.

[6]   SESANA, L., et al., Long period study of outdoor radon concentration in Milan and correlation between its temporal variation and dispersion properties of the atmosphere, J. Environ. Rad. **65** (2003) 147.

[7]   VECCHI, R., et al., The role of atmospheric dispersion in the seasonal variation of PM1 and PM2.5 concentration and composition in the urban area of Milan (Italy), Atmos. Environ. **38** (2004) 4437.

[8]   PERRINO, C., et al., A new beta gauge monitor for the measurement of PM10 air concentration EMEP/CCC Report 9/2000 (Proc. of the EMEP-WMO workshop on fine particles – emissions, modelling and measurements) J.E. Hanssen, R. Ballaman and R. Gehrig Eds. (2000) 147–152.

[9]   PERRINO, C., et al., Influence of natural events on the concentration and composition of atmospheric particulate matter, Atmos. Environ (2009), doi:10.1016/j.atmosenv. 2008.06.035.

CONTRIBUTORS TO DRAFTING AND REVIEW

Arnold, D.	Technical University of Catalonia (UPC), Spain
Brandys, I.	Israel Atomic Energy Commission, Israel
Burian, I.	State Office for Nuclear Safety, Czech Republic
Conen, F.	University of Basel, Switzerland
Fathabadi, N.	National Radiation Protection Department, Islamic Republic of Iran
Gaigl, F.A.	International Atomic Energy Agency
Galmarini, S.	JRC, ISPRA, European Union
Gnoni, G.A.	Autoridad Regulatoria Nuclear, Argentina
Grossi, C.	Technical University of Catalonia (UPC), Spain
Hirao, S.	Nagoya University, Japan
Jalkanen, L.	World Meteorological Organization (WMO), Switzerland
Kim, C-K.	International Atomic Energy Agency
Kobal, I.	Jozef Stefan Institute, Department of Physical and Environmental Chemistry, Slovenia
Magnoni, M.	ISPRA, Arpa Piemonte, Italy
Martin, P.	International Atomic Energy Agency
Neubert, R.E.M.	State University of Groningen, Centre for Isotope Research, Netherlands
Nir, J.	Israel Atomic Energy Commission, Israel
Otahal, P.	State Office for Nuclear Safety, Czech Republic
Perrino, C.	ISPRA – CNR Institute of Atmospheric Pollution, Italy
Quindos Poncela, L.S.	Universidad de Cantabria, Spain
Sansone, U.	International Atomic Energy Agency
Schery, S.	NASA/Ames, United States of America
Schmidt, M.	CEA, France
Seibert, P.	BOKU, Austria
Steinkopff, T.	Federal Ministry of Economics and Technology (BMWI), Germany

Stoehlker, U.	Bundesamt für Strahlenschutz, BFS Department of Radiation Protection and the Environment, Germany
Taguchi, S.	AIST, Japan
Vargas, A.	Universidad Técnica de Cataluña Instituto de Tecnologìas de Energìa, Spain
Vaupotic, J.	Josef Stefan Institute, Slovenia
Verheggen, B.	Energy Research Centre of the Netherlands (ECN), Netherlands
Yamazawa, H.	Nagoya University, Japan
Zahorowski, W.	ANSTO, Australia

IAEA/WMO Technical Meeting

22–24 June 2009, Vienna, Austria

IAEA
International Atomic Energy Agency

Where to order IAEA publications

In the following countries IAEA publications may be purchased from the sources listed below, or from major local booksellers. Payment may be made in local currency or with UNESCO coupons.

AUSTRALIA
DA Information Services, 648 Whitehorse Road, MITCHAM 3132
Telephone: +61 3 9210 7777 • Fax: +61 3 9210 7788
Email: service@dadirect.com.au • Web site: http://www.dadirect.com.au

BELGIUM
Jean de Lannoy, avenue du Roi 202, B-1190 Brussels
Telephone: +32 2 538 43 08 • Fax: +32 2 538 08 41
Email: jean.de.lannoy@infoboard.be • Web site: http://www.jean-de-lannoy.be

CANADA
Bernan Associates, 4501 Forbes Blvd, Suite 200, Lanham, MD 20706-4346, USA
Telephone: 1-800-865-3457 • Fax: 1-800-865-3450
Email: customercare@bernan.com • Web site: http://www.bernan.com

Renouf Publishing Company Ltd., 1-5369 Canotek Rd., Ottawa, Ontario, K1J 9J3
Telephone: +613 745 2665 • Fax: +613 745 7660
Email: order.dept@renoufbooks.com • Web site: http://www.renoufbooks.com

CHINA
IAEA Publications in Chinese: China Nuclear Energy Industry Corporation, Translation Section, P.O. Box 2103, Beijing

CZECH REPUBLIC
Suweco CZ, S.R.O., Klecakova 347, 180 21 Praha 9
Telephone: +420 26603 5364 • Fax: +420 28482 1646
Email: nakup@suweco.cz • Web site: http://www.suweco.cz

FINLAND
Akateeminen Kirjakauppa, PO BOX 128 (Keskuskatu 1), FIN-00101 Helsinki
Telephone: +358 9 121 41 • Fax: +358 9 121 4450
Email: akatilaus@akateeminen.com • Web site: http://www.akateeminen.com

FRANCE
Form-Edit, 5, rue Janssen, P.O. Box 25, F-75921 Paris Cedex 19
Telephone: +33 1 42 01 49 49 • Fax: +33 1 42 01 90 90
Email: formedit@formedit.fr • Web site: http://www. formedit.fr

Lavoisier SAS, 145 rue de Provigny, 94236 Cachan Cedex
Telephone: + 33 1 47 40 67 02 • Fax +33 1 47 40 67 02
Email: romuald.verrier@lavoisier.fr • Web site: http://www.lavoisier.fr

GERMANY
UNO-Verlag, Vertriebs- und Verlags GmbH, Am Hofgarten 10, D-53113 Bonn
Telephone: + 49 228 94 90 20 • Fax: +49 228 94 90 20 or +49 228 94 90 222
Email: bestellung@uno-verlag.de • Web site: http://www.uno-verlag.de

HUNGARY
Librotrade Ltd., Book Import, P.O. Box 126, H-1656 Budapest
Telephone: +36 1 257 7777 • Fax: +36 1 257 7472 • Email: books@librotrade.hu

INDIA
Allied Publishers Group, 1st Floor, Dubash House, 15, J. N. Heredia Marg, Ballard Estate, Mumbai 400 001,
Telephone: +91 22 22617926/27 • Fax: +91 22 22617928
Email: alliedpl@vsnl.com • Web site: http://www.alliedpublishers.com

Bookwell, 2/72, Nirankari Colony, Delhi 110009
Telephone: +91 11 23268786, +91 11 23257264 • Fax: +91 11 23281315
Email: bookwell@vsnl.net

ITALY
Libreria Scientifica Dott. Lucio di Biasio "AEIOU", Via Coronelli 6, I-20146 Milan
Telephone: +39 02 48 95 45 52 or 48 95 45 62 • Fax: +39 02 48 95 45 48
Email: info@libreriaaeiou.eu • Website: www.libreriaaeiou.eu